Universidade de Aveiro Departamento de Química
2019

Elaine Fabre

Tratamento de águas contaminadas com metais potencialmente tóxicos e não essenciais usando biossorventes e materiais zeolíticos

Treatment of contaminated waters with non-essential and potentially toxic metals using biosorbents and zeolite materials

Universidade de Aveiro Departamento de Química
2019

Elaine Fabre

Tratamento de águas contaminadas com metais potencialmente tóxicos e não essenciais usando biossorventes e materiais zeolíticos

Treatment of contaminated waters with non-essential and potentially toxic metals using biosorbents and zeolite materials

Tese apresentada à Universidade de Aveiro para cumprimento dos requisitos necessários à obtenção do grau de Doutor em Engenharia Química, realizada sob a orientação científica do Doutor Carlos Manuel Santos Silva, Professor Associado do Departamento de Química da Universidade de Aveiro, e coorientação científica da Doutora Maria Eduarda Pereira, Professora Associada do Departamento de Química da Universidade de Aveiro.

Este trabalho foi financiado pelo Conselho Nacional de Desenvolvimento Científico e Tecnológico (CNPQ) do Brasil através de uma bolsa de doutoramento (234372/2014-1). Esta pesquisa enquadra-se também no âmbito do projeto CICECO- Instituto de Materiais de Aveiro (FCT Ref. UID/CTM/50011/2019) financiado pela Fundação para a Ciência e a Tecnologia (FCT).

"*Remember to look up at the stars and not down at your feet. Try to make sense of what you see and wonder about what makes the Universe exist. Be curious. And however difficult life may seem, there is always something you can do and succeed at*."

(Stephen Hawking)

o júri

presidente

Professor Doutor António José Arsénia Nogueira
professor catedrático da Universidade de Aveiro

Professor Doutor Miguel Ângelo Pardal
professor catedrático da Faculdade de Ciências e Tecnologia da Universidade de Coimbra

Professor Doutor João Carlos Moura Bordado
professor catedrático do Instituto Superior Técnico da Universidade de Lisboa

Prof. Doutora Helena Maria Vieira Monteiro Soares
professora auxiliar da Faculdade de Engenharia da Universidade do Porto

Doutor Carlos Alberto Garcia do Vale
investigador do Centro Interdisciplinar de Investigação Marinha e Ambiental- CIIMAR

Prof. Doutora Maria Eduarda da Cunha Pereira
professora associada do Departamento de Química da Universidade de Aveiro

agradecimentos

Aos meus orientadores, Doutor Carlos Manuel Silva e a Doutora Eduarda Pereira pela orientação científica, incentivos e tranquilidade transmitidos, que tornaram possível a realização deste trabalho e, sobretudo, pela confiança, apoio e amizade que contribuíram para o meu crescimento profissional e pessoal.

À Doutora Inês Portugal pela simpatia e ensinamentos científicos.

Ao Doutor Carlos Vale pela sua incansável disponibilidade demonstrada ao longo do desenvolvimento deste trabalho e pelos ensinamentos científicos e amizade.

À Cláudia Lopes, pelos ensinamentos, orientação, paciência e amizade.

Ao Bruno Henriques pela orientação científica, disponibilidade, amizade e ajuda em todas as minhas solicitações.

Aos meus colegas de trabalho, pela disponibilidade alegria e motivação sempre.

À todos os meus amigos, que são incríveis e muito especiais, pela motivação, carinho e apoio.

À minha família por todo o amor e compreensão, em especial à minha mãe Roselana que sempre me apoiou incondicionalmente, ao meu pai Clezio pelo carinho, à minha irmã Jamile pelas palavras de apoio e motivação e à minha afilhada Fernanda pelos incentivos.

À empresa N9VE pelo suporte e auxílio financeiro.

Finalmente, agradeço ao apoio financeiro que me foi concedido pelo CNPq.

.

palavras-chave

Biossorventes, permuta ionica, mercúrio, contaminantes, modelação, sorção, materiais de síntese, tratamento de águas

resumo

O crescimento populacional e a industrialização têm reduzido drasticamente a qualidade da água devido à descarga de diversos metais tóxicos nos corpos aquáticos. Entre esses contaminantes, o mercúrio é considerado um dos mais perigosos devido à sua capacidade de acumulação nos organismos vivos e ampliação ao longo da cadeia alimentar. Mesmo em concentrações muito baixas esse metal persiste no ambiente e afeta os ecossistemas e a saúde humana. Agências governamentais como a Organização Mundial da Saúde (OMS) e a União Europeia (UE) têm reconhecido a importância e urgência de remover esse contaminante das águas residuais. A Diretiva 2013/39/UE da União Europeia classifica o mercúrio como uma substância perigosa prioritária que deve ser progressivamente eliminada das emissões até 2021 e incentiva o desenvolvimento de tecnologias de tratamento de águas mais baratas e inovadoras para sua remoção.

Apesar do grande número de trabalhos publicados sobre esse assunto, a maioria destes relata sistemas usando condições irreais, tais como elevadas concentrações de mercúrio e matrizes simples de água. Ainda há uma grande carência de pesquisas e aplicações de materiais em condições ambientais, com o objetivo de efetivamente oferecer uma alternativa aos métodos convencionais. Nesse sentido, este estudo investigou a capacidade de vários sorventes naturais e sintéticos para remover principalmente mercúrio de soluções contaminadas com concentrações baixas a moderadas deste metal. Esses dois tipos de sorventes têm vantagens diferenciadas e sua adequação ao processo depende da aplicação pretendida. No presente estudo, os testes foram realizados em condições controladas em laboratório, usando água desionizada, água da torneira e água do mar com concentrações de mercúrio entre 50 µg dm^{-3} e 1000 µg dm^{-3}. Além disso, um efluente diluído também foi utilizado para testar a viabilidade dos procedimentos em condições realistas. Os sorventes usados foram: AM-11, AM-14, cascas de banana, cascas de batata, cascas de ovo, cascas de *Eucalyptus globulus*, jacinto d'água, resíduo de café, *Ulva intestinalis*, *Ulva lactuca*, *Fucus spiralis*, *Fucus vesiculosus*, *Gracilaria* sp. e *Osmundea pinnatifida*.

Esses sorventes foram estudados em várias condições operacionais, simulando várias águas contaminadas, como as comumente encontradas em sistemas aquáticos ou efluentes industriais. Entre os sorventes testados, os materiais sintéticos apresentaram maiores capacidades de remoção do Hg evidenciando seu potencial para tratamentos de efluentes industriais. Pequenas doses de AM-11, como 14 mg dm^{-3}, foram capazes de remover mais de 99 % de mercúrio de soluções contaminadas com 1000 µg dm^{-3}. As capacidades calculadas através da isotérmica de Langmuir para AM-11 e AM-14 foram 161 e 304 mg g^{-1}, respetivamente. O uso de biossorventes amplamente abundantes na natureza, como resíduos agrícolas ou industriais ou macroalgas marinhas, representa outra alternativa promissora aos métodos já existentes. Nesse contexto, cascas de banana, *Ulva intestinalis*, *Ulva lactuca* e *Gracilaria* sp. exibiram os melhores desempenhos, sendo capazes de remover mais de 98 % de Hg(II) de águas salgadas com concentração de inicial de 50 µg dm^{-3} e obter soluções com qualidade de águas para consumo (ou seja, concentração de Hg menor que 1 µg dm^{-3}). Esses biossorventes se destacaram por sua cinética mais rápida (remoção de mais de 80 % de mercúrio após 48 horas de exposição) e capacidade de atuar igualmente bem na presença de outros iões competidores. Além disso, esses biossorventes têm custos insignificantes, oferecendo excelentes opções para proteger os sistemas aquáticos.

keywords

biosorbents; ion exchange, mercury, contaminants, modelling, sorption, synthetic materials, water treatment.

abstract

The growth of population and industrialization has dramatically reduced the water quality due to the release of diverse toxic metals into the aquatic bodies. Among these contaminants, mercury is considered one of the most hazardous because of its ability of accumulation in the living organisms and magnification along the food chain. Even at very low concentrations this metal persists in the environment and impacts ecosystems and human health. Governmental agencies like World Health Organization (WHO) and European Union (EU) have recognized the importance and urgency of remove this contaminant from waste waters. The Directive 2013/39/EU of the European Union classifies mercury as a priority substance that must be progressive eliminated of the emissions by 2021 and promotes the development of innovative cheaper technologies for its removal in water treatments.

Despite the large number of works published in this subject, most of them report systems using unrealistic conditions such as high mercury concentrations and simple water matrices. There is still a big lack concerning the search and application of materials under environmental conditions with the aim to effectively offer an alternative to the conventional methods. In this sense, this study investigated the ability of various natural and synthetic sorbents to remove mainly mercury at low to moderate concentrations in spiked solutions. These two types of sorbents have advantages and their suitability to the process depend on the intended application. In the present study, tests were performed under laboratory-controlled conditions, using deionised water, tap water and seawater spiked from 50 µg dm^{-3} to 1000 µg dm^{-3}. In addition, a diluted effluent was also used to test the viability of the procedures under realistic conditions. The sorbents applied in the experiments were: AM-11, AM-14, banana and potato peels, eggshells, *Eucalyptus globulus* barks, water hyacinth, coffee waste, *Ulva intestinalis*, *Ulva lactuca*, *Fucus spiralis*, *Fucus vesiculosus*, *Gracilaria* sp. and *Osmundea pinnatifida*.

These sorbents were studied under several operating conditions simulating various contaminated waters, as those commonly reported in aquatic systems or industrial effluents. Among the sorbents tested, the synthetic materials presented higher capacities prospecting their potential for treating industrial effluents. Small doses as low as 14 mg dm^{-3} of AM-11 were able to remove more than 99 % of 1000 µg dm^{-3} of the mercury from spiked solutions. The capacities calculated from Langmuir isotherm for AM-11 and AM-14 were 161 and 304 mg g^{-1}, respectively. The use of biosorbents largely abundant in nature, such as agricultural or industrial wastes or marine macroalgae represent another promising alternative to conventional methods. In this context, banana peels, *Ulva intestinalis*, *Ulva lactuca* and *Gracilaria* sp. exhibited the best performances, being able to remove more than 98 % of Hg(II) from spiked seawaters with Hg(II) concentration of 50 µg dm^{-3} and to accomplish drinking water quality (*i.e.* Hg(II) concentration lower than 1 µg dm^{-3}). These biosorbents stood out for their faster kinetic (removing more than 80 % of Hg after 48 h of exposure), and ability to perform equally well in the presence of other competitive ions. In addition, these biosorbents have negligible costs offering excellent options for protecting water bodies.

Index

List of Figures

List of Tables

Chapter I
Introduction

Index

I. Introduction

I.1. The problem of water contamination

Scarcity and the unequal distribution of water are issues facing humanity in nowadays. Despite the nomenclature of “Water Planet” and the fact that water cover 70 % of the Earth, actually only 3 % of this water is fresh water and the small part of 1/3 of that is the fraction available for use in all the anthropogenic activities (World Water Assessment Programme (United Nations), 2015). Population growth, together with the economic development and increasing consumption has led to the rise in water demand approximately 1 % per year since 1980s and it tends to keep enhancing in similar rates until 2050. Currently, over 2 billion people live with lack of water with enough quality for consuming and more than 4 billion experience scarcity of water at least one month a year (World Water Assessment Programme (United Nations), 2019). The scenario for 2050 points to up 3.2 billion of people living with severe water scarcity and up to 5.7 billion will experience water stress at least one month a year (Burek et al., 2016). Among the sectors, agriculture is the major consumer of water around the world (see Figure I.1), except in Europe, in which industry takes 54 % of the available water. The projections for the 2050 show that agriculture will continue by far leading the water consumption globally, however the domestic and industrial use tend to rise, mainly due to the increase in population (Burek et al., 2016; World Water Assessment Programme (United Nations), 2019).

The availability of water is directly related with its quality, since water contamination may prevent its use. Increased generation of untreated or inadequately treated wastewaters from sewage, agricultural or industry, leads to the reduction of the quality of water worldwide and causes drastic impacts on human health and ecosystems (World Water Assessment Programme (United Nations), 2017).

The 2030 Agenda for Sustainable Development incentives the improvement of water quality by reducing the elimination of chemicals, hazardous substances and materials and the treatment of wastewaters for recycling and reuse. The effective

treatment of effluents and wastewaters allows the improvement of water supply and its redirection to diverse demanding activities, like irrigation, saving freshwater for consumption and other uses that requires higher standard quality.

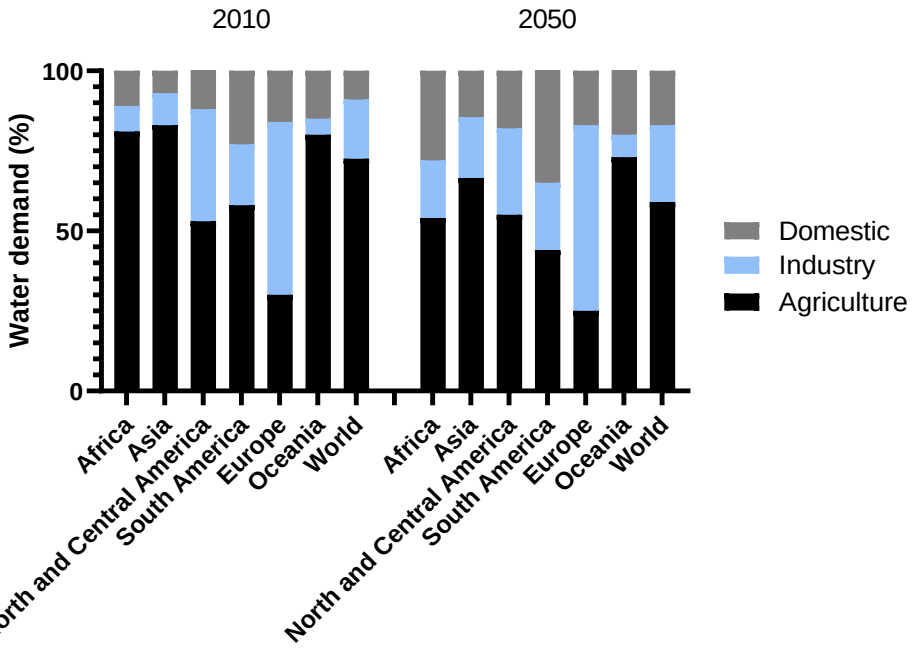

Figure I.1. Water distribution by region and sector in 2010 and the projection for 2050 (adapted from Burek et al. (2016)).

I.2. Contaminants

The large number of elements present in nature can be classified as essentials and non-essentials based on their participation and contribution on the metabolic activities of the living organisms (Torres et al., 2008). Micronutrients are needed to sustain the biological reactions and should be included in the daily diet, like for instance, iron (Fe) and copper (Cu). These two elements are responsible for the transfer of electrons in many cellular processes and without Fe most of the respiration processes would not occur (Torres et al., 2008). However, there is a fine line between classifying these elements as nutrients or poisons. In proper doses, manganese (Mn) is an essential element for the survival of the human beings, but in high doses it is dangerous and has been associated

with Parkinson's symptoms (Ash and Stone, 2003). On the other hand, some elements have no benefits to the organisms and are potentially harmful even at very low concentrations. These non-essential elements include Hg, Cd, Pb, and other elements which can be assimilated by the nutritional strategy of the organisms and interfere in the enzymatic functioning causing several toxic effects (Ash and Stone, 2003; Torres et al., 2008).

Several compounds are contributing for the contamination of the aquatic bodies, but the non-essential toxic metals have increased global concerns due to their persistent character. They easily accumulate in the living cells and are transmitted and amplified along the food chain, being the man the most affected at the top, exposed to concentrations much higher than the ones in the environment (Ayangbenro and Babalola, 2017; Brandão, 1998). On the contrary of the other organic contaminants, these metals are non-degradable into non-toxic forms and they can even associate with functional groups on the tissues of the cells and form more stable and more toxic complexes (Aryal and Liakopoulou-Kyriakides, 2015; Ayangbenro and Babalola, 2017). The damages caused by these metals have drawn much attention because their noxious effects are only observed in the organisms when the levels of these elements exceed the toxic limits (Gautam et al., 2013).

Recently, another group of elements named as rare earth elements (REEs) has been regarded as non-essential contaminants due to the high growth of technological devices production. As a result of the technological innovations, the appliances are becoming increasingly replaceable, generating annually tons of electronic wastes and contaminated wastewaters. Hence, their presence should be considered and as well as the toxic metals they should be removed in order to obtain high quality treated waters (Ishii et al., 2006; Jacinto et al., 2018).

Anthropogenic activities are the main responsible for the release of the non-essential elements in nature, for instance, from sewage, landfill leachate, atmospheric deposition and many industrial activities such as the production of batteries, electrical devices, fertilizers, pesticides, lamps, monitors, photographic materials, printing

pigments, mining, refining ores, pulp and paper, etc (Ayangbenro and Babalola, 2017; Hashim et al., 2011; Nguyen et al., 2013). Despite the greater awareness about the negative impacts of the emission of contaminants, the growth of industrialization has been dramatically reducing the quality of the aquatic bodies.

The World Health Organization (WHO), the European Union (EU) and many government environmental protection agencies have recognized the importance of eliminating those toxic contaminants of water systems and have very strict regulations for their maximum level in drinking waters as presented in Table I.1. The Agency for Toxic Substances and Disease Registry regularly lists the most dangerous substances in order of priority, based on their toxicity, frequencies and potential for human exposure ("ATSDR, Priority list of hazardous substances," 2017). In this list, As, Pb and Hg are occupying the first positions and Cd is the next metal, at the seventh place ("ATSDR, Priority list of hazardous substances," 2017).

Because of its high toxicity and severe damages caused to human health, and the enormous challenges associated with its elimination and quantification, mercury was considered the focus of this work.

Table I.1. Guidelines of the maximum concentration of toxic metals in drinking waters by different regulations (μg dm^{-3}) ("Council Directive 98/83/EC of 3 November 1998 on the quality of water intended for human consumption," 1998, National Primary Drinking Water Regulations, 2009; Organization., 2006; Schroeder, 1998; Zhao et al., 2016).

Metal	WHO	E.U.	U.S.	Brazil	Canada	China
Hg	6	1	2	0.2	1	1
Cd	3	5	5	1	5	5
Pb	10	10	15	10	10	10
Cr	50	50	100	50	50	50
Cu	2000	2000	1300	9	1000	1000
Ni	70	20	-	25	-	20

I.2.1.Mercury – an important contaminant

The contamination of the environment by the presence of mercury is a worldwide concern because this metal is toxic for all organisms and ecosystems, influencing their reproduction, growth and behavior (Wang et al., 2012). Moreover, once released in the atmosphere it can persist for months and be transported thousands of kilometers until being again deposited on the earth surface (Schroeder, 1998; Selin, 2009; Wang et al., 2012).

The utilization of mercury has been reported in history since 1600 BC. when it was used for religious ceremonies, decoration and cosmetics by the Egyptians. In 500 BC. it started to be used in gold mining extractions and since then this metal has been included in many activities (Paasivirta, 1991; Pereira, 1996). However, its toxic effects only began to receive proper attention in the 1950s, when the first occurrences of the biggest disaster involving the population and the release of mercury, known as "Minamata Disease", appeared. Installed in Japan, the Nippon Nitrogen Fertilizer company used mercury as a catalyst in the production of acetic acid and its derivatives and released mercury into the factory effluents. At that time little was known about mercury toxicity and all the effluents were dumped directly into the Minamata bay. Consequently, high fish mortality, population neurological disorders and deaths were reported related to ingestion of contaminated fish or seafood from Minamata. In 1977, the process of depollution was initiated by dragging sediments from the bottom of the bay and only ended in 1991. Mercury concentrations higher than 25 mg kg^{-1} were found in the contaminated sludge (Harada, 1995; Selin, 2009)

Currently, the northern region of Brazil is severely affected by mercury contamination from legal and illegal gold mining activities. During the exploration of gold, mercury is used to bind tiny gold particles, forming amalgams and separating it from sediments. The amalgams are then burned, the mercury is released as steam to atmosphere and all the gold present is recovered. Aggravating this situation is the fact that the main mining areas are near large rivers such as Amazonas and Madeira,

spreading this contaminant over many kilometers away and affecting the entire riverside population (Drasch et al., 2004). This problematic situation has led the ratification the of Minamata Convention in Brazil in 2018 in order to determine sustainable ways to reduce Hg emissions and promote safer alternatives to substitute its use ("Brasil promulga Convenção de Minamata sobre Mercúrio | WWF Brasil," 2018).

Mercury is a silver-white transition metal, liquid at room temperature, poorly soluble in water and the most volatile of metals (Wang et al., 2012). Its atomic mass is 200.6 and it has a boiling point of 396 ℃ and a melting point of -39 ℃. This metal can exist in three oxidation states 0, +1 and +2, (but the state +1 is very rare) and occurs naturally as six main isotopes (masses ordered in order of abundance) 202 > 200 > 199 > 201 > 198 > 204 (Drasch et al., 2004). Mercury is environmentally found as elemental form, or in organic or inorganic compounds (Schroeder, 1998). The most toxic form of mercury is the methyl mercury (MeHg) species, which are obtained through the conversion of inorganic mercury by metabolic processes of the living organisms. The high stability of MeHg allows its accumulation and magnification up to millionfold along the food chain (Schroeder, 1998). Its estimated half-life of Hg in the environment can be 58 days for elemental mercury, 70–80 days for MeHg and up to 30– 60 days for inorganic forms (De et al., 2014; Holmes et al., 2009).

Natural and anthropogenic activities are responsible for the release of mercury into the aquatic systems. Natural sources include weathering of rocks, volcanic events and geothermal activity (Nriagu and Becker, 2003; Wang et al., 2012). Anthropogenic activities include metal finishing, welding, production of batteries, fluorescent lamps and electronic devices, alloy manufacturing plants, chloralkali and pulp and paper industries, petroleum refining, coal combustion and waste incineration (Costley et al., 2000; Inglezakis et al., 2002).

Most of the virgin Hg comes from the mining of Cinnabar (HgS) but the liquid mercury (Hg^0) can also be found. The largest mines of Hg extraction were located in the European Union (Almadén, Spain), USSR and China, however most of mining extraction of Hg has been ceased. Since 2008 the European Union has banned the exportation of Hg

and in 2017 imposed restrictions to its importation (European Parliament, 2017). In the same line, the USA was the first country to sign the Minamata convention in 2013 to reduce Hg pollution and end mercury mining ("Mercury - United States Department of State," 2019)).

The primary route of mercury for humans is by food ingestion, mainly by fish consumption (Pickhardt et al., 2006). Once fishes are exposed to contaminated waterborne, Hg is rapidly accumulated in their tissues and most of it is methylated and transmitted by dietary route. Additionally, direct bioaccumulation from water may occur simultaneously. In fishes, about 80-90 % of methyl mercury is uptake from food and the remained from water, while for inorganic Hg, the dietary ingestion can represent 32-92 % (Bradley et al., 2017; Hrenchuk et al., 2012; Pickhardt et al., 2006; R. Wang et al., 2010).

All these forms of mercury, elemental, inorganic or organic, undergo interconversion inside the organism. The major problem occurs when the transformation to the organic forms (MeHg) is more often than the reverse reactions (De et al., 2014).

Mercury presents high affinity to sulfhydryl groups of amino acids such as cysteine and methionine, interfering in the enzymatic activity and cellular membrane properties which explains its high toxicity (Drasch et al., 2004; Pereira, 1996). Methyl mercury can cross the membrane that protects the brain from toxins and penetrate the blood-brain causing diverse neurodegenerative illnesses, such as Amyotrophic lateral sclerosis, Alzheimer's and Parkinson's diseases (Wang et al., 2012). The same can occur in the placenta, affecting the growth and formation of the fetus. Other health impacts reported are disfunction on renal, cardiovascular, immune and nervous systems (Wang et al., 2012).

In water systems Hg(II) can exist as metal ions, bound to organic or inorganic ligands and its distribution depends on the chemical parameters of the water such as pH, salinity, temperature, etc. (Raspor, 2004). In seawater Hg(II) is mostly present in inorganic forms of chloro-complexes, such as $HgCl_4^{-2}$ and $HgCl_3^-$, $HgCl_2$ or $HgCl^+$ or bound to humid acids while in fresh waters, the main forms are the organometallic methylated

compounds or inorganic complexes with, carbonates, sulphur and chlorine among others (Stumm and Morgan, 1996).

I.2.2.Other non-essential toxic elements

Cadmium (Cd), lead (Pb), chromium (Cr), copper (Cu) and nickel (Ni), together with mercury, are regarded as the most concerning metals due to their significant threats to the environment and human health and their high occurrence in the aquatic systems. The presence of these metals in waters is controlled by atmospheric precipitation and the weathering processes on soil and bedrocks, which have been modified by humans and industrialization, increasing their flux and distribution in waters resources (Stumm and Morgan, 1996).

Cadmium has been largely used for batteries, pigments, plastic stabilizers and fertilizers production (Yu, 2001), lead has been applied in various sectors of the materials industry, such as production of glass, paints, building materials, pipes and the armaments industry (Yu, 2001), chromium is present in metallurgical and refractory industries to impart corrosion resistance (Stoecker, 2004), copper is mainly applied as conductor of heat and electricity (Momc, 2004) and nickel is used to constitute many metal alloys (Caledonia, 2004)

Besides the above mentioned toxic metals, rare earth elements (REEs), such as europium (Eu), neodymium (Nd), dysprosium (Dy), gadolinium (Gd), lanthanum (La), terbium (Tb), cerium (Ce), praseodymium (Pr) and yttrium (Y) are recently becoming issues for the water bodies. These elements are largely used to produce many technology devices, such as monitors, phones, computers, lamps, etc. and are indiscriminately disposed into environment with the industrial effluents. In addition, unlike toxic metals, these elements have no regulatory guidelines for their maximum allowable concentrations in discharges or drinking water (Goering, 2004).

Other contamination sources of the aquatic systems include the release of effluents containing pharmaceutical products, plastics, synthetic materials, and organic

compounds due to the absence of strong regulations. The occurrence of these contaminants in the environment impacts the consuming water quality, biota and ecosystems. However , their consequences may be attenuated by degradation of these pollutants in non-toxic or less toxic substances.

I.3. Analytical techniques and quality control of the results

I.3.1.Mercury quantification

In the last three decades the quantification techniques of cold vapour atomic absorption spectroscopy (CV-AAS) and cold vapour atomic fluorescence spectroscopy (CV-AFS) have been largely used because of their simplicity and sensibility, allowing determination of Hg in the range of 0.01-1 μg kg^{-1} (CV-AAS) and 0.001-0.01 μg kg^{-1} (CV-AFS) (Drasch et al., 2004). Other methods used are neutron activation analysis (NAA), inductively coupled plasma mass spectrometry (ICP-MS), inductively coupled plasma atomic emission spectrometry (ICP-AES) and gas and liquid chromatography, coupled with various detectors. The detection limits of those methods are summarized in Table I.2 (Drasch et al., 2004). The choice of the right technique is directly related with the type of Hg sample (water matrix and Hg concentration levels) and it is a determinant factor to ensure the quality of results.

Table I.2. Mercury quantification and the detection limits of several methods (adapted from Drasch et al. (2004)).

Method	Detection limits (μg kg^{-1})
Cold vapour atomic absorption spectroscopy (CV-AAS)	0.01-1.00
Cold vapour atomic fluorescence spectroscopy (CV-AFS)	0.001-0.010
Neutron activation analysis in instrumental mode (INAA)	1.0-10.0
Neutron activation analysis in radiochemical mode (RNAA)	0.01-1.00
Gas chromatography (GC) coupled with electron capture detector	0.01-0.05
Gas chromatography (GC) coupled with atomic emission detector	0.05

Gas chromatography (GC) coupled with mass spectrometer	0.1
High-performance liquid chromatography (HPLC) UV	1.0
High-performance liquid chromatography (HPLC) CVAAS	0.5
High-performance liquid chromatography (HPLC) CVAFS	0.08
High-performance liquid chromatography (HPLC) coupled with electrochemical detectors	0.1-1.0
Inductively coupled plasma mass spectrometry (ICP-MS)	0.01
Inductively coupled plasma atomic emission spectrometry (ICP-AES)	2.0

I.3.1.1. Cold vapour atomic fluorescence spectroscopy

Cold vapour atomic fluorescence spectroscopy (CV-AFS) is used for quantification of volatile metals with high vapour pressure in order to allow its vapour measurement at room temperature, dispensing the use of external sources to promote the vaporization of the sample. The technique is based on the atomic fluorescence radiation emitted when excited atoms return to ground electronic state. The excitation is promoted by an ultraviolet radiation and the frequency of the radiation emitted by the sample is measured and compared with the incident frequency. The absorption and the subsequent atomic emission occur at specific wavelengths characteristic of the atomic species present (Sanchez-rodas, 2010). According to the frequencies emitted the fluorescence can be classified as resonance (when incident and emitted frequencies are equal) or non-resonance (when incident and emitted frequencies are different) (Atkins and Paula, 2006).

The analytical procedure is simplified in Figure I.2. For quantification, Hg samples, the reducing solution and ultrapure water must be, at the same time, pumped from the storage flasks by peristaltic pumps with adjustable flow rates into the mixing cell. The reducing agent normally used is $SnCl_2$ 2 % (w/v), prepared with tin(II) and hydrochloric

acid 10 % (v/v). When in contact with the Hg solution, vapour of Hg is produced by the reduction reaction bellow:

$$Hg^{2+} + Sn^{2+} \rightarrow Hg^{0} + Sn^{4+} \quad \text{(I.1)}$$

Afterwards, a mixture containing elemental Hg goes out of the mixing cell and enters in the gas-liquid separation cell. This cell receives continuously injection of argon, which is the carrier gas and promotes the separation of vapour of Hg from the other components. The vapour stream is then conducted through a drying membrane with air K to remove some water vapour remained with the flow. After drying, the vapour of Hg finally reaches the AFS detector and is quantified.

It is important to mention that this method is used to determine total inorganic mercury, and so it is mandatory that all mercury compounds from the samples are converted in forms of Hg(II).

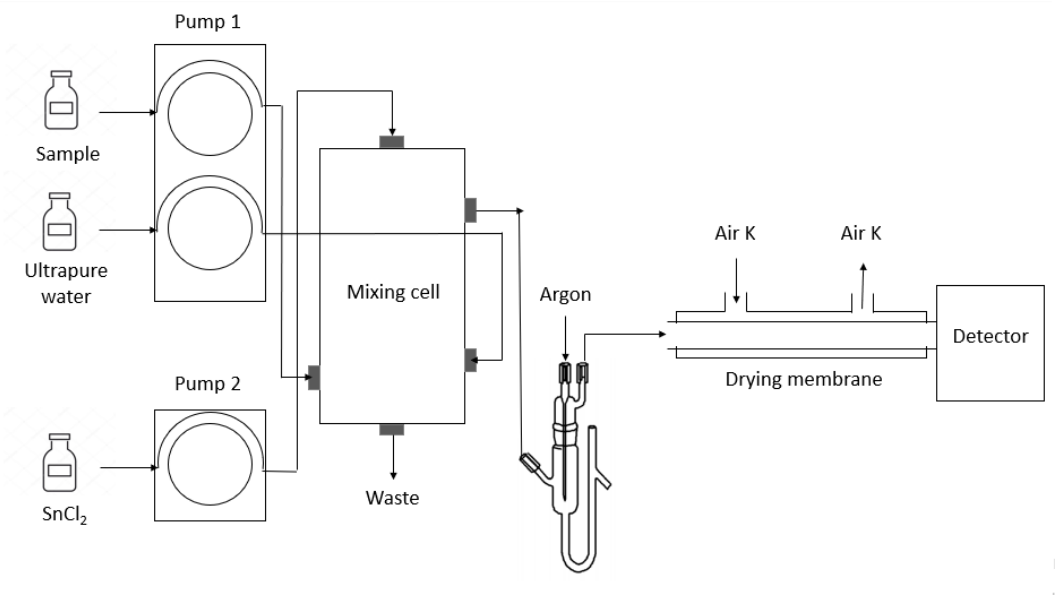

Figure I.2. Schematic representation of a CV-AFS for mercury quantification (adapted from Sanchez-rodas (2010)

In the detector (Figure I.3.), a radiation is emitted perpendicularly to the sample in order to avoid interferences and another argon flow rate is provided to keep the sample as uniform as possible. The intensity read by the detector is proportional to the concentration of analyte in the sample and it is reported as a signal converted to concentration by calibration curves.

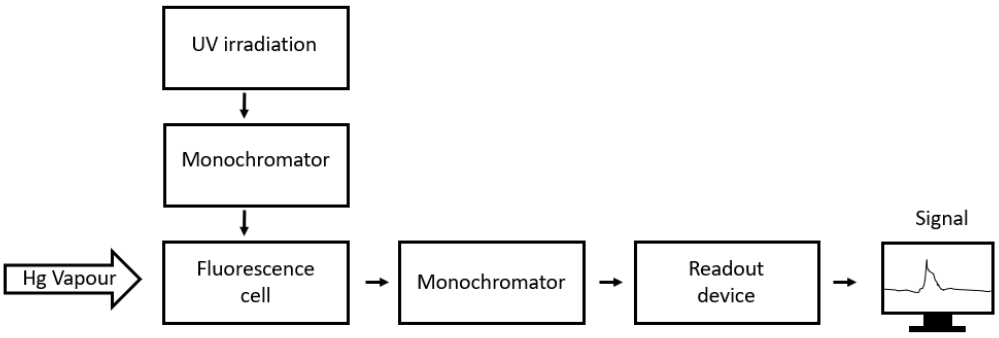

Figure I.3. Scheme of the detector of CV-AFS.

The calibration curves for the determination of Hg(II) concentration are prepared by diluting a stock commercial solution of Hg in nitric acid 2 % (v/v) for the desired concentrations (minimum of 5 standards is recommended). Each standard should be read at least in duplicate per each curve and standards should be read between samples to ensure the quality of the measurements. For quantification of the Hg(II) samples, at least three measures should be performed and blank solutions must be analyzed between samples.

The quality control of the results is performed by evaluation of detection limits and precision as well as the implementation and monitorization of control solutions.

The limit of detection (LoD, μg dm^{-3}) is calculated from the calibration curves because in this method the blank solution did not differ the baseline. The LoD equation is represented as follows:

$$LoD = b + 3\sqrt{\frac{\sum(y_i - \hat{y}_i)^2}{n-2}} \qquad \text{(I.2)}$$

where b is the intercept of the linear equation, n is the number of standards and $y_i$and $\widehat{y_i}$ are the experimental and calculated values, respectively. The values of LoD vary from curve to curve, depending on the sensitivity of the equipment.

The precision of the measures can be determined by the coefficient of variation (CV, %) between analyses of replicates, calculated by the ratio standard deviation/ average of the signals obtained for the samples.

The use of control solutions allows to determine possible experimental losses of the process, *e.g*. by volatilization or adsorption on the vessels. They contain only the contaminated solution (without sorbent), with all the experimental conditions exactly equal the assays, and are run in parallel with the experiments.

I.3.2. Other elements quantification

Other elements such as Cd, Pb, Cr, Cu, Ni, Eu, Nd, Dy, Gd, La, Tb, Ce, Pr and Y can be quantified by inductively coupled plasma atomic emission spectrometry (ICP-AES). This spectrometric technique has become one of the most used and allows to analyse simultaneously different elements (Smith and Nordberg, 2015). The plasma generated by a stream of argon has very high temperature which will dry and atomize the analytes. This high energy of the plasma is important to break the molecular bonds and guarantee the excitation and atomization of the elements. When the excited atoms return to the ground state, they emit electromagnetic radiation that will be detected by chances in the wavelengths and converted in concentration using a calibration curve, similar to the procedure for Hg quantification (Smith and Nordberg, 2015).

The average limit of detection of this method for all the elements was 10 µg dm^{-3} and the coefficients of variation (CV) of the results between replicates were lower than 10 %.

I.4. Processes related to removal of contaminants from water

A wide variety of conventional and modern methods have been applied in recent decades to separate contaminants from wastewaters and effluents. Chemical

precipitation, electrochemical treatments, membrane separation, and sorption processes such as ion exchange and adsorption with activated carbon are among the most studied and applied methods so far (Lopes et al., 2012). However, new technologies using biological materials, such as biosorption and bioaccumulation have attracted much attention and are promising alternatives in the scope of circular economy and sustainability (Chojnacka, 2010). A brief description of the mentioned methods is given below:

I.4.1.Chemical Precipitation

Chemical precipitation is largely used for the removal of metals from wastewater because of its simplicity, efficiency and inexpensive cost for the treatment of large volumes of contaminated waters (Álvarez-Ayuso and García-Sánchez, 2007). By the addition of chemicals into solution, metals can form insoluble compounds which deposit as precipitates. The solid precipitated formed may be further separated by sedimentation or filtration. Reagents used in this process usually include hydroxides or sulphides (Fu and Wang, 2011).

The disadvantages associated with its use are the generation of large amount of contaminated sludge and the fact that the final concentrations achieved rarely comply the limits for discharge imposed by regulations, therefore, this process is more commonly applied as a pre-treatment step (Álvarez-Ayuso and García-Sánchez, 2007).

I.4.2.Electrochemical techniques

This process involves the reduction and electrodeposition of metal ions on a charged surface and allows recover metals in their elemental state with high purity (Wang et al., 2012). Electrochemical techniques do not require the use of chemicals and allows to treat waters containing high metal concentrations with considerable selectivity and great efficiency (O'Connell et al., 2008).

The application of these technologies involves a large capital investment and a high energy cost for their maintenance and therefore these treatments were not widely used in the past. However, because of the stricter regulations limiting the discharge of

wastewater these techniques have gained its importance and have become more applied (Wang et al., 2012).

I.4.3.Membrane filtration

Membrane filtration techniques are, basically, processes where the water passes through a semipermeable membrane. They are especially attractive for water treatment since they are easily operable, require little space and may be highly efficient and selective to the metal of interest (O'Connell et al., 2008). Nevertheless, as well as with the electrochemical techniques the high installation and operating costs limit their use in water treatments and other disadvantages may include the low flow rates of the solution across the membrane and its fouling (O'Connell et al., 2008).

The main membrane processes for metal removal are ultrafiltration, nanofiltration, reverse osmosis and electrodialysis, which differ basically by the pressure gradient or electric potential (in the case of electrodialysis) and by the size of the particles retained (Fu and Wang, 2011).

The low-pressure processes of reverse osmosis (RO) makes the treatment of higher fluxes of solution possible and can operate over different temperature and pH. The RO processes are attractive alternatives for contaminated waters treatment and have been applied in several fields, such as chemical, textile, petrochemical, electrochemical, pulp and paper, and food industries as well as for the treatment of municipal wastewaters (Madaeni and Mansourpanah, 2003).

I.4.4.Sorption processes

Sorption processes are mass transport separations which involve selective transfer of a component from a fluid phase to the surface and/or into a solid or liquid and include absorption, adsorption and ion exchange (Seader and Henley, 1998). Absorption is a process of incorporating a component from one phase to another, while adsorption and ion exchange are surface processes in which certain components are accumulated on the

surface of a solid suspended in a flask or packed in columns (Seader and Henley, 1998). The substance being sorbed is termed sorbate and the solid is termed sorbent (De Gisi et al., 2016). Figure I.4. summarizes the main terms used in sorption processes.

Concerning the applicability for water remediation, the sorption processes of more interess are adsorption and ion exchange. They have been extensively studied and applied in industry because of their selectivity to the target pollutant, ease of implementation and operation, efficiency and the most important, unlike most of the conventional methods, they are able to produce high-quality treated effluents and cumply with the standards imposed by water regulations (Bhatnagar et al., 2015; De Gisi et al., 2016; Fu and Wang, 2011; Hashim et al., 2011; Saunders et al., 2012).

The main types of sorption are classified as follows (De Gisi et al., 2016; Park et al., 2010):

(i) Physical sorption or physical adsorption is a reversible process in which the molecules are sorbed by intermolecular attractions and involves weak forces such as Van der Walls;

(ii) Chemical sorption or chemisorption is the sorption that occurs by the sharing of electrons between the specific surface sites and the solute. Chemisorption presents stronger bonds and the energy involved is higher than the energy of physical sorption;

(iii) Ion exchange is the separation process governed by coulombic forces between ions and charged functional groups with the exchange of ions in solution and the exchangable ions on the solid surface.

All the processes above mentioned can occur simultaneously or alternatively. The understanding of the sorption mechanism as well as the potential application of the sorbents depends on the properties of the sorbate and sorbent. The sorbent characteristics include chemical composition, functional groups, surface area, porosity and surface morphology (Tran et al., 2015). While the most relevant sorbate properties in the case of metal removal are hydrated ionic radii (Nguyen et al., 2013) eletronegativity and metal speciation (Carro et al., 2010). However, the sorption may be influenced by

several other factors, such as the number and accessibility of the active sorption sites, their chemical state and affinity between the sites and the sorbate (Igwe et al., 2008).

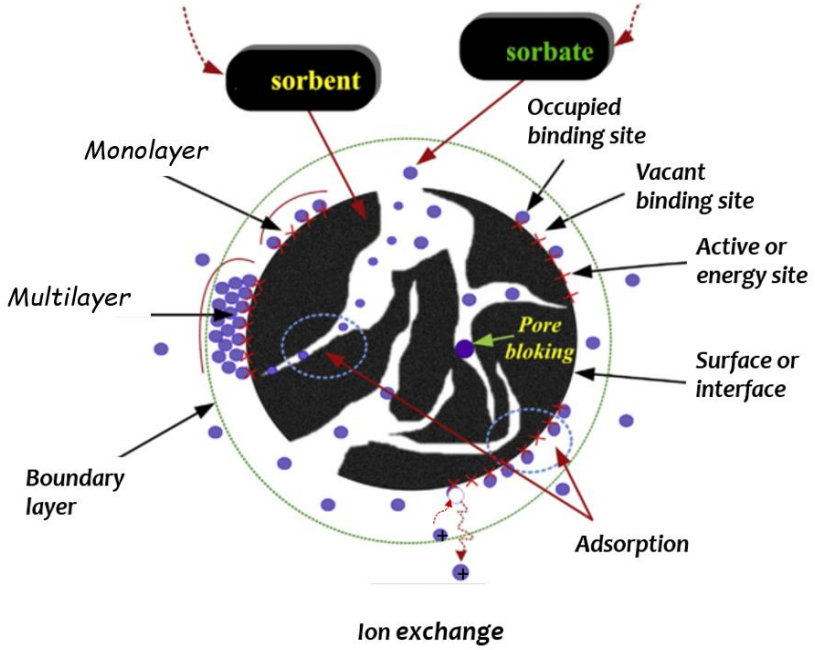

Figure I.4. Examples of terminologies of sorption processes (adapted from Tran et al. (2017)).

I.4.4.1. Adsorption with activated carbon

Activated carbon (AC) is the most adopted adsorbent to remove organic and inorganic contaminants. Its wide application is acribed to the large volume of micropores and mesopores, providing large surface areas and more active sites for the removal (Fu and Wang, 2011). However, this sorbent is moderately expensive and the ratio AC/metal demanded for proper water treatment is significantly high which limits its use (De et al., 2013). In this sense, the research for new materials, less costly, regenerable and equaly or more efficient to substitute the ACs plays an urgent need for water treatment technologies.

I.4.4.2. Ion exchange

Ion exchange is a process where positive or negative charges in solution are stoichiometrically replaced by ions of the same charge contained in a solid named ion exchanger (Seader and Henley, 1998).

An ion exchanger (see Figure I.5) is a solid formed by an insoluble polymeric or mineral matrix which carries immobile, and permanently bound ions. This surplus charge of the framework is balanced by mobile counter-ions with opposite sign which can be exchanged for a equivalent amount of other ions with the same charge from electrolytic solution. The ion exchangers may be called cation exchangers if the counter-ions are cations, anion exchangers if the counter-ions are anions or amphoteric ion exchanger if they carry both, cations and anions (Helfferich, 1962; Seader and Henley, 1998).

Ion exchange is normally (with very rare exceptions) a reversible process in which the counter-ions in the solid (B) and in solution (A) will exchange until reach the equilibrium as represented in the following equation:

$$z_A\overline{B^{z_B}} + z_B A^{z_A} \leftrightarrow z_B\overline{A^{z_A}} + z_A B^{z_B} \qquad \text{(I.3)}$$

where z_A and z_B are the cations valences, the bar above "A" and "B" represents the cations in the solid and its absence represents the cations in solution.

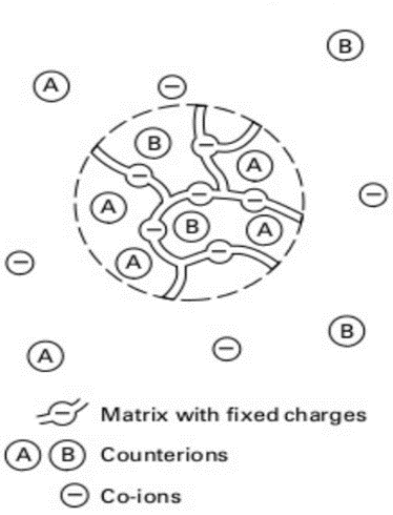

Figure I.5. Representation of an ion exchanger (Seader and Henley, 1998).

The first application of ion exchange in water treatment was in water-softening, by removing ions like Ca from the solution. A natural zeolite was iniatially applied but since

1935 diverse synthetic resins ion exchangers have been produced and they are largely employed to this day (Seader and Henley, 1998). The most commonly found cationic resins contain sulfonic or carboxylic acid functional groups, wherein the hydrogen present in these groups will be exchanged with the metals in solution (Fu and Wang, 2011).

Different ion exchangers resins have been applied for metal removal in water treatment, as may cite, Amberlite IR-120 and Dowex 2-X4 which were investigated for Zn(II), Cr(III) and Cr(VI) sorption (Idrisb et al., 1996) and IRN77 and SKN1 applied for Cr(III) elimination (Rengaraj et al., 2001).

The efficiency of the ion exchange is conditionated on the ability of the solid as exchanger, defined by its ion exchange capacity, which is the magnitude of the counter-ions content in the material. This parameter represents the amount of exchangable ions and it is independent of its nature (Helfferich, 1962). A great advantage of using ion exchangers is that they are easily regenerated by applying the reverse process, with a solution containing excess of the previous counter-ions of the ion exchanger. This allows the reuse of the solids and reduces significantly the operating costs making this method much more attractive than the conventional techniques (Helfferich, 1962).

Zeolites, natural and synthetic, have been increasingly used in ion exchange processes due to their abundance, low-cost and great ion exchange capacities (Czarna et al., 2018). Recently, researchers have synthetized zeolite-type materials displaying improved properties like higher capacities, faster kinetics and more selectivity to the target toxic metal for application in sorption processes. Microporous materias like titanium silicates (ETS-4, ETS-10, AM-2) and zirconium silicates (AV-13) are examples of good zeolite-type ion exchangers applied for Hg(II) removal from aqueous solutions (Cardoso et al., 2013; Lopes et al., 2007, 2008, 2009).

I.4.4.3. Biosorption

Biosorption is defined as a sorption process in which the sorbent is from biological orign, then called biosorbent. The advantages of the biosorption processes are low-operational costs, low environmental impacts and possibility of biosorbent regeneration

and/or recovery of metal. Moreover, in the case of using wastes or by-products as biosorbents this process aditionally may eliminate some disposal costs of these residues (Nguyen et al., 2013).

Normally, a sorbent can be classified as low-cost if it needs little or no processing, and it is largely available in nature, or is a waste or industrial by-product (Farooq et al., 2010). Biosorbents are living or dead materials obtained from different sources, including lignocellulosic materials, algae, chitin/chitosan, bacteria, fungae, and etc. (Farooq et al., 2010; Tran et al., 2015).

It has been documented that several functional groups are present on the biosorbents cell walls, such as carboxyl, hidroxyl, amines, amides, sulphydryl, alcohols and ester. These functional groups can interact with the metals in solution in several ways, for instance, by substituting hydrogen ions for metal ions or donating an electron pair to form complexes with metals (Farooq et al., 2010). These attractive features make the biosorbents excellent options for metal removal and their performances can be comparable and even better than the commercial sorbents (Huang and Lin, 2015; Singh Ahluwalia and Goyal, 2007). In the case of mercury, the use o biosorbents may enhance its removal due to its strong afinity with sulphur-groups present on the biosorbents surfaces. Such afinity is explained by the high values of stability constants for the formation of complexes between Hg and surphur-groups (Stumm and Morgan, 1996).

Several works have reported the use of biosorbents for mercury removal. In fact, colleting data from the Web of Science database from 2008 to 2018 it was possible to find 92 papers containing the keywords “mercury removal”, “biosorbent” and/or “sorption”. Evaluating the selected articles in greater detail, some of them presented more than one biosorbent or more than one system being tested (single or multi-elemental contamination and batch or column operation) and they were considered as different works for further discussion. So, in total, the works equaled 210 studies.

Figure I.6 illustrates the distribution of these studies for the types of systems. 87 % of the studies were performed under batch conditions and only 13 % were done in column configuration. Batch conditions with single element removal were the most

frequent works developed in this topic (124 studies or 59 %). Even more, considering the type of water matrix, the simple waters such as deionized and distilled waters were used in 37 % and 23 % of the total works, respectively and not available information (N.a.) represented 23 % of the total. Complex matrices include mainly natural waters, seawater, real effluents and river waters and they were present in only 16 % of the works and, going deeper, only 8 % of these studies have tested Hg(II) eliminations with initial concentration lower than 500 µg dm^{-3}.

Despite all the research done so far it is clear that several gaps still exist and more realistic environmental conditions should be studied in order to improve the effective implementation of the biosorbents in water treatment processes. Afroze and Sen (2018) suggest the use of the biosorbents for multi-elemental removal and a real industrial scale application. Salman et al. (2015) completes that, by stating that mono-elemental systems are important but they are not enough to quantify the true capacities for metal removal under competitive effect in natural or residual waters.

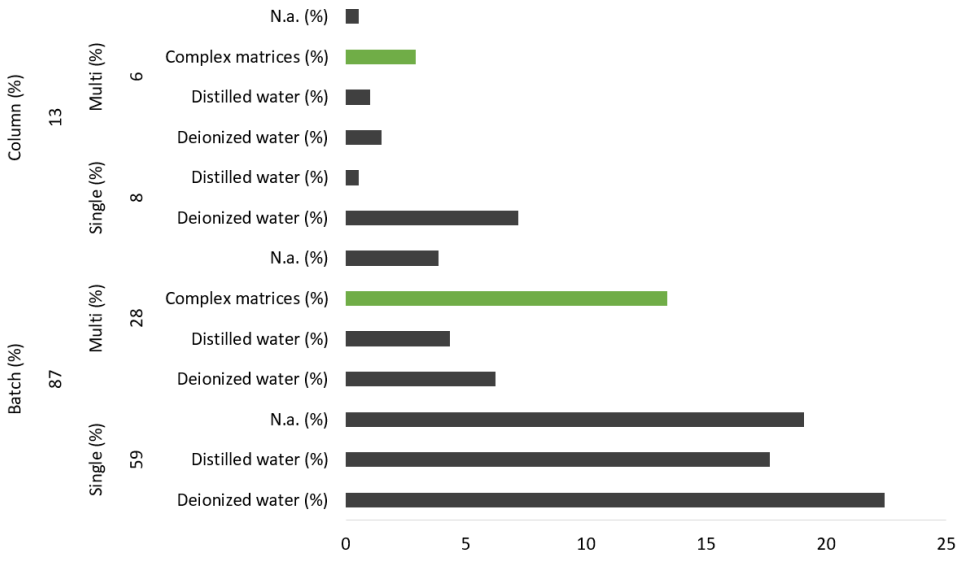

Figure I.6. Record of the number of publications on Web of Science database from 2008 to 2018 for mercury removal separated by the types os systems studied. (Source: Web of Science, searched April 10, 2019).

I.4.5. Bioaccumulation of contaminants

Bioaccumulation is defined as a process that uses living biosorbents for elements uptake from aqueous solutions. This process can be simplified in two stages (Figure I.7): the first one involves the fast uptake of the target element through metabolically passive mass transport by physical-chemical means, similar to biosorption, while the second stage is the slower intracellular accumulation which depends on the metabolic activities (Chojnacka, 2010; Veglio and Beolchini, 1997).

The organisms may interact with the sorbates (i) by promoting their active transport across the cells membranes, and (ii) by releasing sulfides or phosphates ions to the solution, as a defense strategy, which will complex with the metal ions. Beyond that, some living organisms, like algae, use CO_2 as a source of carbon for growth processes. However, the culture medium is composed by bicarbonates and they need to convert them by the reaction $HCO_3^- \rightarrow CO_2 + OH^-$ to properly functioning. Such reaction provides an excess of OH^- in the medium that may bind metals in solution and precipitate as insoluble hydroxydes (Chojnacka, 2010; Stumm and Morgan, 1996).

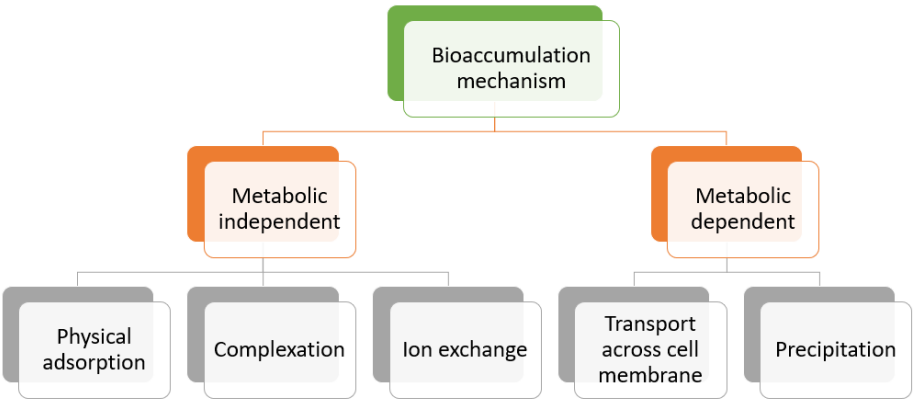

Figure I.7. Bioaccumulation mechanisms according to the dependence and independency of metabolic activity of the biosorbent (adapted from Veglio and Beolchini (1997)).

The transport of metals into the cells are mainly performed by carrier proteins that complex with the metals in the solid surface. The natural processes of nutrient uptake are not very specific for the target elements and thus, when metals are present in solution , due to competition they can replace the nutrients, be transported instead of them and get access to the inside of the cells. In the cells, these metals can participate in the biochemical processes or be transformed in biological inactive forms by complexation with proteins rich in thiol groups, like metallothionenins, released by the detoxication defense mechanisms of the cells (Stumm and Morgan, 1996).

Bioaccumulation differs from biosorption mainly because bioaccumulation is a non-equilibrium process. When metal sorbed on the biosorbent surface crosses the membranes into the cells it makes available previously occupied active sites, constantly providing new sorption sites and, hence, equilibrium state is never reached (Chojnacka, 2010; Ishii et al., 2006; Stumm and Morgan, 1996). Besides that, bioaccumulation dismisses the biosorbent separation step, frequently necessary on biosorption because the solids are mostly used as powder, and that may represents adittional costs on the process application (Chojnacka, 2010; Henriques et al., 2017). Other steps of biomass drying, milling and storage can be eliminated in bioaccumulation (Chojnacka, 2010).

The most important limiting factors of bioaccumulation are related with the resistance of the organisms to the contaminated solutions and the supply of nutrient and energy for their growth. Organisms like yeasts and molds have been extensivelly used for metals bioaccumulation. Other biosorbents applied include bacteria species like *Pseudomonas*, *Enterobacter*, *Bacillus*, and *Micrococcus*, and red, brown or green algae (Ayangbenro and Babalola, 2017). If the conditions are favorable, the organisms can grow at high rates and it is possible to construct a self-replenishing system, where the biosorbents are cultivated in the presence of contaminants (Aksu and Dönmez, 2005; Chojnacka, 2010).

I.5. Variables influencing mercury sorption processes

The metals sorption can be influenced by different operation parameters, such as pH, initial metal concentration, temperature, sorbent dosage, coexistence of other ions, etc (Nguyen et al., 2013; Park et al., 2010). The performance of the biosorbent, and the feasibility and efficiency of the process will be determined by these variables. The effect of these parameters has been widely investigated and a short discussion of their impact on mercury removal is given below.

I.5.1.pH

The influence of the pH is one of the most important factors to evalute during the sorption of metals. The pH impacts the sorbent surface charge, the degree of ionization and speciation of metals, and the competition with coexisting ions in solution (Nguyen et al., 2013). Generally, the higher the pH, the greater the sorption of cations until an optimum value, which then decreases with further pH enhance (Park et al., 2010).

The electrical state of the sorbent surface is determined by the point zero charge (PZC), which is defined as the pH of the solution when the density charge of the solid surface is zero, *i.e.* it is independent of the ionic strenght of the medium. Bellow the PZC the surface has positive charge and above the PZC as the pH enhances the surface becomes increasingly negative (Nguyen et al., 2013; Tran et al., 2017). The charge accounted by PZC represents the net total charge of the solid, which are the external and internal charges of the sorbent surface (Tran et al., 2017). Additionally, in order to properly understand the chemistry of the interactions between mercury and the sorbent, the pK_a of the functional groups present on their surfaces, like carboxyl (pKa 1.7-4.7) and hidroxyl (9.5-13) also must be considered, since when pH > pK_a these functional groups will dissociate in anionic forms and then the cations uptake is favoured (Tran et al., 2017; Volesky, 2007).

Moreover, acid pH affects sorption by the competition between the coexisting ions in solution, H^+ and the Hg(II), while higher pH may promote the precipitation of mercury as hydroxides forms (Park et al., 2010).

The distribution and occurrence of the most important Hg(II) species (which are Hg^{2+}, $Hg(OH)^{+}$ and $Hg(OH)_2$) are conditioned by the pH of the solution and are normally represented in a speciation diagram built with the ionization factors ($\alpha_0, \alpha_1, \alpha_2$). Mercury is a soft Lewis acid and its hydrolysis reactions and values of K_α are (Devani et al., 2017; Lopes, 2009):

$$Hg^{2+}_{(aq.)} + 2H_2O_{(aq.)} \leftrightarrow Hg(OH)^{+}_{(aq.)} + H_3O^{+}_{(aq.)} \quad K_{\alpha 1} = 10^{-3.5} \tag{I.4}$$

$$Hg(OH)^{+}_{(aq.)} + 2H_2O_{(aq.)} \leftrightarrow Hg(OH)_{2(aq.)} + H_3O^{+}_{(aq.)} \quad K_{\alpha 2} = 10^{-2.7} \tag{I.5}$$

The ionization factors are given by the following expressions:

$$\alpha_0 = \frac{[Hg^{2+}]}{[Hg^{2+}] + [Hg(OH)^{+}] + [Hg(OH)_2]} = \frac{[H_3O^{+}]^2}{[H_3O^{+}]^2 + K_{\alpha 1}[H_3O^{+}] + K_{\alpha 1}K_{\alpha 2}} \tag{I.6}$$

$$\alpha_1 = \frac{[Hg(OH)^{+}]}{[Hg^{2+}] + [Hg(OH)^{+}] + [Hg(OH)_2]} = \frac{K_{\alpha 1}[H_3O^{+}]}{[H_3O^{+}]^2 + K_{\alpha 1}[H_3O^{+}] + K_{\alpha 1}K_{\alpha 2}} \tag{I.7}$$

$$\alpha_2 = \frac{[Hg(OH)_2]}{[Hg^{2+}] + [Hg(OH)^{+}] + [Hg(OH)_2]} = \frac{K_{\alpha 1}K_{\alpha 2}}{[H_3O^{+}]^2 + K_{\alpha 1}[H_3O^{+}] + K_{\alpha 1}K_{\alpha 2}} \tag{I.8}$$

The dependence of pH on mercury uptake differs depending on the type or category of biosorbent due to the distinct distribution of functional groups on their surfaces (Nguyen et al., 2013). Consequently, the studies reported in literature have found different pH values for the best performances of the biosorbents for mercury removal. Despite the variations, many experiments using algae were better performed approximately in the range 4.5-8.0 (Carro et al., 2011; Esmaeili et al., 2015; Figueira et al., 2016; Henriques et al., 2017, 2015; Mokone et al., 2018; Plaza et al., 2011; Solisio et al., 2019; Vijayaraghavan and Joshi, 2012; Zaib et al., 2016; Zarei and Niad, 2017), chitin/chitosan assays were within the range of 3.0-7.0 (Allouche et al., 2014; Azari et al., 2017; Hou et al., 2018; Rae et al., 2009; Zhou et al., 2010), lignocellulosic biosorbents were better to remove Hg close to the neutral pH (5.0-7.5) (Al Rmalli et al., 2008; Boutsika

et al., 2014; Carro et al., 2010; Devani et al., 2017, 2015; Igwe et al., 2008; Krishnani et al., 2008; Lopes et al., 2014; Raza et al., 2015; Rocha et al., 2014; Saravanan et al., 2012; Singanan, 2015; Vinod et al., 2011), bacteria experiments were better in the range of pH 4.0-6.0 (Cain et al., 2008; Jafari and Cheraghi, 2014; Kinoshita et al., 2013; M. Kılıç et al., 2008; Mehmet Kılıç et al., 2008; Sulaymon et al., 2014; Wang and Sun, 2013; X. S. Wang et al., 2010) and the fungal group was very restrict being the best removals between pH 5.0 and 6.0 (Bayramoğlu and Arıca, 2008; Khambhaty et al., 2008; Martínez-Juárez et al., 2012; Nirmal Kumar et al., 2010; Sarı et al., 2012; Tuzen et al., 2009).

In the case of ion exchangers, besides the strong competition with H^+ ions in solution, low pH may also collapse the structure of the materials. For that reason, normally the optimum pH is close to neutral. Synthesized hierarchical ZSM-5 zeolite was tested for Hg(II) sorption under pH range of 3.0-10.0 and best performance was reported at pH 7.0 (Rostami et al., 2018). The effect of pH was evaluated for mercury ion exchange by ETS-4 and optimum pH was in the range 4.0-6.0 (Lopes et al., 2010). In another work, the greater sorption of Hg(II) by dithizone-immobilized natural zeolite was accomplished at pH 5.0 (Mudasir et al., 2016). More recently, the effect of pH on Hg(II) removal onto magnetic nanoparticle (AC@Fe_3 O_4 -NH_2 -COOH) was investigated in the range 2.0-11.0. From 2.0 to 7.0 the effect of this variable played an important role in the process and increased Hg(II) elimination, in contrast, above 7.0 the pH only increased mildly the removal efficiency (Pazouki et al., 2018)

I.5.2. Temperature

Temperature changes affect the diffusion and solubility of the metals in solution and can impact the capacity of the sorbents in different ways depending on the solid used (Arief et al., 2008; Nguyen et al., 2013). Normally the temperature study is performed within the range of 283-333 K and according to Sağ (Sağ, 2001), between 293 and 308 K it seems to have lesser impact in the sorption.

Important thermodynamic parameters, such as enthalpy ($\Delta H°$), entropy ($\Delta S°$), and Gibbs free energy ($\Delta G°$), can be determined by equations with equilibrium constants as a function of temperature. They provide valuable information about the endothermic or

exothermic nature of the sorption, the randomness and spontaneity of the process generally needed for practical applications (Arief et al., 2008).

Temperature alter the mercury sorption equilibrium depending on the type of process (Arief et al., 2008). Authors have reported the process as endothermic (Devani et al., 2017; Omorogie et al., 2012; Rajamohan et al., 2014; Raza et al., 2015; Singanan, 2015), exothermic (Johari et al., 2014; Lopes et al., 2010; Nirmal Kumar et al., 2010; Rakhshaee et al., 2009; Song et al., 2014; Tuzen et al., 2009; Vinod et al., 2011) or temperature independent (Khambhaty et al., 2008). However, considering the cost of application and operation of the sorption systems, the room temperature is the most commonly chosen (Nguyen et al., 2013).

High temperatures may damage the physical structure of the sorbents or destroy some binding active sites for sorption (Park et al., 2010). In this sense, usually synthetic materials have the advantage of being able to perform at higher temperatures than biological sorbents.

I.5.3. Sorbent dosage

Several studies have reported the effect of sorbent dosage (Bailey, S.E., Olin, T.J., Bricka, R.M., and Adrian, 1999; Caledonia, 2004; Lopes et al., 2009). They have found that the increase in the sorbent mass increases the number of active sorption sites to bind with mercury ions resulting in higher removal percentages. However, higher amounts of solid added in solution might result in some aggregation of the particles, restricting the access of the sorbate ions to some sorption sites available on the surfaces of biomasses. Regarding the uptake capacity of the solid, it decreases with higher masses of solid in solution, mainly due to the fact that some active sites remain free and unsaturated during the sorption processes (Vinod et al., 2011). The removal of Hg(II) improved from 71 % to almost 100 % when the mass of malt spent rootlet biochar was enhanced from 0.3 to 1 g dm^{-3} (Boutsika et al., 2014). A similar trend has been observed in the Hg(II) sorption by ETS-4, the higher the mass (from 0.6 to 16.2 mg dm^{-3}) the higher the removal (62-100 %) and the smaller was the Hg(II) concentration on the solid surface (from 108.0 to 6.1 mg g^{-1}) (Lopes et al., 2009). An increase in the mass of *Phoenix dactylifera* biomass from 0.5 to

3.0 g dm^{-3} led to an improvement on mercury uptake from 32 to 82 % and no relevant changes from 3 to 4 g dm^{-3} (Rajamohan et al., 2014).

I.5.4.Initial metal concentration

The initial concentration of metal in solution is an important factor in the sorption process. The driving force that promotes the mass transport of sorbate ions to the surface of the sorbent particles is the gradient of concentration between the mercury free sorbent and the initial mercury concentration in solution. The higher this difference, the higher (and normally faster) is the ions transport and higher removal performances are observed (Arief et al., 2008). However, such improvement occurs until the sorbent reach the saturation of the active sorption sites and further initial concentration enhances will not improve the Hg(II) uptake capacity (Arief et al., 2008). Aman et al. (2018) studied the effect of initial metal concentration on mercury removal by rose biomass. With constant pH, mass of sorbent and contact time, they noticed an increase of Hg(II) concentration on the solid from 1.40 mg g^{-1} with 10 mg dm^{-3} of Hg(II) initially in solution to 7.62 mg g^{-1} with initial Hg(II) concentration of 100 mg dm^{-3}. In the study of Hg(II) removal by *Zygnema fanicum* algae the amount of Hg(II) uptake per gram of sorbent increased when the Hg(II) initial concentration improved from 1.5 to 6.5 mg dm^{-3} and after that no relevant changes in the solid concentration were observed until Hg(II) initial concentration of 8 mg dm^{-3} pointing to the achievement of the sorbent capacity (Shams Khoramabadi et al., 2008). Similar behavior was reported by Nirmal Kumar et al. (2010) for mercury sorption by *Aspergillus niger*, with Hg(II) initial concentrations ranging to 20 to 200 mg dm^{-3} the biomass was able to capture more Hg from solution, but above this Hg(II) concentration the sorbent saturation was achieved.

I.5.5.Coexistence of other ions

Industrial effluents, real wastewaters, and aquatic systems generally contain several toxic metals or contaminants, without mentioning the presence of other metal ions like Na^{+}, K^{+}, Mg^{2+}, and Ca^{2+}. The presence of other ions affects the ionic strength of the solution and usually an increase in the presence of other cations may lead to a decrease on mercury elimination, attributed by the competition for the binding sites.

Usually sorption is more impacted by divalent ions, which have greater affinity for the active sites on sorbent surface and may compete more strongly than monovalent ions. The presence of anions in solution, for instance Cl^-, may decrease mercury sorption by the formation of stable complexes with this metal precluding or making difficult its removal (Liu et al., 2016).

In the work of Al Rmalli et al. (2008) the presence of the foreign ions Na^+, K^+, Mg^{2+}, Ca^{2+}, Cl^- or SO_4^{2-} had no relevant limitation on mercury removal by castor leaves (*Ricinus communis L*.). Similar results were found by Liu et al. (2016) for Hg(II) sorption onto cetylpyridinium bromide modified zeolite in a presence of competitive ions of Pb^{2+}, Zn^{2+}, Cd^{2+}, Cl^-, HCO_3^- and SO_4^{2-}. However, in the binary systems, the presence of Cr(II), Cu(II) and Cd(II) ions decreased the mercury sorption and Pb slightly increased Hg(II) sorption. Carro et al. (2010) evaluated the mercury elimination by fern in binary systems with Cd(II), Pb(II), Cu(II), Mg(II) and Ca(II) and only for high concentrations of Pb(II) (1036 mg dm^{-3}) and Cu(II) (318 mg dm^{-3}) the mercury removal percentages were altered and showed a decreases in the removal up to 15 %.

I.6. Kinetic and equilibrium modelling

Sorption is a separation process determined by the interaction between a sorbate in solution and a porous sorbent. The molecules of the sorbate face some “difficulties” to find their place in the interior of this porous medium. These adversities found are related with diffusional resistances toward the sorbate flow and will determine the kinetics of the process. How much the sorbate can be accumulated in the sorbent is defined as capacity of the sorbent and its understanding is domain of the equilibrium study (Do, 1998). Kinetics and equilibrium evaluation give information about speed of the process, affinities between sorbate and sorbent, the main mechanisms involved and the efficiency of the sorption, essentials for practical applications.

I.6.1.Kinetic models

Several kinetic models have been developed for sorption description and in general, they can be separated in two groups quite different in concept, namely, diffusion-based and reaction-based models (Qiu et al., 2009).

Diffusion-based models consider that sorption occurs following three steps: (i) diffusion of sorbate across the liquid film surrounding the sorbent; (ii) intraparticle diffusion in the liquid into the pores of the sorbent or along its pore walls; (iii) sorption/desorption itself on the active sites. Reaction-based models were derived assuming the whole process of sorption as a chemical reaction, instead of these three steps above mentioned (Qiu et al., 2009).

I.6.1.1. Diffusion-based models

When the sorption at sorbent surface is rapid, the transport of solute is controlling the overall rate of the process. In this case, the kinetics limiting step may be the transport across the liquid film, intraparticle diffusion or a combination of both. The film diffusion limitation is highly dependent of stirring and normally in systems well agitated (liquid film layer is very thin) this effect is eliminated or it controls the process only for the first few minutes (Ho et al., 2000).

Considering an uniform sorbent spherical particle and constant diffusivity (D_{eff}), the material balance combined with Fick's first law is given by (Helfferich, 1962):

$$\frac{\partial}{\partial t} q(t,r) = D_{\text{eff}} \left[\frac{\partial^2}{\partial r^2} q(t,r) + \frac{2}{r} \frac{\partial}{\partial r} q(t,r) \right] \tag{I.9}$$

where r is radial position. Assuming a perfectly stirred batch system of infinite volume (no film resistance), a solution for the average concentration in the particles is represented as (Boyd et al., 1947; Crank, 1975):

$$F(t) = \frac{q_{\text{A}}}{q_{\text{Ae}}} = 1 - \left(\frac{6}{\pi^2} \right) \sum_{n=1}^{\infty} \frac{1}{n^2} \exp\left(-n^2 B t\right) \tag{I.10}$$

where $B \equiv \pi^2 D_{\text{eff}}/R_{\text{p}}^2$ and R_{p} is particle radius. The simplified form of Eq. (I.10) for long times is known as Boyd's equation (Largitte and Pasquier, 2016). Reichenberg, (1953) managed this expression to obtain the following approximations (Largitte and Pasquier, 2016; Malash and El-Khaiary, 2010):

$$Bt = -0.4977 - \ln(1 - F(t)) \qquad \text{for } F(t) > 0.85, \tag{I.11a}$$

$$Bt = \left(\sqrt{\pi} - \sqrt{\pi - \left(\frac{\pi^2 F(t)}{3}\right)}\right)^2 \qquad \text{for } F(t) < 0.85, \tag{I.11b}$$

Another equation applied for sorption is the Webber's intraparticle diffusion model (Weber and Morris, 1963), expressed bellow:

$$q_{\text{A}} = k_{\text{i}} t^{0.5} + C \tag{I.12}$$

k_{i} is the intraparticle diffusion parameter (mg $g^{-1}h^{-0.5}$) and C (mg g^{-1}) is a constant related with the effect of limitation by film diffusion (Tran et al., 2017). According to Webber's model, if the intraparticle transport is the rate controlling step, C tends to zero and then the plot of *q versus* $t^{0.5}$ is a straight line with null intercept.

I.6.1.2. Reaction-based models

The most known reaction-based models applied to describe adsorption and ion exchange processes are the pseudo-first order, pseudo-second order and Elovich models (T. C. Ho et al., 2002; Ho et al., 2000; Largitte and Pasquier, 2016; Rocha et al., 2016).

The pseudo-first order model was proposed by Lagergren (1898) to describe the sorption kinetics of oxalic acid and malonic acid onto charcoal, and takes into account the follow assumptions: (i) sorption takes place on localized sites and there is no interactions between the species sorbed on the active sites; (ii) the energy of sorption is independent of the coverage of the surface; (iii) the capacity of the sorbent corresponds to the saturation of the monolayer; (iv) the concentration of sorbate in solution (M) is constant; (v) the sorption follows a kinetic of first order, given by the irreversible reaction

S+M→MS, where S represents the free active sites and MS the occupied sites (Largitte and Pasquier, 2016). Considering the concentration of solute on the sorbent at any time t (h^{-1}) as q (mg g^{-1}) and at equilibrium as q_e (mg g^{-1}), the sorption can be represented as a function of the distance to the equilibrium concentration:

$$\frac{dq}{dt} = k_1(q_e - q) \tag{I.13}$$

where k_1 (h^{-1}) is the rate constant of the model. After integration and application of the initial condition of clean particle at initial time ($t = 0$, $q_A = 0$) one becomes:

$$\ln(q_e - q) = \ln q_e - k_1 t \tag{I.14}$$

The pseudo-second order model (Ho and McKay, 1999), is based on the same hypotheses of the pseudo-first order model (i-iv) and only differs for the consideration of sorption as a second order rate equation: $2S + M \rightarrow MS_2$, which can be expressed in terms of solid concentration by:

$$\frac{dq}{dt} = k_2(q_e - q)^2 \tag{I.15}$$

where k_2 (g mg^{-1} h^{-1}) is the rate constant of the model. The integrated (for $t = 0$, $q_A = 0$) and linearized form is represented as:

$$\frac{t}{q} = \frac{1}{k_2\, q_e^2} + \frac{1}{q_e} t \tag{I.16}$$

The Elovich model was initially proposed by Roginsky and Zeldovich, (1934) for the adsorption of carbon monoxide onto manganese dioxide. It assumes that (i) the solute is sorbed on specific sorption sites, (ii) there is interaction between the sorbed species, (iii) the metal concentration is constant in solution, (iv) the sorbate uptake is governed by a zero order rate equation, and (v) the energy of sorption increases linearly with the coverage of surface (Largitte and Pasquier, 2016). The Elovich is equation is given by:

$$\frac{dq_{\mathrm{A}}}{dt} = \alpha e^{-\beta q_{\mathrm{A}}} \tag{I.17}$$

where α is the initial sorption rate (mg g^{-1} h^{-1}) and β (g mg^{-1}) is the desorption constant of the model. After integration and assuming the simplification proposed by Chien and Clayton (1980), αβt >>1, the equation becomes:

$$q_{\mathrm{A}} = \frac{1}{\beta}\ln(\alpha\beta) + \frac{1}{\beta}\ln t \tag{I.18}$$

I.6.2. Equilibrium isotherms modelling

I.6.2.1. Langmuir isotherm

Langmuir isotherm is the most known and applied model in sorption processes. This theory is based on a monolayer sorption on an ideal sorbent surface. By ideal, it means that the energy is constant over the sorption sites, the distances between them are the same and each sorption site accommodates only one sorbate molecule. The solute is sorbed at definite sites and for that reason the sorption is called localized. Moreover, the heat released upon sorption is uniform and independently of the other active sites. Langmuir theory considers a continuous process where the molecules are constantly bombarding the surface and being desorbed at the same rate and the net rate of accumulation at equilibrium is equal to zero (Do, 1998; Langmuir, 1916). The Langmuir isotherm is represented by:

$$q_{\mathrm{e}} = \frac{q_{\mathrm{m,L}} K_{\mathrm{L}} C_{\mathrm{e}}}{1 + K_{\mathrm{L}} C_{\mathrm{e}}} \tag{I.19}$$

where $q_{\mathrm{m,L}}$ (mg g^{-1}) is the sorption capacity, related with monolayer coverage, and K_{L} (dm^3 mg^{-1}) is the Langmuir equilibrium constant or affinity constant between sorbate and the sorbent surface, the larger is this constant stronger are their affinity (Do, 1998).

I.6.2.2. Freundlich isotherm

This is the first empirical equation used to describe equilibrium data (Freundlich, 1906). This isotherm assumes that sorbent surface is heterogeneous and is formed by patches in which the sorption sites with the same energy are grouped (Do, 1998). These patches are different and independent and their energy distribution follow an exponential decay function (Do, 1998). Hence, some patches have sites with high energy that bind the sorbate molecules strongly and some are less energetic and interact weakly with the sorbed species. In fact, in some sites the energy of sorption is so strong that makes possible to form multilayers of coverage on the sorbent surface (Cooney, 1998; Lopes, 2009).

The equation of Freundlich is expressed by:

$$q_{\mathrm{e}} = K_{\mathrm{F}} C_{\mathrm{e}}^{1/n_{\mathrm{F}}} \tag{I.20}$$

here, K_{F} ($\mathrm{mg}^{1-1/n\mathrm{F}}\ \mathrm{dm}^{3/n\mathrm{F}}\ \mathrm{g}^{-1}$) and n_{F} are the Freundlich constants. The parameter n_{F} is related with the nonlinearity of the model and the higher is this value, more nonlinear is the behaviours of the isotherm (Do, 1998). Limitations of this model are that it does not proper recover at Henry's law at low concentrations as expected and it breaks down when concentrations are very high. However, it is valid in the narrow range of sorption conditions normally studied (Do, 1998).

I.6.2.3. Temkin isotherm

This equation was originally proposed to describe chemisorption of hydrogen on platinum electrodes in acid medium and considers a linear decrease of the heat of sorption, E_θ, with fractional coverage θ (Bourane et al., 2002; Do, 1998). As in the case of Freundlich isotherm, it does not exhibit a finite saturation limit (Do, 1998). It is mathematically given by:

$$q_{\mathrm{Ae}} = Bln(AC_{\mathrm{Ae}}) \tag{I.21}$$

where A (dm^3 mg^{-1}) is the isotherm equilibrium binding constant and $B = q_{\mathrm{m,T}}RT/\Delta E$ (mg g^{-1}) is the Temkin constant related with the heat of sorption, where ΔE (J mol^{-1}) represents the variation of the heats of sorption, $R = 8.314$ J mol^{-1} K^{-1} is the ideal gas constant, T (K) is the absolute temperature and $q_{\mathrm{m,T}}$ is the sorption capacity.

I.6.2.4. Dubinin- Radushkevich isotherm

The premise of this equation is that sorption occurs by pore volume filling mechanism instead of a layer-by-layer onto pore walls (Do, 1998). This equation was originally developed for adsorption based on the potential theory of Polanyi (Polanyi, 1914), relating the amount sorbed in equivalent liquid volume with the sorption potential. It assumes an energetic heterogeneity of the sorbent surface and it is largely applied for systems using activated carbon and zeolites (Dubinin, 1960; Inglezakis, 2007). The mathematical expression of this isotherm is given by:

$$q_{\mathrm{e}} = q_{\mathrm{m,DR}} e^{-B_{\mathrm{DR}}\,\varepsilon^2} \tag{I.22}$$

$$\varepsilon = RT\ln\left[1 + \frac{1}{\mathrm{C_e}}\right] \text{ and } E = \left[\frac{1}{\sqrt{2B_{\mathrm{DR}}}}\right] \tag{I.23}$$

$q_{\mathrm{m,DR}}$ (mg g^{-1}) is the solid capacity, B_{DR} (mol^2 J^{-2}) is the Dubinin-Radushkevich constant, ε (J mol^{-1}) is the Polanyi potential and E denotes the free energy change when 1 mol of solute is transferred to the surface of the solid. The magnitude of E values gives insights about the sorption mechanisms and may be used to distinguish physical and chemical sorption (Foo and Hameed, 2010).

I.6.2.5. Sips isotherm

This three parameters isotherm was proposed by Sips as a modified extension of Freundlich isotherm in such way that it has a finite limit under high concentrations. This isotherm is commonly named Langmuir-Freundlich because combines characteristics of

both models (Do, 1998). In its form, this equation differs Langmuir equation by the third parameter, n_S, added. When n_S is equal to 1 this isotherm becomes the Langmuir isotherm and the surface of the sorbent is assumed homogeneous. Hence, this parameter is associated with heterogeneity of the system (regarded to sorbate, sorbent or both) and the greater is n more heterogeneous is the system (Do, 1998). As Freundlich isotherm, this equation has the limitation of not behaving according to Henry's law at low concentrations (Do, 1998; Y. S. Ho et al., 2002). It is written as follows:

$$q_e = \frac{q_{m,S}(K_S C_e)^{1/n_S}}{1 + (K_S C_e)^{1/n_S}} \quad \text{(I.24)}$$

where $q_{m,S}$ (mg g^{-1}) is the capacity of the material, K_S(dm^3 mg^{-1})^{nS} is the affinity constant of the model, and n_S is the heterogeneity index.

I.6.2.6. Redlich-Peterson isotherm

This is a hybrid equation with characteristics of both Langmuir and Freundlich isotherms. For high concentrations it approaches Freundlich isotherm while for low concentrations is embodies Langmuir isotherm and the Henry's law is recovery (Y. S. Ho et al., 2002). It can be expressed as follows:

$$q_{Ae} = \frac{K_{RP} C_{Ae}}{1 + a_{RP} C_{Ae}^{n_{RP}}} \quad \text{(I.25)}$$

where K_{RP} (dm^3 g^{-1}) and a_{RP} (dm^3 mg^{-1})^{nRP} are the Redlich-Peterson constants, and n_{RP} is the isotherm exponent.

I.6.2.7. Toth isotherm

In contrast with Sips and Redlich-Peterson, this three parameters isotherm has no limitations in the two end limits of concentration (Do, 1998). This model was developed to improve Langmuir isotherm and fit data of heterogeneous sorption system (Foo and Hameed, 2010). It considers the potential theory and assumes a quasi-Gaussian energy

distribution (Foo and Hameed, 2010; Y. S. Ho et al., 2002). It is represented by the following equation:

$$q_{\mathrm{e}} = \frac{q_{\mathrm{m,Th}} C_{\mathrm{e}}}{(a_{\mathrm{Th}} + C_{\mathrm{e}}^{n_{\mathrm{Th}}})^{1/n_{\mathrm{Th}}}} \quad \text{(I.26)}$$

where $q_{\mathrm{m,Th}}$ (mg g^{-1}) is the solid capacity, a_{Th} (mg $dm^{-3})^{n_{\mathrm{Th}}}$ is the Toth isotherm constant, and n_{Th} the isotherm exponent related with heterogeneity of the system and it is normally lower than unity.

I.7. Promising sorbents for mercury removal

A large diversity of solids can be used as sorbent materials, however only a few of them have high uptake capacity that makes them commercially viable (Seader and Henley, 1998). The performance of the sorbent is strongly dependent on its surface area since the larger it is the more sites may be available for metal sorption. This area can be increased through chemical or thermal activation processes, which consist of increasing the porosity of the material resulting in microporous structures with typical surface areas between 300 and 1200 m^2 g^{-1} (Seader and Henley, 1998).

From the economic point of view, among the wide options of sorbents, the biosorbents are especially attractive because they allow the treatment of large volumes of effluents at very low cost and may offer a waste management alternative. On the other hand, zeolitic materials have high selectivity and removal efficiencies, usually present faster sorption kinetics and are easy to recover. Therefore, even with higher costs, these solids are equally excellent choices

I.7.1.Zeolite and zeolite-type materials

Zeolites are crystalline solids that are part of a larger group called molecular sieves that also includes glass, carbons and oxides. Due to their three-dimensional microporous structure, zeolites are widely used industrially, being present in water treatment, petrochemical industry, agriculture, horticulture and nuclear waste treatment, among others (Li and Yu, 2014; Mishra.Meeta, 2011).

Zeolites may be natural or synthetic and have a tetrahedral structure of AlO_4 and SiO_4 connected to each other via oxygen atoms (Helfferich, 1962). These tetrahedra can be linked by different ways, which justifies the existence of a wide variety of zeolitic structures (Li and Yu, 2014). The lattice structure is negative charged and is balanced by alkali or alkaline-earth metals that act as counter ions and can be exchanged with cations in solution (Helfferich, 1962). Examples of the most common natural zeolites are clinoptilolite, natrolite, stilbite and chabazite (Helfferich, 1962; Mishra.Meeta, 2011). Although these natural zeolites are abundant, not expensive and to possess excellent properties for ion exchange application, they have not been widely applied for water treatment due to impurities and some structure imperfections (Chester and Derouane, 2009; Koohsaryan and Anbia, 2016). Synthetic zeolites like A, X and Y, and ZSM-5 are widely used in industry, mainly due to their beneficial characteristics such as non-toxicity, high surface areas, flexible composition and low costs (Chester and Derouane, 2009; Koohsaryan and Anbia, 2016). However, some new materials, with features like zeolite but improved properties such as more resistance or selectivity for target metals have been synthesized. These materials are called zeolite-type and have structure in which Al is replaced by other elements, like Ti, Nb, V, Zr, *etc* (Brandão et al., 2002; Camarinha et al., 2009; Cardoso et al., 2013; Lopes et al., 2008, 2009; Rocha et al., 1998).

In relation to Hg(II) sorption, microporous titanosilicates such as ETS-4 [$Na_9Ti_5Si_{12}O_{38}(OH).12H_2O$] (Lopes et al., 2008, 2009, 2010; Otero et al., 2009), ETS-10 [$(Na,K)_2TiSi_5\ O_{13}.4H_2O$] (Lopes et al., 2007), AM-2 [$K_2TiSi_3O_9$.H2 O], (Lopes et al., 2007) and zirconium silicates like AV-3 [$Na_5Zr_2Si_6\ O_{18}(Cl,OH).nH_2O$] and AV-13 $Na_{(2+x)}ZrSi_3O_9Cl_x.2H_2O$ (Lopes et al., 2008) have been reported as good ion exchangers for mercury removal.

I.7.2.Biosorbents

A large variety of solids have been used as biosorbents, and generally they can be separated into lignocellulosic biosorbents, algae, chitin/chitosan, bacteria and fungi.

Lignocellulosic solids are composed by cellulose, hemi- cellulose, lignin and a little amount of pectin, protein, vitamins, lipids, extractives (Tran et al., 2015). They are normally agricultural, household or industrial by-products discarded as wastes and find no

application anywhere (Bhatnagar et al., 2015). Living or dead algae are reported to have high metal uptake capacities and resistance to contaminated media (Carro et al., 2011; Henriques et al., 2015). Their composition vary according to the type of algae, brown algae are composed mainly by cellulose, alginic acid and sulfated polysaccharides, while red and green algae have cellulose, agar, sulfated polysaccharides, and glycoproteins (Henriques et al., 2015; Romera et al., 2007). Bacteria are organisms composed by peptidoglycan, teichoic and teichuronic acids, phospholipids, lipopolysaccharides, and various proteins (Aryal and Liakopoulou-Kyriakides, 2015; Prakash Williams et al., 2012). Chitin/chitosan-based biosorbents are regarded as promising bio-polymeric-materials due to their biocompatibility and biodegradability, strong sorption capability, and large functionalized potential (Hou et al., 2018). Chitin is a naturally mucopolysaccharide created by several living creatures such as crabs and other arthropods and it is the second most commom polymer in nature, only behind of cellulose. Chitosan is derived from chitin after a process of deacetylation (Tran et al., 2015). Chitin is formed by 2-acetamido-2-deoxy-b-D-glucose through a b (1–4) linkage while chitosan contains D-glucosamine and N-acetyl-D-glucosamine units (Kumar, 2000; Tran et al., 2015). In relation to fungal biosorbents, their cell walls mainly consists of polysaccharides, proteins and lipids (Nirmal Kumar et al., 2010) and they have the advantage of fast and easy growth with simple cellulose sources (Bayramoğlu and Arıca, 2008).

Among all the biosorbents, the ones from lignocellulosic sources have been widely used for mercury removal because of their great availability in nature and innumerable options of sources. Leaves (Al Rmalli et al., 2008; Sen et al., 2011; Singanan, 2015; Zolgharnein and Shahmoradi, 2010), flowers (Cecilia Soto-Ríos et al., 2018), husks (Devani et al., 2017; El-Shafey, 2010; Krishnani et al., 2008; Rizzuti et al., n.d.; Rocha et al., 2014), bagasse (Khoramzadeh et al., 2013; Krishnani et al., 2009), peels (Ahmed et al., 2018) and seeds (Omorogie et al., 2012) are just some examples of the diversity of biosorbents in this category. The most attractive factor of using these biosorbents remains in the use of industrial or agricultural wastes in order to add value to these by-products while promoting their sustainable management by providing a viable and effective technology for water treatment.

Furthermore, the search for new innovative alternatives has led to an advance in the use of micro and macroalgae for metals removal (Huang and Lin, 2015; Plaza et al., 2011; Shams Khoramabadi et al., 2008; Solisio et al., 2019). These biosorbents are reported as excellent options for Hg accumulation attributed to the structural and chemical composition of their cell walls which have in their constitution amino, carboxyl, sulfate and hydroxyl group(Carro et al., 2011; Henriques et al., 2015; Hou et al., 2018; Shams Khoramabadi et al., 2008). For the presence of S and N in these functional groups are attributed their exceptional affinity toward Hg(II) (Hou et al., 2018). In addition, algae are renewable natural biomes that proliferate abundantly in the coastal areas, often causing environmental disrupts (Vijayaraghavan and Joshi, 2012).

I.8. Thesis structure and work innovation

Uncontrolled growth of population and industrialization lead humanity to face water scarcity all over the world. In order to reduce the lack of drinking water and avoid water depletion, it is necessary to promote its recycling and reuse. In this line, sustainable technologies, aiming the removal of contaminants from aquatic systems, wastewaters and industrial effluents with the concern to offer treated waters with very low final concentrations of contaminants, not only to accomplish the guidelines of regulations but to obtain high water quality for reuse must be pursued.

The main goal of this PhD was to develop alternatives in the scope of metals removal for water treatment, focusing on mercury. Mercury stands out for its high toxicity and the fact that it is not as investigated as other potential toxic metals, mainly due to the inherent difficulties in the quantification of this metal. Innovative aspects of this work are the study of new zeolite-type materials (never tested for mercury removal) or different biosorbents for the removal of this target contaminant under various operating conditions similar to real systems found in the environment or industry. These two types of sorbents have many advantages and their suitability to the process depends on the intended application. The outcomes from this PhD contribute to improve knowledge in this field and offer promising sorbents alternatives for application in water treatment technologies.

Beyond this introductory chapter, this thesis is structured by chapters which represent one or more manuscripts published or submitted to recognized international scientific journals. The chapters were separated by the nature of the sorbent used for mercury (and eventually other metals) removal from aqueous solutions and each manuscript is presented in its integral form as it was submitted. The chapters are briefly described as follows:

Chapter 2 ("The use of zeolite-type materials"): In this work the ability of two zeolite-type microporous materials, a niobium silicate, called AM-11 (Aveiro-Manchester No 11), and a vanadium silicate, AM-14 (Aveiro-Manchester No 14), were investigated for mercury removal under batch conditions, at fixed temperature and pH.

Chapter 3 ("Agricultural and industrial wastes as biosorbents"): This chapter comprises a set of three works developed with the aim to reuse residues or by-products with low commercial costs and add-value to them through their use as biosorbents for mercury removal from realistic aqueous solutions.

Chapter 4 ("Use of living macroalgae"): This chapter include two works in which six living macroalgae, namely *Ulva intestinalis*, *Ulva lactuca*, *Fucus spiralis*, *Fucus vesiculosus*, *Gracilaria* sp. and *Osmundea pinnatifida* were tested for mercury removal from synthetic seawater under different mono and multi-contaminated scenarios.

Chapter 5 ("Final remarks and future work"): This chapter presents the main conclusions of the work and suggest some potential future work to be developed.

This thesis led to the following scientific publications:

- **Purification of mercury-contaminated water using new AM-11 and AM-14 microporous silicates**

  Elaine Fabre, Arany Rocha, Simão P. Cardoso, Paula Brandão, Carlos Vale, Cláudia B. Lopes, Eduarda Pereira, Carlos M. Silva

  Submitted to Separation and Purification Technology (Accepted for publication)

- **Agricultural and industrial wastes as promising biosorbents to remove mercury in water treatments**

  Elaine Fabre, Carlos Vale, Eduarda Pereira, Carlos M. Silva

  Submitted to Journal of Water Process Engineering (Under Review)

- **Valuation of banana peels as an effective biosorbent for mercury removal under low environmental concentrations**

  Fabre, E., Lopes, C. B., Vale, C., Pereira, E., & Silva, C. M. (2019). Valuation of banana peels as an effective biosorbent for mercury removal under low environmental concentrations. Science of The Total Environment, 135883. doi:10.1016/j.scitotenv.2019.135883

- **Experimental measurement and modeling of Hg(II) removal from aqueous solutions using *Eucalyptus globulus* bark: effect of pH, salinity and biosorbent dosage**

  Fabre, E.; Vale, C.; Pereira, E.; Silva, C.M. Experimental Measurement and Modeling of Hg(II) Removal from Aqueous Solutions Using *Eucalyptus globulus* Bark: Effect of pH, Salinity and Biosorbent Dosage. *Int. J. Mol. Sci.* **2019**, *20*, 5973.

- **Fast and efficient removal of mercury from contaminated waters by green, brown and red living marine macroalgae: a promising alternative for water treatment**

  Elaine Fabre, Mariana Dias, Bruno Henriques, Thainara Viana, Nicole Ferreira, José Soares, João Pinto, Carlos Vale, José M. P. Torres, Carlos M. Silva, Eduarda Pereira

  Submitted to Separation and Purification Technology

- **Negligible effect of potential toxic elements and rare earth elements on mercury removal from contaminated waters by green, brown and red living marine macroalgae**

Elaine Fabre, Mariana Dias, Marcelo Costa, Bruno Henriques, Carlos Vale, Cláudia B. Lopes, José M. P. Torres, Carlos M. Silva, Eduarda Pereira

Submitted to Journal of Hazardous Materials (under Review)

I.8. References

Afroze, S., Sen, T.K., 2018. A Review on Heavy Metal Ions and Dye Adsorption from Water by Agricultural Solid Waste Adsorbents. Water, Air, Soil Pollut. 229, 225. https://doi.org/10.1007/s11270-018-3869-z

Ahmed, D., Abid, H., Riaz, A., 2018. Lagenaria siceraria peel biomass as a potential biosorbent for the removal of toxic metals from industrial wastewaters Lagenaria siceraria peel biomass as a potential biosorbent for the removal of toxic metals from industrial wastewaters. Int. J. Environ. Stud. 75, 763–773. https://doi.org/10.1080/00207233.2018.1457285

Aksu, Z., Dönmez, G., 2005. Combined effects of molasses sucrose and reactive dye on the growth and dye bioaccumulation properties of Candida tropicalis. Process Biochem. 40, 2443–2454. https://doi.org/10.1016/j.procbio.2004.09.013

Al Rmalli, S.W., Dahmani, A.A., Abuein, M.M., Gleza, A.A., 2008. Biosorption of mercury from aqueous solutions by powdered leaves of castor tree (Ricinus communis L.). J. Hazard. Mater. 152, 955–959. https://doi.org/10.1016/J.JHAZMAT.2007.07.111

Allouche, F.-N., Guibal, E., Mameri, N., 2014. Preparation of a new chitosan-based material and its application for mercury sorption. Colloids Surfaces A Physicochem. Eng. Asp. 446, 224–232. https://doi.org/10.1016/J.COLSURFA.2014.01.025

Álvarez-Ayuso, E., García-Sánchez, A., 2007. Removal of cadmium from aqueous solutions by palygorskite. J. Hazard. Mater. 147, 594–600. https://doi.org/10.1016/j.jhazmat.2007.01.055

Aman, A., Ahmed, D., Asad, N., Masih, R., Muhammad Abd ur Rahman, H., 2018. Rose biomass as a potential biosorbent to remove chromium, mercury and zinc from

contaminated waters Rose biomass as a potential biosorbent to remove chromium, mercury and zinc from contaminated waters. Int. J. Environ. Stud. 75, 774–787. https://doi.org/10.1080/00207233.2018.1429130

Arief, V.O., Trilestari, K., Sunarso, J., Indraswati, N., Ismadji, S., Mandala, W., Catholic, S., Mandala, W., Catholic, S., 2008. Review Recent Progress on Biosorption of Heavy Metals from Liquids Using Low Cost Biosorbents : Characterization , Biosorption Parameters and Mechanism Studies. Clean 36, 937–962. https://doi.org/10.1002/clen.200800167

Aryal, M., Liakopoulou-Kyriakides, M., 2015. Bioremoval of heavy metals by bacterial biomass. Environ. Monit. Assess. 187, 4173. https://doi.org/10.1007/s10661-014-4173-z

Ash, C., Stone, R., 2003. A question of dose. Science (80-.). 300, 925. https://doi.org/10.1126/science.300.5621.925

Atkins, P., Paula, J. de, 2006. Physical Chemistry, 8 th. ed. W. H. Freeman.

ATSDR, Priority list of hazardous substances [WWW Document], 2017. URL https://www.atsdr.cdc.gov/spl/ (accessed 2.22.17).

Ayangbenro, A., Babalola, O., 2017. A New Strategy for Heavy Metal Polluted Environments: A Review of Microbial Biosorbents. Int. J. Environ. Res. Public Health 14, 94. https://doi.org/10.3390/ijerph14010094

Azari, A., Gharibi, H., Kakavandi, B., Ghanizadeh, G., Javid, A., Mahvi, A.H., Sharafi, K., Khosravia, T., 2017. Magnetic adsorption separation process: an alternative method of mercury extracting from aqueous solution using modified chitosan coated Fe3O4 nanocomposites. J. Chem. Technol. Biotechnol. 92, 188–200. https://doi.org/10.1002/jctb.4990

Bailey, S.E., Olin, T.J., Bricka, R.M., and Adrian, D.D., 1999. A review of pontentially low-cost sorbents for heavy metals. Wat. Res. 33, 2469–2479. https://doi.org/10.1016/S0043-1354(98)00475-8

Bayramoğlu, G., Arıca, M.Y., 2008. Removal of heavy mercury(II), cadmium(II) and zinc(II) metal ions by live and heat inactivated Lentinus edodes pellets. Chem. Eng. J. 143, 133–140. https://doi.org/10.1016/J.CEJ.2008.01.002

Bhatnagar, A., Sillanpää, M., Witek-Krowiak, A., 2015. Agricultural waste peels as versatile biomass for water purification - A review. Chem. Eng. J. 270, 244–271. https://doi.org/10.1016/j.cej.2015.01.135

Bourane, A., Nawdali, M., Bianchi, D., 2002. Heats of Adsorption of the Linear CO Species Adsorbed on a Ir/Al 2 O 3 Catalyst Using in Situ FTIR Spectroscopy under Adsorption Equilibrium. J. Phys. Chem. B 106, 2665–2671. https://doi.org/10.1021/jp0137322

Boutsika, L.G., Karapanagioti, H.K., Manariotis, I.D., 2014. Aqueous mercury sorption by biochar from malt spent rootlets. Water. Air. Soil Pollut. 225, 2007–2013. https://doi.org/10.1007/s11270-013-1805-9

Boyd, G.E., Adamson, A.W., Myers, L.S., 1947. The Exchange Adsorption of Ions from Aqueous Solutions by Organic Zeolites; Kinetics. J. Am. Chem. Soc. 69, 2836–2848. https://doi.org/10.1021/ja01203a066

Bradley, M., Barst, B., Basu, N., 2017. A Review of Mercury Bioavailability in Humans and Fish. Int. J. Environ. Res. Public Health 14, 169. https://doi.org/10.3390/ijerph14020169

Brandão, P., 1998. “Síntese, Estrutura e Reatividade de Novos Materiais Microporosos.” Universidade de Aveiro.

Brandão, P., Philippou, A., Hanif, N., Ribeiro-Claro, P., Ferreira, A., Anderson, M.W., Rocha, J., 2002. Synthesis and characterization of two novel large-pore crystalline vanadosilicates. Chem. Mater. 14, 1053–1057. https://doi.org/10.1021/cm010613q

Brasil promulga Convenção de Minamata sobre Mercúrio | WWF Brasil [WWW Document], 2018. URL https://www.wwf.org.br/?67122/Brasil-promulga-Conveno-de-Minamata-sobre-Mercrio (accessed 10.10.19).

Burek, P., Satoh, Y., Fischer, G., Kahil, M.T., Scherzer, A., Tramberend, S., Nava, L.F., Wada,

Y., Eisner, S., Flörke, M., Hanasaki, N., Magnuszewski, P., Cosgrove, B., Wiberg, D., 2016. Water Futures and Solution: Fast Track Initiative (Final Report). Laxemburgue.

Cain, A., Vannela, R., Woo, L.K., 2008. Cyanobacteria as a biosorbent for mercuric ion. Bioresour. Technol. 99, 6578–6586. https://doi.org/10.1016/J.BIORTECH.2007.11.034

Caledonia, N., 2004. Nickel, in: Merian, E., Anke, M., Ihnat, M., Stoeppler, M. (Eds.), Elements and Their Compounds in the Environment. WILEY-VCH Verlag GmbH&Co. KGaA, Weinheim, pp. 841–865.

Camarinha, E.D., Lito, P.F., Antunes, B.M., Otero, M., Lin, Z., Rocha, J., Pereira, E., Duarte, A.C., Silva, C.M., 2009. Cadmium(II) removal from aqueous solution using microporous titanosilicate ETS-10. Chem. Eng. J. 155, 108–114. https://doi.org/10.1016/j.cej.2009.07.015

Cardoso, S.P., Lopes, C.B., Pereira, E., Duarte, A.C., Silva, C.M., 2013. Competitive Removal of Cd2+ and Hg2+ Ions from Water Using Titanosilicate ETS-4: Kinetic Behaviour and Selectivity. Water, Air, Soil Pollut. 224, 1535. https://doi.org/10.1007/s11270-013-1535-z

Carro, L., Anagnostopoulos, V., Lodeiro, P., Barriada, J.L., Herrero, R., Sastre de Vicente, M.E., 2010. A dynamic proof of mercury elimination from solution through a combined sorption–reduction process. Bioresour. Technol. 101, 8969–8974. https://doi.org/10.1016/J.BIORTECH.2010.06.118

Carro, L., Barriada, J.L., Herrero, R., Sastre de Vicente, M.E., 2011. Adsorptive behaviour of mercury on algal biomass: Competition with divalent cations and organic compounds. J. Hazard. Mater. 192, 284–291. https://doi.org/10.1016/J.JHAZMAT.2011.05.017

Cecilia Soto-Ríos, P., Antonio León-Romero, M., Sukhbaatar, O., Nishimura, O., 2018. Biosorption of Mercury by Reed (Phragmites australis) as a Potential Clean Water Technology. Water, Air, Soil Pollut. 229, 328. https://doi.org/10.1007/s11270-018-3978-8

Chester, A.W., Derouane, E.G. (Eds.), 2009. Zeolite Characterization and Catalysis. Springer, New York.

Chien, S.H., Clayton, W.R., 1980. Application of Elovich Equation to the Kinetics of Phosphate Release and Sorption in Soils1. Soil Sci. Soc. Am. J. 44, 265. https://doi.org/10.2136/sssaj1980.03615995004400020013x

Chojnacka, K., 2010. Biosorption and bioaccumulation – the prospects for practical applications. Environ. Int. 36, 299–307. https://doi.org/10.1016/J.ENVINT.2009.12.001

Cooney, D.O., 1998. Adsorption design for wastewater treatment. Lewis Publishers.

Costley, C.T., Mossop, K.F., Dean, J.R., Garden, L.M., Marshall, J., Carroll, J., 2000. Determination of mercury in environmental and biological samples using pyrolysis atomic absorption spectrometry with gold amalgamation. Anal. Chim. Acta 405, 179–183. https://doi.org/10.1016/S0003-2670(99)00742-4

Council Directive 98/83/EC of 3 November 1998 on the quality of water intended for human consumption, 1998. . Off. J. Eur. Communities 330, 32–54.

Crank, J., 1975. The mathematics of diffusion, 2nd ed. Oxford University Press.

Czarna, D., Baran, P., Kunecki, P., Panek, R., Żmuda, R., Wdowin, M., 2018. Synthetic zeolites as potential sorbents of mercury from wastewater occurring during wet FGD processes of flue gas. J. Clean. Prod. 172, 2636–2645. https://doi.org/10.1016/J.JCLEPRO.2017.11.147

De Gisi, S., Lofrano, G., Grassi, M., Notarnicola, M., 2016. Characteristics and adsorption capacities of low-cost sorbents for wastewater treatment: A review. Sustain. Mater. Technol. 9, 10–40. https://doi.org/10.1016/j.susmat.2016.06.002

De, J., Dash, H.R., Das, S., 2014. Mercury Pollution and Bioremediation-A Case Study on Biosorption by a Mercury-Resistant Marine Bacterium, in: Microbial Biodegradation and Bioremediation. Elsevier Inc., pp. 138–166. https://doi.org/10.1016/B978-0-12-800021-2.00006-6

De, M., Azargohar, R., Dalai, A.K., Shewchuk, S.R., 2013. Mercury removal by bio-char based modified activated carbons. Fuel 103, 570–578. https://doi.org/10.1016/j.fuel.2012.08.011

Devani, M.A., Munshi, B., Kennedy Oubagaranadin, J.U., Bihari Lal, B., Mandal, S., 2017. Environmental Technology Remediation of Hg(II) from solutions using Cajanus cajan husk as a new sorbent Remediation of Hg(II) from solutions using Cajanus cajan husk as a new sorbent. Environ. Technol. 3815, 1878–1886. https://doi.org/10.1080/21622515.2016.1240240

Devani, M.A., Munshi, B., Oubagaranadin, J.U.K., 2015. Characterization and use of chemically activated Butea monosperma leaf dust for mercury(II) removal from solutions. J. Environ. Chem. Eng. 3, 2212–2218. https://doi.org/10.1016/J.JECE.2015.07.028

Do, D.D., 1998. Adsorption analysis: equilibria and kinetics. Imperial College Press, London.

Drasch, G., Horvat, M., Stoeppler, Markus, 2004. Mercury, in: Merian, E., Anke, M., Ihnat, M., Stoeppler, M. (Eds.), Elements and Their Compounds in the Environment. WILEY-VCH Verlag GmbH&Co. KGaA, Weinheim, pp. 931–1005.

Dubinin, M.M., 1960. The Potential Theory of Adsorption of Gases and Vapors for Adsorbents with Energetically Nonuniform Surfaces. Chem. Rev. 60, 235–241. https://doi.org/10.1021/cr60204a006

El-Shafey, E.I., 2010. Removal of Zn(II) and Hg(II) from aqueous solution on a carbonaceous sorbent chemically prepared from rice husk. J. Hazard. Mater. 175, 319–327. https://doi.org/10.1016/J.JHAZMAT.2009.10.006

Esmaeili, A., Saremnia, B., Kalantari, M., 2015. Removal of mercury(II) from aqueous solutions by biosorption on the biomass of Sargassum glaucescens and Gracilaria corticata. Arab. J. Chem. 8, 506–511. https://doi.org/10.1016/J.ARABJC.2012.01.008

European Parliament, 2017. Regulation (EU) 2017/852 of the European Parliament and of

the Council of 17 May 2017 on mercury, and repealing Regulation (EC) No 1102/2008. Off. J. Eur. Union 2017.

Farooq, U., Kozinski, J.A., Khan, M.A., Athar, M., 2010. Biosorption of heavy metal ions using wheat based biosorbents – A review of the recent literature. Bioresour. Technol. 101, 5043–5053. https://doi.org/10.1016/J.BIORTECH.2010.02.030

Figueira, P., Henriques, B., Teixeira, A., Lopes, C.B., Reis, A.T., Rui, &, Monteiro, J.R., Duarte, A.C., Pardal, M.A., Pereira, E., 2016. Comparative study on metal biosorption by two macroalgae in saline waters: single and ternary systems. Environ. Sci. Pollut. Res. 23, 11985–11997. https://doi.org/10.1007/s11356-016-6398-6

Foo, K.Y., Hameed, B.H., 2010. Insights into the modeling of adsorption isotherm systems. Chem. Eng. J. 156, 2–10. https://doi.org/10.1016/j.cej.2009.09.013

Freundlich, H., 1906. Concerning adsorption in solutions. Zeitschrift Fur Phys. Chemie-Stochiometrie Und Verwandstchaftslehre 57, 385–470.

Fu, F., Wang, Q., 2011. Removal of heavy metal ions from wastewaters: A review. J. Environ. Manage. 92, 407–418. https://doi.org/10.1016/j.jenvman.2010.11.011

Gautam, R.K., Chattopadhyaya, M.C., Sharma, S.K., 2013. Biosorption of heavy metals: Recent trends and challenges, in: Sharma, S.K., Sanghi, R. (Eds.), Wastewater Reuse and Management. Springer Science+Business Media, Dordrecht, pp. 1–500. https://doi.org/10.1007/978-94-007-4942-9

Goering, P.L., 2004. The Lanthanides, in: Merian, E., Anke, M., Ihnat, M., Stoeppler, M. (Eds.), Elements and Their Compounds in the Environment. WILEY-VCH Verlag GmbH&Co. KGaA, Weinheim, pp. 867–878.

Harada, M., 1995. Minamata Disease : Methylmercury Poisoning in Japan Caused by Environmental Pollution 25, 1–24.

Hashim, M.A., Mukhopadhyay, S., Sahu, J.N., Sengupta, B., 2011. Remediation technologies for heavy metal contaminated groundwater. J. Environ. Manage. 92, 2355–2388. https://doi.org/10.1016/J.JENVMAN.2011.06.009

Helfferich, F.G., 1962. Ion Exchange. McGraw-Hill, New York.

Henriques, B., Lopes, C.B., Figueira, P., Rocha, L.S., Duarte, A.C., Vale, C., Pardal, M.A., Pereira, E., 2017. Bioaccumulation of Hg, Cd and Pb by Fucus vesiculosus in single and multi-metal contamination scenarios and its effect on growth rate. Chemosphere 171, 208–222. https://doi.org/10.1016/J.CHEMOSPHERE.2016.12.086

Henriques, B., Rocha, L.S., Lopes, C.B., Figueira, P., Monteiro, R.J.R., Duarte, A.C., Pardal, M.A., Pereira, E., 2015. Study on bioaccumulation and biosorption of mercury by living marine macroalgae: Prospecting for a new remediation biotechnology applied to saline waters. Chem. Eng. J. 281, 759–770. https://doi.org/10.1016/J.CEJ.2015.07.013

Ho, T.C., Kobayashi, N., Lee, Y.K., Lin, C.J., Hopper, J.R., 2002. Modeling of mercury sorption by activated carbon in a confined, a semi-fluidized, and a fluidized bed. Waste Manag. 22, 391–398. https://doi.org/10.1016/S0956-053X(02)00021-1

Ho, Y.S., McKay, G., 1999. Pseudo-second order model for sorption processes. Process Biochem. 34, 451–465. https://doi.org/10.1016/S0032-9592(98)00112-5

Ho, Y.S., Ng, J.C.Y., McKay, G., 2000. Kinetics of pollutant sorption by biosorbents: Review. Sep. Purif. Methods 29, 189–232. https://doi.org/10.1081/SPM-100100009

Ho, Y.S., Porter, J.F., Mckay, G., 2002. Equilibrium isotherm studies for the sorption of divalentmetal ions onto peat: copper, nickel and lead single component systems. Water, Air, Soil Pollut. 141, 1–33. https://doi.org/10.1023/A:1021304828010

Holmes, P., James, K.A.F., Levy, L.S., 2009. Is low-level environmental mercury exposure of concern to human health? Sci. Total Environ. 408, 171–182. https://doi.org/10.1016/j.scitotenv.2009.09.043

Hou, C., Zhao, D., Zhang, S., Wang, Y., 2018. Highly selective adsorption of Hg(II) by the monodisperse magnetic functional chitosan nano-biosorbent. Colloid Polym. Sci. 296, 547–555. https://doi.org/10.1007/s00396-017-4253-z

Hrenchuk, L.E., Blanch, P.J., Paterson, M.J., Hintelmann, H.H., 2012. Dietary and

Waterborne Mercury Accumulation by Yellow Perch : A Field Experiment. Environ. Sci. Technol. 46, 509–516. https://doi.org/10.1021/es202759q

Huang, S., Lin, G., 2015. Biosorption of Hg(II) and Cu(II) by biomass of dried Sargassum fusiforme in aquatic solution. J. Environ. Heal. Sci. Eng. 13, 21. https://doi.org/10.1186/s40201-015-0180-4

Idrisb, A., Hisham, N., Hamidc, A., 1996. Total removal of heavy metal from mixed plating rinse wastewater. Desalination 106, 419–422.

Igwe, J.C., Abia, A.A., Ibeh, C.A., 2008. Adsorption kinetics and intraparticulate diffusivities of Hg, As and Pb ions on unmodified and thiolated coconut fiber. Int. J. Environ. Sci. Technol. 5, 83–92. https://doi.org/10.1007/BF03326000

Inglezakis, V.J., 2007. Solubility-normalized Dubinin–Astakhov adsorption isotherm for ion-exchange systems. Microporous Mesoporous Mater. 103, 72–81. https://doi.org/10.1016/J.MICROMESO.2007.01.039

Inglezakis, V.J., Loizidou, M.D., Grigoropoulou, H.P., 2002. Equilibrium and kinetic ion exchange studies of Pb2+, Cr3+, Fe3+ and Cu2+ on natural clinoptilolite. Water Res. 36, 2784–2792. https://doi.org/10.1016/S0043-1354(01)00504-8

Ishii, N., Tagami, K., Uchida, S., 2006. Removal of rare earth elements by algal flagellate Euglena gracilis. J. Alloys Compd. 408–412, 417–420. https://doi.org/10.1016/J.JALLCOM.2004.12.105

Jacinto, J., Henriques, B., Duarte, A.C., Vale, C., Pereira, E., 2018. Removal and recovery of Critical Rare Elements from contaminated waters by living Gracilaria gracilis. J. Hazard. Mater. 344, 531–538. https://doi.org/10.1016/J.JHAZMAT.2017.10.054

Jafari, S.A., Cheraghi, S., 2014. Mercury removal from aqueous solution by dried biomass of indigenous Vibrio parahaemolyticus PG02: Kinetic, equilibrium, and thermodynamic studies. Int. Biodeterior. Biodegradation 92, 12–19. https://doi.org/10.1016/J.IBIOD.2014.01.024

Johari, K., Saman, N., Song, S.T., Heng, J.Y.Y., Mat, A.H., 2014. Study of Hg(II) Removal

From Aqueous Solution Using Lignocellulosic Coconut Fiber Biosorbents: Equilibrium and Kinetic Evaluation. Chem. Eng. Comm. 201, 1198–1220. https://doi.org/10.1080/00986445.2013.806311

Khambhaty, Y., Mody, K., Basha, S., Jha, B., 2008. Hg(II) Removal from Aqueous Solution by Dead Fungal Biomass of Marine Aspergillus niger: Kinetic Studies Hg(II) Removal from Aqueous Solution by Dead Fungal Biomass of Marine Aspergillus niger: Kinetic Studies. Sep. Sci. Technol. 43, 1221–1238. https://doi.org/10.1080/01496390801888235

Khoramzadeh, E., Nasernejad, B., Halladj, R., 2013. Mercury biosorption from aqueous solutions by Sugarcane Bagasse. J. Taiwan Inst. Chem. Eng. 44, 266–269. https://doi.org/10.1016/J.JTICE.2012.09.004

Kinoshita, H., Sohma, Y., Ohtake, F., Ishida, M., Kawai, Y., Kitazawa, H., Saito, T., Kimura, K., 2013. Biosorption of heavy metals by lactic acid bacteria and identification of mercury binding protein. Res. Microbiol. 164, 701–709. https://doi.org/10.1016/J.RESMIC.2013.04.004

Kılıç, M., Keskin, M.E., Mazlum, S., Mazlum, N., 2008. Effect of conditioning for Pb(II) and Hg(II) biosorption on waste activated sludge. Chem. Eng. Process. Process Intensif. 47, 31–40. https://doi.org/10.1016/J.CEP.2007.07.019

Kılıç, Mehmet, Keskin, M.E., Mazlum, S., Mazlum, N., 2008. Hg(II) and Pb(II) adsorption on activated sludge biomass: Effective biosorption mechanism. Int. J. Miner. Process. 87, 1–8. https://doi.org/10.1016/J.MINPRO.2008.01.001

Koohsaryan, E., Anbia, M., 2016. Nanosized and hierarchical zeolites: A short review. Chinese J. Catal. 37, 447–467. https://doi.org/10.1016/S1872-2067(15)61038-5

Krishnani, K.K., Meng, X., Christodoulatos, C., Boddu, V.M., 2008. Biosorption mechanism of nine different heavy metals onto biomatrix from rice husk. J. Hazard. Mater. 153, 1222–1234. https://doi.org/10.1016/J.JHAZMAT.2007.09.113

Krishnani, K.K., Meng, X., Dupont, L., 2009. Metal ions binding onto lignocellulosic

biosorbent. J. J. Environ. Sci. Heal. Part A 44, 688–699. https://doi.org/10.1080/10934520902847810

Kumar, M.N.V.R., 2000. A review of chitin and chitosan applications. React. Funct. Polym. 46, 1–27. https://doi.org/10.1016/S1381-5148(00)00038-9

Lagergren, S., 1898. Zur theorie der sogenannten adsorption gel Zur theorie der sogenannten adsorption gelster stoffe, Kungliga Svenska Vetenskapsakademiens. Handlingar 24, 1–39.

Langmuir, I., 1916. The adsorption of gases on plane surface of glass, mica and platinum. J.Am, Chem.Soc 40, 1361–1368.

Largitte, L., Pasquier, R., 2016. A review of the kinetics adsorption models and their application to the adsorption of lead by an activated carbon. Chem. Eng. Res. Des. 109, 495–504. https://doi.org/10.1016/J.CHERD.2016.02.006

Li, Y., Yu, J., 2014. New Stories of Zeolite Structures: Their Descriptions, Determinations, Predictions, and Evaluations. Chem. Rev. 114, 7268–7316. https://doi.org/10.1021/cr500010r

Liu, J., Huang, H., Huang, R., Zhang, J., Hao, S., Shen, Y., Chen, H., 2016. Mechanisms of CPB Modified Zeolite on Mercury Adsorption in Simulated Wastewater. Water Environ. Res. 88, 490–499. https://doi.org/10.2175/106143016x14504669767850

Lopes, C.B., Coimbra, J., Otero, M., Pereira, E., Duarte, A.C., Lin, Z., Rocha, J., 2008. Uptake of Hg2+from aqueous solutions by microporous titano- and zircono-silicates. Quim. Nova 31, 321–325. https://doi.org/10.1590/S0100-40422008000200025

Lopes, C.B., Lito, P.F., Cardoso, S.P., Pereira, E., Duarte, A.C., Silva, C.M., 2012. Metal recovery, separation and/or pre-concentration, in: Inamuddin, Luqma, M. (Eds.), Ion Exchange Technology II – Applications. Springer, pp. 237–322.

Lopes, C.B., Oliveira, J.R., Rocha, L.S., Tavares, D.S., Silva, C.M., Silva, S.P., Hartog, N., Duarte, A.C., Pereira, E., 2014. Cork stoppers as an effective sorbent for water treatment: the removal of mercury at environmentally relevant concentrations and

conditions. Environ. Sci. Pollut. Res. 21, 2108–2121.

Lopes, C.B., Otero, M., Coimbra, J., Pereira, E., Rocha, J., Lin, Z., Duarte, A., 2007. Removal of low concentration Hg2+ from natural waters by microporous and layered titanosilicates. Microporous Mesoporous Mater. 103, 325–332. https://doi.org/10.1016/j.micromeso.2007.02.025

Lopes, C.B., Otero, M., Lin, Z., Silva, C.M., Pereira, E., Rocha, J., Duarte, A.C., 2010. Effect of pH and temperature on Hg2+water decontamination using ETS-4 titanosilicate. J. Hazard. Mater. 175, 439–444. https://doi.org/10.1016/j.jhazmat.2009.10.025

Lopes, C.B., Otero, M., Lin, Z., Silva, C.M., Rocha, J., Pereira, E., Duarte, A.C., 2009. Removal of Hg2+ ions from aqueous solution by ETS-4 microporous titanosilicate — Kinetic and equilibrium studies. Chem. Eng. J. 151, 247–254. https://doi.org/10.1016/j.cej.2009.02.035

Lopes, C.M.B., 2009. Mercury (II) removal from aqueous solutions by microporous materials. Univeristy of Aveiro.

Madaeni, S.S., Mansourpanah, Y., 2003. COD Removal from Concentrated Wastewater Using Membranes. Filtr. Sep. 40, 40–46. https://doi.org/10.1016/S0015-1882(03)00635-9

Malash, G.F., El-Khaiary, M.I., 2010. Piecewise linear regression: A statistical method for the analysis of experimental adsorption data by the intraparticle-diffusion models. Chem. Eng. J. 163, 256–263. https://doi.org/10.1016/j.cej.2010.07.059

Martínez-Juárez, V.M., Cárdenas-González, J.F., Torre-Bouscoulet, M.E., Acosta-Rodríguez, I., 2012. Biosorption of mercury (II) from aqueous solutions onto fungal biomass. Bioinorg. Chem. Appl. 2012, 5–10. https://doi.org/10.1155/2012/156190

Mercury - United States Department of State [WWW Document], 2019. URL https://www.state.gov/key-topics-office-of-environmental-quality-and-transboundary-issues/u-s-actions-to-reduce-mercury-pollution-from-transboundary-sources/ (accessed 11.21.19).

Mishra.Meeta, J.S.K., 2011. Properties and applications of zeolites: A Review. Pro. Nat. Acad. Sci. India. Sect. B 81, 250–259.

Mokone, J.G., Tutu, H., Chimuka, L., Cukrowska, E.M., 2018. Optimization and Characterization of Cladophora sp. Alga Immobilized in Alginate Beads and Silica Gel for the Biosorption of Mercury from Aqueous Solutions. Water, Air, Soil Pollut. 229, 215. https://doi.org/10.1007/s11270-018-3859-1

Momc, B., 2004. The Copper Group, in: Merian, E., Anke, M., Ihnat, M., Stoeppler, M. (Eds.), Elements and Their Compounds in the Environment. WILEY-VCH Verlag GmbH&Co. KGaA, Weinheim, pp. 731–750.

Mudasir, M., Karelius, K., Aprilita, N.H., Wahyuni, E.T., 2016. Adsorption of mercury(II) on dithizone-immobilized natural zeolite. J. Environ. Chem. Eng. 4, 1839–1849. https://doi.org/10.1016/J.JECE.2016.03.016

National Primary Drinking Water Regulations, 2009.

Nguyen, T.A.H., Ngo, H.H., Guo, W.S., Zhang, J., Liang, S., Yue, Q.Y., Li, Q., Nguyen, T.V., 2013. Applicability of agricultural waste and by-products for adsorptive removal of heavy metals from wastewater. Bioresour. Technol. 148, 574–585. https://doi.org/10.1016/J.BIORTECH.2013.08.124

Nirmal Kumar, J.I., George, B., Kumar, R.N., Sajish, P.R., Viyol, S., 2010. Biosorption of mercury and lead by dried Aspergillus niger Tiegh. isolated from estuarine sediments. Int. J. Environ. Stud. 67, 735–746. https://doi.org/10.1080/00207233.2010.517644

Nriagu, J., Becker, C., 2003. Volcanic emissions of mercury to the atmosphere: global and regional inventories. Sci. Total Environ. 304, 3–12. https://doi.org/10.1016/S0048-9697(02)00552-1

O'Connell, D.W., Birkinshaw, C., O'Dwyer, T.F., 2008. Heavy metal adsorbents prepared from the modification of cellulose: A review. Bioresour. Technol. 99, 6709–6724. https://doi.org/10.1016/j.biortech.2008.01.036

Omorogie, M.O., Babalola, J.O., Unuabonah, E.I., Gong, J.R., 2012. Kinetics and thermodynamics of heavy metal ions sequestration onto novel Nauclea diderrichii seed biomass. Bioresour. Technol. 118, 576–579. https://doi.org/10.1016/J.BIORTECH.2012.04.053

Organization., W.H., 2006. Guidelines for Drinking-water Quality.

Otero, M., Lopes, C.B., Coimbra, J., Ferreira, T.R., Silva, C.M., Lin, Z., Rocha, J., Pereira, E., Duarte, A.C., 2009. Priority pollutants (Hg2+ and Cd2+) removal from water by ETS-4 titanosilicate. Desalination 249, 742–747. https://doi.org/10.1016/j.desal.2009.04.008

Paasivirta, J., 1991. Mercury in the environment, in: Chemical Ecotoxicology. Lewis Publishers, Inc., pp. 107–125.

Park, D., Yun, Y.-S., Park, J.M., 2010. The Past, Present, and Future Trends of Biosorption. Biotechnol. Bioprocess Eng. 15, 86–102. https://doi.org/10.1007/s12257-009-0199-4

Pazouki, M., Zabihi, M., Shayegan, J., Fatehi, M.H., 2018. Mercury ion adsorption on AC@Fe3O4-NH2-COOH from saline solutions: Experimental studies and artificial neural network modeling. Korean J. Chem. Eng. 35, 671–683. https://doi.org/10.1007/s11814-017-0293-9

Pereira, E., 1996. Distribuição , Reactividade e Transporte do Mercúrio na Ria de Aveiro. University of Aveiro.

Pickhardt, P.C., Stepanova, M., Fisher, N.S., 2006. Contrasting uptake routes and tissue distributions of inorganic and methylmercury in mosquitofish (Gambusia affinis) and redear sunfish (Lepomis microlophus). Environ. Toxicol. Chem. 25, 2132–2142.

Plaza, J., Viera, M., Donati, E., Guibal, E., 2011. Biosorption of mercury by Macrocystis pyrifera and Undaria pinnatifida: Influence of zinc, cadmium and nickel. J. Environ. Sci. 23, 1778–1786. https://doi.org/10.1016/S1001-0742(10)60650-X

Polanyi, M., 1914. Adsorption from the point of view of the Third Law of Thermodynamics. Verh. Deut. Phys. Ges 16, 1012–1016.

Prakash Williams, G., Gnanadesigan, M., Ravikumar, S., 2012. Biosorption and bio-kinetic studies of halobacterial strains against Ni2+, Al3+ and Hg2+ metal ions. Bioresour. Technol. 107, 526–529. https://doi.org/10.1016/J.BIORTECH.2011.12.054

Qiu, H., Lv, L., Pan, B.-C., Zhang, Q.-J., Zhang, W.-M., Zhang, Q.-X., 2009. Critical review in adsorption kinetic models *. J Zhejiang Univ Sci A 10, 716–724. https://doi.org/10.1631/jzus.A0820524

Rae, I.B., Gibb, S.W., Lu, S., 2009. Biosorption of Hg from aqueous solutions by crab carapace. J. Hazard. Mater. 164, 1601–1604. https://doi.org/10.1016/j.jhazmat.2008.09.052

Rajamohan, N., Rajasimman, M., Dilipkumar, M., 2014. Parametric and kinetic studies on biosorption of mercury using modified Phoenix dactylifera biomass. J. Taiwan Inst. Chem. Eng. 45, 2622–2627. https://doi.org/10.1016/J.JTICE.2014.07.004

Rakhshaee, R., Giahi, M., Pourahmad, A., 2009. Studying effect of cell wall's carboxyl–carboxylate ratio change of Lemna minor to remove heavy metals from aqueous solution. J. Hazard. Mater. 163, 165–173. https://doi.org/10.1016/j.jhazmat.2008.06.074

Raspor, B., 2004. Elements and Elemental Compounds in Waters and the Aquatic Food Chain, in: Merian, E., Anke, M., Ihnat, M., Stoeppler, M. (Eds.), Elements and Their Compounds in the Environment. WILEY-VCH Verlag GmbH&Co. KGaA, Weinheim, pp. 127–147. https://doi.org/10.1002/9783527619634.ch7

Raza, M.H., Sadiq, A., Farooq, U., Athar, M., Hussain, T., Mujahid, A., Salman, M., 2015. *Phragmites karka* as a Biosorbent for the Removal of Mercury Metal Ions from Aqueous Solution: Effect of Modification. J. Chem. 2015, 1–12. https://doi.org/10.1155/2015/293054

Reichenberg, D., 1953. Properties of Ion-Exchange Resins in Relation to their Structure. III. Kinetics of Exchange. J. Am. Chem. Soc. 75, 589–597. https://doi.org/10.1021/ja01099a022

Rengaraj, S., Yeon, K.-H., Moon, S.-H., 2001. Removal of chromium from water and wastewater by ion exchange resins. J. Hazard. Mater. 87, 273–287. https://doi.org/10.1016/S0304-3894(01)00291-6

Rizzuti, A.M., Ellis, F.L., Cosme, L.W., n.d. Biosorption of Mercury from Dilute Aqueous Solutions Using Soybean Hulls and Rice Hulls. Waste and Biomass Valorization 6. https://doi.org/10.1007/s12649-015-9391-2

Rocha, J., Brandao, P., Phillippou, A., Anderson, M.W., 1998. Synthesis and characterisation of a novel microporous niobium silicate catalyst. Chem Commun 2687–2688. https://doi.org/Doi 10.1039/A808264b

Rocha, L.S., Almeida, Â., Nunes, C., Henriques, B., Coimbra, M.A., Lopes, C.B., Silva, C.M., Duarte, A.C., Pereira, E., 2016. Simple and effective chitosan based films for the removal of Hg from waters: Equilibrium, kinetic and ionic competition. Chem. Eng. J. 300, 217–229. https://doi.org/10.1016/j.cej.2016.04.054

Rocha, L.S., Lopes, I., Lopes, C.B., Henriques, B., Soares, A.M.V.M., Duarte, A.C., Pereira, E., 2014. Efficiency of a cleanup technology to remove mercury from natural waters by means of rice husk biowaste: ecotoxicological and chemical approach. Env. Sci Pollut Res 21, 8146–8156. https://doi.org/10.1007/s11356-014-2753-7

Roginsky, S., Zeldovich, Y.B., 1934. The catalytic oxidation of carbon monoxide on manganese dioxide. Acta Phys. Chem. USSR 1, 554.

Romera, E., González, F., Ballester, A., Blázquez, M.L., Muñoz, J.A., 2007. Comparative study of biosorption of heavy metals using different types of algae. Bioresour. Technol. 98, 3344–3353. https://doi.org/10.1016/J.BIORTECH.2006.09.026

Rostami, S., Azizi, S.N., Asemi, N., 2018. Removal of mercury(II) from aqueous solutions via Box–Behnken experimental design by synthesized hierarchical nanoporous ZSM-5 zeolite. J. Iran. Chem. Soc. 15, 1741–1754. https://doi.org/10.1007/s13738-018-1371-6

Sağ, Y., 2001. Biosorption of heavy metals by fungal biomass and modeling of fungal

biosorption: a review. Sep. Purif. Methods 30, 1–48. https://doi.org/10.1081/SPM-100102984

Sanchez-rodas, D., 2010. Atomic Fluorescence Spectrometry : A suitable detection technique in speciation studies for arsenic , selenium , antimony and mercury Atomic Fluorescence Spectrometry : a suitable detection technique in speciation studies for arsenic , selenium , antimony. J. Anal. At. Spectrom. 25, 933–946. https://doi.org/10.1039/b917755h

Saravanan, P., Vinod, V.T.P., Sreedhar, B., Sashidhar, R.B., 2012. Gum kondagogu modified magnetic nano-adsorbent: An efficient protocol for removal of various toxic metal ions. Mater. Sci. Eng. C 32, 581–586. https://doi.org/10.1016/J.MSEC.2011.12.015

Sarı, A., Tüzen, M., Cıtak, D., 2012. Equilibrium, Thermodynamic and Kinetic Studies on Biosorption of Mercury from Aqueous Solution by Macrofungus (Lycoperdon perlatum) Biomass. Sep. Sci. Technol. 478, 1167–1176. https://doi.org/10.1080/01496395.2011.644615

Saunders, R.J., Paul, N.A., Hu, Y., de Nys, R., 2012. Sustainable Sources of Biomass for Bioremediation of Heavy Metals in Waste Water Derived from Coal-Fired Power Generation. PLoS One 7, e36470. https://doi.org/10.1371/journal.pone.0036470

Schroeder, H., 1998. Atmospheric mercury- an over view. Atmos. Environ. 32, 809–822.

Seader, J.D., Henley, E.J., 1998. Separation Process Principles. John Wiley & Sons, Inc., New York.

Selin, N.E., 2009. Global Biogeochemical Cycling of Mercury : A Review. Annu. Rev. ofEnvironment Resour. 34, 43–63. https://doi.org/10.1146/annurev.environ.051308.084314

Sen, T.K., Azman, A.F. Bin, Maitra, S., Dutta, B.K., 2011. Removal of Mercury(II) from Aqueous Solutions Using the Leaves of the Rambai Tree (<I>Baccaurea motleyana</I>). Water Environ. Res. 83, 834–842. https://doi.org/10.2175/106143011X12989211841098

Shams Khoramabadi, G., Jafari, A., Hasanvand Jamshidi, J., 2008. Biosorption of Mercury (II) from Aqueous Solutions by Zygnema fanicum Algae. J. Appl. Sci. 8, 2168–2172.

Singanan, M., 2015. Biosorption of Hg(II) ions from synthetic wastewater using a novel biocarbon technology. Environ. Eng. Res. 20, 33–39. https://doi.org/10.4491/eer.2014.032

Singh Ahluwalia, S., Goyal, D., 2007. Microbial and plant derived biomass for removal of heavy metals from wastewater. Bioresour. Technol. 98, 2243–2257. https://doi.org/10.1016/j.biortech.2005.12.006

Smit, B., Maesen, T., 2008. Molecular simulations of zeolites : Adsorption , diffusion , and shape selectivity. Chem. Rev. 108, 4125–4184. https://doi.org/10.1021/cr8002642

Smith, D.R., Nordberg, M., 2015. General chemistry, sampling, analytical methods, and speciation∗, in: Handbook on the Toxicology of Metals. Elsevier, pp. 15–44. https://doi.org/10.1016/B978-0-444-59453-2.00002-0

Solisio, C., Al Arni, S., Converti, A., 2019. Adsorption of inorganic mercury from aqueous solutions onto dry biomass of Chlorella vulgaris: kinetic and isotherm study. Environ. Technol. 40, 664–672. https://doi.org/10.1080/09593330.2017.1400114

Song, S.-T., Saman, N., Johari, K., Mat, H., 2014. Biosorption of Mercury from Aqueous Solution and Oilfield Produced Water by Pristine and Sulfur Functionalized Rice Residues. Environ. Prog. Sustain. Energy 33, 482–489. https://doi.org/10.1002/ep

Stoecker, B., 2004. Chromium, in: Merian, E., Anke, M., Ihnat, M., Stoeppler, M. (Eds.), Elements and Their Compounds in the Environment. WILEY-VCH Verlag GmbH&Co. KGaA, Weinheim, pp. 709–729.

Stumm, W., Morgan, J.J., 1996. Aquatic Chemistry: chemical equilibria and rates in natural waters. John Wiley & Sons, Inc.

Sulaymon, A.H., Yousif, S.A., Al-Faize, M.M., 2014. Competitive biosorption of lead mercury chromium and arsenic ions onto activated sludge in fixed bed adsorber. J. Taiwan Inst. Chem. Eng. 45, 325–337. https://doi.org/10.1016/j.jtice.2013.06.034

Torres, M.A., Barros, M.P., Campos, S.C.G., Pinto, E., Rajamani, S., Sayre, R.T., Colepicolo, P., 2008. Ecotoxicology and Environmental Safety Biochemical biomarkers in algae and marine pollution : A review 71, 1–15. https://doi.org/10.1016/j.ecoenv.2008.05.009

Tran, H.N., You, S.-J., Hosseini-Bandegharaei, A., Chao, H.-P., 2017. Mistakes and inconsistencies regarding adsorption of contaminants from aqueous solutions: A critical review. Water Res. 120, 88–116. https://doi.org/10.1016/J.WATRES.2017.04.014

Tran, V.S., Ngo, H.H., Guo, W., Zhang, J., Liang, S., Ton-That, C., Zhang, X., 2015. Typical low cost biosorbents for adsorptive removal of specific organic pollutants from water. Bioresour. Technol. 182, 353–363. https://doi.org/10.1016/j.biortech.2015.02.003

Tuzen, M., Sari, A., Mendil, D., Soylak, M., 2009. Biosorptive removal of mercury(II) from aqueous solution using lichen (Xanthoparmelia conspersa) biomass: Kinetic and equilibrium studies. J. Hazard. Mater. 169, 263–270. https://doi.org/10.1016/j.jhazmat.2009.03.096

Veglio, F., Beolchini, F., 1997. Removal of metals by biosorption: A review. Hydrometallurgy 44, 301–316.

Vijayaraghavan, K., Joshi, U.M., 2012. Interaction of Mercuric Ions with Different Marine Algal Species. Bioremediat. J. 16, 225–234. https://doi.org/10.1080/10889868.2012.731443

Vinod, V.T.P., Sashidhar, R.B., Sivaprasad, N., Sarma, V.U.M., Satyanarayana, N., Kumaresan, R., Rao, T.N., Raviprasad, P., 2011. Bioremediation of mercury (II) from aqueous solution by gum karaya (Sterculia urens): A natural hydrocolloid. Desalination 272, 270–277. https://doi.org/10.1016/J.DESAL.2011.01.027

Volesky, B., 2007. Biosorption and me. Water Res. 41, 4017–4029. https://doi.org/10.1016/j.watres.2007.05.062

Wang, J., Feng, X., Anderson, C.W.N., Xing, Y., Shang, L., 2012. Remediation of mercury contaminated sites – A review. J. Hazard. Mater. 221, 1–18. https://doi.org/10.1016/j.jhazmat.2012.04.035

Wang, R., Wong, M., Wang, W., 2010. Mercury exposure in the freshwater tilapia Oreochromis niloticus. Environ. Pollut. 158, 2694–2701. https://doi.org/10.1016/j.envpol.2010.04.019

Wang, T., Sun, H., 2013. Biosorption of heavy metals from aqueous solution by UV-mutant Bacillus subtilis. Env. Sci Pollut Res 20, 7450–7463. https://doi.org/10.1007/s11356-013-1767-x

Wang, X.S., Li, F.Y., He, W., Miao, H.H., 2010. Hg(II) removal from aqueous solutions by Bacillus subtilis biomass. Clean - Soil, Air, Water 38, 44–48. https://doi.org/10.1002/clen.200900201

Weber, W.J., Morris, J.C., 1963. Kinetics of Adsorption on Carbon from Solution. J. Sanit. Eng. Div. 89, 31–60.

World Water Assessment Programme (United Nations), 2019. The United Nations world water development report 2019: leaving no one behind - UNESCO Digital Library. UNESCO on behalf of UN-Water.

World Water Assessment Programme (United Nations), 2017. Wastewater : the untapped resource : the United Nations world water development report 2017.

World Water Assessment Programme (United Nations), 2015. The United Nations World Water Development Report 2015: Water for a Sustainable World. UNESCO on behalf of UN-Water, Paris.

Yu, M.-H., 2001. Environmental Toxicology: impacts of environmental toxicants on living systems. Lewis Publishers, Boca Raton.

Zaib, M., Makshoof Athar, M., Saeed, A., Farooq, U., Salman, M., Nouman Makshoof, M., 2016. Green Chemistry Letters and Reviews Equilibrium, kinetic and thermodynamic biosorption studies of Hg(II) on red algal biomass of Porphyridium cruentum. Green

Chem. Lett. Rev. 94, 179–189. https://doi.org/10.1080/17518253.2016.1185166

Zarei, S., Niad, M., 2017. Cystoseira myricaas for mercury (II) uptake: Isotherm, kinetics, thermodynamic, response surface methodology and fuzzy modeling. J. Taiwan Inst. Chem. Eng. 81, 247–257. https://doi.org/10.1016/J.JTICE.2017.10.010

Zhao, X., Wang, H., Tang, Z., Zhao, T., Qin, N., 2016. Amendment of water quality standards in China : viewpoint on strategic considerations. Environ. Sci. Pollut. Res. 25, 3078–3092. https://doi.org/10.1007/s11356-016-7357-y

Zhou, L., Liu, Z., Liu, J., Huang, Q., 2010. Adsorption of Hg(II) from aqueous solution by ethylenediamine-modified magnetic crosslinking chitosan microspheres. Desalination 258, 41–47. https://doi.org/10.1016/J.DESAL.2010.03.051

Zolgharnein, J., Shahmoradi, A., 2010. Characterization of Sorption Isotherms, Kinetic Models, and Multivariate Approach for Optimization of Hg(II) Adsorption onto Fraxinus Tree Leaves. J. Chem. Eng. Data 55, 5040–5049. https://doi.org/10.1021/je1006218

Chapter II

Zeolite-type materials towards water treatment

This chapter presents the study of the ability of two microporous materials, a niobium silicate, called AM-11 (Aveiro-Manchester No 11), and a vanadium silicate, AM-14 (Aveiro-Manchester No 14), for mercury removal under batch conditions, at fixed temperature and pH. Because of their excellent ion exchange properties, equilibrium and kinetics assays were performed using only a few mg dm^{-3} of material. The most relevant two- and three-parameter isotherms and kinetic models were used to fit the experimental data. In the end, the performances of these two microporous materials to remove mercury were compared with other sorbents.

This chapter is the manuscript accepted for publication.

Index

Work submitted as scientific article

Purification of mercury-contaminated water using new AM-11 and AM-14 microporous silicates

Abstract

Water is an essential resource on Earth and the maintenance of its quality led to the incentive of water reuse programmes. Among the most relevant contaminants, mercury is recognized for its toxicity and biomagnifications along the food chain, reason why its removal from aqueous solutions was studied in this essay using two microporous materials for the first time. The ability of a niobium silicate, called AM-11 (Aveiro-Manchester No 11), and of a vanadium silicate, AM-14 (Aveiro-Manchester No 14), were assessed under batch conditions, at fixed temperature and pH. These microporous materials were synthesized and characterized by SEM, PXRD, ICP-OES, TGA and elemental analysis. Because of their excellent ion exchange properties, equilibrium and kinetics assays were performed using only a few mg dm^{-3} of material. The most relevant two- and three-parameter isotherms were used to fit the experimental data. Langmuir isotherm adjusted better the AM-11 data (deviation of 3.58 %, R^2_{adj}=0.980, AIC=52.8), predicting a maximum uptake of 161 mg g^{-1}, while the AM-14 data were better fitted by the Temkin model (deviation of 3.92 %, R^2_{adj}=0.985, AIC=54.2). The kinetic study was performed using Elovich, pseudo-first order and pseudo-second order models. The pseudo–second order and Elovich equations provided the best fits for both materials. The Elovich equation achieved a better correlation in the initial branch while the pseudo-second order expression was more efficient for the horizontal branch. The intraparticle diffusivities of counter ions were also assessed using a kinetic model based on the Nernst-Plank equations. Performance of these two microporous materials to remove mercury has been compared with other sorbents, highlighting their potential as ion exchangers.

II.1. Purification of mercury-contaminated water using new AM-11 and AM-14 microporous silicates

II.1.1. Introduction

The contamination of waters and aquatic systems due to the discharge of toxic elements has caused worldwide concern for the last years, due to their well-known effects on biota and human health (Meena et al., 2005; Sousa et al., 2010). Several industries are responsible for the discharge of metals into the aquatic system including the production of lamps, batteries, electronic devices, chlor-alkali production and petroleum refining (Liu et al., 2018). Mercury is considered one of the most hazardous non-essential metals, occupying the third position in the rank of the most dangerous substances of the Agency for Toxic Substances & Disease Registry (ATSDR), which is elaborated based on a combination of its environmental frequency, toxicity, and potential for human exposure ("Substance Priority List | ATSDR"). Mercury dangerousness is due to its persistent character, ease of accumulation and amplification along the food chain causing a lot of toxic effects on living organisms (C B Lopes et al., 2008; Lopes et al., 2009; Qi et al., 2017). Therefore, its removal from water and wastewaters is a key issue in water remediation technologies and that is not a trivial task. The study of Hg removal is delicate and the efficiency of the process is highly dependent on the speciation, transformation and reactivity of Hg(II) species in waters (Johs et al., 2019). In fresh waters the interactions between Hg(II) and the dissolved organic matters strongly influence its removal due to the high thermodynamic stability of the organic mercury complexes formed, which are several orders of magnitude higher than non-sulfidic Hg complexes (Dong et al., 2010; Johs et al., 2019).

A variety of processes are available for the treatment of aqueous streams contaminated with toxic metals. The most important are electrochemical techniques, chemical precipitation, membrane processes, flotation, solvent extraction, ion exchange

and adsorption (Baral et al., 2009; Barreira et al., 2009; Huang et al., 2016; Ihsanullah, 2019; Ihsanullah et al., 2016; C. B. Lopes et al., 2012; Sajid et al., 2018). However, many of these methods exhibit high operating and maintenance costs, difficult sludge disposal and are non-effective to treat water with low metal concentrations (Bhatnagar et al., 2015; C B Lopes et al., 2008; Meena et al., 2005). Comparatively, the ion exchange is widely used in industry, because of its simple operation and efficiency to treat large volumes of dilute solutions (Camarinha et al., 2009; Dąbrowski et al., 2004; C B Lopes et al., 2008). Here, the need for low cost, accessible and recoverable sorbents guides the research and development of new materials to replace the ion exchange resins largely used (C B Lopes et al., 2008; Wierzba and Kłos, 2019).

Zeolites and other zeolite-type materials are receiving special attention in ion exchange processes due to their structure, high surface areas and selectivity, which provide good cost-benefit ratios (Ahmed et al., 1998; Araki et al., 2019; Biškup and Subotić, 2004; Czarna et al., 2018). The negative charge of the porous framework of these materials is balanced by the presence of exchangeable cations electrostatically held within their channels and/or cavities, which makes them adequate for cationic exchange (Lito et al., 2012). Despite the great interest in ion exchange using microporous materials, only a few publications have addressed realistic and low concentrated solutions. Recently, titanium silicates, displaying zeolite-type properties, have attracted much interest (Noh et al., 2012). Materials like ETS-4 and ETS-10 have been used for Hg(II) and Cd(II) removal from diluted aqueous solutions and these materials have been proposed as good exchangers (Barreira et al., 2009; Camarinha et al., 2009; Cardoso et al., 2013; Ferreira et al., 2009; C B Lopes et al., 2008). As an extension of these works, novel microporous niobium and vanadium silicates have been synthesized and studied here for Hg(II) removal, namely, AM-11 (Aveiro-Manchester microporous solid no. 11), as an example of a niobium silicate, and AM-14 (Aveiro-Manchester microporous solid no. 14), as an example of vanadium silicate (Brandão et al., 2002a; Rocha et al., 1998). The crystal structure of AM-11 and AM-14 materials are still unknown. Nevertheless, from a wide range of characterisation techniques one may say that both materials exhibit three-dimensional network of interconnected channels, composed by tetrahedral SiO_4 units and

octahedral Nb^{5+} atoms for AM-11 (Brandão et al., 2002b) and V^{4+} for AM-14 (Brandão et al., 2002a). The pore size of these two silicates were accessed by adsorption isotherms of different organic molecules (n-hexane, benzene, tripropylamine) indicating that AM-11 contains medium pore size of 4 Å and AM-14 possess a median pore size of 6.8 Å (Brandão et al., 2002a; Rocha et al., 1998). The NH_4^+ ions are the counter ions used to balance the charge associated with niobium framework (Brandão et al., 2002b) and its theoretical capacity is 2.12 meq g^{-1}, while in the case of AM-14 the Na^+ cations are the neutralizing species and its theoretical capacity is 5.20 meq g^{-1} (Brandão et al., 2002a).

Taking into account the small pore diameters mentioned above for AM-11 and AM-14 (4 Å and 6.8 Å, respectively) along with the strong and long-range nature of the electrostatic interactions, and the Donan exclusion principle (*i.e*., solution co-ions cannot penetrate the zeolite materials), the diffusing species never escape from the force field of the solid matrix and thus the sorption mechanism of mercury is ion exchange. Accordingly, the systems of interest in this work are Hg(II)/AM-11 and Hg(II)/AM-14.

In line with one of the goals of 2030 Agenda for Sustainable Development of United Nations, which includes improving water quality by reducing pollution, minimizing the presence of hazardous chemicals, and to substantially increase water recycling and safe reuse, here we investigate the applicability of AM-11 and AM-14 to remove Hg(II) from diluted solutions, prospecting their potential for treating contaminated waters and industrial effluents. Batch experiments were carried out for two systems (Hg(II)/AM-11 and Hg(II)/AM-14), for which the kinetics and equilibrium were investigated experimentally and theoretically by applying well-known kinetic equations and isotherms. To the best of our knowledge these microporous materials have never been applied in ion exchange processes. With this study, we intend to contribute to the better knowledge of Hg(II) removal process, searching alternative materials for improving water quality and contributing to sustainable development goals of United Nations.

II.1.2. Materials and methods

II.1.2.1. Chemicals

All reagents used in this work were of analytical grade. They were purchased and used without additional purification. The certified standard solution of mercury(II) nitrate (1000 ±2 mg dm^{-3}), the sodium hydroxide (≥ 99 %), the ammonia solution (25 %), the sodium silicate solution (≥ 25 %) and the vanadium(IV) oxide sulfate hydrate (≥ 99 %) were purchased from Merck. The tetraethyl orthosilicate (≥ 99 %), sodium chloride (≥ 99 %), and niobium chloride (≥ 99 %), were acquired from Aldrich. All working solutions, including standards for the calibration curves, were obtained by dissolving or diluting the corresponding stock solution in high purity water (18.2 MΩ cm, Milli-Q system).

II.1.2.2. Sorbents materials

II.1.2.2.1. Synthesis

AM-11 and AM-14 were studied for Hg(II) removal from aqueous solution. The AM-11 sample used in this work was prepared using NH^{4+} as cation. Briefly, AM-11 was synthesized as follows: a solution was made by mixing 0.193 g of $NbCl_5$, with 3 cm^3 of HCl (37 %). A second solution was made by mixing 4 cm^3 of H_2O and 1.28 g of tetraethyl orthosilicate. These two solutions were combined and stirred thoroughly, then 50 cm^3 of ammonium solution (25 %) was added. The gel was autoclaved for 15 days at 200 °C. The resulting crystalline product was filtered off, washed with distilled water and then dried at room temperature The final product obtained was an off-white microcrystalline powder (Rocha et al., 1998).

The synthesis of AM-14 started with an alkaline solution, by dissolving 5.02 g of sodium silicate solution, 9.05 g of H_2O, 0.540 g of NaOH and 0.760 g of NaCl. A second solution was prepared by mixing 6.66 g of H_2O with 1.44 g of $VOSO_4 \cdot 5H_2O$. The AM-14 gel was autoclaved for 3 days at 230 °C. The crystalline green powder was filtered out, washed and dried at room temperature (Brandão et al., 2002a).

II.1.2.2.2. Structural and chemical characterization

The crystal morphology of AM-11 and AM-14 was analysed using scanning electron microscopy (SEM) on a Hitachi SU-70 SEM microscope with a Bruker Quantax 400 detector operating at 20 kV. The powder X-Ray diffraction (PXRD) patterns of both samples were recorded on an Empyrean PANalytical diffractometer equipped with a Cu-Kα monochromatic radiation source. Inductively coupled plasma optical emission spectroscopy (ICP-OES) analyses (for Si, Nb, V and Na) were carried out on a Horiba Jobin Yvon Activa M spectrometer (detection limit of *ca.* 20 μg dm^{-3}; experimental range of error of *ca.* 5 %). Elemental analysis of nitrogen present in AM-11 sample was performed using a Truspec 630-200-200 instrument. Thermogravimetric analysis curves were measured with Shimadzu TGA-50. The heating rate was 10 °C min^{-1} from room temperature until 800 °C for AM-11 and until 700 °C for AM-14. The point zero charge (PZC) of AM-11 was determined according to an adaptation of the immersion method proposed by Fiol and Villaescusa (2009) using an incubator shaker HWY-200D and the solution pH was measured on a WTW series 720 meter. In the case of AM-14, the measurement was not performed over all pH range (0-9) as in the case of AM-11, due to material stability.

II.1.2.3. Batch sorption experiments

All the material was washed before the experiments with nitric acid 25 % for 24 hours and then plenty rinsed with ultra-pure water. The ability of niobium and vanadium silicates to sorb Hg(II) from solution was assessed by contacting each microporous material with solutions of fixed concentration for a determined period of time. All assays were performed in batch conditions, at 22 ± 1 °C in 1 dm^3 volumetric flasks magnetically stirred at 500 rpm. The Hg(II) solutions were prepared diluting the standard solution in high purity water (18.2 MΩ) to the desired initial concentration (1 mg dm^{-3}). The pH of the solutions was adjusted to 6 with 0.1 mol dm^{-3} NaOH. A blank experiment (without the niobium or vanadium silicate) was always run as control under the same operating conditions. Rigorous masses of AM-11 or AM-14 were added to the previous aqueous solutions and this moment was considered the initial time of the experiment. Solution

samples were withdrawn at increasing times, filtered with a Millipore membrane of 0.45 μm, adjusted to pH < 2 with HNO_3 and immediately analysed afterwards. The concentration of Hg(II) in the samples was measured using a cold vapour atomic fluorescence spectroscope (CV-AFS), on a PSA cold vapour generator (model 10.003) coupled to a Merlin PSA detector (model 10.023). The liquid samples containing mercury were introduced in the equipment, the Hg(II) was reduced by $SnCl_2$ to its elemental form and quantified in the detector. The response was obtained as a signal and converted to concentration through a calibration curve.

For AM-11, twelve experiments were accomplished: ten to determine equilibrium points and two to measure kinetic removal curves (in this case, the final points were also used to get additional equilibrium data). For AM-14, eleven experiments were carried out: nine to obtain isotherm points, and the remaining two to generate removal curves (and also two extra equilibrium data). The detailed experimental conditions can be found in Table II.1.1.

Table II.1.1. Experimental conditions studied: Temperature = 22 ± 1 °C, solution volume = 1 dm^3, initial Hg(II) concentration = 1 mg dm^{-3}.

No. of Exp. for AM-11	**1**	**2**	**3**	**4**	**5**	**6**	**7**	**8**	**9**	**10**	**11**	**12**
Mass of AM-11 (mg)	1.0	1.5	2.5	3.7	5.1	6.0	7.0	8.0	10.0	12.1	6.5	14.0
Data measured	Equilibrium										Kinetic and equilibrium	
No. of Exp. for AM-14	**13**	**14**	**15**	**16**	**17**	**18**	**19**	**20**	**21**	**22**		**23**
Mass of AM-14 (mg)	1.5	2.0	2.5	3.0	3.8	4.0	5.0	10.0	12.0	6.5		3.5
Data measured	Equilibrium									Kinetic and Equilibrium		Kinetic

The average amount of sorbed Hg(II) per unit mass of microporous material, q_A (mg g^{-1}), was calculated by material balance to the whole system at time t:

$$q_A = \frac{V_L}{m_S}(C_{A0} - C_A) \quad \text{(II.1.1)}$$

where subscript A denotes mercury(II), V_{L} (dm^3) is the solution volume, m_{S} (g) is the mass of AM-11 or AM-14, C_{A0} (mg dm^{-3}) is the initial concentration of Hg(II) in solution, and C_{A} (mg dm^{-3}) is its concentration at any time t

II.1.2.4. Kinetic and equilibrium modelling

II.1.2.4.1. Kinetic models

The kinetics of Hg(II) ion exchange on AM-11 and AM-14 was experimentally studied by batch ion exchange assays. Kinetic data depend on the chemical and structural properties of the materials, stirring velocity, and the inherent transport properties of the system. The pursue of sorption elucidate the viability of the ion exchange process to remove contaminants (Azizian, 2004).

Ion exchange is essentially a diffusion process subject to a stoichiometric restriction, therefore its rate depends on the mobilities of both counter ions. This process is distinct from a chemical reaction in the usual sense, though some simple empirical or semi-empirical expressions, which were initially derived for adsorption considering the process as a chemical reaction, are frequently adopted to fit ion exchange kinetic data with the aim to evaluate the behaviour of the process. One may cite, for instance, the pseudo-first order (PFO), pseudo-second order (PSO) and Elovich equations. Accordingly, the significance of the intrinsic parameters has little in common with the rate constants of chemical reactions (Helfferich, 1962). Phenomenological principles-based models should be preferred in order to obtain theoretically consistent information about the process. Rodrigues and Silva (Rodrigues and Silva, 2016) compared the PFO equation with the linear driving force model of Glueckauf, and demonstrated that the kinetic constants of both models showed relevant differences mainly in their temperature dependence. Nonetheless, in the case of linear isothermal conditions the two models are formally equivalent. In this work, the above mentioned models were applied to fit the experimental data and extract information about the Hg(II) removal from aqueous solutions.

The PFO equation of Lagergren (Aksu, 2005; Lagergren, 1898) assumes that the uptake kinetics is proportional to the distance to the final equilibrium concentration:

$$\frac{dq_A}{dt} = k_1(q_{Ae} - q_A) \quad \text{(II.1.2)}$$

where k_1 (h^{-1}) is a rate constant, q_{Ae} (mg g^{-1}) is the concentration of sorbed metal at final equilibrium, and t (h) is time. After integration from the initial clean particle condition ($t = 0$, $q_A = 0$) to any time t and solid loading q_A, one obtains:

$$ln(q_{Ae} - q_A) = ln\, q_{Ae} - k_1 t \quad \text{(II.1.3)}$$

The PSO model (Ho and McKay, 1999) can also be applied to represent the ion exchange kinetics along time. Its corresponding differential and integrated expressions embody a rate constant (k_2, g mg^{-1} h^{-1}) and are given by:

$$\frac{dq_A}{dt} = k_2(q_{Ae} - q_A)^2 \quad \text{(II.1.4)}$$

$$\frac{t}{q_A} = \frac{1}{k_2 q_{Ae}^2} + \frac{1}{q_{Ae}} t \quad \text{(II.1.5)}$$

The Elovich equation (Ho et al., 2002; Roginsky and Zeldovich, 1934) describes the sorption kinetics on heterogeneous surfaces, and it is represented by:

$$\frac{dq_A}{dt} = \alpha e^{-\beta q_A} \quad \text{(II.1.6)}$$

$$q_A = \frac{1}{\beta} ln(\alpha\beta) + \frac{1}{\beta} ln\, t \quad \text{(II.1.7)}$$

where α is the initial sorption rate (mg g^{-1} h^{-1}) and β (g mg^{-1}) is the desorption constant.

With the objective to estimate the intraparticle diffusion coefficient of the counter ions of interest, a phenomenological model based on the kinetic equations of Nernst-Plank formalism (Cardoso et al., 2016; Helfferich, 1962; Lito et al., 2013, 2012) has also been included in the calculations.

II.1.2.4.2. Equilibrium models

The study of equilibrium is essential for evaluating the viability of sorption processes. Relevant properties and the affinity of the ion exchange system can be disclosed by isotherms, being important for the effective design of metal removal process (Ho et al., 2002). The most relevant two-parameter isotherms (Langmuir, Freundlich, Temkin and Dubinin-Radushkevich) and three-parameter isotherms (Langmuir-Freundlich, Redlich-Peterson and Toth) were selected in this essay to represent the experimental data.

Langmuir Isotherm. This is the most known isotherm and assumes that the sorbent contains a finite number of equivalent active sites, the sorption energy is uniform, the sorbed phase is ideal and forms a monolayer at solid surface (Dada et al., 2012; Langmuir, 1916). It is given by:

$$q_e = \frac{q_{m,L} K_L C_e}{1 + K_L C_e} \quad \text{(II.1.8)}$$

where $q_{\mathrm{m,L}}$ (mg g^{-1}) is the sorption capacity, related with monolayer coverage, and K_{L} (dm^3 mg^{-1}) is the Langmuir equilibrium constant.

Freundlich Isotherm. This equation is applied to non-ideal systems, with heterogeneous surfaces and multilayer sorption, and assumes an exponentially decaying function of site density with respect to the sorption energy (Freundlich, 1906; Ho et al., 2002):

$$q_e = K_F C_e^{1/n_F} \quad \text{(II.1.9)}$$

Here, K_{F} ($mg^{1-1/nF}$ $dm^{3/nF}$ g^{-1}) and n_{F} are the Freundlich constants. The parameter n_{F} is related with the nonlinearity of the model: the larger is this value, more nonlinear is the isotherm (Do, 1998). One limitation of Freundlich model is that under extremely low concentrations it does not recover the Henry's law, which would be expected in advance.

Temkin Isotherm. This equation assumes that the heat of sorption, E_θ, decreases linearly with fractional coverage θ (Bourane et al., 2002). As in the case of Freundlich isotherm, it does not exhibit a finite saturation limit (Do, 1998). It is mathematically given by:

$$\theta = \frac{RT}{\Delta E} ln(AC_{Ae}) \quad \text{(II.1.10)}$$

where ΔE (J mol^{-1}) represents the variation of the heats of sorption corresponding to the particle initially free of solute ($\theta = 0$) and at maximum coverage ($\theta = 1$), $R = 8.314$ J mol^{-1} K^{-1} is the ideal gas constant, T (K) is the absolute temperature, and A (dm^3 mg^{-1}) is the isotherm equilibrium binding constant. Setting $B = q_{\mathrm{m,T}} RT/\Delta E$ (mg g^{-1}), the equation is rewritten as:

$$q_{Ae} = B ln(AC_{Ae}) \quad \text{(II.1.11)}$$

Dubinin-Radushkevich Isotherm. This equation was originally developed for adsorption and is based on the potential theory of Polanyi (Polanyi, 1914). The process relies on the micropore volume filling concept instead of a layer-by-layer adsorption onto pore walls, and takes into account the energetic heterogeneity of the solid and the interactions between sorbed species (Dubinin, 1960; Inglezakis, 2007). It is frequently extended to ion exchange equilibrium (Ali Khan et al., 1994; Rashid et al., 2014). The isotherm is described by:

$$q_e = q_{m,DR} e^{-B_{DR}\,\varepsilon^2} \quad \text{(II.1.12)}$$

$$\varepsilon = RT\, ln[1 + \frac{1}{C_e}] \quad \text{and} \quad E = [\frac{1}{\sqrt{2B_{DR}}}] \quad \text{(II.1.13)}$$

where $q_{\mathrm{m,DR}}$ (mg g^{-1}) is the solid capacity, B_{DR} (mol^2 J^{-2}) is the Dubinin-Radushkevich constant, ε (J mol^{-1}) is the Polanyi potential**.** The magnitude of E represents the free

energy change when 1 mol of solute is transferred to the surface of the solid and may be used to distinguish the sorption mechanisms**.**

Langmuir-Freundlich isotherm. At low concentrations, this three-parameter isotherm is essentially the Freundlich isotherm and, at high sorbate concentrations, it predicts a monolayer sorption characteristic of Langmuir model (Figueira et al., 2011; Ho et al., 2002). The Langmuir-Freundlich equation is given by:

$$q_{Ae} = \frac{q_{m,LF}(K_{LF}C_{Ae})^{n_{LF}}}{1 + (K_{LF}C_{Ae})^{n_{LF}}} \quad \text{(II.1.14)}$$

where $q_{\mathrm{m,LF}}$ (mg g^{-1}) is the capacity of the material, K_{LF}(dm^3 mg^{-1})$^{n\mathrm{LF}}$ is the Langmuir-Freundlich constant, and n_{LF} is the heterogeneity index, which varies from 0 to 1. If the material is homogeneous, n_{LF} is assumed to be 1, if the material is heterogeneous, n_{LF} gets values lower than 1 (Umpleby et al., 2001).

Redlich-Peterson Isotherm. This model embodies characteristics of both Langmuir and Freundlich isotherms (Ho et al., 2002). It can be expressed as follows:

$$q_{Ae} = \frac{K_{RP}C_{Ae}}{1 + a_{RP}C_{Ae}^{n_{RP}}} \quad \text{(II.1.15)}$$

where K_{RP} (dm^3 g^{-1}) and a_{RP} (dm^3 mg^{-1})$^{n\mathrm{RP}}$ are the Redlich-Peterson constants, and n_{RP} is the isotherm exponent. At low concentrations the Henry's law is recovered and at high concentrations it approaches Freundlich behaviour (Ho et al., 2002).

Toth Isotherm. This model is derived considering the potential theory and it is applicable to heterogeneous sorption. It assumes a quasi-Gaussian energy distribution and most sites exhibits sorption energies lower than the mean value (Allen et al., 2004; Ho et al., 2002). It is represented by the following equation:

$$q_e = \frac{q_{m,Th} C_e}{(a_{Th} + C_e^{n_{Th}})^{1/n_{Th}}} \quad \text{(II.1.16)}$$

where $q_{\mathrm{m,Th}}$ (mg g^{-1}) is the solid capacity, a_{Th} (mg dm^{-3})$^{n_{\mathrm{Th}}}$ is the Toth isotherm constant, and n_{Th} the isotherm exponent.

II.1.2.4.3. Error analysis

All the parameters of the kinetic and equilibrium models were obtained by nonlinear regression using the Nelder-Mead simplex algorithm to minimize the error between calculated and experimental data. With the aim to find out the most suitable models, the coefficient of determination (R^2), the adjusted coefficient of determination (R^2_{adj}), the average absolute relative deviation ($AARD$), the sum of squares (SS), and the Akaike's Information Criterion (AIC) (Malash and El-Khaiary, 2010) were calculated. The corresponding definitions and mathematical expressions are given by:

$$R^2 = 1 - \frac{\sum(\hat{y}_i - y_i)^2}{\sum(y_i - \bar{y})^2} \quad \text{(II.1.17)}$$

$$R^2_{adj} = 1 - (1 - R^2)\frac{(N_{DP}-1)}{(N_{DP}-N_P-1)} \quad \text{(II.1.18)}$$

$$AARD(\%) = \frac{100}{N_{DP}} \sum_{i=1}^{N_{DP}} \frac{|\hat{y}_i - y_i|}{y_i} \quad \text{(II.1.19)}$$

$$SS = \sum(\hat{y}_i - y_i)^2 \quad \text{(II.1.20)}$$

$$AIC = N_{DP}\, ln\left(\frac{SS}{N_{DP}}\right) + 2N_P + \frac{2N_P(N_P+1)}{N_{DP}-N_P-1} \quad \text{(II.1.21)}$$

where N_{DP} is the number of data points, N_{P} is the number of parameters, y_{i} and $\hat{y}_{\mathrm{i}}$ are the experimental and calculated values for point i, respectively, and $\bar{y}$ is the average of all observed values. The value of AIC determines which model is more likely to be correct and quantifies how much more likely. The lower the AIC (on a scale from -∞ to +∞) the

better is the model to describe the experimental data than the alternative models (Malash and El-Khaiary, 2010).

II.1.3. Results and discussion

III.1.3.1. Characterization of AM-11 and AM-14 microporous materials

Figure II.1.1 shows the X-Ray diffractograms of the synthesized AM-11 and AM-14 used for the Hg(II) removal studies, revealing that they are identical to those published by Rocha et al.(1998) and Brandão et al. (2002a), respectively. SEM images presented in Figure II.1.2 reveal that both microporous materials contain only a single phase: the AM-11 crystals are needles with *ca*. 10 µm in length and AM-14 consists of thin plates with size of *ca*. 1-2 µm. Table II.1.2 shows the percentages of N, Si and Nb for AM-11, and of Na, Si and V for AM-14, as well as the main molar ratios. The molar ratio between Si and Nb in AM-11 is 4.5, and in AM-14 Si/V is 4, which are in accordance to the values published previously. The theoretical ion exchange in AM-14 is performed by 2 mol of Na for each mol of V, and in AM-11, according with the amount of nitrogen (Table II.1.2), by one cation NH_4^+ for each Nb present. The TGA curves shown in Figures II.1.3a and II.1.3b were obtained under air for both materials. The curves reveal a gradual weight loss from room temperature until 800 °C for AM-11, and until 700 °C for AM-14. Total mass losses were 13 % (AM-11) and 14 % (AM-14), although only 4-5 % were observed below 100 °C, suggesting loss of adsorbed water. Losses at higher temperatures were most likely due to the release of water molecules strongly coordinated with the cations, which is related with the structure of the materials.

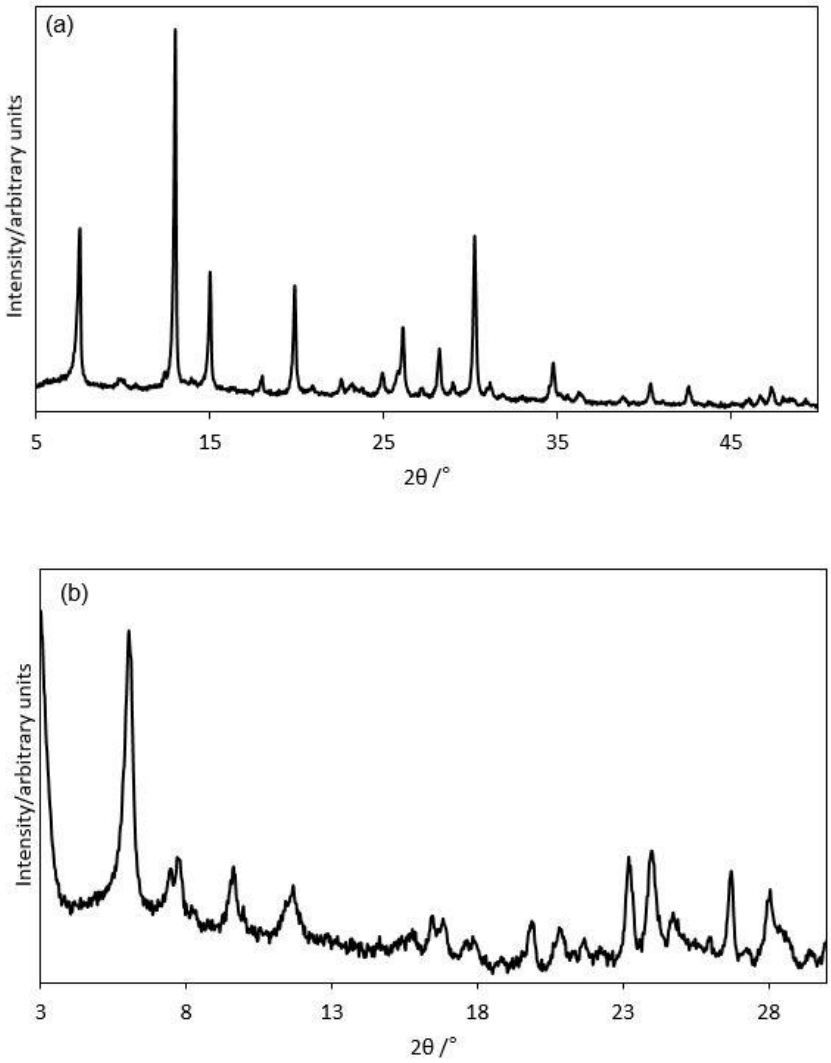

Figure II.1.1. PXRD patterns of AM-11 (a) and AM-14 (b).

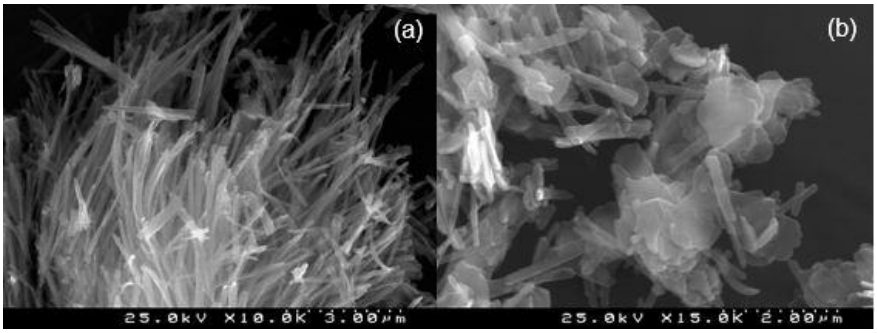

Figure II.1.2. SEM images of AM-11 (a) and AM-14 (b)

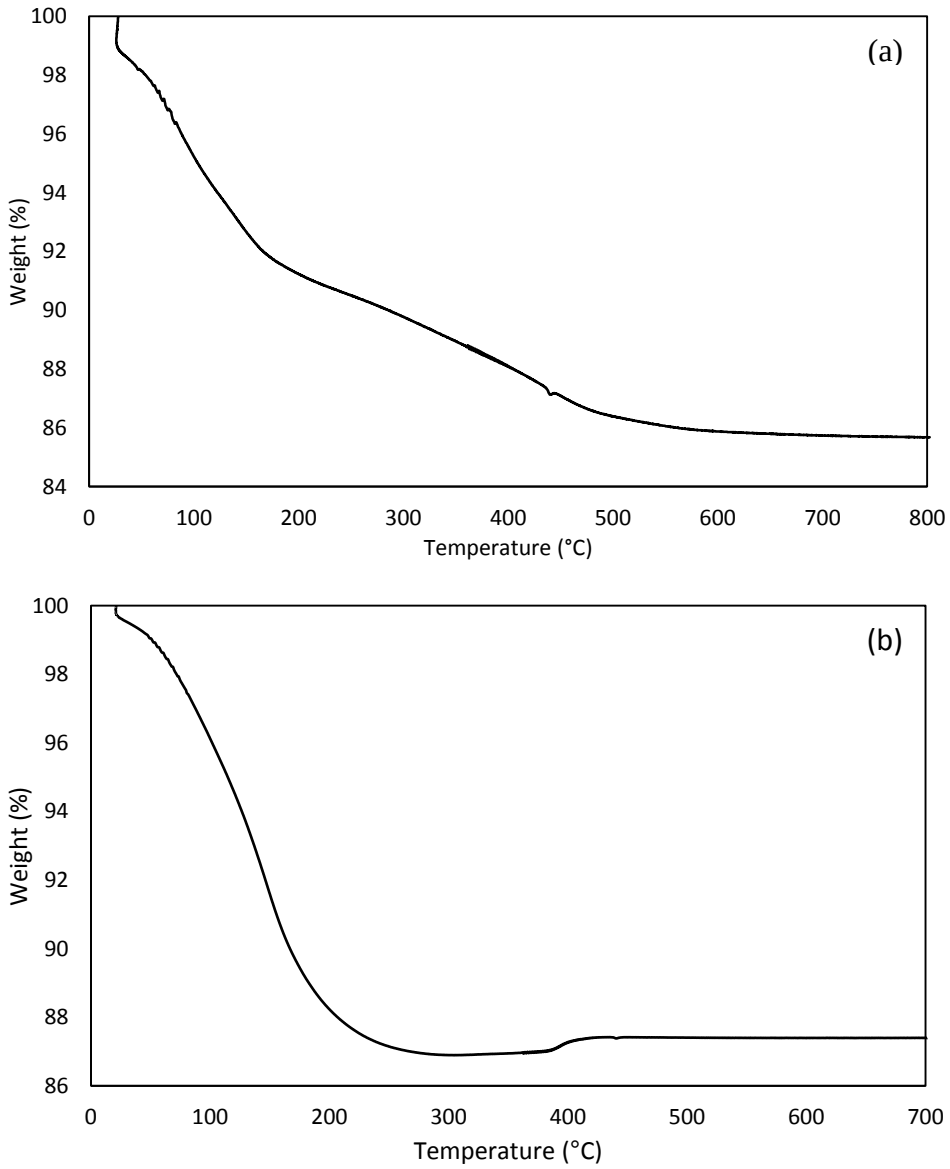

Figure II.1.3. TGA curve of AM-11 (a) and AM-14 (b).

Table II.1.2. Composition of AM-11 and AM-14

Material	Concentrations (wt.%)			Molar ratios (mol/mol)	
AM-11	N	Si	Nb	Si/Nb	N/Nb (mol/mol)
	2.7	23	17	4.5	1.0
AM-14	Na	Si	V	Si/V	Na/V
	8.7	27	10	4.0	2.0

The measurement of the Point of Zero Charge (PZC) of both materials was also considered (see Figure II.1.4): in the case of AM-11, the characteristic |ΔpH| versus initial pH curve is always negative over pH range 0-9, which means the microporous silicate surface is negatively charged, with advantage for cation exchange (in this essay, pH was constant and equal to 6). In the case of AM-14 the same occurs at pH 6, i.e. surface is negatively charged, and similar conclusions may be drawn.

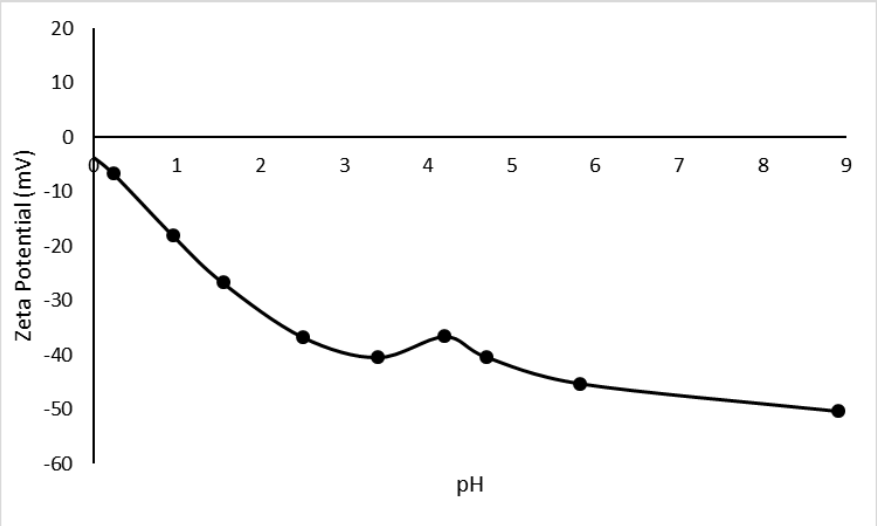

Figure II.1.4. Point of Zero Charge plot (measured |ΔpH| against initial pH) of AM-11.

II.1.3.2. Removal of Hg(II) by AM-11 and AM-14 materials

The variation with time of the normalized Hg(II) concentration, for two masses of AM-11 and AM-14, is presented in Figure II.1.5. During ion exchange, it is possible to distinguish two periods for the two quantities of materials. In the first 48 h the removal is faster than the slower subsequent period towards the equilibrium. This pattern mirrors the large driving force for mass transport at the beginning of the process, when particles are free of Hg(II) or contain negligible quantities of the metal.

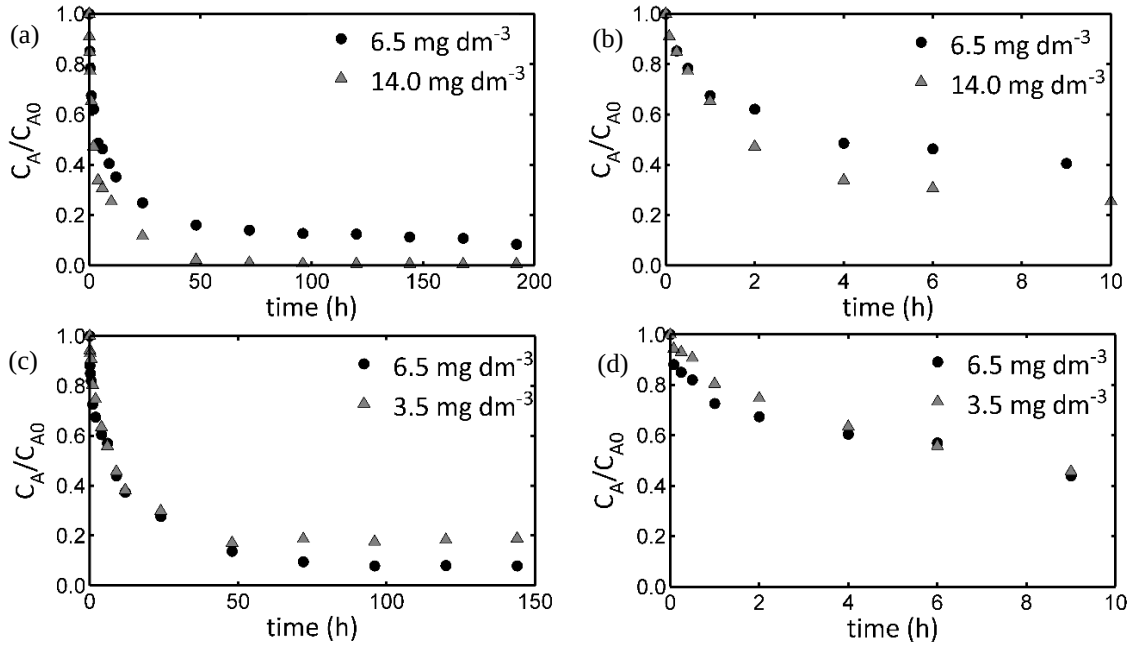

Figure II.1.5. Normalized Hg(II) concentration in the liquid phase for AM-11 ((a) and (b)) and AM-14 ((c) and (d)); two quantities of sorbents were tested

Despite the differences between AM-11 and AM-14, the kinetic curves and the removal efficiencies of both materials towards Hg(II) are very similar under the same operating conditions. For instance, only 6.5 mg dm^{-3} of microporous materials were able to remove 92 % of the Hg(II) initially present in solution, reflecting the great ion exchange capacity of AM-11 and AM-14. Moreover, no relevant differences were observed on the kinetics of the two materials: the initial rates had the same order of magnitude (0.607 and 0.528 mg dm^{-3} h^{-1}, values calculated from the first derivate of $C_A = f(t)$ at $t = 0$), and the equilibrium time was approximately 96 h for both, although the dimensionless concentration in the case of AM-11 decreased smoothly until 192 h.

The experiments performed with two material doses emphasize the effect of mass on the removal process. Increasing the dose of AM-11 from 6.5 to 14.0 mg dm^{-3} led to an additional removal from 92 to 99 % of Hg(II) from solution, while the dose increment of AM-14 from 3.5 to 6.5 mg dm^{-3} resulted in the uptake of 81 to 92 % of the Hg(II) initially present in solution. These results are naturally due to the fact that more mass provides additional sorption sites available for ion exchange. The equilibrium time was not very sensitive to the changes in the amount of material, although slightly smaller equilibrium

time was found for the higher mass of AM-11. Both materials showed fast kinetics, even smaller masses being sufficient to remove more than 70 % of the Hg(II) in solution during the first 24 hours.

In Figure II.1.6 it is plotted the mercury speciation in aqueous solution for the experimental conditions of this essay, namely, initial metal concentration of 1 mg dm^{-3} and temperature of 22±1 °C. It is possible to conclude that mercury occurs as neutral ($Hg(OH)_2$) and positive ($[Hg(OH)]^+$ and Hg^{2+}) species, while complexes with NO^{3-} are negligible and thus not represented. At pH 6 the predominant form is $Hg(OH)_2$ and no precipitation was detected. This fact implies that at particle surface the solution equilibrium is shifted to the mercury(II) form, and then ion exchange proceeds subjected to the already discussed steric and Donan restrictions.

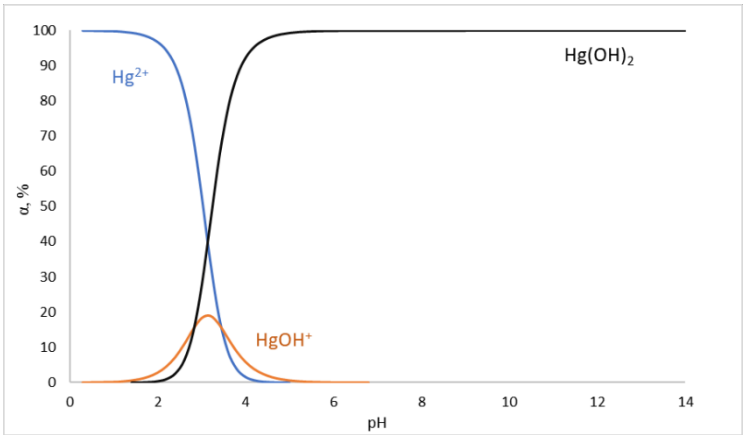

Figure II.1.6. Mercury speciation in aqueous solution at 22 °C for an initial metal concentration of 1 mg dm^{-3}.

The excellent performances of AM-11 and AM-14 obtained in this work are very promising for waters treatment, though real systems involve competitive ions that may interfere with the Hg(II) uptake. Nonetheless, studies in literature using zeolites report little or no impacts upon Hg(II) removal by the presence of competitive ions in solution (Czarna et al., 2018; Cláudia B Lopes et al., 2008). Materials like ETS-10, ETS-4, AM-2 and AV-13 exhibited similar sorption efficiencies in seawater or in solutions containing $MgSO_4$ or NaCl (Cláudia B Lopes et al., 2008). Furthermore, the performances of the zeolites Ag-X, Na-A, Na-X, 13X and 4A for Hg(II) removal from an industrial wastewater were not penalized by the presence of foreign ions (Czarna et al., 2018). On the other hand, Hg(II)

sorption using biosorbents, like E. globulus bark, decreased with increasing NaCl concentration in solution (Fabre et al., 2019b). The same happened in the case of bracken ferns (Carro et al., 2010) but no influence was observed in the case of Hg(II) removal by banana peels (Fabre et al., 2019a). In another study, the addition of NaCl and Cu(II) decreased Hg(II) sorption using Cystoseira baccat, while the existence of Cd(II), Mg(II), Zn(II) and Ca(II) did not penalize Hg(II), and the presence of Pb(II) improved the biosorbent removal efficiency (Herrero et al., 2005).

Desorption studies also need to be considered in order to reuse the synthetic materials and recover the sorbed metal if it is of interest. Depending on the easiness of desorption, the solid may be subsequently applied for several cycles as long as its efficiency, stability and structure are maintained (Melamed and da Luz, 2006). For instance, in the particular case of mercury, its desorption from functionalized zeolite PPy/SH-Beta/MCM-41 using 0.5 M H_2SO_4 was able to recover more than 90 % of the metal. The efficiency of the sorbent was analysed during five cycles and it was possible to remove Hg(II) in all of them, although metal removal was decreasing along the cycles (Javadian and Taghavi, 2014). In a different work, Hg(II) was removed from aqueous solutions using titanosilicate ETS-4 in fixed-bed (C B Lopes et al., 2012) and its regeneration was successfully accomplished with a concentration gradient (0.05–0.25 M) of EDTA-Na_2 solution. The metal recovery was very fast and reached 98 % with a concentration factor of 920 (ratio between the maximum peak concentration during elution and the initial metal concentration). The utilization of $NaNO_3$ solutions (10-3 M) was also tested to guarantee the complete elution of Hg(II) and Cd(II) from loaded ETS-4 (Otero et al., 2009).

II.1.3.3. Modelling

The solid loadings along time were modelled by PFO, PSO and Elovich equations. The variation with time of the experimental and calculated Hg(II) concentrations in the materials are shown in Figures II.1.7 and II.1.8. The PSO and Elovich models show the best fit to the experimental data. The PSO model have presented good description of the kinetic data from other mercury removal processes reported in the literature (Figueira et

al., 2011; Zandi-Atashbar et al., 2018). In general, there is a good agreement between the Elovich fitting and the experimental q_A values for the ascend branch, while the PSO expression achieved a better performance on the horizontal branches of each curve. Moreover, the AARDs found for the microporous materials in the first 6 h were between 2.96 % and 8.18 % for the Elovich model and between 12.1 % and 24.6 % for the PSO model, which confirms the above mentioned. The best fit parameters are shown in Table II.1.3, and the values of the rate constants (k_1, k_2 and α) of the PFO, PSO and Elovich models follow the sorbent mass tendency, lower values for the smaller doses of material.

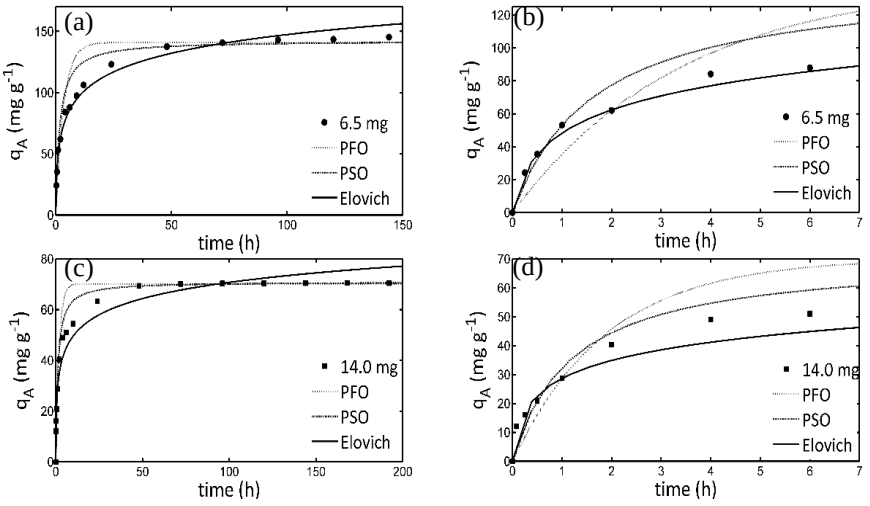

Figure II.1.7. Sorption kinetics modelling for the AM-11 particles: (a) and (b) represent the sorbent dosage of 6.5 mg dm^{-3}, (c) and (d) represent the sorbent dosage of 14.0 mg dm^{-3}.

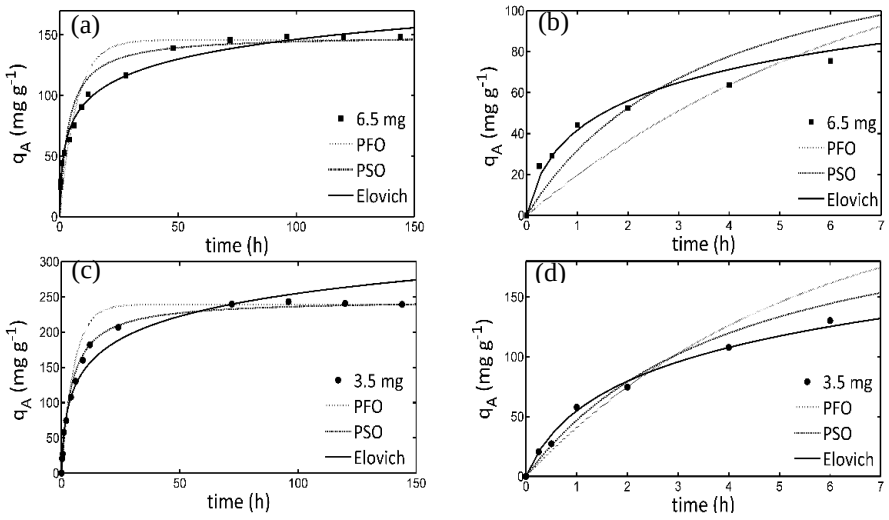

Figure II.1.8. Sorption kinetics modelling on the AM-14 particles ((a) and (b) represent the sorbent dosage of 6.5 mg dm^{-3}, (c) and (d) represent the sorbent dosage of 3.5 mg dm^{-3}

Table II.1.3. PFO, PSO and Elovich constants for Hg(II) sorption on AM-11 and AM-14.

Kinetic Model	**Fitted parameters of AM-11**			R^2	R^2_{adj}	*AARD*	*AIC*
PFO	$q_{e\,Exp}$ (mg g^{-1})	$q_{e\,Adj}$ (mg g^{-1})	k_1(h^{-1})				
6.50 mg	150	1419	0.291	0.916	0.902	16.5	98.7
14.0 mg	70.5	70.1	0.526	0.940	0.930	15.1	69.6
PSO	$q_{e\,Exp}$ (mg g^{-1})	$q_{e\,Adj}$ (mg g^{-1})	k_2(g·mg^{-1}·h^{-1})				
6.50 mg	150	142	0.00420	0.951	0.943	9.93	87.5
14.0 mg	70.5	71.0	0.0118	0.977	0.973	9.44	55.9
Elovich		α (mg g^{-1} h^{-1})	β (g mg^{-1})				
6.50 mg		176	0.0453	0.987	0.985	4.17	67.6
14.0 mg		198	0.108	0.972	0.967	7.70	71.7
Kinetic Model	**Fitted parameters of AM-14**			R^2	R^2_{adj}	*AARD*	*AIC*
PFO	$q_{e\,Exp}$ (mg g^{-1})	$q_{e\,Adj}$ (mg g^{-1})	k_1(h^{-1})				
6.50 mg	148	146	0.223	0.949	0.941	19.8	84.9
3.50 mg	239	239	0.187	0.970	0.964	13.9	87.0
PSO	$q_{e\,Exp}$ (mg g^{-1})	$q_{e\,Adj}$ (mg g^{-1})	k_2(g·mg^{-1}·h^{-1})				
6.50 mg	148	152	0.0017	0.960	0.953	14.3	76.2
3.50 mg	239	246	0.0010	0.993	0.992	6.97	59.9
Elovich		α (mg g^{-1} h^{-1})	β (g mg^{-1})				
6.50 mg		114	0.0422	0.990	0.988	5.21	52.7
3.50 mg		104	0.0212	0.974	0.969	7.48	80.7

With respect to the calculated results achieved by the Nernst-Plank based model and the corresponding intraparticle diffusivities of counter ions, the following points can be highlighted: (i) AARD = 16.9 % for AM-11 and AARD = 10.1 % for AM-14. These are good results taking into account that the two curves for the same material were fitted simultaneously with only two parameters. (ii) The self-diffusivity of Hg(II) was 2.561×10^{-19} m^2 s^{-1} for AM-11 and 3.342×10^{-19} m^2 s^{-1} for AM-14. These values can be directly ascribed to the larger pore diameter of AM-14 (6.8 Å) in comparison with AM-11 (4 Å). (iii) The self-diffusivity of the counter ion of AM-11 (NH_4^+) was 4.593×10^{-19} m^2 s^{-1}, while for AM-14 (Na^+) it was 1.480×10^{-18} m^2 s^{-1}. The faster kinetics found in the case of AM-14 dues to the combined action of two positive effects, namely, the larger pore size of this solid and the smaller diameter of Na^+ (in opposition to NH_4^+). (IV) Finally, the estimated convective mass transfer coefficients were k_f(AM-11) = 8.5×10^{-4} m s^{-1} and k_f(AM-14) = 2.5×10^{-3} m s^{-1}.

The properly understanding about the ion exchange systems involves a good description of the equilibrium behaviour. The analysis of the isotherm curves allows to find out the best equation for design purposes, and their parameters unveil information about the surface characteristics and metal-sorbent affinity (Ho et al., 2002; Maleki et al., 2019). The main two-parameter and three-parameter isotherms are plotted for AM-11 and AM-14 in Figure II.1.9, together with the experimental data. Both materials display favourable isotherms, and the uptake ability increases until it reaches a saturation *plateau* for AM-11, which establishes the capacity of this material. However, the same behaviour cannot be observed for AM-14 since the uptake continues to improve along the range of tested conditions. Agreeing with the Giles classification (Giles et al., 1960), which divides all isotherms into four main classes according with their initial slope and curve trend – S, L ("Langmuir"), H ("high affinity") and C ("constant partition") – the ion exchange of Hg(II) by AM-11 follows the H-type curve pattern while in the case of AM-14 it seems to follows the L-type. In the L-type isotherm the initial curvature shows that as more sites in the AM-14 are filled it becomes increasingly difficult for Hg(II) to find a vacant site available (Giles et al., 1960). The H-type is considered a special case of the L-type curve, in which the initial part of the isotherm is vertical due to the high affinity of the solute by the sorbent. Hence, in dilute solutions the solute tends to be completely

sorbed, or at least there is no measurable amount remaining in solution (Giles et al., 1960).

The optimized parameters of the equilibrium models, the adjusted coefficient of determination, the average absolute relative deviations and the values of Akaike's Information Criterion are listed in Table II.1.4 for AM-11 and in Table II.1.5 for AM-14.

In general, the AM-11 and AM-14 equilibrium results are well described by all isotherms excluding Freundlich. According to the results obtained, the Langmuir equation describes better the Hg(II)/AM-11 system ($AARD$=3.58 %, R^2_{adj}=0.980) and the lowest AIC value observed (52.8) corroborates with this statement. The sorbent achieves a *plateau*, in accordance with the monolayer sorption characteristic of this model, and indicates an uptake capacity of 161 mg g^{-1}. The model also suggests that all active sites on the AM-11 surface possess equal affinity for Hg(II) and constant sorption energy (Ho et al., 2002). The mean sorption energy (E, kJ mol^{-1}) can be calculated through the Dubinin-Radushkevich parameter. The calculated value of $E = 9.91$ kJ mol^{-1} denotes the free energy change when the Hg(II) is sorbed onto the solid surface. According to Helfferich (1962), as ion exchange is not a chemical reaction, the values of heat involved in the processes should be small. Normally such energy is lower than 8 kJ mol^{-1}, but values up to 40 kJ mol^{-1} have been observed in exceptional cases (Helfferich, 1962). Therefore, it is possible to conclude that in the case of the system Hg(II)/AM-11 the removal is conducted by ion exchange. The difference between the experimental (1.60 meq g^{-1}) and theoretical (2.12 meq g^{-1}) ion exchange capacity of AM-11 suggests that some active sites may be not accessible to Hg ions.

Table II.1.4. Isotherm parameters for Hg(II) sorption on AM-11.

No. of param	Model	Fitted parameters			R^2	R^2_{adj}	AARD	AIC
2	Langmuir	qm_L (mg g^{-1})	K_L (dm^3 mg^{-1})					
		161	149		0.984	0.980	3.58	52.8
2	Freundlich	K_F (mg$^{1-1/nF}$ dm$^{3/nF}$ g^{-1})	n_F					
		181	7.03		0.901	0.879	9.00	76.1
2	Temkin	A (dm^3 mg^{-1})	B (mg g^{-1})					
		1.81E+04	18.1		0.922	0.905	8.07	71.6
2	Dubinin-Radushkevich	qm_{DR}(mg g^{-1})	B_{DR} (mol^2 kJ^{-2})					
		171	5.09E-09		0.953	0.942	5.65	67.6
3	Langmuir-Freundlich	qm_{LF} (mg g^{-1})	K_{LF} (dm^3 mg^{-1})^{nLF}	n_{LF}				
		162	143	0.898	0.981	0.974	3.58	60.0
3	Redlich-Peterson	K_{RP} (dm^3 g^{-1})	a_{RP} (dm^3 mg^{-1})^{nRP}	n_{RP}				
		2.26E+04	141	1.02	0.983	0.977	3.56	55.4
3	Toth	qm_{Th} (mg g^{-1})	a_{Th} (mg dm^{-3})^{nTh}	n_{Th}				
		160	3.30E-03	1.18	0.984	0.978	3.56	54.3

Table II.1.5. Isotherm parameters for Hg(II) sorption on AM-14.

No. of param.	Model	Fitted parameters			R^2	R^2_{adj}	$AARD$	AIC
2	Langmuir	qm_L (mg g^{-1})	K_L (dm^3 mg^{-1})					
		304	10.8		0.983	0.978	3.93	59.3
2	Freundlich	K_F (mg$^{1-1/nF}$ dm$^{3/nF}$ g^{-1})	n_F					
		343	2.63		0.968	0.959	7.11	66.6
2	Temkin	A (dm^3 mg^{-1})	B (mg g^{-1})					
		135	61.4		0.988	0.985	3.92	54.2
2	Dubinin-Radushkevich	qm_{DR}(mg g^{-1})	B_{DR} (mol^2 kJ^{-2})					
		292	1.74E-08		0.988	0.984	4.30	55.5
3	Langmuir-Freundlich	qm_{LF} (mg g^{-1})	K_{LF} (dm^3 mg^{-1})^{nLF}	n_{LF}				
		337	8.92	0.799	0.988	0.982	3.72	58.4
3	Redlich-Peterson	K_{RP} (dm^3 g^{-1})	a_{RP} (dm^3 mg^{-1})^{nRP}	n_{RP}				
		5.30E+03	16.8	0.860	0.989	0.983	3.63	58.1
3	Toth	qm_{Th} (mg g^{-1})	a_{Th} (mg dm^{-3})^{nTh}	n_{Th}				
		369	0.162	0.628	0.988	0.982	3.69	58.5

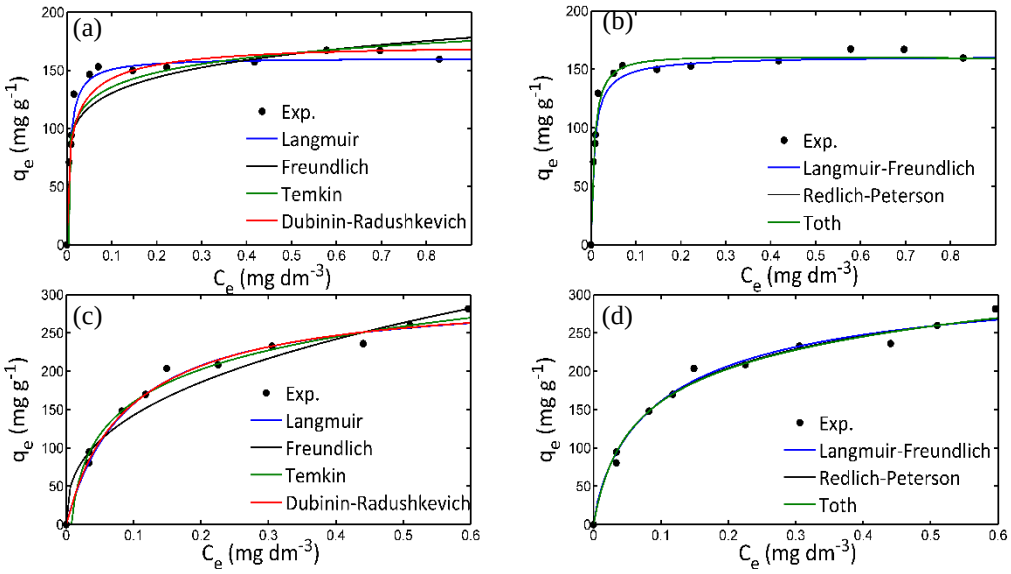

Figure II.1.9. Sorption equilibrium isotherms on the AM-11((a) two parameters and (b) three parameters) and AM-14 ((c) two parameters and (d) three parameters).

The experimental data of the Hg(II)/AM-14 system are slightly better fitted by Temkin isotherm ($AARD$=3.92 %, R^2_{adj}=0.985, AIC=54.2), disclosing that the solid surface is more heterogeneous. Despite the measured data do not achieve an horizontal branch under the operating conditions of this study, the highest uptake observed was 280 mg g^{-1} (or 2.79 meq g^{-1}) and the capacity obtained by the Langmuir model is 304 mg g^{-1} (3.03 meq g^{-1}). Once again, the estimated value of 3.03 meq g^{-1} is inferior to the theoretical ion exchange capacity (5.20 meq g^{-1}), and the sorption energy calculated from the Dubinin-Radushkevich parameters is characteristic of an ion exchange mechanism (E =5.36 kJ mol^{-1}). It is also interesting to mention a previous study performed with Hg(II)/ETS-4, for which the counter ions (Na^+ and Hg^{2+}) are the same as in AM-14, and the calculated sorption energy is quite similar, E =6.38 kJ mol^{-1} (Lopes et al., 2009).

II.1.3.4. Comparison with other sorbents

In the following it is accomplished a comparison between the performance of AM-11 and AM-14 with other materials from the literature, namely: titanosilicate ETS-4; a modified zeolitic mineral of clinoptiolite-heulandite called ZNaSS; activated carbon, considered an universal adsorbent; and magnetic nanoparticles functionalized with a high Hg-affinity funtional group (dithiocarbamate). The comparison was based on the

following quantities: sorbent doses used, initial mercury concentration and uptake removal (Table II.1.6).

Satisfactory Hg(II) removals are reported in various works. For example, ETS-4 (Lopes et al., 2009) showed a removal capacity of 246.3 mg g^{-1} and the dithiocarbamate grafted on magnetite particles (Figueira et al., 2011) presented an uptake capacity of 142.0 mg g^{-1} under the same initial Hg(II) concentration of 50 μg dm^{-3}. The sorption experiments using ZNaSS (Gebremedhin-Haile et al., 2003) and activated carbon (Ranganathan, 2003) were carried out under higher initial Hg(II) concentrations, in the range of 6.20-62.2 mg dm^{-3} for ZNaSS and 20.0 mg dm^{-3} for activated carbon, and the capacities reported for these materials are 10.1 and 13.3 mg g^{-1} respectively. The uptake capacities ($q_{\mathrm{m,L}}$) found for the microporous materials AM-11 (161 mg g^{-1}) and AM-14 (304 mg g^{-1}) were comparable and even higher than the other selected materials (Table II.1.6). These values were obtained using very low exchanger doses and highlight the great capacity of AM-14 and AM-11. The use of small quantities of AM-n materials is an advantage to treat a large volume of water, since small packed beds or stirred vessels are necessary to meet design specifications.

Table II.1.6. Parameters related to the Hg(II) removal by various sorbents performed at temperature of 22 ℃

Material	Sorbent doses studied (mg dm^{-3})	Hg(II) initial conc. (mg dm^{-3})	pH	q_{max} (mg g^{-1})	Reference
ETS-4	0.290-8.11	5.00E-02	4.0-5.0	246	(Lopes et al., 2009)
ZNaSS **	1.00E+04	6.20-62.2	3.0	10.1	(Gebremedhin-Haile et al., 2003)
Activated Carbon *	1.50E+03	20.0	5.5	43.9	(Ranganathan, 2003)
Dithiocarbamate grafted on Fe_3O_4 particles	0.248-6.13	5.00E-02	7.0	142	(Figueira et al., 2011)
AM-11	1.00-14.0	1.00	6.0	161	This study
AM-14	1.50-12.0	1.00	6.0	304	This study

(*) Experiment carried out at 30 ℃. (**) No information available about temperature.

II.1.4. Conclusions

The sorption ability of AM-11 and AM-14 towards Hg(II) was investigated carrying out batch stirred tank experiments. Even small masses of those sorbents are able to achieve trace final concentrations of mercury. The Hg(II) removal increased with increasing contact time and mass, being possible to distinguish a fast removal in the first 48 h followed by a slower removal towards the equilibrium. PSO and Elovich models are adequated to describe the ion exchange kinetics of both materials. The values of the rate constants found (k_1, k_2 and β) agree with the mass trend, *i.e*. higher initial rates for higher masses and *vice-versa*.

The Langmuir isotherm provides the best fit to the Hg(II)/AM-11 data, predicting a sorption capacity of 161 mg g^{-1} at room temperature and pH 6 (typical of various industrial effluents and other wastewaters). The experimental data of Hg(II)/AM-14 is slightly better fitted by Temkin model and despite the full capacity of the material was not attained under the conditions studied, the highest uptake observed was 280 mg g^{-1} and the maximum uptake predicted by Langmuir model is 304 mg g^{-1}. The low mean sorption energies calculated on the basis of Dubinin-Radushkevich equation indicate that ion exchange is the mechanism for Hg(II) removal by AM-11 and AM-14. For both systems, the theoretical exchange capacity is not achieved, which may suggest that some sites are not accessible to Hg(II) ions. The performance of these two microporous niobium and vanadium silicates to uptake Hg(II) from aqueous solutions was generally excellent in comparison with other sorbents published in the literature, emphasising its high potential as ion exchangers for wastewaters treatments.

II.1.5 References

Ahmed, S., Chughtai, S., Keane, M.A., 1998. The removal of cadmium and lead from aqueous solution by ion exchange with Na-Y zeolite. Sep. Purif. Technol. 13, 57–64.

https://doi.org/10.1016/S1383-5866(97)00063-4

Aksu, Z., 2005. Application of biosorption for the removal of organic pollutants: a review. Process Biochem. 40, 997–1026. https://doi.org/10.1016/j.procbio.2004.04.008

Ali Khan, S., Riaz-ur-Rehman, Ali Khan, M., 1994. Sorption of cesium on bentonite. Waste Manag. 14, 629–642. https://doi.org/10.1016/0956-053X(94)90035-3

Allen, S.J., Mckay, G., Porter, J.F., 2004. Adsorption isotherm models for basic dye adsorption by peat in single and binary component systems. J. Colloid Interface Sci. 280, 322–333. https://doi.org/10.1016/J.JCIS.2004.08.078

Araki, S., Li, T., Li, K., Yamamoto, H., 2019. Preparation of zeolite hollow fibers for high-efficiency cadmium removal from waste water. Sep. Purif. Technol. 221, 393–398. https://doi.org/10.1016/j.seppur.2019.04.011

Azizian, S., 2004. Kinetic models of sorption: a theoretical analysis. J. Colloid Interface Sci. 276, 47–52. https://doi.org/10.1016/j.jcis.2004.03.048

Baral, S.S., Das, N., Ramulu, T.S., Sahoo, S.K., Das, S.N., Chaudhury, G.R., 2009. Removal of Cr(VI) by thermally activated weed Salvinia cucullata in a fixed-bed column. J. Hazard. Mater. 161, 1427–1435. https://doi.org/10.1016/j.jhazmat.2008.04.127

Barreira, L.D., Lito, P.F., Antunes, B.M., Otero, M., Lin, Z., Rocha, J., Pereira, E., Duarte, A.C., Silva, C.M., 2009. Effect of pH on cadmium (II) removal from aqueous solution using titanosilicate ETS-4. Chem. Eng. J. 155, 728–735.

Bhatnagar, A., Sillanpää, M., Witek-Krowiak, A., 2015. Agricultural waste peels as versatile biomass for water purification - A review. Chem. Eng. J. 270, 244–271. https://doi.org/10.1016/j.cej.2015.01.135

Biškup, B., Subotić, B., 2004. Kinetic analysis of the exchange processes between sodium ions from zeolite A and cadmium, copper and nickel ions from solutions. Sep. Purif. Technol. 37, 17–31. https://doi.org/10.1016/S1383-5866(03)00220-X

Bourane, A., Nawdali, M., Bianchi, D., 2002. Heats of Adsorption of the Linear CO Species Adsorbed on a Ir/Al 2 O 3 Catalyst Using in Situ FTIR Spectroscopy under Adsorption Equilibrium. J. Phys. Chem. B 106, 2665–2671. https://doi.org/10.1021/jp0137322

Brandão, P., Philippou, A., Hanif, N., Ribeiro-Claro, P., Ferreira, A., Anderson, M.W., Rocha, J.,

2002a. Synthesis and characterization of two novel large-pore crystalline vanadosilicates. Chem. Mater. 14, 1053–1057. https://doi.org/10.1021/cm010613q

Brandão, P., Philippou, A., Rocha, J., Anderson, M.W., 2002b. Dehydration of alcohols by microporous niobium silicate AM-11. Catal. Letters 80, 99–102. https://doi.org/10.1023/A:1015444005961

Camarinha, E.D., Lito, P.F., Antunes, B.M., Otero, M., Lin, Z., Rocha, J., Pereira, E., Duarte, A.C., Silva, C.M., 2009. Cadmium(II) removal from aqueous solution using microporous titanosilicate ETS-10. Chem. Eng. J. 155, 108–114. https://doi.org/10.1016/j.cej.2009.07.015

Cardoso, S.P., Azenha, I.S., Lin, Z., Portugal, I., Rodrigues, A.E., Silva, C.M., 2016. Experimental measurement and modeling of ion exchange equilibrium and kinetics of cadmium(II) solutions over microporous stannosilicate AV-6. Chem. Eng. J. 295, 139–151. https://doi.org/10.1016/j.cej.2016.03.007

Cardoso, S.P., Azenha, I.S., Portugal, I., Lin, Z., Rodrigues, A.E., Silva, C.M., 2017. Single and binary surface diffusion permeation through zeolite membranes using new Maxwell-Stefan factors for Dubinin-type isotherms and occupancy-dependent kinetics. Sep. Purif. Technol. 182, 207–218. https://doi.org/10.1016/j.seppur.2017.03.036

Cardoso, S.P., Lopes, C.B., Pereira, E., Duarte, A.C., Silva, C.M., 2013. Competitive Removal of Cd2+ and Hg2+ Ions from Water Using Titanosilicate ETS-4: Kinetic Behaviour and Selectivity. Water, Air, Soil Pollut. 224, 1535. https://doi.org/10.1007/s11270-013-1535-z

Carro, L., Anagnostopoulos, V., Lodeiro, P., Barriada, J.L., Herrero, R., Sastre de Vicente, M.E., 2010. A dynamic proof of mercury elimination from solution through a combined sorption–reduction process. Bioresour. Technol. 101, 8969–8974. https://doi.org/10.1016/J.BIORTECH.2010.06.118

Czarna, D., Baran, P., Kunecki, P., Panek, R., Żmuda, R., Wdowin, M., 2018. Synthetic zeolites as potential sorbents of mercury from wastewater occurring during wet FGD processes of flue gas. J. Clean. Prod. 172, 2636–2645. https://doi.org/10.1016/J.JCLEPRO.2017.11.147

Dąbrowski, A., Hubicki, Z., Podkościelny, P., Robens, E., 2004. Selective removal of the heavy metal ions from waters and industrial wastewaters by ion-exchange method. Chemosphere 56, 91–106. https://doi.org/10.1016/j.chemosphere.2004.03.006

Dada, A.., Olalekan, A.., Olatunya, A.., Dada, O., 2012. Langmuir , Freundlich , Temkin and Dubinin

– Radushkevich Isotherms Studies of Equilibrium Sorption of Zn 2 + Unto Phosphoric Acid Modified Rice Husk. IOSR J. Appl. Chem. 3, 38–45. https://doi.org/10.9790/5736-0313845

Do, D.D., 1998. Adsorption analysis: equilibria and kinetics. Imperial College Press, London.

Dong, W., Liang, L., Brooks, S., Southworth, G., Gu, B., 2010. Roles of dissolved organic matter in the speciation of mercury and methylmercury in a contaminated ecosystem in Oak Ridge, Tennessee. Environ. Chem. 7, 94–102. https://doi.org/10.1071/EN09091

Dubinin, M.M., 1960. The Potential Theory of Adsorption of Gases and Vapors for Adsorbents with Energetically Nonuniform Surfaces. Chem. Rev. 60, 235–241. https://doi.org/10.1021/cr60204a006

Fabre, E., Lopes, C.B., Vale, C., Pereira, E., Silva, C.M., 2019a. Valuation of banana peels as an effective biosorbent for mercury removal under low environmental concentrations. Sci. Total Environ. https://doi.org/DOI: 10.1016/j.scitotenv.2019.135883

Fabre, E., Vale, C., Pereira, E., Silva, C.M., 2019b. Experimental Measurement and Modeling of Hg(II) Removal from Aqueous Solutions Using Eucalyptus globulus Bark: Effect of pH, Salinity and Biosorbent Dosage. Int. J. Mol. Sci. 20, 5973. https://doi.org/10.3390/ijms20235973

Ferreira, T.R., Lopes, C.B., Lito, P.F., Otero, M., Lin, Z., Rocha, J., Pereira, E., Silva, C.M., Duarte, A., 2009. Cadmium(II) removal from aqueous solution using microporous titanosilicate ETS-4. Chem. Eng. J. 147, 173–179. https://doi.org/10.1016/j.cej.2008.06.032

Figueira, P., Lopes, C.B., Daniel-da-Silva, A.L., Pereira, E., Duarte, A.C., Trindade, T., 2011. Removal of mercury (II) by dithiocarbamate surface functionalized magnetite particles: application to synthetic and natural spiked waters. Water Res. 45, 5773–5784. https://doi.org/10.1016/j.watres.2011.08.057

Fiol, N., Villaescusa, I., 2009. Determination of sorbent point zero charge: usefulness in sorption studies. Environ. Chem. Lett. 7, 79–84. https://doi.org/10.1007/s10311-008-0139-0

Freundlich, H., 1906. Concerning adsorption in solutions. Zeitschrift Fur Phys. Chemie-Stochiometrie Und Verwandstchaftslehre 57, 385–470.

Gebremedhin-Haile, T., Olguín, M.T., Solache-Ríos, M., 2003. Removal of mercury ions from mixed aqueous metal solutions by natural and modified zeolitic minerals. Water. Air. Soil Pollut. 148, 179–200.

Giles, C.., MacEwan, T.., Nakhwa, S.., Smith, D., 1960. Studies in adsorption. Part XI. A system of classification of solution adsorption isotherms, and its use in diagnosis of adsorption mechanisms and in measurement of specific surface areas of solids. J. Chem. Soc. 786, 3973–3993. https://doi.org/10.1016/S0008-6223(03)00002-2.

Helfferich, F.G., 1962. Ion Exchange. McGraw-Hill, New York.

Herrero, R., Lodeiro, P., Rey-Castro, C., Vilariño, T., Sastre De Vicente, M.E., 2005. Removal of inorganic mercury from aqueous solutions by biomass of the marine macroalga Cystoseira baccata. Water Res. 39, 3199–3210. https://doi.org/10.1016/j.watres.2005.05.041

Ho, Y.S., McKay, G., 1999. Pseudo-second order model for sorption processes. Process Biochem. 34, 451–465. https://doi.org/10.1016/S0032-9592(98)00112-5

Ho, Y.S., Porter, J.F., Mckay, G., 2002. Equilibrium isotherm studies for the sorption of divalentmetal ions onto peat: copper, nickel and lead single component systems. Water, Air, Soil Pollut. 141, 1–33. https://doi.org/10.1023/A:1021304828010

Huang, Y., Wu, D., Wang, X., Huang, W., Lawless, D., Feng, X., 2016. Removal of heavy metals from water using polyvinylamine by polymer-enhanced ultrafiltration and flocculation. Sep. Purif. Technol. 158, 124–136. https://doi.org/10.1016/j.seppur.2015.12.008

Ihsanullah, 2019. Carbon nanotube membranes for water purification: Developments, challenges, and prospects for the future. Sep. Purif. Technol. 209, 307–337. https://doi.org/https://doi.org/10.1016/j.seppur.2018.07.043

Ihsanullah, Abbas, A., Al-Amer, A.M., Laoui, T., Al-Marri, M.J., Nasser, M.S., Khraisheh, M., Atieh, M.A., 2016. Heavy metal removal from aqueous solution by advanced carbon nanotubes: Critical review of adsorption applications. Sep. Purif. Technol. 157, 141–161. https://doi.org/10.1016/j.seppur.2015.11.039

Inglezakis, V.J., 2007. Solubility-normalized Dubinin–Astakhov adsorption isotherm for ion-exchange systems. Microporous Mesoporous Mater. 103, 72–81. https://doi.org/10.1016/J.MICROMESO.2007.01.039

Javadian, H., Taghavi, M., 2014. Application of novel Polypyrrole/thiol-functionalized zeolite Beta/MCM-41 type mesoporous silica nanocomposite for adsorption of Hg 2+ from aqueous solution and industrial wastewater: Kinetic, isotherm and thermodynamic studies. Appl. Surf. Sci. 289, 487–494. https://doi.org/10.1016/j.apsusc.2013.11.020

Johs, A., Eller, V.A., Mehlhorn, T.L., Brooks, S.C., Harper, D.P., Mayes, M.A., Pierce, E.M., Peterson, M.J., 2019. Dissolved organic matter reduces the effectiveness of sorbents for mercury removal. Sci. Total Environ. 690, 410–416. https://doi.org/10.1016/j.scitotenv.2019.07.001

Lagergren, S., 1898. Zur theorie der sogenannten adsorption gel Zur theorie der sogenannten adsorption gelster stoffe, Kungliga Svenska Vetenskapsakademiens. Handlingar 24, 1–39.

Langmuir, I., 1916. The adsorption of gases on plane surface of glass, mica and platinum. J.Am, Chem.Soc 40, 1361–1368.

Lito, P.F., Aniceto, J.P.S., Silva, C.M., 2013. Maxwell – Stefan based modelling of ion exchange systems containing common species (Cd 2 + , Na +) and distinct sorbents. Int. J. Environ. Sci. Technol. https://doi.org/10.1007/s13762-013-0438-2

Lito, P.F., Cardoso, S.P., Loureiro, J.M., Silva, C.M., 2012. Ion Exchange Equilibria and Kinetics, in: Inamuddin, Luqman, M. (Eds.), Ion Exchange Technology I – Applications. Springer, pp. 51–120.

Liu, Chao, Peng, J., Zhang, L., Wang, S., Ju, S., Liu, Chenhui, 2018. Mercury adsorption from aqueous solution by regenerated activated carbon produced from depleted mercury-containing catalyst by microwave-assisted decontamination. J. Clean. Prod. 196, 109–121. https://doi.org/10.1016/J.JCLEPRO.2018.06.027

Lopes, Cláudia B, Coimbra, J., Otero, M., Pereira, E., Duarte, A.C., Lin, Z., Rocha, J., 2008. Uptake of Hg2+ from aqueous solutions by microporous titano- and zircono-silicates. Quim. Nov. 31, 321–325.

Lopes, C. B., Lito, P.F., Cardoso, S.P., Pereira, E., Duarte, A.C., Silva, C.M., 2012. Metal recovery, separation and/or pre-concentration, in: Inamuddin, Luqma, M. (Eds.), Ion Exchange Technology II – Applications. Springer, pp. 237–322.

Lopes, C B, Lito, P.F., Otero, M., Lin, Z., Rocha, J., Silva, C.M., Pereira, E., Duarte, A.C., 2008. Mercury removal with titanosilicate ETS - 4 : Batch experiments and modelling. Microporous Mesoporous Mater. 115, 98–105. https://doi.org/10.1016/j.micromeso.2007.10.055

Lopes, C.B., Otero, M., Lin, Z., Silva, C.M., Rocha, J., Pereira, E., Duarte, A.C., 2009. Removal of Hg2+ ions from aqueous solution by ETS-4 microporous titanosilicate-Kinetic and equilibrium studies. Chem. Eng. J. 151, 247–254. https://doi.org/10.1016/j.cej.2009.02.035

Lopes, C B, Pereira, E., Lin, Z., Pato, P., Otero, M., Silva, C.M., Rocha, J., Duarte, A.C., 2012. Microporous and Mesoporous Materials Fixed-bed removal of Hg 2 + from contaminated water by microporous titanosilicate ETS-4 : Experimental and theoretical breakthrough curves. Microporous Mesoporous Mater. 145, 32–40. https://doi.org/10.1016/j.micromeso.2011.04.019

Malash, G.F., El-Khaiary, M.I., 2010. Piecewise linear regression: A statistical method for the analysis of experimental adsorption data by the intraparticle-diffusion models. Chem. Eng. J. 163, 256–263. https://doi.org/10.1016/j.cej.2010.07.059

Maleki, A., Hajizadeh, Z., Sharifi, V., Emdadi, Z., 2019. A green, porous and eco-friendly magnetic geopolymer adsorbent for heavy metals removal from aqueous solutions. J. Clean. Prod. 215, 1233–1245. https://doi.org/10.1016/j.jclepro.2019.01.084

Meena, A.K., Mishra, G.K., Rai, P.K., Rajagopal, C., Nagar, P.N., 2005. Removal of heavy metal ions from aqueous solutions using carbon aerogel as an adsorbent. J. Hazard. Mater. 122, 161–170. https://doi.org/10.1016/J.JHAZMAT.2005.03.024

Melamed, R., da Luz, A.B., 2006. Efficiency of industrial minerals on the removal of mercury species from liquid effluents. Sci. Total Environ. 368, 403–406. https://doi.org/10.1016/j.scitotenv.2005.09.091

Noh, Y.D., Komarneni, S., MacKenzie, K.J.D., 2012. Titanosilicates: Giant exchange capacity and selectivity for Sr and Ba. Sep. Purif. Technol. 95, 222–226. https://doi.org/10.1016/j.seppur.2012.05.013

Otero, M., Lopes, C.B., Coimbra, J., Ferreira, T.R., Silva, C.M., Lin, Z., Rocha, J., Pereira, E., Duarte, A.C., 2009. Priority pollutants (Hg2+ and Cd2+) removal from water by ETS-4 titanosilicate. Desalination 249, 742–747. https://doi.org/10.1016/j.desal.2009.04.008

Polanyi, M., 1914. Adsorption from the point of view of the Third Law of Thermodynamics. Verh. Deut. Phys. Ges 16, 1012–1016.

Qi, C., Ma, X., Wang, M., Ye, L., Yang, Y., Hong, J., 2017. A case study on the life cycle assessment of recycling industrial mercury-containing waste. J. Clean. Prod. 161, 382–389. https://doi.org/10.1016/J.JCLEPRO.2017.05.023

Ranganathan, K., 2003. Adsorption of Hg(II) ions from aqueous chloride solutions using powdered activated carbons. Carbon N. Y. 41, 1087–1092. https://doi.org/10.1016/S0008-

6223(03)00002-2

Rashid, M., Khan, F., Lutfullah, 2014. Removal of Pb(II) ions from aqueous solutions using hybrid organic–inorganic composite material: Zr(IV) iodosulphosalicylate. J. Water Process Eng. 3, 53–61. https://doi.org/10.1016/J.JWPE.2014.07.003

Rocha, J., Brandao, P., Phillippou, A., Anderson, M.W., 1998. Synthesis and characterisation of a novel microporous niobium silicate catalyst. Chem Commun 2687–2688. https://doi.org/Doi 10.1039/A808264b

Rodrigues, A.E., Silva, C.M., 2016. What's wrong with Lagergreen pseudo first order model for adsorption kinetics? Chem. Eng. J. 306, 1138–1142. https://doi.org/10.1016/j.cej.2016.08.055

Roginsky, S., Zeldovich, Y.B., 1934. The catalytic oxidation of carbon monoxide on manganese dioxide. Acta Phys. Chem. USSR 1, 554.

Sajid, M., Nazal, M.K., Ihsanullah, Baig, N., Osman, A.M., 2018. Removal of heavy metals and organic pollutants from water using dendritic polymers based adsorbents: A critical review. Sep. Purif. Technol. 191, 400–423. https://doi.org/10.1016/j.seppur.2017.09.011

Smit, B., Maesen, T., 2008. Molecular simulations of zeolites : Adsorption , diffusion , and shape selectivity. Chem. Rev. 108, 4125–4184. https://doi.org/10.1021/cr8002642

Sousa, R.N., Veiga, M.M., Klein, B., Telmer, K., Gunson, A.J., Bernaudat, L., 2010. Strategies for reducing the environmental impact of reprocessing mercury-contaminated tailings in the artisanal and small-scale gold mining sector: insights from Tapajos River Basin, Brazil. J. Clean. Prod. 18, 1757–1766. https://doi.org/10.1016/J.JCLEPRO.2010.06.016

Substance Priority List | ATSDR [WWW Document], 2017. URL https://www.atsdr.cdc.gov/spl/ (accessed 2.2.19).

Umpleby, R.J., Baxter, S.C., Chen, Y., Shah, R.N., Shimizu, K.D., 2001. Characterization of molecularly imprinted polymers with the Langmuir-Freundlich isotherm. Anal. Chem. 73, 4584–91.

Wierzba, S., Kłos, A., 2019. Heavy metal sorption in biosorbents – Using spent grain from the brewing industry. J. Clean. Prod. 225, 112–120. https://doi.org/10.1016/J.JCLEPRO.2019.03.286

Zandi-Atashbar, N., Ensafi, A.A., Ahoor, A.H., 2018. Magnetic Fe2CuO4/rGO nanocomposite as an efficient recyclable catalyst to convert discard tire into diesel fuel and as an effective mercury adsorbent from wastewater. J. Clean. Prod. 172, 68–80. https://doi.org/10.1016/J.JCLEPRO.2017.10.146

Chapter III

Biosorbents towards water treatment

This chapter focuses on the use of residues from agriculture and industry as biosorbents for mercury removal. This chapter comprises three different works, presented in the same way they were submitted to scientific journals or with minor changes in the structure of presentation. They are briefly described below.

In the first work, the performances of six different biomasses, namely banana and potato peels, eggshells, *Eucalyptus globulus* barks, water hyacinth and coffee waste were evaluated and compared for mercury removal from tap water under the same batch conditions and Hg(II) initial concentration of 50 μg dm^{-3}. These biosorbents embrace natural "undesirable" wastes such as agricultural wastes, industrial by-products and an aquatic plant considered as pest.

Due to the fact that banana peels presented the best performance in the first work, this biosorbent was studied more deeply in the second work. Here, the impact of the operating conditions such as biosorbent dosage, contact time, and ionic strength were investigated on the efficiency of Hg(II) sorption from contaminated solutions with realistic initial concentrations. Additionally, real waters, like seawater and an industrial effluent were used as matrices.

A new approach has been proposed in the third work by applying the Response Surface Methodology to extract information about the significance of the factors (pH salinity and biosorbent dosage) on Hg(II) removal by *Eucalyptus globulus* barks and to obtain a model that describes the sorption process. Results were generated through the Design of Experiments using the methodology of three-factor and three-level Box–Behnken. *Eucalyptus globulus* barks were chosen because this biomass is a representative waste from pulp and paper industry.

Index

Work submitted as scientific article

Agricultural and industrial wastes as promising biosorbents to remove mercury in water treatments

Abstract

Agricultural and industrial wastes are produced in abundance in many agro-industrial activities and expensive disposal costs led to the search for new alternatives to use them. Mercury is a potential contaminant of the aqueous systems that needs to be removed from wastewaters even in trace concentrations. The Hg(II) ions can establish bonds with the functional groups present on lignocellulosic biomasses, making these types of biosorbents excellent alternatives to remove mercury in water treatments. In this work six biosorbents (banana and potato peels, eggshells, *Eucalyptus globulus* bark, water hyacinth and coffee waste) were tested and compared under the same batch conditions with an initial mercury concentration of 50 μg dm^{-3} in order to determine their removal performances. Several reaction- and diffusion-based models were adjusted to the experimental data to analyze the limiting sorption mechanisms. Sorption experiments and modelling results evidenced distinct affinities of those biosorbents to Hg(II), banana peels being the best alternative due to the fast removal kinetics and capacity. Chemical and physical characteristics of the solids are involved in Hg(II) elimination, as reported by FTIR-ATR and SEM studies.

III.1. Agricultural and industrial wastes as promising biosorbents to remove mercury in water treatments

III.1.1. Introduction

The removal of toxic contaminants from aqueous waste streams can be accomplished by a variety of processes, such as chemical precipitation, membrane processes like reverse osmosis, flotation, adsorption and ion exchange (Lito et al., 2012; Lopes et al., 2012). Most of these technologies is expensive, requires high energy and reagents costs, involves toxic secondary sludge production and is ineffective to treat low metal concentration waters (Abdolali et al., 2014). Sorption processes are considered better alternatives for metal removal because they are easy to operate, economic and allow to treat contaminated waters of trace realistic concentrations (Bhatnagar et al., 2015; Lito et al., 2012; Lopes et al., 2012; Rao et al., 2002). Activated carbon is the most used adsorbent (Carro et al., 2011; Zhang et al., 2005), but its cost is a limiting factor. Hence, research of new materials capable to operate successfully in water treatment processes under lower costs is hence a pertinent issue (Rosales et al., 2017).

By-products from agricultural or industrial operations have received attention because of the many advantages inherent to their availability at low cost and favoured chemical composition (Bhatnagar et al., 2015; Nguyen et al., 2013). Agricultural wastes typically are composed by lignin, cellulose and other components with polar functional groups such as alcohols, aldehydes, ketones, carboxylic, phenolic, and ether groups. These groups are capable to establish bonds with pollutants through different mechanisms, for instance, substituting their hydrogen ions by metal ions or donating electron pairs to form complexes with the metal in solution (Bailey, S.E., Olin, T.J., Bricka, R.M., and Adrian, 1999; Jiménez-Cedillo et al., 2013; Pérez Marín et al., 2010; Zafar et al., 2007). It is worth to highlight that these types of wastes are formed during industrial processing and they represent disposal problems, since they need to be managed or re-utilized (Tran et al., 2015). They are often incinerated to produce energy for the own industrial process (Luo et al., 2019). Alternative application as biosorbents symbolizes a

benefit since value is added to these solids and the contaminated waters are treated applying a much lower cost operation.

Many studies have compared biosorbents ability considering their cations removal percentages although performed under different experimental conditions (Abdolali et al., 2014; Bailey, S.E., Olin, T.J., Bricka, R.M., and Adrian, 1999). Moreover, various works used contaminant concentrations up to 2000 mg dm^{-3} of Hg(II) (Devani et al., 2015; Igwe et al., 2008; Omorogie et al., 2012; Singanan, 2015), which are much higher than the ones found in the environment. The present study tested and compared the ability of banana peels, potato peels, eggshells, *Eucalyptus globulus* bark, water hyacinth and coffee waste as biosorbents to remove mercury from tap water contaminated with 50 µg dm^{-3} of metal. The most known reaction-based and diffusion-based kinetic models were adopted to represent the experimental data and examine the wastewater remediation results. Mercury was chosen due to the worldwide concern about its emissions and release, causing dangerous impacts on environment, biomagnifications through the wed chain, and effects on human health (Carro et al., 2010; Rao et al., 2009). Industrial activities are the major anthropogenic source of mercury contamination into the aquatic systems such as metal finishing, welding, alloy manufacturing plants, pulp industries and petroleum refining (Inglezakis et al., 2002).

III.1.2. Materials and methods

III.1.2.1. Chemicals and instrumentation

All glassware used in the experiments was acid-washed prior to use, with nitric acid 25 % for 24 hours, and then plenty rinsed with ultra-pure water (18.2 MΩ cm, Milli-Q system). All necessary chemicals were of analytical grade, obtained from commercial suppliers and used without further purification. The certified standard solution of mercury(II) nitrate (1000 ±2 mg dm^{-3}) was purchased from Merck. The standard solutions for the calibration curves were obtained by diluting the corresponding stock solution in ultra-pure water.

The quantification of Hg(II) in the solutions was performed by cold vapour atomic fluorescence spectroscopy (CV-AFS), on a PSA cold vapour generator, model 10.003, coupled to a Merlin PSA detector, model 10.023, and using $SnCl_2$ as reducing agent. This technique can measure mercury concentrations as low as 1.0 ng dm^{-3} (Lopes et al., 2008; Otero et al., 2009).

III.1.2.2. Biosorbent materials collection

All biosorbents used in this work were applied without any chemical pretreatment. The coffee waste was a mixture of chicory, barley, coffee and cereals, and the water hyacinth was a combination of leaves (65 wt.%) and branches (35 wt.%). A food company granted the coffee waste, and the *Eucalyptus globulus* bark was provided by a pulp and paper industry. The other sorbents were obtained from a local market. The sorbents (banana and potato peels, eggshells, water hyacinth and coffee waste) were rinsed with tap and distilled water and oven dried afterwards, except the potato and banana peels that were lyophilized. Materials were milled and separated in particles sizes of less than 1 mm diameter. *Eucalyptus globulus* bark was cut in similar pieces with medium size of 1 cm length.

III.1.2.3. Biosorbents characterization

Fourier Transform Infrared (FTIR) analyses of all biosorbents were performed in a Bruker optics tensor 27 spectrometer coupled to a horizontal attenuated total reflectance (ATR) cell using 256 scans at a resolution of 4 cm^{-1} and the spectra were recorded from 4000 to 400 cm^{-1}. The samples were examined directly and data were obtained as absorbance. The morphology surface was studied by Scanning Electron Microscopy (SEM) using a Hitachi SU-70 SEM microscope with a Bruker Quantax 400 detector operating at 20 kV.

III.1.2.4. Batch sorption experiments

Sorption experiments were performed in batch conditions at room temperature (22 ± 1 °C) in 1 dm^3 volumetric flasks magnetically stirred at 650 rpm. The ability of the

biosorbents to remove Hg(II) from solution was assessed by contacting the materials with a Hg(II) solution of fixed concentration for a determined period of time. The solutions were prepared diluting the mercury standard solution in tap water (pH≈6.3) to a concentration of 50 μg dm^{-3}. Each amount of biosorbent was added into the flasks (dose of 0.5 g dm^{-3}) and this was considered the start point of the experiments. Different runs were performed for each biosorbent during a maximum time of 72 hours. Water samples were collected at increasing times, filtered with a 0.45 μm Millipore filter, adjusted to pH < 2 with HNO_3, stored at 4 °C and then analyzed. A blank experiment (*i.e.*, without biosorbent) was always run as control to check the mercury sorbed on the vessel walls or lost by volatilization. The mercury concentration was quantified by CV-AFS and the obtained signal was converted in Hg(II) concentration through a calibration curve as reported by Cardoso et al., (2013).

The average amount of sorbed Hg(II) per unit mass of solid, q_A (mg g^{-1}), was calculated by material balance to the sorber (*i.e.,* solid and solution) at time t:

$$q_A = \frac{V_L}{m_S}(C_{A0} - C_A) \qquad \text{(III.1.1)}$$

where subscript A denotes Hg(II), V_L is the solution volume (dm^3), m_S is the mass of biosorbent (g), C_{A0} is the initial concentration of Hg(II) in solution and C_A is its concentration at time t (mg dm^{-3}).

The studied biosorbents were compared in terms of their Hg(II) removal and sorption uptake. The removal efficiency was calculated as follows:

$$Removal\ (\%) = 100 \times \frac{C_{A0} - C_{Af}}{C_{A0}} \qquad \text{(III.1.2)}$$

where C_{Af} is the Hg(II) final concentration in the liquid phase.

III.1.2.5. Modelling of mercury(II) removal

In order to investigate the mechanism of Hg(II) sorption by the biosorbents and the potential rate-controlling steps, the experimental results were analysed by the most

relevant and representative models of the literature, which may be grouped into two large classes: reaction-based models and diffusion-based models (Qiu et al., 2009).

The reaction-based models include the pseudo-first order (PFO), pseudo-second order (PSO) and Elovich equations, and have been derived for adsorption assuming the process as a chemical reaction. These models have been frequently used to fit kinetic data to evaluate the behaviour of ion exchange and adsorption processes (Ho, 2006; Ho et al., 2000; Largitte and Pasquier, 2016; Rocha et al., 2016).

The PFO and PSO equations were derived considering five assumptions: (i) Sorption only occurs on specific sites and there is no interaction between sorbed species, (ii) the energy of sorption is independent of the surface coverage, (iii) the sorption capacity is achieved when the monolayer is saturated, (iv) the sorbate concentration is uniform in the particle, (v) the sorbate concentration is considered constant, and (vi) the solute capture is described according to a first order rate equation (in the case of PFO model) or by a second order rate equation (in the case of PSO model) (Largitte and Pasquier, 2016).

The PFO equation of Lagergren takes sorption as an irreversible reaction, $S + M \rightarrow MS$, where S represents the free active sites, M the sorbate in solution, and MS the occupied sites (Lagergren, 1898; Largitte and Pasquier, 2016). Representing the concentration of the sorbed species at final equilibrium by q_{Ae} and its concentration at any time t by q_{A}, the removal kinetics gets proportional to the distance to the final equilibrium concentration, $(q_{\mathrm{Ae}} - q_{\mathrm{A}})$:

$$\frac{dq_A}{dt} = k_1(q_{Ae} - q_A) \qquad \text{(III.1.3)}$$

where k_1 (h^{-1}) is the rate constant of the model, and q_{Ae} and q_{A} may be expressed in mg g^{-1}. After integration from the initial clean particle condition ($t = 0$, $q_{\mathrm{A}} = 0$) one gets:

$$ln(q_{Ae} - q_A) = ln\, q_{Ae} - k_1 t \qquad \text{(III.1.4)}$$

In the case of the PSO model (Ho and McKay, 1999), the sorption is based on the reaction $2S + M \rightarrow MS_2$, becoming mathematically expressed by:

$$\frac{dq_A}{dt} = k_2(q_{Ae} - q_A)^2 \quad \text{(III.1.5)}$$

where k_2 (g mg^{-1} h^{-1}) is the rate constant of the model. After integration and linearization, the final equation is given by:

$$\frac{t}{q_A} = \frac{1}{k_2 q_{Ae}^2} + \frac{1}{q_{Ae}} t \quad \text{(III.1.6)}$$

The Elovich model was initially proposed by Roginsky and Zeldovich, (1934) for the adsorption of carbon monoxide onto manganese dioxide. It describes the kinetics of sorption on heterogeneous surfaces and is given by:

$$\frac{dq_A}{dt} = \alpha e^{-\beta q_A} \quad \text{(III.1.7)}$$

where α is the initial sorption rate (mg g^{-1} h^{-1}) and β (g mg^{-1}) is the desorption constant of the model. Assuming that αβt >>1, one obtains after common integration:

$$q_A = \frac{1}{\beta} ln(\alpha\beta) + \frac{1}{\beta} ln\, t \quad \text{(III.1.8)}$$

With respect to the diffusion-based models, they consider that the overall sorption rate is controlled by film diffusion, intraparticle diffusion or a combination of both (Malash and El-Khaiary, 2010). In the following, three modelling approaches of this type are focused: the equations of Crank, Boyd and co-workers, and Webber.

For the simplest case of uniform sorbent particles with spherical geometry and constant effective diffusivity (D_{eff}), the material balance combined with Fick's first law is given by (Helfferich, 1962):

$$\frac{\partial}{\partial t} q_A(t,r) = D_{eff}\left[\frac{\partial^2}{\partial r^2} q_A(t,r) + \frac{2}{r}\frac{\partial}{\partial r} q_A(t,r)\right] \quad \text{(III.1.9)}$$

where r is radial position. Crank reported a solution for the average concentration in the particles – also represented hereafter by q_{A} – of a perfectly stirred batch system of infinite volume (Hartley and Crank, 1949):

$$F(t) = \frac{q_A}{q_{Ae}} = 1 - \left(\frac{6}{\pi^2}\right)\sum_{n=1}^{\infty}\frac{1}{n^2}exp\,(-n^2Bt) \qquad \text{(III.1.10)}$$

Here, $B \equiv \pi^2 D_{\text{eff}}/R_{\text{p}}^2$ and R_{p} is particle radius. The simplified form of Eq. (III.1.10) for long times is known as Boyd's equation (Largitte and Pasquier, 2016). Reichenberg, (1953) managed this expression to obtain the following approximations:

$$Bt = -0.4977 - ln\big(1 - F(t)\big), \quad \text{for } F(t) > 0.85 \qquad \text{(III.1.11.a)}$$

$$Bt = \left(\sqrt{\pi} - \sqrt{\pi - \left(\frac{\pi^2 F(t)}{3}\right)}\right)^2, \quad \text{for } F(t) < 0.85 \qquad \text{(III.1.11.b)}$$

Plotting Bt against time one may disclose the mechanism controlling the rate of removal: if the plot is linear with null origin intercept then intraparticle diffusion controls the process; on the contrary, if it is nonlinear or does not pass through the origin, the film diffusion or the local binding (sorption) may control the process (Boyd et al., 1947; Jeong and Park, 2008; Malash and El-Khaiary, 2010; Reichenberg, 1953). Equations (III.1.11.a) and (III.1.11.b) will be henceforth called Boyd *et al.* equations.

Webber's intraparticle diffusion model (Eq. (III.1.12)) is derived from Fick's second law. It assumes the film diffusion is negligible or it is only significant for a short period of time at the beginning of the process (Weber and Morris, 1963):

$$q_A = k_i t^{0.5} \qquad \text{(III.1.12)}$$

Here, k_{i} is the intraparticle diffusion parameter (mg $g^{-1}h^{-0.5}$). According to Webber's model, if the intraparticle transport is the rate controlling step then the plot of q_{A} *versus* $t^{0.5}$ is a straight line with null intercept.

The parameters of the reaction-based models were obtained by simultaneous numerical integration and optimization of Eqs. (III.1.3), (III.1.5) and (III.1.7). All programs were coded in Matlab R2014a, finite differences of second order were used, and the Nelder-Mead simplex algorithm was adopted to minimize the error between experimental and calculated data ($AARD$, Eq. (III.1.14)). In the case of the diffusion-based models (Eqs. (III.1.11) and (III.1.12)), the parameters were obtained by piecewise linear

regression (PLR) using a Microsoft® Excel™ worksheet developed by Malash and El-Khaiary, (2010). The method segments the independent variable and performs the regression analysis separately for each interval. The parameters are determined by the method of least squares by minimizing the sum of squared deviations between experimental and calculated values.

The goodness of the fits was assessed by the coefficient of determination (R^2) and the average absolute relative deviation ($AARD$):

$$R^2 = 1 - \frac{\sum(\hat{y}_i - y_i)^2}{\sum(y_i - \bar{y})^2} \quad \text{(III.1.13)}$$

$$AARD(\%) = \frac{100}{N_{DP}} \sum_{i=1}^{N_{DP}} \frac{|\hat{y}_i - y_i|}{y_i} \quad \text{(III.1.14)}$$

where y_{i} represents the experimental data, $\hat{y}_{\mathrm{i}}$ the calculated values, $\bar{y}$ is the mean of experimental data, and N_{DP} is the number of data points.

III.1.3. Results and discussion

III.1.3.1. Biosorbent characteristics

The morphology of the studied biosorbents is presented in Figure III.1.1. Water hyacinth has a strongly rough structure, banana peels and *Eucalyptus globulus* bark surfaces have well defined protrusions, while coffee waste and eggshells are characterized by a heterogeneous surface with some roughness and slight protuberances. The potato peels structure showed an apparent smooth surface.

In general, all the materials (excluding the eggshells) showed resembling FTIR spectra as can be observed in Figure III.1.2. Banana peels are composed mainly by cellulose, hemicellulose, pectin, chlorophyll and other low molecular weight species (Bhatnagar et al., 2015). The band observed in the region of 3305 cm^{-1} represent O-H and N-H vibrations (Abdel-Khalek et al., 2017). The double peak at 2800-3000 cm^{-1} may be due to the C-H stretching vibrations (Rao et al., 2009), while the band at 1740 cm^{-1} (C=O

bonds) was reflective of esters bands of fatty acids, hydroxy fatty acids, and diacids in lipids and suberin polymers (Liang and McDonald, 2014). The vibration observed at 1600 cm^{-1} is attributed to C=C stretching frequencies which is ascribed, in general, to the vibration of the aromatic ring present in lignin (Liang and McDonald, 2014). The peak of 1378 cm^{-1} corresponds to aliphatic C-H stretching (Liang and McDonald, 2014), and the strong band ranging from 1200 to 900 cm^{-1} is related to -C-O-C- vibration of the cellulose (Rafatullah et al., 2009). Like the banana peels, the biosorbents coffee waste, potato peels, water hyacinth and *Eucalyptus globulus* bark are lignocellulosic materials as may be inferred by their similar FTIR spectra. The coffee waste presented stronger fat acids peak at 1730 cm^{-1} and another peak at 1528 cm^{-1} corresponding to N-H bending (Arami et al., 2006). As opposed to the banana peels, the potato peels presented only one peak at the region between 2800 and 3000 cm^{-1}. The water hyacinth showed higher intensity peak at 1635 cm^{-1} which is related with the aromatic ring in lignin as mentioned above (Ibrahim et al., 2012). *Eucalyptus globulus* bark spectrum exhibited less intensity peaks related with C-H stretching vibrations. The eggshells spectrum has markedly different characteristics, there are three prominent peaks at 1410, 880 and 712 cm^{-1} which are the characteristic peaks for calcium carbonate, a major constituent of eggshells (Salaudeen et al., 2018).

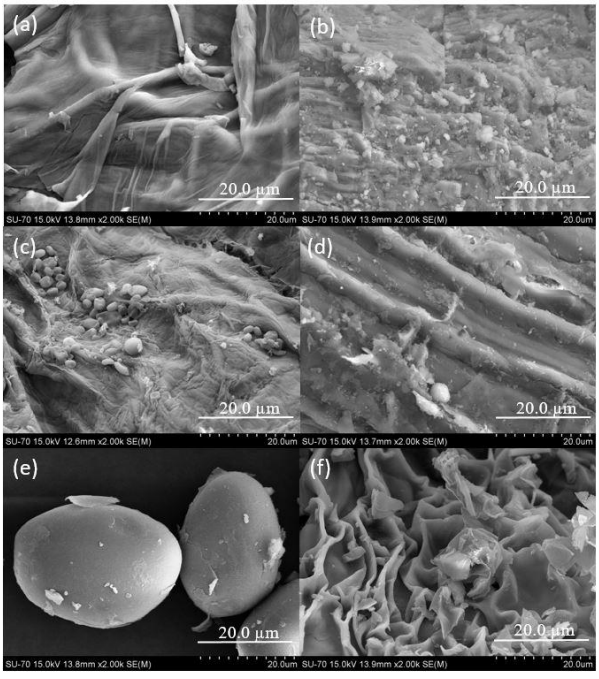

Figure III.1.1. SEM images of (a) banana peels, (b) eggshells, (c) coffee waste, (d*) Eucalyptus globulus* bark, (e) potato peels and (f) water hyacinth.

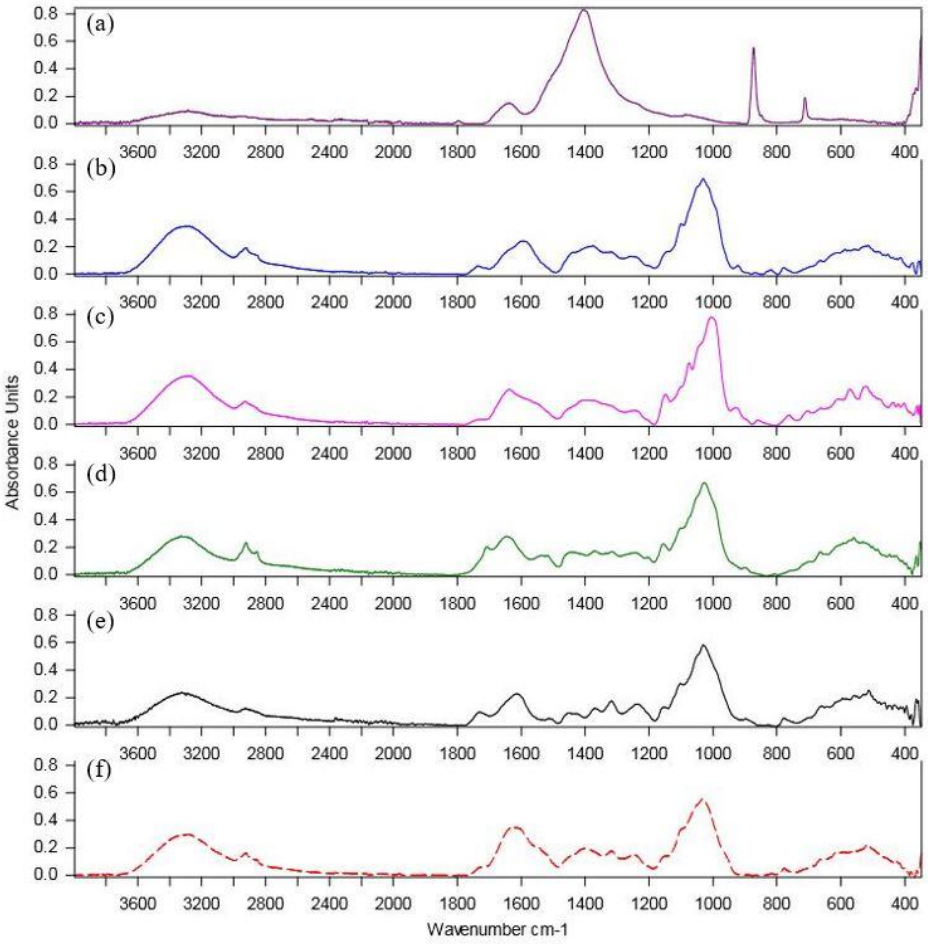

Figure III.1.2. FTIR spectra of (a) eggshells,(b) banana peels, (c) potato peels, (d) coffee waste, (e) *Eucalyptus globulus* bark and (f) water hycacinth.

III.1.3.2. Removal of mercury by biosorbents

Figure III.1.3 shows the uptake of Hg(II) by the studied biosorbents over time under batch conditions. The plots express the Hg(II) concentration in solution at each time (C_A) normalized in relation to its initial value (C_{A0}) for all those materials. In general, the kinetic profiles found were similar, characterized by a fast decrease of C_A/C_{A0} at initial times, followed by a stage where the rate of sorption becomes slower. This behaviour can be ascribed to the large driving force for ions transport at the beginning of the process, because the materials were initially free of Hg(II) and the free active binding sites were

largely available. However, with increasing coverage, the available fraction of active sites rapidly diminished penalizing the removal.

Although all the materials are able to reduce satisfactorily the Hg(II) initially in solution, it is possible to observe differences in the metal uptake related to the biosorbent used. Differences were more remarkable at the first hours, which indicates that some biosorbents exhibit higher affinity to capture Hg(II) from solution. Materials like banana peels and water hyacinth have achieved, after 72 hours of contact, residual Hg(II) concentrations of 4.8 and 4.0 μg dm^{-3} respectively (less than 10 % of the initial concentration), and the experiments suggest that they could remove even more, since the equilibrium time has not been reached. Moreover, the equilibrium time varied among the biosorbents. For instance, potato peels have attained the equilibrium at *ca.* 6 hours, while for the *Eucalyptus glubulus* bark the time required was *ca.* 11 hours and for the eggshells it was *ca.* 48 hours.

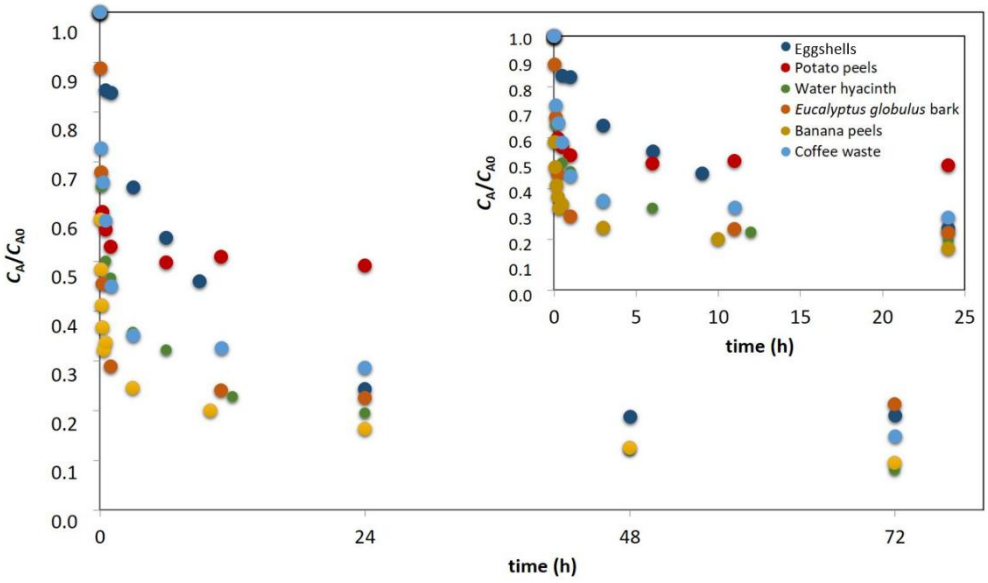

Figure III.1.3. Normalized Hg(II) concentration (C_A/C_{A0}) in solution *versus* time for the studied biosorbents.

In terms of efficiency (Figure III.1.4) the best removal values were obtained by the water hyacinth (91.9 %) and banana peels (90.5 %), with uptake loadings of 0.0898 and 0.0919 mg g^{-1} respectively, despite the relevant differences noted at the beginning of the sorption process. Even with the fastest kinetics, only 50.9 % of the mercury initially in

solution was removed by the potato peels. The other biosorbents showed similar final removal percentages of around 80 %, corresponding to approximated residual concentration of 10 µg dm^{-3}. It should be emphasized that more than 70 % of the mercury content was reduced during the first 24 hours by all the materials (except potato peels). These results highlight the fast and effective mercury uptake ability of these biosorbent materials.

According to Panda et al., (2007), Jiménez-Cedillo et al., (2013) and Pérez Marín et al., (2010) functional groups like carboxyl and hydroxyl, observed on the surface of the studied biosorbents, might be involved in the metal sorption. Consequently, the best performance observed for the removal of mercury by the water hyacinth and banana peels may be related to the peaks of O-H and C=O. Although potato peels present bands associated with the main groups involved in the sorption processes, this biomass showed the worst performance. Most likely, other factors such as porosity and particle size may play a stronger influence on the uptake than the chemical composition of the sorbent, at least from the kinetic point of view.

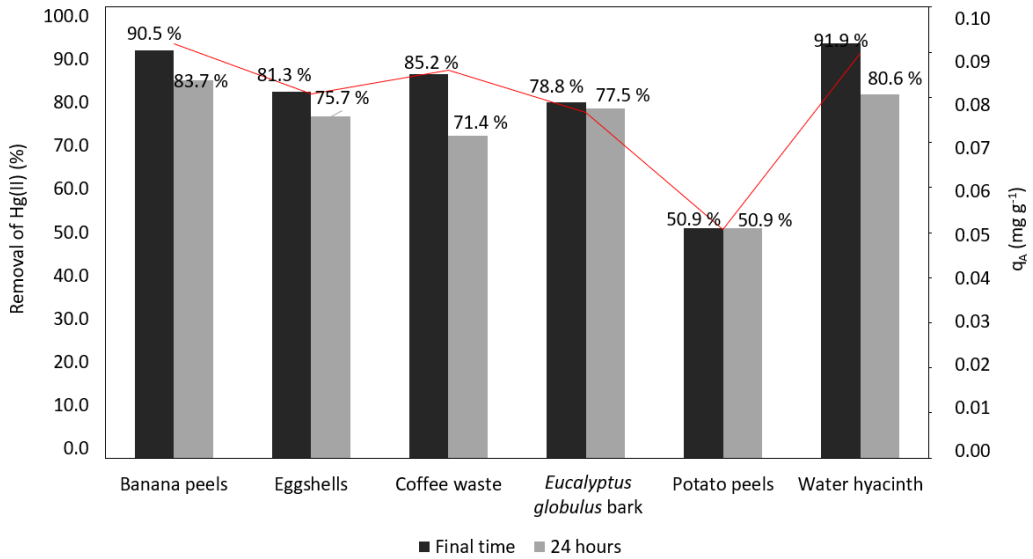

Figure III.1.4. Hg(II) removal (%) at the end of the experiment (dark bar) and after 24 hours (grey bar) for all the studied biosorbents.

III.1.3.3. Kinetic data modelling

The fittings to experimental data of Hg(II) uptake along time, by all the materials tested, by PFO, PSO and Elovich models are plotted in Figure III.1.5. The obtained values of the different kinetic parameters as well as the coefficients of determination and the average absolute relative deviations are summarized in Table III.1.1.

In general, the PFO model presented the poorest fit to the experimental data over the whole period of time, as shown by the low values of R^2 found (0.814-0.992). The only exception was observed for the *Eucalyptus globulus* bark which was better described by this model and showed values of R^2 of 0.992 and $AARD$ of 6.84 %. These values reflect the good adjustment of the PFO model in the range between the ascendant branch and the horizontal branch, where the PSO model fails. The value of q_{Ae} correlated by PFO equation is 0.0754 mg g^{-1} and agrees with the observed value of 0.0766 mg g^{-1} (relative error of 1.50 %).

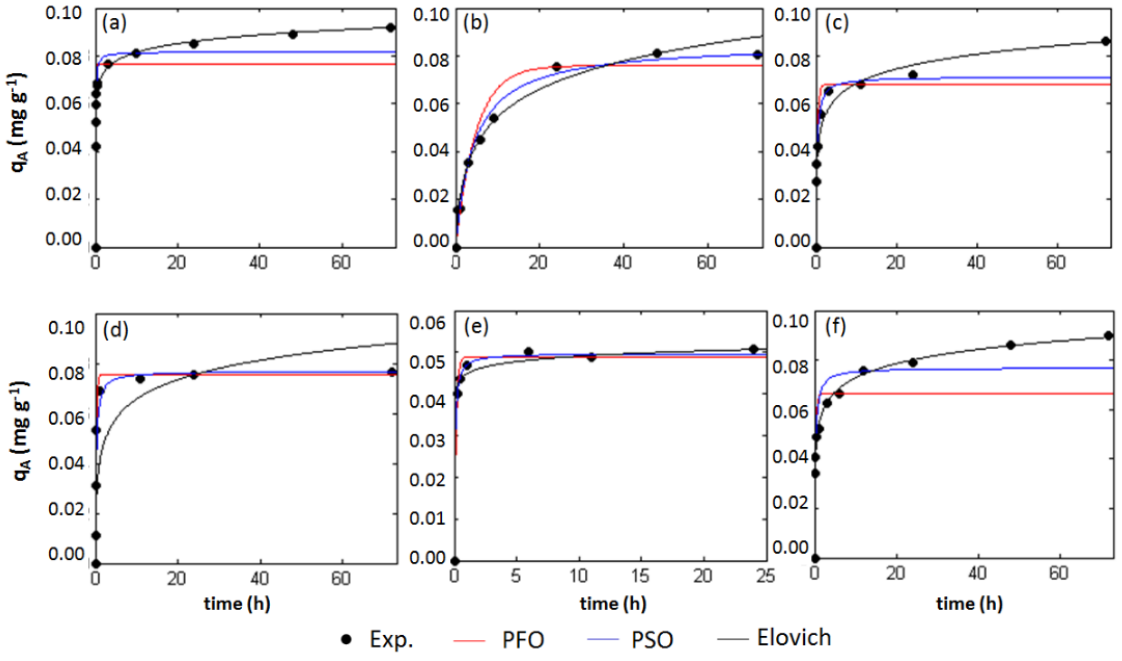

Figure III.1.5. Kinetic modelling of the experimental data of Hg(II) sorption onto (a) banana peels, (b) eggshells, (c) coffee waste, (d) *Eucalyptus globulus* bark, (e) potato peels and (f) water hyacinth. Reaction-based models applied PFO, PSO and Elovich.

The best fits for the eggshells and potato peels data were achieved by the PSO model. The adjusted q_{Ae} values (0.0855 and 0.0497 mg g^{-1}, respectively) were similar to

the experimental ones (0.0807 and 0.0507 mg g^{-1}) achieving small relative errors of 5.95 % (eggshells) and 1.97 % (potato peels). The k_2 rate constant of the PSO model for potato peels was a hundred times bigger in comparison with the eggshells, confirming the faster equilibration time discussed above.

The Elovich model was better for the kinetics of the banana peels, coffee waste and water hyacinth data. Normally, systems with a mildly rising tendency of q_{A} are well described by this equation as demonstrated by Wu et al., (2009), who studied the characteristics of the kinetic curves through a dimensionless equilibrium parameter ($1/(q_{\mathrm{Ae}}\beta)$). They classified the curves tendency according to the value of this equilibrium parameter in four types of rise: slow, mildly, rapidly and instantly equilibrium approaches. They showed that the systems which are better fitted by the Elovich equation fall into the zone of mildly rising (Devani et al., 2015). The correlated desorption constant (β) was similar for the three biosorbents, while the obtained constants of initial sorption rate (α) were in the same order of magnitude for the coffee waste and water hyacinth. Furthermore, it is more than one thousand times higher for the banana peels emphasizing the advantages to use this biosorbent in mercury removal treatments.

Globally, it can be concluded from the reaction-based models that the biosorption of Hg(II) by *Eucalyptus globulus* bark is better described by a PFO kinetics, while eggshells and potato peels follow a PSO kinetics. On the other hand, banana peels, coffee waste and water hyacinth are better represented by the Elovich model.

The equations of Boyd *et al*. and Webber for intraparticle diffusion were used to unveil the sorption mechanisms involved in the Hg(II) uptake. Table III.1.2 compiles the numerical results of piecewise linear regression (PLR) applied to the experimental data.

Table III.1.1. Parameters of the PFO, PSO and Elovich models for Hg(II) sorption on biosorbents.

	PFO model				**PSO model**				**Elovich model**			
	k_1 (h^{-1})	q_{Ae} (mg g^{-1})	R^2	$AARD$ (%)	k_2 (g mg^{-1} h^{-1})	q_{Ae} (mg g^{-1})	R^2	$AARD$ (%)	α (mg g^{-1} h^{-1})	β (g mg^{-1})	R^2	$AARD$ (%)
Banana peels	11.60	0.0765	0.896	9.22	220.00	0.0817	0.967	4.48	2.52E+03	189.00	0.974	4.49
Eggshells	0.21	0.0760	0.962	12.79	2.72	0.0855	0.987	7.55	3.72E-02	57.46	0.984	7.12
Coffee waste	2.83	0.0680	0.895	11.83	52.74	0.0712	0.952	6.95	1.86	111.93	0.977	4.22
Eucalyptus globulus bark	4.34	0.0754	0.992	6.84	59.43	0.0769	0.973	9.84	0.37	88.55	0.808	20.30
Potato peels	6.79	0.0489	0.989	2.67	329.78	0.0497	0.999	0.96	5.32E+07	538.00	0.994	2.06
Water hyacinth	3.78	0.0663	0.814	14.60	58.00	0.0769	0.908	10.40	4.93	119.00	0.998	1.41

For the equations of Boyd *et al*. it is not recommended to extend the plot close to equilibrium (Malash and El-Khaiary, 2010), hence in this study Bt values higher than 2.2 were excluded from the calculations since enough data are still included to obtain the segments. The plots of Boyd *et al*. (see Figure III.1.6) for the banana peels, coffee waste and water hyacinth were characterized by two linear segments, but only in the case of the coffee waste the interval of the intercept (with 95 % confidence limits) includes zero, what suggests that intraparticle diffusion controls the mass transfer rate. On the other hand, the intercept confidence interval of the first segments of the banana peels and water hyacinth does not include zero, which means the Hg(II) sorption may be controlled by film diffusion during the initial times.

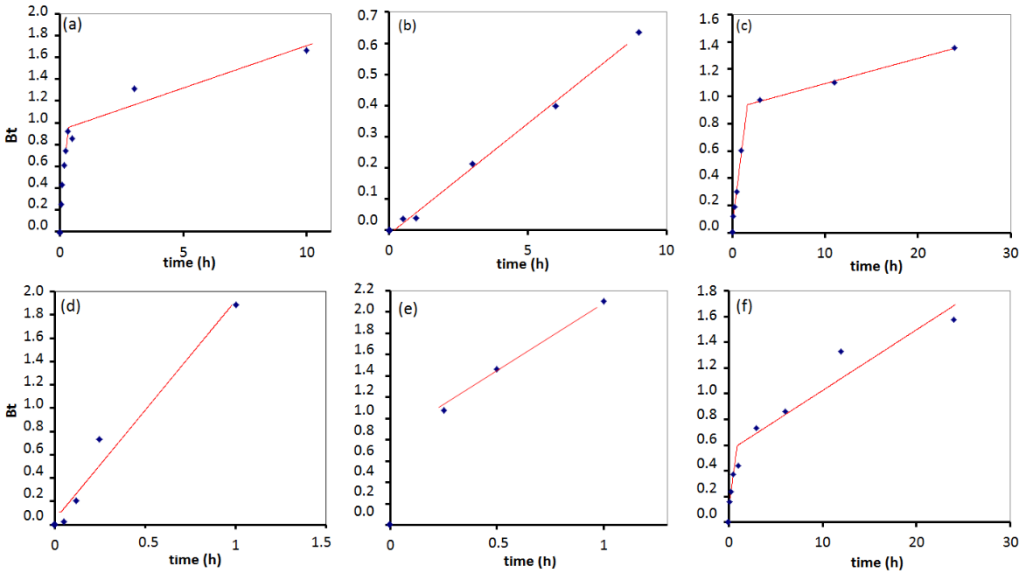

Figure III.1.6. Kinetic modelling of the experimental data of Hg(II) sorption using Boyd et al. diffusion model for: (a) banana peels), (b) eggshells, (c) coffee waste, (d) *Eucalyptus globulus* bark, (e) potato peels and (f) water hyacinth.

The eggshells, *Eucalyptus globulus* bark and potato peels plots evidenced only one linear segment, being the intercept of the first two ones statistically equal to zero, what indicates that intraparticle diffusion may be the rate controlling mechanism. Regarding to the potato peels, the film diffusion may be the prevailing mechanism.

The Webber's plots are shown in Figure III.1.7. After application of PLR, the decision about the assumed number of linear segments was taken based on the Akaike's

Information Criterion (AIC) and the evidence ratio analysis. The lower the AIC value (on a scale from -∞ to +∞) the better, and the evidence ratio means the number of times is more likely the model to be correct than the alternative model. The lower AIC values found for all biosorbents were obtained for two linear segments instead of three and the evidence ratio data were between 1.30×10^3 and 5.10×10^{15}.

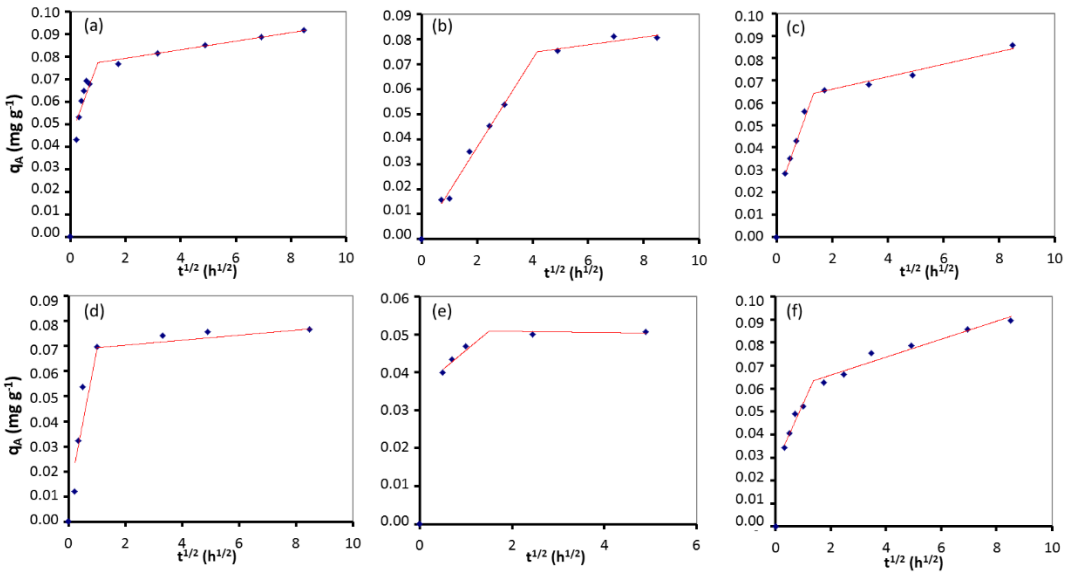

Figure III.1.7. Kinetic modelling of the experimental data of Hg(II) sorption using Webber's intraparticle diffusion model for: (a) banana peels), (b) eggshells, (c) coffee waste, (d) *Eucalyptus globulus* bark, (e) potato peels and (f) water hyacinth.

Considering the results obtained by the Webber's model, since the plots for banana and potato peels, coffee waste and water hyacinth are not intercepting the origin, the trends found can be explained by an initial period of an external diffusion limitation, followed by a stage of intraparticle diffusion towards equilibrium. In relation to the potato peels the second segment is a plateau, which points out that practically no pore diffusion limitations occur, and the mass transfer is controlled by the film. The breakpoints (time where the two linear segments intersect, Table III.1.2) give the calculated time for the transition from film to intraparticle diffusion.

The two stages observed for the eggshells and *E. globulus* bark disclose two diffusional sorption periods. The breakpoints in these cases indicate the time of the

transition between consecutive intraparticle diffusion regimes. Table III.1.2 shows that higher k_{i} values were obtained for the first linear sections as expected.

In general, comparing the classes of equations under analysis, the reaction-based models achieved the best fittings (higher R^2 and lower $AARD$), which emphasises that the mercury(II) uptake by the biosorbents is better explained assuming a chemical reaction between the metal and active sites. However, for the coffee waste the diffusion-based model of Webber offered the best fit, what may suggest that the removal is essentially diffusional and the sorption involves only pure physical interactions.

Table III.1.2. Parameters of the diffusion-based models for Hg(II) sorption on biosorbents.

	Boyd *et al.* intraparticle diffusion model				**Webber's intraparticle diffusion model**			
	Stage	**Intercept & confidence interval**	R^2	**Breakpoint (h)**	k_i **(mg g^{-1} h$^{-0.5}$)**	**Intercept & confidence interval**	R^2	$AARD$ **(%)**
Banana peels	1st	0.187 [0.074, 0.300]	0.983	1.0	0.0333	0.0445 [0.0299, 0.0590]	0.855	4.90
	2nd	0.930 [-1.175, 3.036]	0.889		0.0019	0.0755 [0.0731, 0.0780]	0.988	
Eggshells	1st	-0.014 [-0.057, 0.029]	0.996	17.2	0.0177	0.0018 [-0.0068, 0.0104]	0.982	5.37
	2nd				0.0015	0.0687 [-0.0038, 0.1410]	0.775	
Coffee waste	1st	0.052 [-0.010, 0.114]	0.996	1.7	0.0353	0.0180 [0.0138, 0.0223]	0.997	1.98
	2nd	0.908 [0.727, 1.089]	0.998		0.0028	0.0608 [0.0527, 0.0688]	0.973	

Eucalyptus globulus bark	1st	0.044 [-0.496, 0.584]	0.968	1.0	0.0590	0.0105 [-0.0419, 0.0629]	0.844	18.90
	2nd				0.0010	0.0685 [0.0561, 0.0809]	0.874	
Potato peels	1st	0.751 [0.223, 1.280]	0.998	2.3	0.0101	0.0358 [0.0217, 0.0500]	0.989	1.85
	2nd				-0.0002 NP	0.0512 NP	1.000	
Water hyacinth	1st	0.104 [0.061, 0.147]	1.000	1.9	0.0268	0.0271 [0.0126, 0.0416]	0.936	2.76
	2nd	0.552 [0.194, 0.911]	0.900		0.0039	0.0644 [0.0520, 0.0644]	0.955	

NP: It was not possible to calculate confidence limits because the line consists

III.1.4. Conclusions

This work emphasizes the high ability of the tested biosorbents to remove mercury from aqueous streams. All biosorbents have been able to capture Hg(II) from aqueous solutions under environmental realistic conditions. The best performances were accomplished by banana peels and water hyacinth, which removed in 72 hours more than 90 % of the initial mercury in solution (50 μg dm^{-3}) for sorbent doses of 0.5 g dm^{-3}. The different fittings of the kinetic reaction-based equations to the experimental data confirmed the unequal abilities of the biosorbents for Hg(II) uptake, and stressed banana peels as the most promising one for application in water treatments. The diffusion models suggested that the rate of mercury sorption by the potato peels is controlled by film diffusion, while in banana peels, coffee waste and water hyacinth is controlled initially by film diffusion followed by intraparticle diffusion. In the case of eggshells and *Eucalyptus globulus* bark the rate controlling step is intraparticle diffusion. The FTIR-ATR and SEM analyses pointed to the relevance of 0-H and C=O functional groups on the biosorbent surface, eventually combined with its morphology, on the Hg(II) uptake.

III.1.5. References

Abdel-Khalek, M.A., Abdel Rahman, M.K., Francis, A.A., 2017. Exploring the adsorption behavior of cationic and anionic dyes on industrial waste shells of egg. J. Environ. Chem. Eng. 5, 319–327. https://doi.org/10.1016/j.jece.2016.11.043

Abdolali, A., Guo, W.S., Ngo, H.H., Chen, S.S., Nguyen, N.C., Tung, K.L., 2014. Typical lignocellulosic wastes and by-products for biosorption process in water and wastewater treatment: A critical review. Bioresour. Technol. 160, 57–66. https://doi.org/10.1016/j.biortech.2013.12.037

Arami, M., Yousefi Limaee, N., Mahmoodi, N.M., 2006. Investigation on the adsorption capability of egg shell membrane towards model textile dyes. Chemosphere 65, 1999–2008. https://doi.org/10.1016/j.chemosphere.2006.06.074

Bailey, S.E., Olin, T.J., Bricka, R.M., and Adrian, D.D., 1999. A review of pontentially low-

cost sorbents for heavy metals. Wat. Res. 33, 2469–2479. https://doi.org/10.1016/S0043-1354(98)00475-8

Bhatnagar, A., Sillanpää, M., Witek-Krowiak, A., 2015. Agricultural waste peels as versatile biomass for water purification - A review. Chem. Eng. J. 270, 244–271. https://doi.org/10.1016/j.cej.2015.01.135

Boyd, G.E., Adamson, A.W., Myers, L.S., 1947. The Exchange Adsorption of Ions from Aqueous Solutions by Organic Zeolites; Kinetics. J. Am. Chem. Soc. 69, 2836–2848. https://doi.org/10.1021/ja01203a066

Cardoso, S.P., Lopes, C.B., Pereira, E., Duarte, A.C., Silva, C.M., 2013. Competitive Removal of Cd2+ and Hg2+ Ions from Water Using Titanosilicate ETS-4: Kinetic Behaviour and Selectivity. Water, Air, Soil Pollut. 224, 1535. https://doi.org/10.1007/s11270-013-1535-z

Carro, L., Anagnostopoulos, V., Lodeiro, P., Barriada, J.L., Herrero, R., Sastre de Vicente, M.E., 2010. A dynamic proof of mercury elimination from solution through a combined sorption–reduction process. Bioresour. Technol. 101, 8969–8974. https://doi.org/10.1016/J.BIORTECH.2010.06.118

Carro, L., Barriada, J.L., Herrero, R., Sastre de Vicente, M.E., 2011. Adsorptive behaviour of mercury on algal biomass: Competition with divalent cations and organic compounds. J. Hazard. Mater. 192, 284–291. https://doi.org/10.1016/J.JHAZMAT.2011.05.017

Devani, M.A., Munshi, B., Oubagaranadin, J.U.K., 2015. Characterization and use of chemically activated Butea monosperma leaf dust for mercury(II) removal from solutions. J. Environ. Chem. Eng. 3, 2212–2218. https://doi.org/10.1016/J.JECE.2015.07.028

Hartley, G.S., Crank, J., 1949. Some fundamental definitions and concepts in diffusion processes. Trans. Faraday Soc. 45, 801. https://doi.org/10.1039/tf9494500801

Helfferich, F.G., 1962. Ion Exchange. McGraw-Hill, New York.

Ho, Y.-S., 2006. Review of second-order models for adsorption systems. J. Hazard. Mater. 136, 681–689. https://doi.org/10.1016/J.JHAZMAT.2005.12.043

Ho, Y.S., McKay, G., 1999. Pseudo-second order model for sorption processes. Process Biochem. 34, 451–465. https://doi.org/10.1016/S0032-9592(98)00112-5

Ho, Y.S., Ng, J.C.Y., McKay, G., 2000. Kinetics of pollutant sorption by biosorbents: Review. Sep. Purif. Methods 29, 189–232. https://doi.org/10.1081/SPM-100100009

Ibrahim, H.S., Ammar, N.S., Soylak, M., Ibrahim, M., 2012. Removal of Cd(II) and Pb(II) from aqueous solution using dried water hyacinth as a biosorbent. Spectrochim. Acta Part A Mol. Biomol. Spectrosc. 96, 413–420. https://doi.org/10.1016/j.saa.2012.05.039

Igwe, J.C., Abia, A.A., Ibeh, C.A., 2008. Adsorption kinetics and intraparticulate diffusivities of Hg, As and Pb ions on unmodified and thiolated coconut fiber. Int. J. Environ. Sci. Technol. 5, 83–92. https://doi.org/10.1007/BF03326000

Inglezakis, V.J., Loizidou, M.D., Grigoropoulou, H.P., 2002. Equilibrium and kinetic ion exchange studies of Pb2+, Cr3+, Fe3+ and Cu2+ on natural clinoptilolite. Water Res. 36, 2784–2792. https://doi.org/10.1016/S0043-1354(01)00504-8

Jeong, S.H., Park, K., 2008. Drug loading and release properties of ion-exchange resin complexes as a drug delivery matrix. Int. J. Pharm. 361, 26–32. https://doi.org/10.1016/j.ijpharm.2008.05.006

Jiménez-Cedillo, M.J., Olguín, M.T., Fall, C., Colin-Cruz, A., 2013. As(III) and As(V) sorption on iron-modified non-pyrolyzed and pyrolyzed biomass from Petroselinum crispum (parsley). J. Environ. Manage. 117, 242–252. https://doi.org/10.1016/J.JENVMAN.2012.12.023

Lagergren, S., 1898. Zur theorie der sogenannten adsorption gel Zur theorie der sogenannten adsorption gelster stoffe, Kungliga Svenska Vetenskapsakademiens. Handlingar 24, 1–39.

Largitte, L., Pasquier, R., 2016. A review of the kinetics adsorption models and their

application to the adsorption of lead by an activated carbon. Chem. Eng. Res. Des. 109, 495–504. https://doi.org/10.1016/J.CHERD.2016.02.006

Liang, S., McDonald, A.G., 2014. Chemical and thermal characterization of potato peel waste and its fermentation residue as potential resources for biofuel and bioproducts production. J. Agric. Food Chem. 62, 8421–8429. https://doi.org/10.1021/jf5019406

Lito, P.F., Aniceto, J.P.S., Silva, C.M., 2012. Removal of Anionic Pollutants from Waters and Wastewaters and Materials Perspective for Their Selective Sorption. Water, Air, Soil Pollut. 223, 6133–6155. https://doi.org/10.1007/s11270-012-1346-7

Lopes, C.B., Lito, P.F., Cardoso, S.P., Pereira, E., Duarte, A.C., Silva, C.M., 2012. Metal recovery, separation and/or pre-concentration, in: Inamuddin, Luqma, M. (Eds.), Ion Exchange Technology II – Applications. Springer, pp. 237–322.

Lopes, C.B., Lito, P.F., Otero, M., Lin, Z., Rocha, J., Silva, C.M., Pereira, E., Duarte, A.C., 2008. Mercury removal with titanosilicate ETS - 4 : Batch experiments and modelling. Microporous Mesoporous Mater. 115, 98–105. https://doi.org/10.1016/j.micromeso.2007.10.055

Luo, H., He, D., Zhu, W., Wu, Y., Chen, Z., Yang, E.H., 2019. Humic acid-induced formation of tobermorite upon hydrothermal treatment with municipal solid waste incineration bottom ash and its application for efficient removal of Cu(II) ions. Waste Manag. 84, 83–90. https://doi.org/10.1016/j.wasman.2018.11.037

Malash, G.F., El-Khaiary, M.I., 2010. Piecewise linear regression: A statistical method for the analysis of experimental adsorption data by the intraparticle-diffusion models. Chem. Eng. J. 163, 256–263. https://doi.org/10.1016/j.cej.2010.07.059

Nguyen, T.A.H., Ngo, H.H., Guo, W.S., Zhang, J., Liang, S., Yue, Q.Y., Li, Q., Nguyen, T.V., 2013. Applicability of agricultural waste and by-products for adsorptive removal of heavy metals from wastewater. Bioresour. Technol. 148, 574–585. https://doi.org/10.1016/J.BIORTECH.2013.08.124

Omorogie, M.O., Babalola, J.O., Unuabonah, E.I., Gong, J.R., 2012. Kinetics and thermodynamics of heavy metal ions sequestration onto novel Nauclea diderrichii seed biomass. Bioresour. Technol. 118, 576–579. https://doi.org/10.1016/J.BIORTECH.2012.04.053

Otero, M., Lopes, C.B., Coimbra, J., Ferreira, T.R., Silva, C.M., Lin, Z., Rocha, J., Pereira, E., Duarte, A.C., 2009. Priority pollutants (Hg2+ and Cd2+) removal from water by ETS-4 titanosilicate. Desalination 249, 742–747. https://doi.org/10.1016/j.desal.2009.04.008

Panda, G.C., Das, S.K., Bandopadhyay, T.S., Guha, A.K., 2007. Adsorption of nickel on husk of Lathyrus sativus: Behavior and binding mechanism. Colloids Surfaces B Biointerfaces 57, 135–142. https://doi.org/10.1016/J.COLSURFB.2007.01.022

Pérez Marín, A.B., Aguilar, M.I., Ortuño, J.F., Meseguer, V.F., Sáez, J., Lloréns, M., 2010. Biosorption of Zn(II) by orange waste in batch and packed-bed systems. J. Chem. Technol. Biotechnol. 85, 1310–1318. https://doi.org/10.1002/JCTB.2432

Qiu, H., Lv, L., Pan, B.-C., Zhang, Q.-J., Zhang, W.-M., Zhang, Q.-X., 2009. Critical review in adsorption kinetic models *. J Zhejiang Univ Sci A 10, 716–724. https://doi.org/10.1631/jzus.A0820524

Rafatullah, M., Sulaiman, O., Hashim, R., Ahmad, A., 2009. Adsorption of copper (II), chromium (III), nickel (II) and lead (II) ions from aqueous solutions by meranti sawdust. J. Hazard. Mater. 170, 969–977. https://doi.org/10.1016/J.JHAZMAT.2009.05.066

Rao, M., Parwate, A.V., Bhole, A.G., 2002. Removal of Cr6+ and Ni2+ from aqueous solution using bagasse and fly ash. Waste Manag. 22, 821–830. https://doi.org/10.1016/S0956-053X(02)00011-9

Rao, M.M., Reddy, D.H.K.K., Venkateswarlu, P., Seshaiah, K., 2009. Removal of mercury from aqueous solutions using activated carbon prepared from agricultural by-product/waste. J. Environ. Manage. 90, 634–643. https://doi.org/10.1016/j.jenvman.2007.12.019

Reichenberg, D., 1953. Properties of Ion-Exchange Resins in Relation to their Structure. III. Kinetics of Exchange. J. Am. Chem. Soc. 75, 589–597. https://doi.org/10.1021/ja01099a022

Rocha, L.S., Almeida, Â., Nunes, C., Henriques, B., Coimbra, M.A., Lopes, C.B., Silva, C.M., Duarte, A.C., Pereira, E., 2016. Simple and effective chitosan based films for the removal of Hg from waters: Equilibrium, kinetic and ionic competition. Chem. Eng. J. 300, 217–229. https://doi.org/10.1016/j.cej.2016.04.054

Roginsky, S., Zeldovich, Y.B., 1934. The catalytic oxidation of carbon monoxide on manganese dioxide. Acta Phys. Chem. USSR 1, 554.

Rosales, E., Meijide, J., Pazos, M., Sanromán, M.A., 2017. Challenges and recent advances in biochar as low-cost biosorbent: From batch assays to continuous-flow systems. Bioresour. Technol. 246, 176–192. https://doi.org/10.1016/J.BIORTECH.2017.06.084

Salaudeen, S.A., Tasnim, S.H., Heidari, M., Acharya, B., Dutta, A., 2018. Eggshell as a potential CO2 sorbent in the calcium looping gasification of biomass. Waste Manag. 80, 274–284. https://doi.org/10.1016/J.WASMAN.2018.09.027

Singanan, M., 2015. Biosorption of Hg(II) ions from synthetic wastewater using a novel biocarbon technology. Environ. Eng. Res. 20, 33–39. https://doi.org/10.4491/eer.2014.032

Tran, V.S., Ngo, H.H., Guo, W., Zhang, J., Liang, S., Ton-That, C., Zhang, X., 2015. Typical low cost biosorbents for adsorptive removal of specific organic pollutants from water. Bioresour. Technol. 182, 353–363. https://doi.org/10.1016/j.biortech.2015.02.003

Weber, W.J., Morris, J.C., 1963. Kinetics of Adsorption on Carbon from Solution. J. Sanit. Eng. Div. 89, 31–60.

Wu, F.-C., Tseng, R.-L., Juang, R.-S., 2009. Characteristics of Elovich equation used for the analysis of adsorption kinetics in dye-chitosan systems. Chem. Eng. J. 150, 366–373. https://doi.org/10.1016/J.CEJ.2009.01.014

Zafar, M.N., Nadeem, R., Hanif, M.A., 2007. Biosorption of nickel from protonated rice bran. J. Hazard. Mater. 143, 478–485. https://doi.org/10.1016/J.JHAZMAT.2006.09.055

Zhang, F.-S., Nriagu, J.O., Itoh, H., 2005. Mercury removal from water using activated carbons derived from organic sewage sludge. Water Res. 39, 389–395. https://doi.org/10.1016/j.watres.2004.09.027

Work submitted as scientific article

Valuation of banana peels as an effective biosorbent for mercury removal under low environmental concentrations

Abstract

The use of banana peels as biosorbent for mercury sorption from different aqueous solutions was investigated in this work. The impact of the operating conditions, such as biosorbent dosage, contact time and ionic strength was evaluated for realistic initial Hg(II) concentrations of 50 μg dm^{-3}. Biosorbent dosage and contact time showed more influence on Hg(II) removal than ionic strength, and their increase led to improve Hg(II) uptake achieving final concentrations with drinking water quality. The kinetic behaviour of the sorption process was assessed through the reaction-based models of pseudo-first order, pseudo-second order and Elovich, being the last two more appropriated to describe the process. The equilibrium study showed that Freundlich isotherm provided the best fit to the experimental results (R^2=0.991), which may suggest a multilayer mechanism at biosorbent surface, and the sorption capacity of banana peels obtained from Langmuir isotherm was 0.75 mg g^{-1}. The ability of banana peels to sorb Hg(II) was also examined under real waters, like seawater and a wastewater, which confirmed the feasibility of the biosorbent. Additionally, a counter-current two-stages unit has been proposed for the application of banana peels as biosorbent in water treatments for mercury removal.

III.2. Valuation of banana peels as an affective biosorbent for mercury removal under low environmental concentrations

III.2.1. Introduction

Sorption processes have received increasing attention due to their efficient and cheaper application for toxic metals removal in water treatments (Vinod et al., 2011). These processes are based on the separation of metals from a solution by a solid sorbent of synthetic or biological origin (Fabre et al., 2019; Lito et al., 2012; Lopes et al., 2012; Rangabhashiyam et al., 2016). Despite the advantages of synthetic sorbents, such as high affinity and selectivity towards target metals, in general these materials present high costs and the preparing reactions are usually toxic (D Castro et al., 2011). Biosorbents from agricultural and agro-forest residues are promising approaches for metal removal because residues are largely available in nature, have low costs, and require little or no additional processing (Castro et al., 2017; Fabre et al., 2019; Kumar et al., 2019; Nguyen et al., 2013).

Banana is one of the most popular fruit consumed worldwide and its world production increased from 68.2 million tons in 2000 to 117.9 million tons in 2015 (FA0, 2018). The banana peel represents 30-40 % of the banana total weight, generating annually about 50 million tons of wastes (FA0, 2018). In its constitution, banana peel contains high quantities of cellulose, which possesses functional groups able to bind metals (D Castro et al., 2011). In addition, the concepts of circular economy and green processes magnify the interest of using this type of biomass as biosorbent, contributing to the waste management and to add value to this by-product.

Among the toxic metals responsible for the contamination of the aquatic systems, mercury is one of the most troublesome due to its persistence in the environment and magnification along the food chain (Johs et al., 2019; Lopes et al., 2009; Shan et al., 2019). Mercury is listed by the Agency for Toxic Substances & Disease Registry (ATSDR) as the third most dangerous substance (“ATSDR, Priority list of hazardous substances,” 2017)

and can occur as elemental or metallic mercury, organic and inorganic forms (De et al., 2014; Holmes et al., 2009). In the aquatic systems mercury may be converted into various forms, and the environmental toxic effects increase when inorganic mercury is transformed in methylmercury (De et al., 2014). Even trace concentrations of methylmercury exerts considerable health risks, affecting the cardiovascular and central nervous systems (Azevedo et al., 2012), while elemental and inorganic mercury impacts kidneys, lungs, and immune system (Ayangbenro and Babalola, 2017; Wang et al., 2012). Concerns about mercury exposure effects encourage the development of new clean-up technologies. In addition, the 2030 Agenda for Sustainable Development of United Nations promotes minimizing release of hazardous chemicals and materials, fomenting wastewater treatment and recycling and safe water reuse globally.

Several biosorbents have been investigated for mercury removal. *Phragmites karka* untreated and treated with NaOH (0.5 M) and $CaCl_2$ (1.5 M) were used to remove Hg(II) from distilled water with Hg(II) initial concentrations in the range of 10-60 mg dm^{-3} (Raza et al., 2015). Gum karaya (*Sterculia urens*) was used for Hg(II) biosorption from ultrapure water spiked with 50-300 mg dm^{-3} (Vinod et al., 2011). Natural and formaldehyde treated forms of *Lagenaria siceraria* peels were tested for Hg(II) elimination from mono-elemental solutions prepared with distilled water and different mercury concentrations (between 2 and 10 mg dm^{-3}) (Ahmed et al., 2018). In another study, mercury removal (at 100 mg dm^{-3}) was optimized by using 10 g dm^{-3} of algal *Cladophora* sp. (Mokone et al., 2018). A dosage of 20 g dm^{-3} of *Allium Cepa L.* was applied for Hg(II) removal from ultrapure water containing initial concentrations up to 1000 mg dm^{-3} (Balderas-Hernández et al., 2017). Living and dead *Agaricus macrosporus* was used for mercury removal from acid solutions containing initial metal concentration of 100 mg dm^{-3} (Melgar et al., 2007). Recently, *Eucalyptus globulus* bark was used for Hg(II) sorption from natural waters containing initial metal concentration of 50 μg dm^{-3}, with solid dosages of 0.2-0.8 g dm^{-3} (Fabre et al., 2019).

Despite the increasing attention to the biosorption processes and the high number of publications in this field, the use of unrealistic conditions like mono-elemental solutions with high Hg(II) concentrations and simple water matrices hold off the practical

application of the biosorbents. Furthermore, normally high doses of biosorbents are applied and consequently large amounts of contaminated wastes are generated. In this sense, more research should be oriented to conditions more likely to be found in the environment and industrial effluents in order to offer viable alternatives for wastewaters treatment.

The present work reports the performance of banana peels for removal of low mercury concentrations from spiked tap water, seawater and wastewater. Effects of contact time, sorbent dosage and ionic strength were investigated. The kinetic behavior was interpreted using pseudo-first order, pseudo-second order and Elovich models, and the equilibrium study was accomplished with Langmuir and Freundlich isotherms. A proposed two-stage counter-current contactor complements the work for effective application of this biosorbent.

III.2.2. Materials and methods

III.2.2.1. Chemicals and instrumentation

The chemicals used in this work were of analytical grade, obtained from chemical commercial suppliers and used without further purification. The certified standard solution of mercury(II) nitrate (1000 ± 2 mg dm^{-3}), sodium hydroxide (≥ 99 %) and nitric acid (65 %) were purchased from Merck, and the sodium chloride (≥ 99%) was acquired from Applichem Panreac. Standard solutions for the calibration curves were prepared by diluting the corresponding stock solution in high purity water (18 MΩ cm) or nitric acid solution (2 %, v/v). All glassware was acid-washed prior to use, with nitric acid 25 % (v/v) for 24 hours.

The quantification of Hg(II) was performed by atomic fluorescence spectroscopy (CV-AFS), on a PSA cold vapour generator, model 10.003, with Merlin PSA detector, model 10.023 and using $SnCl_2$ as the reducing agent. Fourier Transform Infrared (FTIR) spectra of the biosorbent previous and after sorption were performed using a Bruker optics tensor 27 spectrometer coupled to a horizontal attenuated total reflectance (ATR) cell using 256 scans at a resolution of 4 cm^{-1}. The biosorbent point zero charge (PZC) was determined

according to an adaptation of the immersion method proposed by Fiol and Villaescusa (2009) using an incubator shaker HWY-200D and the solution pH was measured on a WTW series 720 meter. The salinity was determined by Eclipse handheld refractometer model 45-63.

III.2.2.2. Biomass collection

The biosorbent used in this study had no chemical or thermal pre-treatment. Banana peels were only rinsed with tap and distilled water, frozen, lyophilized, milled and separated in particles sizes of less than 1 mm diameter and then stored in plastic containers until use in the further experiments.

III.2.2.3. Batch experiments

In order to investigate the performance of the banana peels, experiments were accomplished in batch conditions at room temperature (22 °C ± 1) in a 1 dm^3 volumetric flasks. Known masses of the biosorbent were added into the spiked tap water solutions with the fixed Hg(II) concentration of 50 µg dm^{-3} and pH about 6.0, and the mixture was magnetically stirred at 650 rpm. Samples were taken at determined times, filtered through a 0.45 µm Millipore filter, adjusted to pH < 2 with HNO_3 65 %, stored at 4 °C and then analyzed. Each experiment was run in parallel with a control experiment (without biosorbent) to check the experimental losses. The effects of the biosorbent dosage and contact time were studied by varying the solid dosages in solution (0.15, 0.25 and 0.50 g dm^{-3}) and collecting samples at different times until 72 hours. For the equilibrium isotherm, several dosages (0.10, 0.15, 0.20, 0.25, 0.40, 0.50, 0.60 and 1.00 g dm^{-3}) were added to Hg(II) solutions with an initial concentration of 50 µg dm^{-3} and the experiments were conducted as previously described until reaching equilibrium. The ionic strength influence on the sorption efficiency was examined by contacting a biosorbent proportion of 0.50 g dm^{-3} with salt solutions prepared with 3, 15 and 30 g dm^{-3} of NaCl. Again, the experiments were conducted as previously described.

To test the ability of banana peels to sorb Hg(II) under more realist conditions, spiked seawater and industrial wastewater were used. Seawater was collected from the Portuguese coast at Vagueira beach (40°33'N, 8°46'W) and the wastewater was kindly provided by ISQ - Instituto de Soldadura e qualidade (Welding and Quality Institute). Seawater used in the experiments was previously spiked with 50 μg dm^{-3} of Hg(II), while the wastewater was analysed to determine the initial metal concentration and then diluted to achieve the same target mercury concentration (50 μg dm^{-3}). In these sorption assays, the same biosorbent concentration of 0.50 g dm^{-3} was used.

The average amount of sorbed Hg(II) per unit mass of biosorbent, q_A (mg g^{-1}) was calculated by global material balance at time t in solution:

$$q_A = \frac{V_L}{m_S}(C_{A0} - C_A) \qquad \text{(III.2.1)}$$

where 'A' represents Hg(II), V_L is the solution volume (dm^3), m_S is the mass of biosorbents (g), C_{A0} is the initial concentration of Hg(II) in solution and C_A is its concentration at time t (mg dm^{-3}).

The removal efficiency was calculated as bellow:

$$Removal\ (\%) = 100 \times \frac{(C_{A0} - C_{Af})}{C_{A0}} \qquad \text{(III.2.2)}$$

where C_{Af} is the Hg(II) concentration at the end of the experimental assay.

III.2.2.4. Kinetics and equilibrium modelling

The kinetic study is important to elucidate the rate of mass transfer between the sorbent and bulk solution, and depends on the chemical and morphological features of the solid. The rate of the contaminants sorption is one of the most essential factors to consider in a system design (Plazinski et al., 2009). The evaluation of the kinetic parameters gives important information about the viability of the process, which is essential for posterior industrial applications (Azizian, 2004). The models of pseudo-first order (PFO), pseudo-second order (PSO), and Elovich were fitted to the experimental data

to describe the process of Hg(II) removal. These models were derived for adsorption, considering that the overall sorption process is controlled by chemical reaction on the sorbent surface and have been largely applied due to their simplicity and ability to represent the removal process (Largitte and Pasquier, 2016; Rudzinski and Plazinski, 2006).

The pseudo-first order equation proposed by Lagergren (1898) assumes that the sorption follows a first order kinetics, as follows :

$$\frac{dq_A}{dt} = k_1(q_{Ae} - q_A) \qquad \text{(III.2.3)}$$

where k_1 (h^{-1}) is the rate constant of the model and q_{Ae} (mg g^{-1}) is the concentration of Hg(II) sorbed at equilibrium.

The pseudo-second-order model (Ho and McKay, 1999) can also be used to describe the kinetics of sorption along time, and its corresponding expression is:

$$\frac{dq_A}{dt} = k_2(q_{Ae} - q_A)^2 \qquad \text{(III.2.4)}$$

where k_2 (g mg^{-1} h^{-1}) is the rate constant of the model.

The Elovich equation (Roginsky and Zeldovich, 1934) is is given by:

$$\frac{dq_A}{dt} = \alpha e^{-\beta q_A} \qquad \text{(III.2.5)}$$

where α is the initial Hg(II) sorption rate (mg g^{-1} h^{-1}) and β (g mg^{-1}) is the desorption parameter.

The equilibrium study also plays an important role in the decision for scale-up applications. The evaluation of the isotherm provides information about the capacity of the material and its surface characteristics. The isotherms of Langmuir and Freundlich were fitted to the experimental data in this work.

Langmuir model predicts a finite number of identical active sites on the sorbent surface with uniform energy sorption. The sorbate is accumulated in a monolayer at solid surface (Langmuir, 1916). It is represented by:

$$q_{Ae} = \frac{qm_L K_L C_{Ae}}{1 + K_L C_{Ae}} \quad \text{(III.2.6)}$$

where qm_{L} (mg g^{-1}) is the sorption capacity, corresponding to the monolayer coverage, and K_{L} (dm^3 mg^{-1}) is the Langmuir equilibrium constant.

Freundlich isotherm assumes a multilayer sorption with an exponentially decaying sorption energy. It is applied to non-ideal systems, with heterogeneous surfaces (Freundlich, 1906; Ho et al., 2002), and it is mathematically represented by:

$$q_{Ae} = K_F C_{Ae}^{1/n_F} \quad \text{(III.2.7)}$$

where, K_{F} ($mg^{1-1/nF}$ $dm^{3/nF}$ g^{-1}) and n_{F} are the Freundlich constants. The parameter n_{F} is related with the nonlinearity of the model. The larger is this value, more nonlinear is the isotherm (Do, 1998).

All the parameters of both kinetic and equilibrium models were obtained by nonlinear regression using Matlab R2014a program, based on the Nelder-Mead simplex algorithm to minimize the average absolute relative deviation ($AARD$). The goodness of the fits were evaluated over the coefficient of determination (R^2) and $AARD$, which are expressed by:

$$R^2 = 1 - \frac{\sum(\hat{y}_i - y_i)^2}{\sum(y_i - \bar{y})^2} \quad \text{(III.2.8)}$$

$$AARD(\%) = \frac{100}{N_{DP}} \sum_{i=1}^{N_{DP}} \frac{|y_i - \hat{y}_i|}{y_i} \quad \text{(III.2.9)}$$

where, y_{i} represents the experimental values, $\hat{y}_{\mathrm{i}}$ are the values calculated by the models, $\bar{y}$ is the mean of the experimental values and N_{DP} is the total number of points.

III.2.3. Results and discussion

III.2.3.1. Biosorbent characterization

Peaks of the functional groups present on biosorbents surfaces obtained by FTIR spectra before and after sorption are presented in Figure III.2.1. The band observed in the region of 3300 cm^{-1} represents O-H and N-H vibrations (Abdel-Khalek et al., 2017). The double peak at 2800-3000 cm^{-1} is due to the C-H stretching vibrations (Rao et al., 2009) and the band at 1740 cm^{-1} is attributed to C=O bonds of carboxylic acids (Liang and McDonald, 2014). The peak at 1588 cm^{-1} is associated with C=C stretching frequencies characteristic of the aromatic ring presents on lignin (Liang and McDonald, 2014). The band at 1372 cm^{-1} corresponds to aliphatic C-H stretching (Liang and McDonald, 2014), and the strong band ranging from 1200 to 900 cm^{-1} is related to -C-O-C- vibration of the cellulose (Rafatullah et al., 2009). The peaks observed at 923, 887 and 515 cm^{-1} are representative of sulfur groups (Awwad et al., 2015). These last groups have been reported as efficient ligands towards mercury (Castro et al., 2003; Pérez-García et al., 2010). Indeed, the comparison between biomass and biomass/Hg(II) spectra showed a shift of the peak at 1588 cm^{-1} to 1631 cm^{-1}, a slight peak rise at 1540 cm^{-1} attributed to N-H bonds (D Castro et al., 2011) and the bands at 923 and 515 cm^{-1} of the sulfur groups disappeared in the loading biosorbent. These changes suggest the involvement of those groups in the process of mercury sorption. Sulfur being a soft base has high affinity and selectivity for soft cations, like Hg^{2+}, as compared to hard cations commonly present in natural waters (Na^{+}, Mg^{2+} or Ca^{2+}) (Stumm and Morgan, 1996).

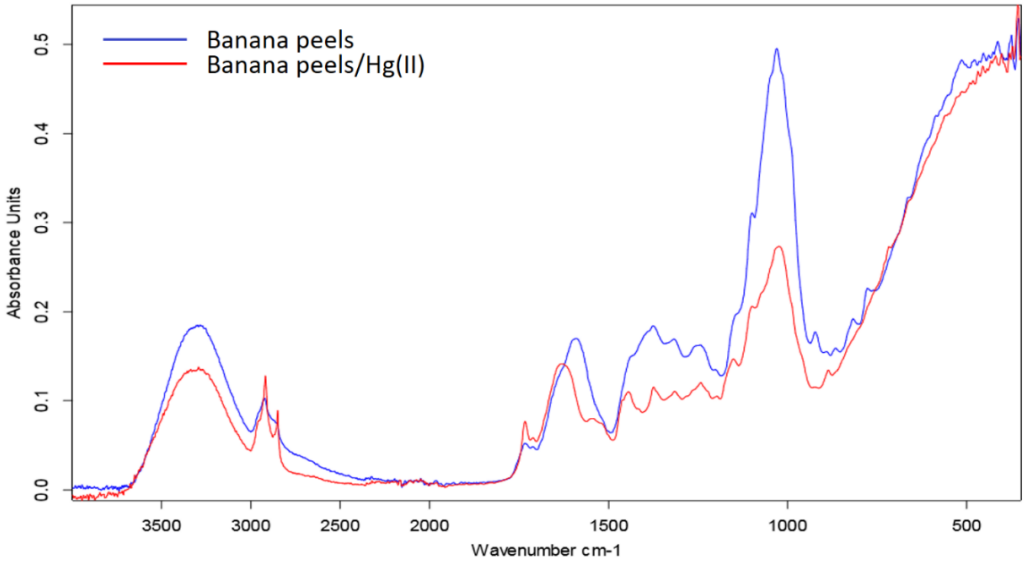

Figure III.2.1. FTIR spectra for the biomass before (blue) and after mercury sorption (red).

The point of zero charge (PZC) of the biosorbent was determined (Figure III.2.2). The method used imposes that PZC is reached when the surface of biosorbents has no charge, at ΔpH ≈ 0. Above this pH the surface donates protons to the solution and becomes negatively charged and, in contrast, below this value the sorbent is positively charged by accepting protons from the solution (Fiol and Villaescusa, 2009). The PZC found for the banana peels used in this study was 5.4, which is in accordance with the value previously reported by Pathak *et al.* (Pathak and Mandavgane, Sachin A. Kulkarni, 2017).

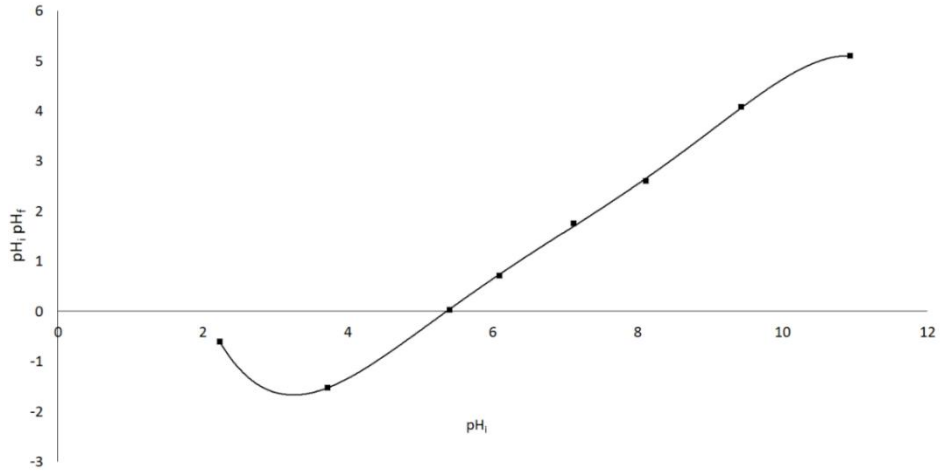

Figure III.2.2. Point zero charge (PZC) of the banana peels.

III.2.3.2. Effect of biosorbent dosage and contact time

The efficiency of sorption processes is highly influenced by the quantity of biosorbent and contact time (Lopes et al., 2009). The effect of biosorbent dosage was studied using 0.15, 0.25 and 0.50 g dm^{-3} of banana peels to remove Hg(II) in batch sorption systems until 72 hours.

Figure III.2.3 shows that Hg(II) removal increased from 73 to 91 % with the increase of banana peels from 0.15 to 0.50 g dm^{-3}. This behaviour has also been observed in other sorption studies (Ajmani et al., 2019b; Fabre et al., 2019; Karthik et al., 2019; Patra et al., 2019; Riaz et al., 2009), and is explained by the increased number of sorption sites available, in this case in higher mass of banana peels. Concerning the Hg(II) sorbed per gram of solid (q_A), the values decreased from 0.246 mg g^{-1} for 0.15 g dm^{-3} to 0.0919 mg g^{-1} for 0.50 g dm^{-3}, due to the dilution effect of Hg(II) in a higher amount of biosorbent.

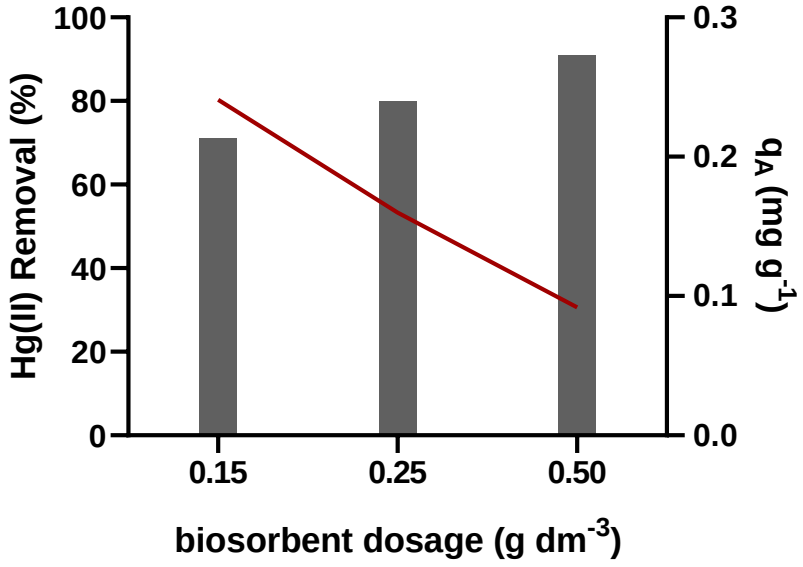

Figure III.2.3. Effect of the biosorbent dosage on Hg(II) sorption after 72 hours of contact, expressed as Hg(II) removal (bars) and as solid loading (line).

Figure III.2.4 shows the kinetic curves corresponding to Hg(II) sorption for the three different dosages of banana peels. For all curves the metal concentration in the liquid phase decreased along time. The observed kinetic profiles exhibited a high dependence on the contact time mainly in the first 10 hours when the sorption is characterized by a pronounced reduction of Hg followed by a decelerating of the Hg(II) removal until 72 hours. At the beginning of the process, the particles are free of Hg(II) and the concentration gradient between the banana peels surface and contaminated water is higher, therefore promotes the diffusion towards the biosorbent. As sorption sites become occupied and Hg(II) concentration in solution decreases, the concentration gradient is reduced conducting the process towards the equilibrium (Seader and Henley, 1998). In addition, the fastest initial sorption rate was observed for the highest biosorbent dose (0.50 g dm^{-3}), the magnitude of initial rates (calculated from the first derivate of $C_A = f(t)$ for initial times, at $t = 0$) were 117, 154 and 175 µg dm^{-3} h^{-1} for the biosorbent doses of 0.15, 0.25 and 0.50 g dm^{-3}.

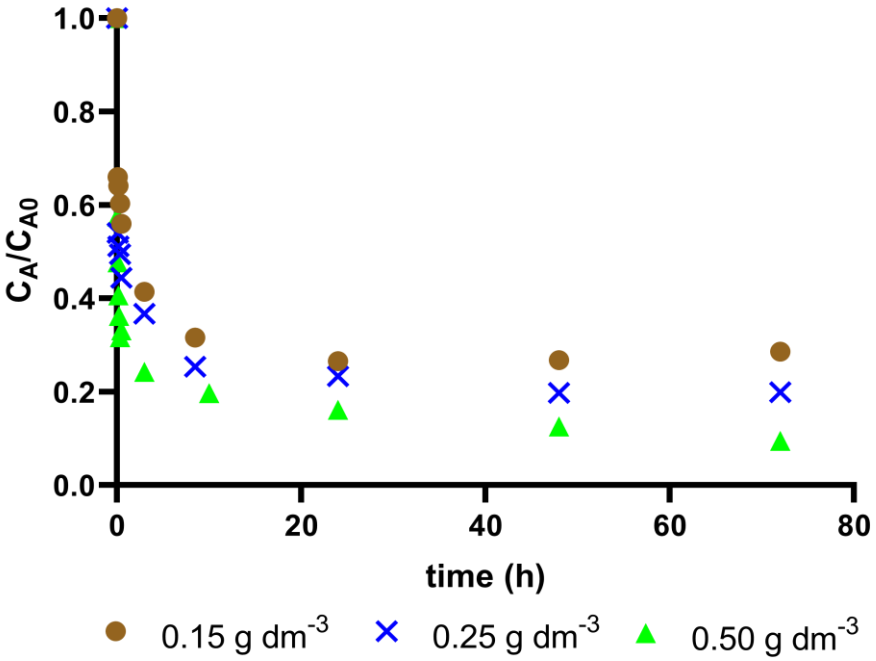

Figure III.2.4. Hg(II) normalized concentration in solution along time for three different biosorbent dosages.

III.2.3.3. Effect of Hg complexation

The effect of salts presence was studied with solutions containing 3, 15 and 30 g dm^{-3} of NaCl. Sodium is common in many wastewaters, and high Na concentrations give rise to high ionic strengths (Schiewer and Wong, 2000). The addition of electrolytes can influence sorption processes in at least two ways: (i) by competition of metal ions for the binding sites on the biomass due to electrostatic effects; (ii) by forming complexes between the ions of the salt and the metal in solution (Carro et al., 2010). These complexes are very stable, and normally they are more difficult to capture from the solution (El-Shafey, 2010). This statement was confirmed by Carro et al. (2010), who observed a drastic drop in the mercury sorption by the addition of NaCl to the solutions. The presence of chloride salts changes completely the mercury speciation as shown in Figure III.2.5. At the conditions of the current sorption assays, Hg(II) is mostly present in the negative forms of $[HgCl_4]^{2-}$ and $[HgCl_3]^{-1}$.

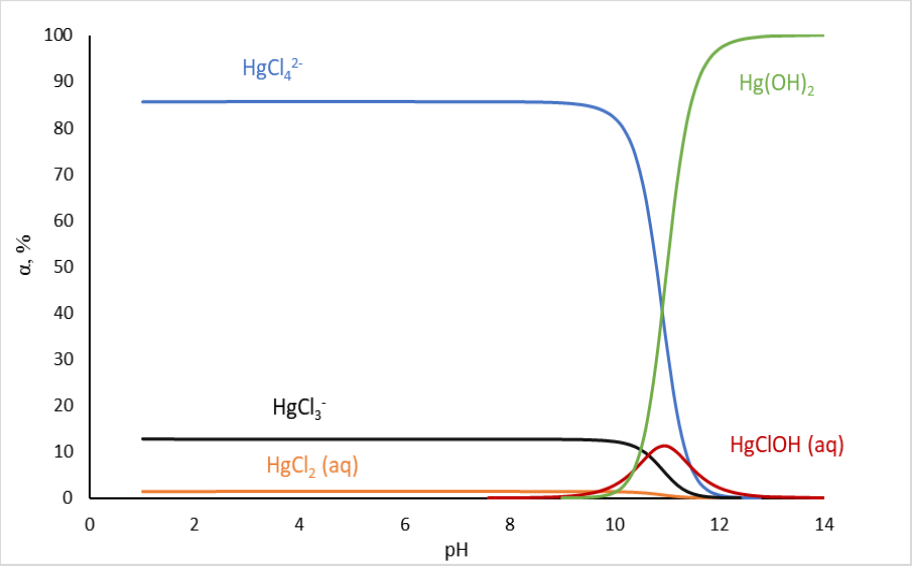

Figure III.2.5. Mercury speciation in NaCl solution (30 g dm^{-3}) at temperature of 22 °C.

Unlike the expected, experimental results indicated that the introduction of electrolytes has enhanced mercury sorption (see Figure III.2.6). The explanation for this phenomenon may be related with the biosorbents surface, which contains sulfur donor groups that according to the Pearson's HSAB (Hard and soft acids and bases) theory (Pearson, 1963) have larger affinity to form complexes with mercury than chloride ions. It is plausible that despite the chloro-complexes formed, there is a preference for Hg to establish coordinate covalent bonds, by sharing or exchanging electrons with the sulfur groups of the biosorbent, suggesting the occurrence of a chemisorption mechanism (Balderas-Hernández et al., 2017; Tavares et al., 2016).

Moreover, the addition of 3 g dm^{-3} of NaCl has improved mercury removal but the increase of further additions of NaCl (15 and 30 g dm^{-3}) had no substantial effect on the Hg sorption efficiency neither on the sorption kinetics. This observation is supported by the fact that 3 g dm^{-3} provide an excess of the chloride ions for the complexation reactions relative to the Hg(II) concentrations present in the solutions (Carro et al., 2010)

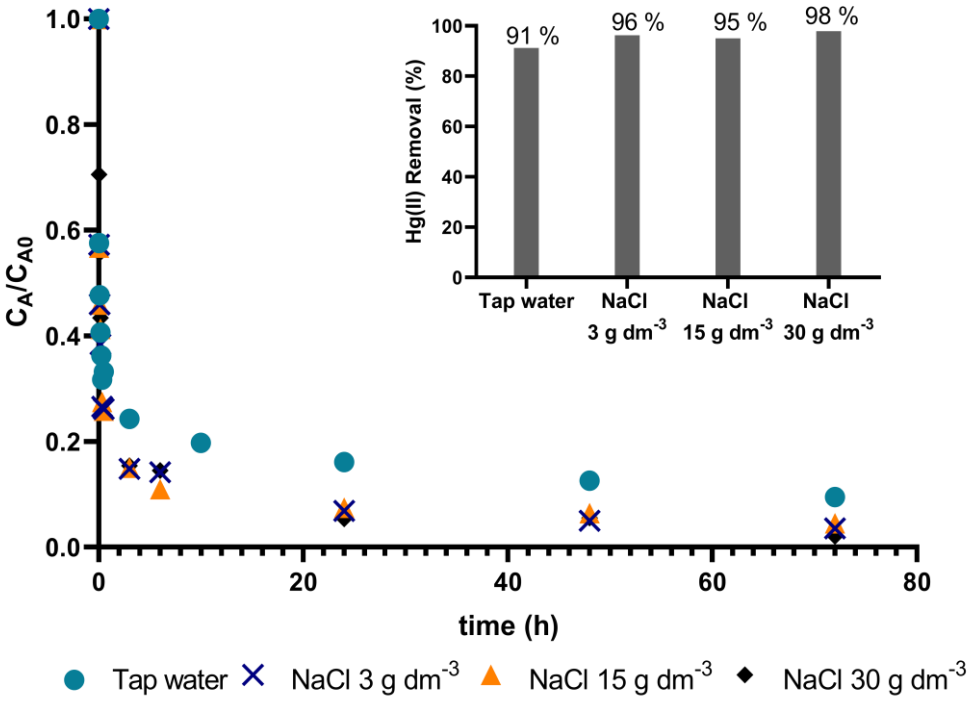

Figure III.2.6. Evaluation of the ionic strength impact on Hg(II) removal along time in tap water and in NaCl solutions. The bars chart presents the removal percentage of Hg(II) after 72 hours of sorption.

Comparing the kinetic sorption behavior of banana peels in Hg(II) spiked tap water and in Hg(II) spiked NaCl solutions, the results presented as normalized Hg(II) concentration in liquid phase along time (Figure III.2.6), highlighted the high affinity between Hg(II) and the biomass in all matrices, with more than 75 % removed in the first 3 hours and being possible to achieve residual Hg(II) concentrations corresponding to the guideline value of the European Union for drinking water quality (≤ 1 μg dm^{-3}) (Directive 2008/105/EC). However, faster removals were observed at the initial times for all the saline solutions when compared with the removal in tap water. Such affirmation is supported by the calculated initial sorption rates (from the first derivate of $C_A = f(t)$ for initial times, at $t = 0$) which were 205, 188 and 191 μg dm^{-3} h^{-1}, for the solutions with 3, 15 and g dm^{-3} of NaCl, higher than the tap water (175 μg dm^{-3} h^{-1}). After 24 hours more than 93 % of the Hg(II) was sorbed from the saline solutions while 83 % was captured from tap water.

III.2.3.4. Application to real matrices

Despite the increasing attention and utilization of the biosorbents in remediation processes, there are still several gaps concerning their application under multi-metal conditions and real matrices systems (Nguyen et al., 2013). In order to fill these gaps and access the performance of the biosorbents towards Hg(II) under realist conditions, two real matrices were tested: seawater and a real wastewater.

Seawater is one of the last receptors of contaminants and the source of water used in many aquacultures (Lopes et al., 2014). Besides the sodium chloride, seawater contains other dissolved ions and organic matter that can influence the efficiency of the sorption. The real wastewaters contain large diversity of other metals and ions, which can compete with Hg(II) ions in solution for the active sorption sites on the biosorbents.

According to the Figure III.2.7, the increase of solution complexity, from tap water to seawater, did not affect mercury removal (variation from 91 to 93 %). That behaviour is

probably assigned to the large number of available sorption sties on the surface of banana peels combined with the strong affinity between Hg(II) and the sulfur functional groups. Furthermore, unlike this work, the uptake ability of several sorbents has been reported to decrease in the presence of other elements in real systems (Lopes et al., 2014; Upadhyay et al., 2017).

Regarding the real wastewater the removal observed was 81 %. This effluent is rich in elements like Ag, Fe and Cr (see Table III.2.1) and the strong competition between mercury and the other metals is playing an important role in this sorption process. Like Hg^{2+}, Ag^{+} ion is also classified as soft acid and due to the similar ionization potential of these two elements, their cations present comparable tendency to accept electrons pairs and form complexes with S ligands on the biosorbents surface (Stumm and Morgan, 1996). Even so, it must be mentioned that under extreme conditions the banana peels were able to successfully reduce mercury levels and achieve very low final concentrations.

The time profiles in the early stages follow the order of the complexity of the aqueous solution. The kinetics was faster for the tap water and became slower for the seawater and real wastewater. At the beginning of the process, the presence of other elements and different mercury speciation may have slowed down the sorption rate.

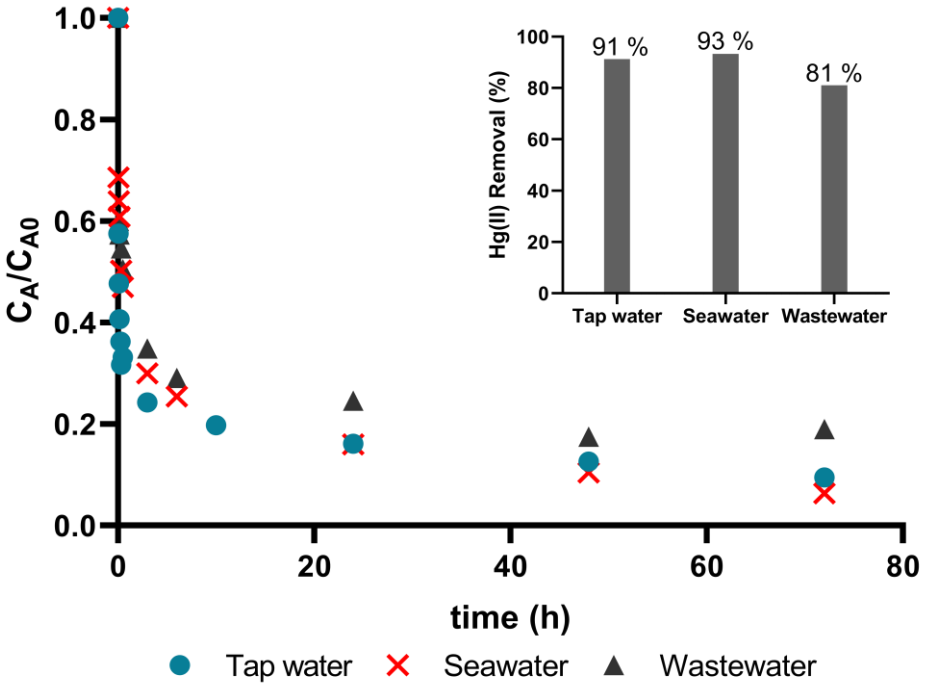

Figure III.2.7. Application of banana peels for Hg(II) reduction in real matrices along time. The bars chart present the removal percentage of Hg(II) after 72 hours of sorption.

Table III.2.1. Main composition of the real wastewater tested

Elements	Concentration (mg dm^{-3})
Ag	885.0
Hg	625.0
Fe	494.5
Cr	166.3
K	130.2
Na	18.9
Si	15.4
Ca	15.2

III.2.3.5. Kinetics and equilibrium modelling

The kinetic profiles of Hg(II) sorption by banana peels along time for the different systems studied in this work (effect of biosorbent dosage, ionic strength and real matrices) were evaluated by fitting the pseudo-first order, pseudo-second order and Elovich models to the experimental data and the obtained parameters are listed in Tables III.2.2, III.2.3 and III.2.4, together with R^2 $AARD$. In order to clarify the visualization of the results only the best fit is shown in Figure III.2.8, together with the experimental data. Among the models, the pseudo-first order equation usually provides the poorest adjust to the kinetic results (Plazinski et al., 2009), as it was confirmed by the lowest values of R^2 (0.792-0.927) and highest $AARDs$ (8.19 %- 16.01 %) obtained. In general, the Elovich model showed the best fit to the experimental data for systems with different biosorbent dosages and real water matrices, with values of R^2 between 0.974 and 0.995 and $AARD$ between 1.67 % and 4.38 %. Such model is associated with sorbents with heterogeneous surfaces (Plazinski et al., 2009). Regarding the systems with different NaCl concentrations, pseudo-second order model provided the best sorption kinetics description, and the coefficients of determination were in the range of 0.968-0.982 and $AARD$ in the range of 3.87-4.64 %.

The parameter α of the Elovich model followed the mass tendency, the higher the solid concentration the higher the initial sorption rate. More biosorbent in solution provides more available active sorption sites and therefore more mercury is sorbed at the initial times. However, it decreased by improving the complexity of the solution to real waters, which may be ascribed to competitive effects or by the different mercury speciation in these media.

Table III.2.2. Modelling parameters of the Hg(II) sorption (concentration of 50 μg dm^{-3}) from tap water by different dosages of banana peels.

	Pseudo-first order				**Pseudo-second order**				**Elovich**			
	k_1 (h^{-1})	q_e (mg g^{-1})	R^2	$AARD$ (%)	k_2 (g·mg^{-1}·h^{-1})	q_e (mg g^{-1})	R^2	$AARD$ (%)	α (mg g^{-1} h^{-1})	β (g mg^{-1})	R^2	$AARD$ (%)
0.15 g	2.4	0.2410	0.860	13.40	27.1	0.2340	0.945	8.64	42.1	46.3	0.982	3.49
0.25 g	3.4	0.1490	0.792	13.10	73.5	0.1500	0.937	7.60	440.0	90.4	0.994	1.67
0.50 g	11.7	0.0769	0.893	9.12	224.8	0.0819	0.966	4.44	3314.0	192.1	0.974	4.38

Table III.2.3. Modelling parameters of the Hg(II) sorption (concentration of 50 μg dm^{-3}) from different salt solutions using 0.5 g dm^{-3} of banana peels.

	Pseudo-first order				**Pseudo-second order**				**Elovich**			
	k_1 (h^{-1})	q_e (mg g^{-1})	R^2	$AARD$ (%)	k_2 (g·mg^{-1}·h^{-1})	q_e (mg g^{-1})	R^2	$AARD$ (%)	α (mg g^{-1} h^{-1})	β (g mg^{-1})	R^2	$AARD$ (%)
Tap water	11.7	0.0769	0.893	9.12	224.8	0.0819	0.966	4.44	3314.0	192.1	0.974	4.38
NaCl 3 g dm^{-3}	10.1	0.0887	0.927	8.19	181.7	0.0905	0.974	3.87	744.4	153.7	0.966	5.95
NaCl 15 g dm^{-3}	9.6	0.0879	0.922	8.78	175.2	0.0888	0.982	4.12	263.8	149.9	0.962	5.93
NaCl 30 g dm^{-3}	7.3	0.0963	0.906	9.40	103.2	0.0984	0.968	4.64	12.9	96.7	0.957	8.36

Table III.2.4. Modelling parameters of Hg(II) sorption (concentration of 50 μg dm^{-3}) by real waters using 0.5 g dm^{-3} of banana peels.

	Pseudo-first order				**Pseudo-second order**				**Elovich**			
	k_1 (h^{-1})	q_e (mg g^{-1})	R^2	$AARD$ (%)	k_2 (g·mg^{-1}·h^{-1})	q_e (mg g^{-1})	R^2	$AARD$ (%)	α (mg g^{-1} h^{-1})	β (g mg^{-1})	R^2	$AARD$ (%)
Tap water	11.7	0.0769	0.893	9.12	224.8	0.0819	0.966	4.44	3314.0	192.1	0.974	4.38
Seawater	4.1	0.0793	0.852	16.01	68.2	0.0817	0.908	11.06	4.4	103.2	0.995	2.69
Wastewater	5.5	0.0795	0.847	13.17	106.5	0.0811	0.928	8.79	28.5	135.3	0.992	2.35

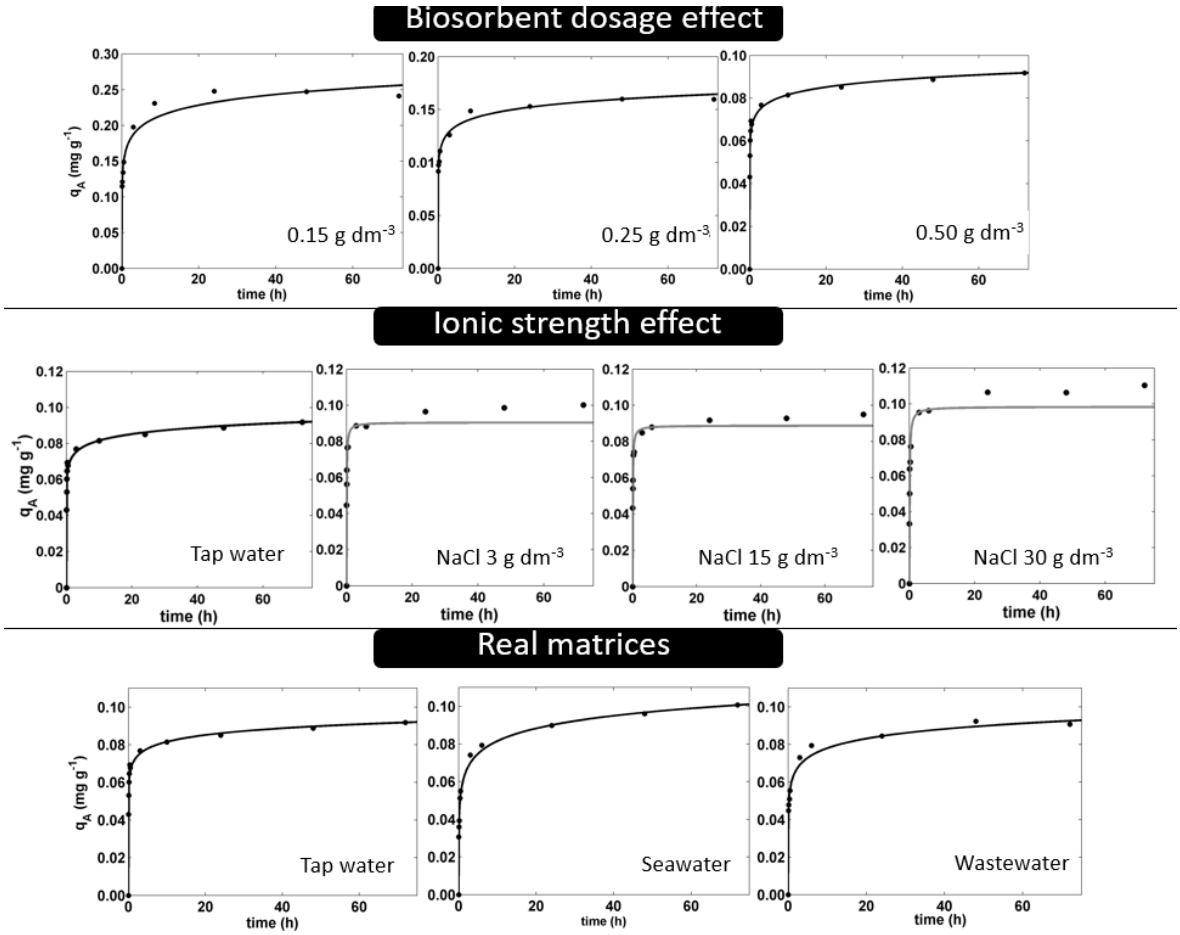

Figure III.2.8. Fitting Elovich model (black line) and pseudo-second order model (grey line) to the experimental data (dots) of the different systems studied.

Moreover, the value of k_2 calculated from the pseudo-second order model improved with higher biosorbent doses and decreased with the increase of NaCl concentration or in real waters. This parameter has been reported as strongly dependent on the experimental conditions, and the higher it is the shorter is the time to reach equilibrium (Plazinski et al., 2009). It has been observed that despite the great performances and low final concentrations achieved, the more complex is the system the slower is the sorption. The q_{Ae} values obtained by the same model presented a good agreement with the experimental results, with relative errors between them ranging in 2.85-18.9 %.

The isotherms of Langmuir and Freundlich were fitted to the experimental data for sorption equilibrium study and the results are exhibited in Figure III.2.9. The calculated

modelling parameters for the two models are presented in Table III.2.5 as well as the R^2 and $AARD$ values. The obtained isotherm is favourable type and the curve seems to continue growing beyond the conditions studied. Freundlich model provides the best description of the data, demonstred by the high value of R^2=0.991 and the low value of $AARD$=4.55 % achieved. According to Freundlich model, the Hg(II) capture may follow a multilayer mechanism on the heterogeneous surface of banana peels and the energy of sorption decays exponentially. The theoretical capacity of the Langmuir isotherm is 0.75 mg g^{-1}, which is much higher than the experimental value here observed and reinforces that this material has excellent potential to sorb Hg(II) and can perform even greater under different conditions.

Table III.2.5. Equilibrium modelling parameters.

Model	**Parameters**			
Langmuir	q_m (mg g^{-1})	K_L (L mg^{-1})	R^2	$AARD$ (%)
	0.75	32.80	0.985	5.57
Freundlich	K_F ($mg^{1-1/n}$ $dm^{3/n}$ g^{-1})	n	R^2	$AARD$ (%)
	7.36	1.24	0.991	4.55

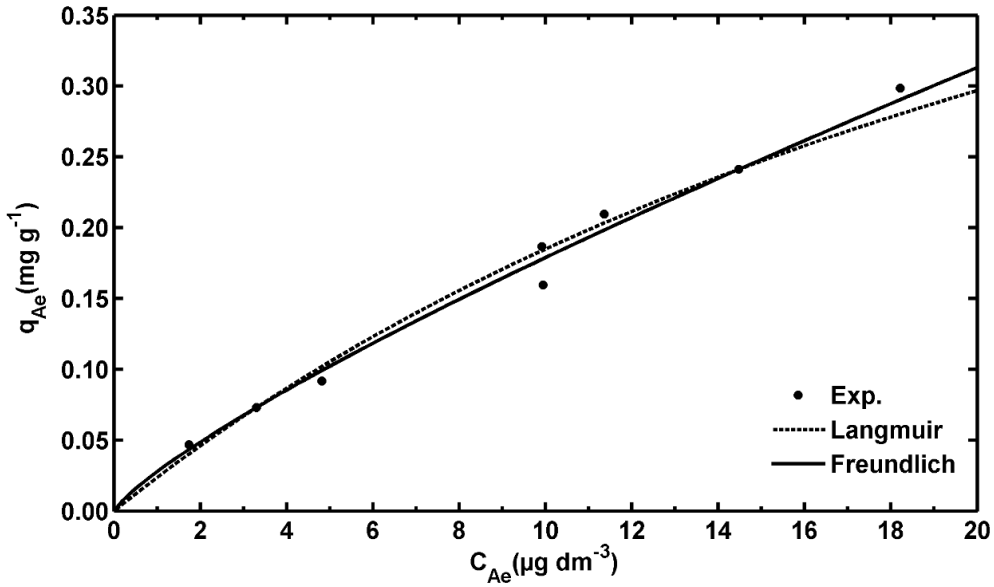

Figure III.2.9. Equilibrium behaviour of Hg(II) sorption onto banana peels.

The theoretical capacities of banana peels (0.75 mg g^{-1}) and other biosorbents applied for mercury removal in literature have been compared, confirming the great potential of this biosorbent in comparison with others. Clam shell wastes were tested to remove Hg(II) from ultrapure waters with the same initial Hg(II) concentration of this study (50 µg dm^{-3}) and the capacity obtained was 0.24 mg g^{-1} (Monteiro et al., 2016). The maximum uptake of dried garlic powder (*Allium sativum L.*) for mercury sorption from ultrapure waters was evaluated by fixing the biosorbent dosage at 12.5 g dm^{-3} and varying the Hg(II) initial concentration in the range of 10-5000 µg dm^{-3}. For these conditions described, the capacity obtained from Langmuir model was 0.65 mg g^{-1} (Eom et al., 2011). Another study reported a biosorbent capacity of 0.037 mg g^{-1} using reed (*Phragmites australis*) to remove Hg(II) from solutions with ultrapure water and Hg(II) initial concentration of 10 mg dm^{-3} (Cecilia Soto-Ríos et al., 2018).

III.2.3.6. Design of a counter-current system for water treatment

The feasibility of biosorption as an alternative to conventional methods depends on factors such as biosorbent availability, cost and uptake capacity (Ajmani et al., 2019a; Chojnacka, 2010; Volesky, 2007). Considering a volume (V_L) of contaminated solution with Hg(II) initial concentration C_{A0}, and the final goal equilibrium concentration as C_{A2}, a two-stage counter-current unit is proposed with an equilibrium raffinate concentration of stage 1 as C_{A1}. This configuration requires much less sorbent amount than a single stage. Its simplified scheme is shown in Figure III.2.10. The solution with initial concentration C_{A0} is fed to stage 1 and the Hg(II) free biosorbent amount (m_S) is introduced into stage 2. Taking into account the Freundlich isotherm (which fitted better the experimental data) already substituted in the overall mass balance (Eq. (III.2.10)) and in the mass balance to stage 1 (Eqs. (III.2.11)), the final equations from which C_{A1} and m_s can be calculated are:

$$V_L C_{A0} = V_L C_{A2} + m_S K_F C_{A1}^{1/n} \quad \text{(III.2.10)}$$

$$V_L C_{A0} + m_S K_F C_{A2}^{1/n} = V_L C_{A1} + m_S K_F C_{A1}^{1/n} \quad \text{(III.2.11)}$$

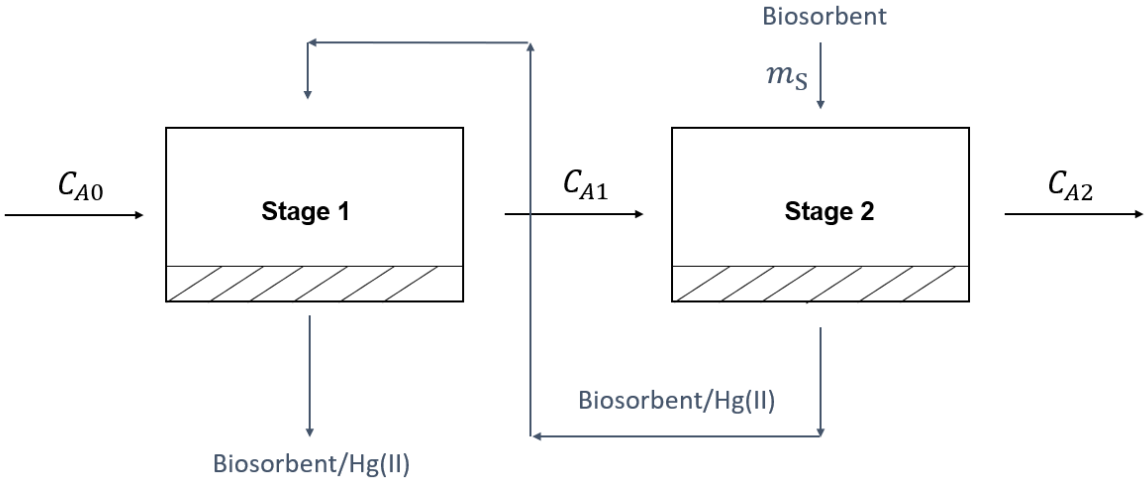

Figure III.2.10. Counter-current two-stages unit for Hg(II) sorption.

Considering, for instance, 1000 dm^{-3} of solution with Hg(II) initial concentration of 50 µg dm^{-3} and final concentration of 1 µg dm^{-3}, the calculated intermediate concentration is C_{A1} =9.2 µg dm^{-3} and 291 g of banana peels are necessary. Such low biosorbent amount reflects the benefits of using this configuration when compared, for example, with a single stage that would need 1749 g of biosorbent to reach the same target. The counter-current design proposed here uses only 17 % of the mass required for the single stage. Nevertheless, both systems exhibit the great advantage of using banana peels as biosorbent, in which only few mg of solid were able to treat a large volume of contaminated solution and accomplished the water quality guideline imposed by the regulations.

III.2.4. Conclusions

Banana peels were applied for the first time to sorb Hg(II) from solutions with environmental realistic concentrations. The efficiency of the process was studied, being possible to conclude it depends clearly on the dosage of banana peels and contact time, but was not penalized by ionic strength and competitive conditions. Even for the harshest competing conditions (*i.e.*, using seawater or 3-30 g dm^{-3} of NaCl in solution), banana

peels doses of 0.5 g dm^{-3} were able to achieve treated waters with residual concentrations of Hg(II) with levels of drinking water regulation (1 μg dm^{-3}).

The biosorption kinetics was well described by Elovich and pseudo-second order models, while equilibrium was well fitted by Freundlich equation, which may suggest a multilayer mechanism behind the separation process.

The successful application in complex water matrices proved the applicability of banana peels in realistic systems with low initial Hg(II) concentrations, like the ones present on environment. Considering an industrial application, the water treatment in a counter-current two-stage unit is able to produce high-quality purified waters with lower dosages of banana peels, generating smaller amounts of contaminated residues.

III.2.5. References

Abdel-Khalek, M.A., Abdel Rahman, M.K., Francis, A.A., 2017. Exploring the adsorption behavior of cationic and anionic dyes on industrial waste shells of egg. J. Environ. Chem. Eng. 5, 319–327. https://doi.org/10.1016/j.jece.2016.11.043

Ahmed, D., Abid, H., Riaz, A., 2018. Lagenaria siceraria peel biomass as a potential biosorbent for the removal of toxic metals from industrial wastewaters Lagenaria siceraria peel biomass as a potential biosorbent for the removal of toxic metals from industrial wastewaters. Int. J. Environ. Stud. 75, 763–773. https://doi.org/10.1080/00207233.2018.1457285

Ajmani, A., Shahnaz, T., Narayanan, S., Narayanasamy, S., 2019a. Equilibrium, kinetics and thermodynamics of hexavalent chromium biosorption on pristine and zinc chloride activated Senna siamea seed pods. Chem. Ecol. 35, 379–396. https://doi.org/10.1080/02757540.2019.1584614

Ajmani, A., Shahnaz, T., Subbiah, S., Narayanasamy, S., 2019b. Hexavalent chromium adsorption on virgin, biochar, and chemically modified carbons prepared from Phanera vahlii fruit biomass: equilibrium, kinetics, and thermodynamics approach.

Environ. Sci. Pollut. Res. 26, 32137–32150. https://doi.org/10.1007/s11356-019-06335-z

ATSDR, Priority list of hazardous substances [WWW Document], 2017. URL https://www.atsdr.cdc.gov/spl/ (accessed 2.22.17).

Awwad, A.M., Salem, N.M., Abdeen, A.O., 2015. Noval approach for synthesis sulfur (S-NPs) nanoparticles using Albizia julibrissin fruits extract. Adv. Mater. Lett. 6, 432–435. https://doi.org/10.5185/amlett.2015.5792

Ayangbenro, A., Babalola, O., 2017. A New Strategy for Heavy Metal Polluted Environments: A Review of Microbial Biosorbents. Int. J. Environ. Res. Public Health 14, 94. https://doi.org/10.3390/ijerph14010094

Azevedo, B.F., Furieri, L.B., Peçanha, F.M., Wiggers, G.A., Frizera Vassallo, P., Ronacher Simões, M., Fiorim, J., Rossi de Batista, P., Fioresi, M., Rossoni, L., Stefanon, I., Alonso, M.J., Salaices, M., Valentim Vassallo, D., 2012. Toxic Effects of Mercury on the Cardiovascular and Central Nervous Systems. J. Biomed. Biotechnol. 2012, 1–11. https://doi.org/10.1155/2012/949048

Azizian, S., 2004. Kinetic models of sorption: a theoretical analysis. J. Colloid Interface Sci. 276, 47–52. https://doi.org/10.1016/j.jcis.2004.03.048

Balderas-Hernández, P., Roa-Morales, G., Ramírez-Silva, M.T., Romero-Romo, M., Rodríguez-Sevilla, E., Esparza-Schulz, J.M., Juárez-Gómez, J., 2017. Effective mercury(II) bioremoval from aqueous solution, and its electrochemical determination. Chemosphere 167, 314–321. https://doi.org/10.1016/J.CHEMOSPHERE.2016.10.009

Carro, L., Anagnostopoulos, V., Lodeiro, P., Barriada, J.L., Herrero, R., Sastre de Vicente, M.E., 2010. A dynamic proof of mercury elimination from solution through a combined sorption–reduction process. Bioresour. Technol. 101, 8969–8974. https://doi.org/10.1016/J.BIORTECH.2010.06.118

Castro, L., Blázquez, M.L., González, F., Muñoz, J.A., Ballester, A., 2017. Biosorption of

Zn(II) from industrial effluents using sugar beet pulp and F . vesiculosus : From laboratory tests to a pilot approach. Sci. Total Environ. 598, 856–866. https://doi.org/10.1016/j.scitotenv.2017.04.138

Castro, M., Cruz, J., Otazo-Sánchez, E., Perez-Marín, L., 2003. Theoretical Study of the Hg 2+ Recognition by 1,3-Diphenyl-Thiourea. J. Phys. Chem. A 107, 9000–9007. https://doi.org/10.1021/jp030768g

Chojnacka, K., 2010. Biosorption and bioaccumulation – the prospects for practical applications. Environ. Int. 36, 299–307. https://doi.org/10.1016/J.ENVINT.2009.12.001

D Castro, R.S., ercio Caetano, L., Ferreira, G., Padilha, P.M., Saeki, M.J., Zara, L.F., Antonio Martines, M.U., Castro, G.R., 2011. Banana Peel Applied to the Solid Phase Extraction of Copper and Lead from River Water: Preconcentration of Metal Ions with a Fruit Waste. Ind. Eng. Chem. Res 50, 3446–3451. https://doi.org/10.1021/ie101499e

De, J., Dash, H.R., Das, S., 2014. Mercury Pollution and Bioremediation-A Case Study on Biosorption by a Mercury-Resistant Marine Bacterium, in: Microbial Biodegradation and Bioremediation. Elsevier Inc., pp. 138–166. https://doi.org/10.1016/B978-0-12-800021-2.00006-6

Do, D.D., 1998. Adsorption analysis: equilibria and kinetics. Imperial College Press, London.

El-Shafey, E.I., 2010. Removal of Zn(II) and Hg(II) from aqueous solution on a carbonaceous sorbent chemically prepared from rice husk. J. Hazard. Mater. 175, 319–327. https://doi.org/10.1016/J.JHAZMAT.2009.10.006

Eom, Y., Won, J.H., Ryu, J.-Y., Lee, T.G., 2011. Biosorption of mercury(II) ions from aqueous solution by garlic (Allium sativum L.) powder. Korean J. Chem. Eng 28, 1439–1443. https://doi.org/10.1007/s11814-010-0514-y

EU, 2008. Directive 2008/105/EC of the European Parliament and of the Council of 16 December 2008 on environmental quality standards in the field of water policy,

amending and subsequently repealing Council Directives 82/176/EEC, 83/513/EEC, 84/156/EEC, 84/491/EEC,. Off. J. Eur. Communities L 348, 84–97.

FA0, 2018. Banana market review: : Preliminary results for 2018. Rome.

Fabre, E., Vale, C., Pereira, E., Silva, C.M., 2019. Experimental Measurement and Modeling of Hg(II) Removal from Aqueous Solutions Using Eucalyptus globulus Bark: Effect of pH, Salinity and Biosorbent Dosage. Int. J. Mol. Sci. 20, 5973. https://doi.org/10.3390/ijms20235973

Fiol, N., Villaescusa, I., 2009. Determination of sorbent point zero charge: usefulness in sorption studies. Environ. Chem. Lett. 7, 79–84. https://doi.org/10.1007/s10311-008-0139-0

Freundlich, H., 1906. Concerning adsorption in solutions. Zeitschrift Fur Phys. Chemie-Stochiometrie Und Verwandstchaftslehre 57, 385–470.

Ho, Y.S., McKay, G., 1999. Pseudo-second order model for sorption processes. Process Biochem. 34, 451–465. https://doi.org/10.1016/S0032-9592(98)00112-5

Ho, Y.S., Porter, J.F., Mckay, G., 2002. Equilibrium isotherm studies for the sorption of divalentmetal ions onto peat: copper, nickel and lead single component systems. Water, Air, Soil Pollut. 141, 1–33. https://doi.org/10.1023/A:1021304828010

Holmes, P., James, K.A.F., Levy, L.S., 2009. Is low-level environmental mercury exposure of concern to human health? Sci. Total Environ. 408, 171–182. https://doi.org/10.1016/j.scitotenv.2009.09.043

Johs, A., Eller, V.A., Mehlhorn, T.L., Brooks, S.C., Harper, D.P., Mayes, M.A., Pierce, E.M., Peterson, M.J., 2019. Dissolved organic matter reduces the effectiveness of sorbents for mercury removal. Sci. Total Environ. 690, 410–416. https://doi.org/10.1016/j.scitotenv.2019.07.001

Karthik, V., Saravanan, K., Patra, C., Ushadevi, B., Vairam, S., Selvaraju, N., 2019. Biosorption of Acid Yellow 12 from simulated wastewater by non-viable T. harzianum: kinetics, isotherm and thermodynamic studies. Int. J. Environ. Sci.

Technol. 16, 6895–6906. https://doi.org/10.1007/s13762-018-2073-4

Kumar, S., Narayanasamy, S., Venkatesh, R.P., 2019. Removal of Cr(VI) from synthetic solutions using water caltrop shell as a low-cost biosorbent. Sep. Sci. Technol. 54, 2783–2799. https://doi.org/10.1080/01496395.2018.1560333

Lagergren, S., 1898. Zur theorie der sogenannten adsorption gel Zur theorie der sogenannten adsorption gelster stoffe, Kungliga Svenska Vetenskapsakademiens. Handlingar 24, 1–39.

Langmuir, I., 1916. The adsorption of gases on plane surface of glass, mica and platinum. J.Am, Chem.Soc 40, 1361–1368.

Largitte, L., Pasquier, R., 2016. A review of the kinetics adsorption models and their application to the adsorption of lead by an activated carbon. Chem. Eng. Res. Des. 109, 495–504. https://doi.org/10.1016/J.CHERD.2016.02.006

Liang, S., McDonald, A.G., 2014. Chemical and thermal characterization of potato peel waste and its fermentation residue as potential resources for biofuel and bioproducts production. J. Agric. Food Chem. 62, 8421–8429. https://doi.org/10.1021/jf5019406

Lito, P.F., Aniceto, J.P.S., Silva, C.M., 2012. Removal of Anionic Pollutants from Waters and Wastewaters and Materials Perspective for Their Selective Sorption. Water, Air, Soil Pollut. 223, 6133–6155. https://doi.org/10.1007/s11270-012-1346-7

Lopes, C.B., Lito, P.F., Cardoso, S.P., Pereira, E., Duarte, A.C., Silva, C.M., 2012. Metal recovery, separation and/or pre-concentration, in: Inamuddin, Luqma, M. (Eds.), Ion Exchange Technology II – Applications. Springer, pp. 237–322.

Lopes, C.B., Oliveira, J.R., Rocha, L.S., Tavares, D.S., Silva, C.M., Silva, S.P., Hartog, N., Duarte, A.C., Pereira, E., 2014. Cork stoppers as an effective sorbent for water treatment: the removal of mercury at environmentally relevant concentrations and conditions. Environ. Sci. Pollut. Res. 21, 2108–2121. https://doi.org/10.1007/s11356-013-2104-0

Lopes, C.B., Otero, M., Lin, Z., Silva, C.M., Rocha, J., Pereira, E., Duarte, A.C., 2009. Removal of Hg2+ ions from aqueous solution by ETS-4 microporous titanosilicate — Kinetic and equilibrium studies. Chem. Eng. J. 151, 247–254. https://doi.org/10.1016/j.cej.2009.02.035

Melgar, M.J., Alonso, J., García, M.A., 2007. Removal of toxic metals from aqueous solutions by fungal biomass of Agaricus macrosporus. Sci. Total Environ. 385, 12–19. https://doi.org/10.1016/j.scitotenv.2007.07.011

Mokone, J.G., Tutu, H., Chimuka, L., Cukrowska, E.M., 2018. Optimization and Characterization of Cladophora sp. Alga Immobilized in Alginate Beads and Silica Gel for the Biosorption of Mercury from Aqueous Solutions. Water, Air, Soil Pollut. 229, 215. https://doi.org/10.1007/s11270-018-3859-1

Monteiro, R.J.R., Lopes, C.B., Rocha, L.S., Coelho, J.P., Duarte, A.C., Pereira, E., 2016. Sustainable approach for recycling seafood wastes for the removal of priority hazardous substances (Hg and Cd) from water. J. Environ. Chem. Eng. 4, 1199–1208. https://doi.org/10.1016/J.JECE.2016.01.021

Nguyen, T.A.H., Ngo, H.H., Guo, W.S., Zhang, J., Liang, S., Yue, Q.Y., Li, Q., Nguyen, T.V., 2013. Applicability of agricultural waste and by-products for adsorptive removal of heavy metals from wastewater. Bioresour. Technol. 148, 574–585. https://doi.org/10.1016/J.BIORTECH.2013.08.124

Pathak, P.D., Mandavgane, Sachin A. Kulkarni, B.D., 2017. Fruit peel waste: characterization and its potential uses. Curr. Sci. 113, 444–454.

Patra, C., Medisetti, R.M.N., Pakshirajan, K., Narayanasamy, S., 2019. Assessment of raw, acid-modified and chelated biomass for sequestration of hexavalent chromium from aqueous solution using Sterculia villosa Roxb. shells. Environ. Sci. Pollut. Res. 26, 23625–23637. https://doi.org/10.1007/s11356-019-05582-4

Pearson, R.G., 1963. Hard and Soft Acids and Bases. J.Am, Chem.Soc 265. https://doi.org/10.1021/ja00905a001

Pérez-García, F., Alvarado-Rodríguez, J.G., Galán-Vidal, C.A., Elena Páez-Hernández, M., Andrade-López, N., Moreno-Esparza, R., 2010. Synthesis, characterization, and crystal structures of n-alkyldiorganodithiophosphates RS2P(OC6H4)2. Struct. Chem. 21, 191–196. https://doi.org/10.1007/s11224-009-9562-5

Plazinski, W., Rudzinski, W., Plazinska, A., 2009. Theoretical models of sorption kinetics including a surface reaction mechanism: A review. Adv. Colloid Interface Sci. 152, 2–13. https://doi.org/10.1016/J.CIS.2009.07.009

Rafatullah, M., Sulaiman, O., Hashim, R., Ahmad, A., 2009. Adsorption of copper (II), chromium (III), nickel (II) and lead (II) ions from aqueous solutions by meranti sawdust. J. Hazard. Mater. 170, 969–977. https://doi.org/10.1016/J.JHAZMAT.2009.05.066

Rangabhashiyam, S., Suganya, E., Lity, A.V., Selvaraju, N., 2016. Equilibrium and kinetics studies of hexavalent chromium biosorption on a novel green macroalgae Enteromorpha sp. Res. Chem. Intermed. 42, 1275–1294. https://doi.org/10.1007/s11164-015-2085-3

Rao, M.M., Reddy, D.H.K.K., Venkateswarlu, P., Seshaiah, K., 2009. Removal of mercury from aqueous solutions using activated carbon prepared from agricultural by-product/waste. J. Environ. Manage. 90, 634–643. https://doi.org/10.1016/j.jenvman.2007.12.019

Raza, M.H., Sadiq, A., Farooq, U., Athar, M., Hussain, T., Mujahid, A., Salman, M., 2015. Phragmites karka as a Biosorbent for the Removal of Mercury Metal Ions from Aqueous Solution: Effect of Modification. J. Chem. 2015, 1–12. https://doi.org/10.1155/2015/293054

Riaz, M., Nadeem, R., Hanif, M.A., Ansari, T.M., Rehman, K.-, 2009. Pb(II) biosorption from hazardous aqueous streams using Gossypium hirsutum (Cotton) waste biomass. J. Hazard. Mater. 161, 88–94. https://doi.org/10.1016/J.JHAZMAT.2008.03.096

Roginsky, S., Zeldovich, Y.B., 1934. The catalytic oxidation of carbon monoxide on manganese dioxide. Acta Phys. Chem. USSR 1, 554.

Rudzinski, W., Plazinski, W., 2006. Kinetics of Solute Adsorption at Solid/Solution Interfaces: A Theoretical Development of the Empirical Pseudo-First and Pseudo-Second Order Kinetic Rate Equations, Based on Applying the Statistical Rate Theory of Interfacial Transport. J. Phys. Chem. B 110, 16514–16525. https://doi.org/10.1021/jp061779n

Schiewer, S., Wong, M.H., 2000. Ionic strength effects in biosorption of metals by marine algae. Chemosphere 41, 271–282.

Seader, J.D., Henley, E.J., 1998. Separation Process Principles. John Wiley & Sons, Inc., New York.

Shan, Y., Yang, W., Li, Y., Liu, Y., Pan, J., 2019. Preparation of microwave-activated magnetic bio-char adsorbent and study on removal of elemental mercury from flue gas. Sci. Total Environ. 697, 134049. https://doi.org/10.1016/j.scitotenv.2019.134049

Soto-Ríos, P.C., León-Romero, M.A., Sukhbaatar, O., Nishimura, O., 2018. Biosorption of Mercury by Reed (Phragmites australis) as a Potential Clean Water Technology. Water, Air, Soil Pollut. 229, 328. https://doi.org/10.1007/s11270-018-3978-8

Stumm, W., Morgan, J.J., 1996. Aquatic Chemistry: chemical equilibria and rates in natural waters. John Wiley & Sons, Inc.

Tavares, D.S., Lopes, C.B., Daniel-da-silva, A.L., Vale, C., Trindade, T., Pereira, M.E., 2016. Mercury in river , estuarine and seawaters e Is it possible to decrease realist environmental concentrations in order to achieve environmental quality standards ? Water Res. 106, 439–449. https://doi.org/10.1016/j.watres.2016.10.031

Upadhyay, K.H., Vaishnav, A.M., Tipre, D.R., Bhargav, P.C., Dave, S.R., 2017. Kinetics and mechanisms of mercury biosorption by an exopolysaccharide producing marine isolate Bacillus licheniformis. 3 Biotech 7, 313. https://doi.org/10.1007/s13205-017-0958-4

Vinod, V.T.P., Sashidhar, R.B., Sivaprasad, N., Sarma, V.U.M., Satyanarayana, N.,

Kumaresan, R., Rao, T.N., Raviprasad D A Jonaki, P., 2011. Bioremediation of mercury (II) from aqueous solution by gum karaya (Sterculia urens): A natural hydrocolloid. Desalination 272, 270–277. https://doi.org/10.1016/j.desal.2011.01.027

Volesky, B., 2007. Biosorption and me. Water Res. 41, 4017–4029. https://doi.org/10.1016/j.watres.2007.05.062

Wang, J., Feng, X., Anderson, C.W.N., Xing, Y., Shang, L., 2012. Remediation of mercury contaminated sites – A review. J. Hazard. Mater. 221, 1–18. https://doi.org/10.1016/j.jhazmat.2012.04.035

Work published as scientific article

Experimental measurement and modeling of Hg(II) removal from aqueous solutions using *Eucalyptus globulus* bark: effect of pH, salinity and biosorbent dosage

Abstract

Different experimental conditions were tested in order to optimize the Hg(II) removal by *Eucalyptus globulus* bark. Response Surface Methodology was applied to extract information about the significance of the factors and to obtain a model describing the sorption. Results were generated through the Design of Experiments applying the methodology of three-factor and three-level Box–Behnken. The factors tested were pH (4.0, 6.5 and 9.0), salinity (0, 15 and 30) and biosorbent dosage (0.2, 0.5 and 0.8 g dm^{-3}) to evaluate the Hg(II) removal using realistic conditions such as contaminated natural waters with initial Hg(II) concentration of 50 µg dm^{-3}. The optimum response provided by the model was 81 % of metal removal under the optimal operating conditions of pH 6.0, no salinity and 0.55 g dm^{-3} of biosorbent dose. Concerning the kinetic, the pseudo-second order equation fitted better to the experimental results with R^2 between 0.973 and 0.996. This work highlighted the promising valorization of this biomass, which is an industrial by-product and made available information about the influence of the variables for Hg(II) removal in water treatment processes.

III.3. Experimental measurement and modeling of Hg(II) removal from aqueous solutions using *Eucalyptus globulus* bark: effect of pH, salinity and biosorbent dosage

III.3.1. Introduction

Mercury is a non-degradable toxic metal classified by the Agency for Toxic Substances & Disease Registry (ATSDR) as the third most dangerous substance. This list is elaborated considering facts such as the toxicity, occurrence in the environment and the risks for human health ("Substance Priority List | ATSDR," 2017). Furthermore, under Directive 2013/39/EU of the European Union, mercury and its compounds are classified as priority substances and must be progressive reduced and eliminated of the emissions by 2021. This Directive also encourages the development of innovative cheaper technologies for the improvement of water quality.

Major anthropogenic sources of mercury are effluents from chloralkali, pulp and paper, petroleum refining, electrical, batteries and lamp production (Baeyens et al., 1996). Technologies, such as membrane processes, chemical precipitation, flotation, coagulation–flocculation and electrochemical techniques reduce metal content present in waters in range concentrations of mg dm^{-3} (Lopes et al., 2012; Romera et al., 2007). However, these conventional methods may be inadequate, expensive, generate secondary sludge and most of the times are not effective to reach final low concentrations (Lopes et al., 2007; Panayotova, 2001). Sorption processes like adsorption and ion exchange are the most applied in industries and despite their efficiency, the cost of the sorbent is a restraining factor for the implementation of this cleanup operation.

The biosorbents have been recognized as good options for trace metal removal from waters. They are usually composed by cellulose, hemi-cellulose and lignin which have a high content of hydroxyl and carboxyl groups (Nguyen et al., 2013). Due to abundant binding groups, their capacities can be equal or even greater compared with the conventional sorbents what makes these materials promising sources for decontaminating toxic metals from wastewaters (Jiménez-Cedillo et al., 2013; Nguyen et

al., 2013; Zafar et al., 2007). Balderas-Hernández et al. (2017) have used 10 g dm^{-3} of *Allium cepa L*. for mercury removal and have got Hg(II) elimination of 99.4 % from solutions with 20 mg dm^{-3} of this metal. Aman et al. (2018) have studied the performance of rose flowers (*Rosa indica*) for mercury sorption and they have found a biosorbent uptake capacity of 11.91 mg g^{-1}. Phragmites australis (dose of 20 g dm^{-3}) has been applied in sorption and have removed 80 % of Hg(II) from solutions spiked with 10 mg of Hg(II) dm^{-3} (Cecilia Soto-Ríos et al., 2018). Despite the several works reported using biosorbents, only a few of them consider realistic low initial concentrations of mercury. These vestigial concentrations are the most common in the aquatic bodies and therefore they are the conditions that must be pursued (Stumm and Morgan, 1996).

Eucalyptus is the most important source of biomass for paper pulp industries which generate large amounts of biomass bark wastes. This by-product has been used as biosorbent for diverse metals uptake. *Eucalyptus globulus* bark pretreated with sulfuric acid has been successfully used for Pb(II) and Cd(II) removal achieving capacities of 26.12 mg g^{-1} for Pb(II) and 35.65 mg g^{-1} for Cd(II) (Dwivedi et al., 2011). In other study, *E. camaldulensis Dehn*. bark was investigated for Cu(II) and Pb(II) sorption after impregnation with phosphoric acid and carbonization. The capacities found were 54.02 mg g^{-1} and 184.41 mg g^{-1} for Cu(II) and Pb(II), respectively (Patnukao et al., 2008). Cr(VI) was completely removed by *Eucalyptus globulus* bark biochar at dose of 2 g dm^{-3} from contaminated groundwater (initial Cr(VI) concentration of 25 g dm^{-3}) in the work of Choudhary et al. (2017).

It is well documented that sorption performance is highly dependent of various operational conditions, such as pH, temperature, ionic strength, sorbent mass, sorbate initial concentration and particle size. (Neris et al., 2019). The influence of pH and ionic strength on mercury elimination was evaluated, for example, in the work of Carro *et al*. (2010) using dry bracken ferns; the effect of pH, metal initial concentration, biosorbent mass and contact time on mercury removal were investigated by Boutsika *et al.* (2014) using biochar produced from malt spent rootlets; the impacts of the initial metal concentration, pH and competitive ions on the sorption of different metals by alkali-treated rice husks as biosorbents were reported in the work of Krishnani *et al.* (2008).

Usually sorption experiments are developed in such way that only one variable, or factor, is evaluated each time while the others remain constant (Devani et al., 2015; Eom et al., 2011; Vinod et al., 2011). Interactions among target factors are hence poorly explored. Multivariate statistics methods allow reducing the experimental efforts and provide information about the impact of individual or combined variables on the obtained responses. In line with this, the Design of Experiments (DoE) is a fundamental tool for searching the best solution and improving the process efficiency (Witek-Krowiak et al., 2014). Response surface methodology is a set of techniques that describes the relation between several independent variables and the respective responses. This procedure describes the process and improve its efficacy while reduce costs and experimental time (Montgomery, 2001; Witek-Krowiak et al., 2014).

The aim of this study is to use raw *Eucalyptus globulus* barks to remove mercury from contaminated waters. The specific objectives are: i) optimize the conditions of pH, biosorbent dosage and salinity in the sorption processes, ii) use the Response Surface Methodology to obtain the appropriate response functions; iii) adjust pseudo-first order, pseudo-second order and Elovich models to the experimental data in order to obtain information about the applicability of this process for the mercury water treatment proposal.

III.3.2. Materials and methods

III.3.2.1. Chemicals

The chemicals used in this work were all of analytical grade, purchased from chemical commercial suppliers and used without any purification. The certified standard solution of mercury(II) nitrate (1000 ± 2 mg dm^{-3}), the sodium hydroxide (≥ 99 %) and the nitric acid (65 %) were purchased from Merck and the sodium chloride (≥ 99 %) was acquired from Applichem Panreac. The standards solutions for the calibration curves were obtained by diluting the corresponding stock solution in high purity water (18 MΩ cm) or nitric acid solution (2 %). All glassware used in the experiments was acid-washed prior to use for at least 24 hours.

III.3.2.2. Biomass characterization

The *E. globulus* bark used in this work was provided by The Navigator Company (Cacia, Portugal), directly from its debarking/crushing unit. The biosorbent was dried under room temperature and humidity conditions, and it was then cut into pieces with *ca.* 1 cm length (see Figure III.3.1). No additional chemical or thermal pretreatments were applied before the sorption assays. The morphology was assessed by SEM using a Hitachi SU-70 SEM microscope with a Bruker Quantax 400 detector operating at 20 kV. The FTIR spectra of the biosorbent before and after sorption were recorded with a Bruker Tensor 27 spectrometer coupled to a horizontal attenuated total reflectance (ATR) cell using 256 scans at a resolution of 4 cm^{-1}. The samples were examined directly, and data were obtained as absorbance from a wavenumber range from 400 to 4000 cm^{-1}. The biosorbent PZC was determined according to the immersion method proposed by Fiol and Villaescusa (2009) using an incubator shaker HWY-200D.

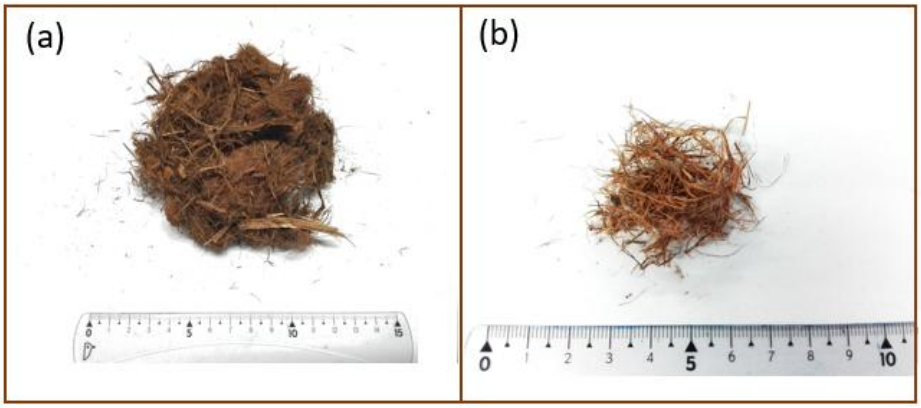

Figure III.3.1. (a) *E. globulus* bark provided by The Navigator Company; (b) *E globulus* bark prepared for use in the sorption experiments.

III.3.2.3. Chemical quantification

The pH was recorded on a WTW series 720 meter and the salinity by Eclipse handheld refractometer model 45-63.

The mercury quantification was performed by a cold vapour atomic fluorescence spectroscopy (CV-AFS), on a PSA cold vapour generator, model 10.003, using a Merlin PSA

detector, model 10.023 and with $SnCl_2$ as reducing agent. In this method, mercury(II) concentration is obtained as a signal and converted to concentration through a calibration curve constructed using five standards solutions (0.0, 0.1, 0.2, 0.3 and 0.5 µg of Hg(II) dm^{-3}). The calibration curves were plotted at least three times a day and the obtained determination coefficient was always ≥ 0.995. Each sample was measured in triplicate with admissible variation coefficient between replicas lower than 10 %. The limit of quantification of this technique was 0.02 µg dm^{-3}.

III.3.2.4. Biosorption experiments

Experiments were performed in batch conditions in 1 dm^{-3} volumetric flasks, magnetically stirred at 650 rpm, under a temperature of 22 ± 1 °C. The capability of the biosorbent to remove Hg(II) was assessed by contacting the biomass with a Hg(II) solution for 48 h (see experimental conditions in Table III.3.1). The mass of *E. globulus* varied between 0.2 and 0.8 g (doses of 0.2–0.8 g dm^{-3}), and the initial metal concentration was fixed at 50 µg dm^{-3}. These solutions were prepared by diluting the mercury stock solution in tap water to the desired mercury concentration, which is the concentration limit for wastewaters discharges (Directive 2008/105/EC). The salinity was adjusted using NaCl (0–30 g dm^{-3}), and pH was fixed between 4 and 9 with NaOH (0.1 mol dm^{-3}) or HNO_3 (0.5 mol dm^{-3}). The starting point of the experiments was the time, when the mass of the biosorbent was added into the flasks, and the samples were collected at different times, filtered with a 0.45 µm Millipore filter, adjusted to a pH value of <2 with HNO_3 and then analyzed for the Hg(II) concentrations in the solutions. A control experiment (without the biosorbent) was always run to check if Hg(II) was sorbed on the vessel walls or lost by volatilization.

The average amount of sorbed Hg(II) per unit mass of solid, q_A (mg g^{-1}) was calculated by global material balance at time t in solution:

$$q_A = \frac{V_L}{m_S}(C_{A0} - C_A) \qquad \text{(III.3.1)}$$

where A denotes Hg(II), V_{L} is the solution volume (dm^3), m_S is the mass of biosorbents (g), C_{A0} (mg dm^{-3}) is the initial concentration of Hg(II) in solution and C_{A} (mg dm^{-3}) is its concentration at time t.

The removal efficiency was calculated as follows:

$$Removal\ (\%) = 100 \times \frac{C_{A0} - C_{Af}}{C_{A0}} \qquad \text{(III.3.2)}$$

where C_{Af} (mg dm^{-3}) is the Hg(II) concentration at the end of the experiments.

III.3.2.5. Response surface methodology

Response surface methodology (RSM) is a statistical tool that describes the relation between several independent factors and one or more responses. The RSM is based on the fit of diverse models (linear, square polynomial functions and others) to the experimental results generated from the design of experiments (DoE) and the verification of the model obtained by means of statistical techniques. The aim of DoE is to improve the efficiency of the process while minimizes the number of experiments without loose the reliability of the results obtained. It reduces the experimental time and, consequently, the costs involved (Montgomery, 2001; Witek-Krowiak et al., 2014).

A Box-Behnken design of 3 factors and 3 levels was selected to evaluate the performance of the *E. globulus* bark as biosorbent to remove mercury from waters in sorption processes. The factors studied were pH (4, 6.5 and 9), sorbent dosage (0.2, 0.5 and 0.8 g dm^{-3}) and salinity (0, 15 and 30) and the response variable was the Hg(II) removal efficiency (%). The performed experimental conditions are listed in Table III.3.1.

The RSM model operates using the variables codified to have a common comparison basis. The coded input values are +1, 0 and -1 and they were obtained transforming the experimental factors using the expression bellow (see Table III.3.2):

$$X_{k} = \frac{x_k - x_0}{\Delta_{x_k}} \qquad \text{(III.3.3)}$$

where X_{k} is the codified value of the independent variable x_{k}, x_0 is the variable value at its center point, and $\Delta_{\mathrm{x_k}}$ is the step change between levels for the k variable.

Table III.3.1. Experimental conditions of the Box–Behnken design. Fixed conditions: temperature of 22 °C, contact time of 48 h, stirring velocity of 650 rpm, and volume of 1 dm^3.

Experiment	pH	Salinity	Biosorbent Mass (g) or Dosage ($g\ dm^{-3}$)
1	4.0	15	0.2
2	9.0	15	0.2
3	4.0	15	0.8
4	9.0	15	0.8
5	6.5	0	0.2
6	6.5	30	0.2
7	6.5	0	0.8
8	6.5	30	0.8
9	4.0	0	0.5
10	4.0	30	0.5
11	9.0	0	0.5
12	9.0	30	0.5
13	6.5	15	0.5
14	6.5	15	0.5
15	6.5	15	0.5

The RSM results were obtained in a form of a second order polynomial equation written as:

$$Y = \beta_0 + \sum_{i=1}^{k} \beta_i X_i + \sum_{i=1}^{k} \beta_{ii} X_i^2 + \sum_{i<j}^{k} \beta_{ij} X_i X_j \qquad \text{(III.3.4)}$$

where Y refers to the response variable studied, β_0 is a constant, β_{i}, β_{ii} and β_{ij} are the model coefficients associated with linear effects, quadratic effects, and interaction effects, respectively.

Table III.3.2. Three factors and three levels of Box-Behnken design and their corresponding experimental conditions

Variable	**Level**		
	-1	0	+1
pH	4.0	6.5	9.0
Salinity	0	15	30
Biosorbent dosage (g dm^{-3})	0.2	0.5	0.8

The software STATISTICA (version 5.1, StatSoft Inc., Tulsa, USA) was applied to treat the results. Analysis of variance (ANOVA) was used to assess the significant factors and interactions using Fisher's test and its associated probability p(F), while t -tests were performed to evaluate the significance of the fitted coefficients of each model. The coefficient of determination, R^2, and the adjusted coefficient of determination, R^2_{Adj}, were used to verify goodness of the fit, and they are expressed as follows:

$$R^2 = 1 - \frac{\sum(\hat{y}_i - y_i)^2}{\sum(y_i - \bar{y}\,)^2} \qquad \text{(III.3.5)}$$

$$R^2_{adj} = 1 - (1 - R^2)\frac{(N_{DP} - 1)}{(N_{DP} - N_P - 1)} \qquad \text{(III.3.6)}$$

where N_{DP} is the number of experimental data, N_{P} is the parameters number, y_{i} are the experimental values, $\hat{y}_{\mathrm{i}}$ are the values calculated by the model and $\bar{y}$ is the mean of the experimental values.

III.3.2.6. Kinetics modelling

In order to obtain information about the kinetics of the sorption of Hg(II) onto the biosorbents, three widely used reaction-based models were fitted to the experimental data, namely pseudo-first order, pseudo-second order and Elovich models.

The pseudo-first order equation (PFO), was suggested by Lagergren (Lagergren, 1898) and describes sorption processes as proportional to the distance to the equilibrium $(q_{Ae} - q_A)$ as follows:

$$\frac{dq_A}{dt} = k_1(q_{Ae} - q_A) \quad \text{(III.3.7)}$$

where k_1 (h^{-1}) is the rate constant the model and q_{Ae} (mg g^{-1}) is the Hg(II) concentration on the solid at equilibrium. After integration from the initial Hg(II) free particle condition ($t = 0$, $q_A = 0$) to $q_A = q_A$, the Eq.(III.3.7) gives:

$$ln(q_{Ae} - q_A) = ln\, q_{Ae} - k_1 t \quad \text{(III.3.8)}$$

The pseudo-second order model (PSO) is represented by (Ho and McKay, 1999):

$$\frac{dq_A}{dt} = k_2(q_{Ae} - q_A)^2 \quad \text{(III.3.9)}$$

where k_2 (g (mg h)$^{-1}$) is the rate constant of the model. After integration, the equation becomes:

$$\frac{t}{q_A} = \frac{1}{k_2 q_{Ae}^2} + \frac{1}{q_{Ae}} t \quad \text{(III.3.10)}$$

The Elovich equation is one of the most useful models to describe reactions involving sorption on heterogeneous surfaces (Roginsky and Zeldovich, 1934) and it is mathematically expressed by:

$$\frac{dq_A}{dt} = \alpha e^{-\beta q_A} \quad \text{(III.3.11)}$$

where α is the initial Hg(II) sorption rate (mg (g h)$^{-1}$) and β (g mg^{-1}) is the desorption constant of the model. Assuming αβt >>1 and applying the conditions $t = 0$ to $t = t$ and $q_A = 0$ to $q_A = q_A$, one obtains:

$$q_A = \frac{1}{\beta} ln(\alpha\beta) + \frac{1}{\beta} ln\, t \qquad \text{(III.3.12)}$$

All the parameters of kinetics models were obtained by nonlinear regression using Matlab R2014a program and they were optimized by the Nelder-Mead simplex algorithm to minimize the error between experimental and predicted data. The fits of the kinetic equations were examined over the coefficient of determination (R^2) (Eq. (III.3.5)) and the average absolute relative deviation ($AARD$), which is mathematically expressed by:

$$AARD(\%) = \frac{100}{N_{DP}} \sum_{i=1}^{N_{DP}} \frac{|\widehat{y}_i - y_i|}{y_i} \qquad \text{(III.3.13)}$$

III.3.3. Results

III.3.3.1 Sorbent characterization

The morphology of the biomass of *E. globulus* bark was studied by Scanning Electron Microscopy (SEM), being possible to observe that it was composed of rough fibres with *ca.* 170 µm thickness; pieces of *ca.* 1 cm length were utilized (see Figure III.3.2a)

The charge of the sorbent surface is important information for sorption processes and is influenced by pH of the contaminated water in contact with the biosorbent. The point of zero charge was determined and the plot expressed in Figure III.3.2b exhibits the |ΔpH| versus the initial pH. According to the method used (Fiol and Villaescusa, 2009), the point of zero charge appears when ΔpH ≈ 0, at the pH of 2.2, and at this pH the surface is neutral and the functional groups do not contribute to the pH of the solution. Above this pH of 2.2, the surface charge becomes negative and below this value the sorbent is positively charged (Marcilla et al., 2007).

FTIR spectra of both *E. globulus* bark, prior and after its use in sorption experiments are shown in Figure III.3.2c. This is a non-destructive technique that allows identifying the main functional groups present on the surface of biomass. The appearance, disappearance or displacement of the vibration frequencies after sorption

may indicate bonds between the functional groups and the sorbate (Dwivedi et al., 2011). The peaks observed at 3300 cm^{-1} are characteristic of -OH and $–NH_2$ groups (Rocha et al., 2016). The emergence of the double peak between 2850 and 2920 cm^{-1} in the loaded biosorbent spectrum is representative of stretching vibrations of for asymmetric and symmetric C-H groups (Choudhary et al., 2017) and suggests their participation in the bonds established between the biosorbent and the Hg(II) in solution. The band at 1730 cm^{-1} is due to C=O bonds and the band at 1620 cm^{-1} is attributed to C=C stretching frequencies which is ascribed, in general, to the vibration of the aromatic ring present on lignin (Liang and McDonald, 2014). The other remarkable peaks are represented by N-H amino at 1520 cm^{-1}, C-O-C- vibration of the cellulose (bands around 850 cm^{-1}) (Rafatullah et al., 2009) and stretching of C-O of a primary alcohol (peak at 1025 cm^{-1})(Rocha et al., 2016). The appearance of the peak at 1120 cm^{-1} after exposure to Hg(II) may be attributed to C–O (COOH) vibration (Dwivedi et al., 2011).

III.3.3.2. Optimization of the Hg(II) removal conditions

Figure III.3.3 shows the curves of the experiments performed by Box-Behnken design. The last three experiments represent replications of the central point and their average is shown together with the error bars. The control results are not shown but the concentrations remained constant along time with variation coefficients lower than 10 %. Results indicate that the major content of Hg(II) is removed during the first hours followed by a period where the sorption kinetics is slower towards the equilibrium. The driving force promoted by the large mercury concentration gradient between mercury in the solution and the biosorbent is higher at the beginning of the process when all sorption sites are available (Rocha et al., 2016). As the process occurs, the sites become occupied and the sorption tends to reach the equilibrium. Although the normalized final mercury concentration has displayed remarkable differences, all the experiments reached the equilibrium after 6 hours.

(a)

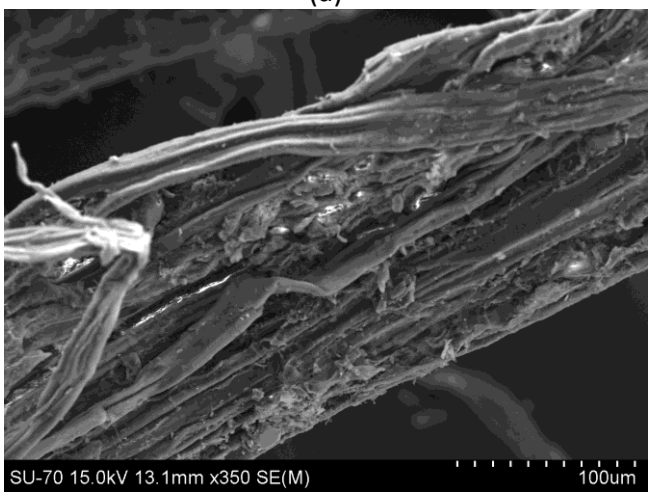

(b)

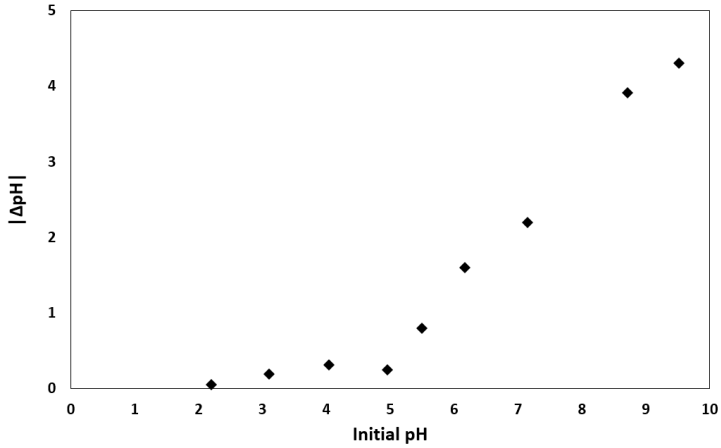

(c)

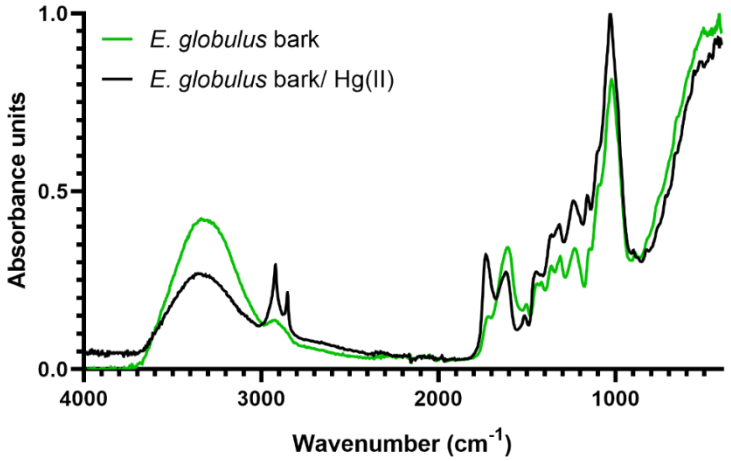

Figure III.3.2. Characterization of the *Eucalyptus globulus* (*E. globulus*) bark utilized in the Hg(II) removal experiments: (a) SEM image; (b) relationship between |ΔpH| and initial pH; (c) FTIR spectra before and after the sorption assays.

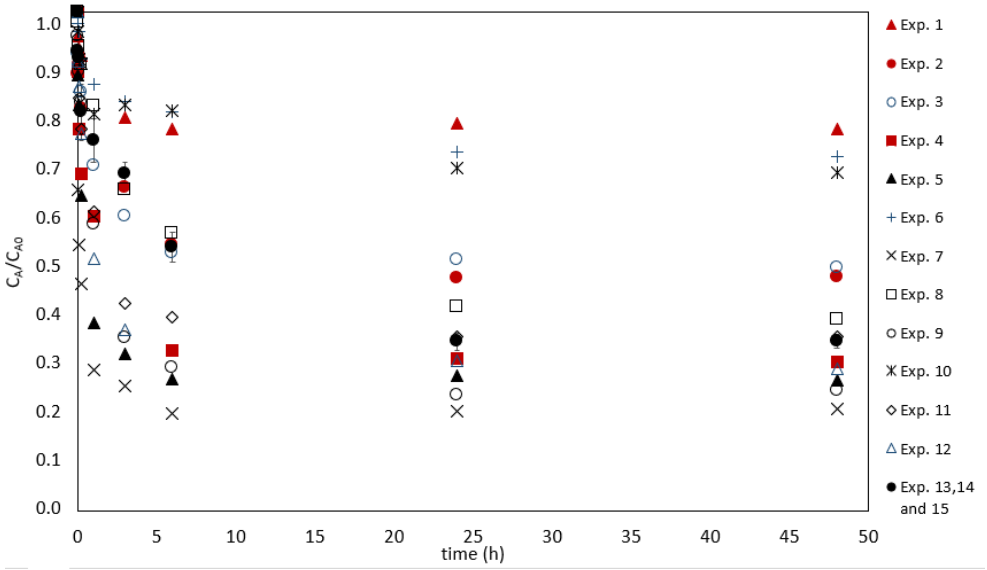

Figure III.3.3. Normalized Hg(II) concentration in a solution as a function of time for different experiments performed according to the conditions (initial Hg(II) concentration of 50 μg dm^{-3}, stirring speed of 650 rpm, and a temperature of 22 ± 1 °C).

The results of the 15 experiments and the Hg(II) removal percentages are presented in Table III.3.3. The experimental conditions and the codified variables are detailed in Materials and Methods section (see Tables III.3.1 and III.3.2; fixed conditions: temperature of 22 °C, contact time of 48 h, and stirring speed of 650 rpm). Regarding the results of the DoE applied, the minimum response observed (% of Hg(II) removal) was 23 % for the Exp. 1 (pH 4.0 (level -1), salinity of 15 (level 0) and biosorbent dosage of 0.2 g dm^{-3} (level -1)) and the maximum was 77 % for Exp. 7 (pH 6.5 (level 0), salinity of 0 (level -1) and biosorbent dosage of 0.8 g dm^{-3} (level +1)). These values are explained by Figure III.3.4 which presents the pareto chart with the linear (L), quadratic (Q) and interaction effects of the factors, obtained at 95 % of confidence level. The significant variables are the ones with score values above the red line (p-value ≤ 0.05) The salinity is the most impactful factor and it is contributing negatively for the removal efficiency. The other variables affected positively the results. The linear effect of the variables, the quadratic effect of the pH and biosorbent dosage as well as the interaction salinity-pH and salinity-biosorbent dosage were considered significant for the model that describes Hg(II) sorption.

The quadratic effect of salinity and the interaction between pH and biosorbent dosage were considered non-significant (p-value > 0.05) and hence were eliminated from the full model to obtain the reduced model (RM) only with the impactful factors for the removal efficiency of the sorption. The coefficients obtained for the reduced model are presented in Table III.3.4. The final uncoded reduced model (Eq. (III.3.14)) was obtained by applying the Eq. (III.3.3) for the back substitution of the variables and it is presented in Table III.3.5 together with the values of R^2 and R^2_{Adj}. The value of the determination coefficient, $R^2 = 0.945$, presented for the reduced equation indicates goodly fit to the experimental data, however the lower value of the adjusted coefficient of determination, $R^2_{\mathrm{Adj}} = 0.793$, represents that the goodness of the fit is due to the large number of parameters instead of the robustness of the proposed function.

Table III.3.3. Results of the experiments performed according to the Box–Behnken design, along with noncodified (Table III.3.1) and codified (Table III.3.2) conditions. Fixed conditions: temperature of 22 °C, contact time of 48 h, and stirring speed of 650 rpm.

Experiment	pH	Salinity	Biosorbent dosage	Removal (%)
1	4.0 (–1)	15 (0)	0.2 (–1)	23
2	9.0 (+1)	15 (0)	0.2 (–1)	53
3	4.0 (–1)	15 (0)	0.8 (+1)	51
4	9.0 (+1)	15 (0)	0.8 (+1)	70
5	6.5 (0)	0 (–1)	0.2 (–1)	74
6	6.5 (0)	30 (+1)	0.2 (–1)	29
7	6.5 (0)	0 (–1)	0.8 (+1)	77
8	6.5 (0)	30 (+1)	0.8 (+1)	62
9	4.0 (–1)	0 (–1)	0.5 (0)	76
10	4.0 (–1)	30 (+1)	0.5 (0)	32
11	9.0 (+1)	0 (–1)	0.5 (0)	65
12	9.0 (+1)	30 (+1)	0.5 (0)	71
13	6.5 (0)	15 (0)	0.5 (0)	68
14	6.5 (0)	15 (0)	0.5 (0)	65

15	6.5 (0)	15 (0)	0.5 (0)	65

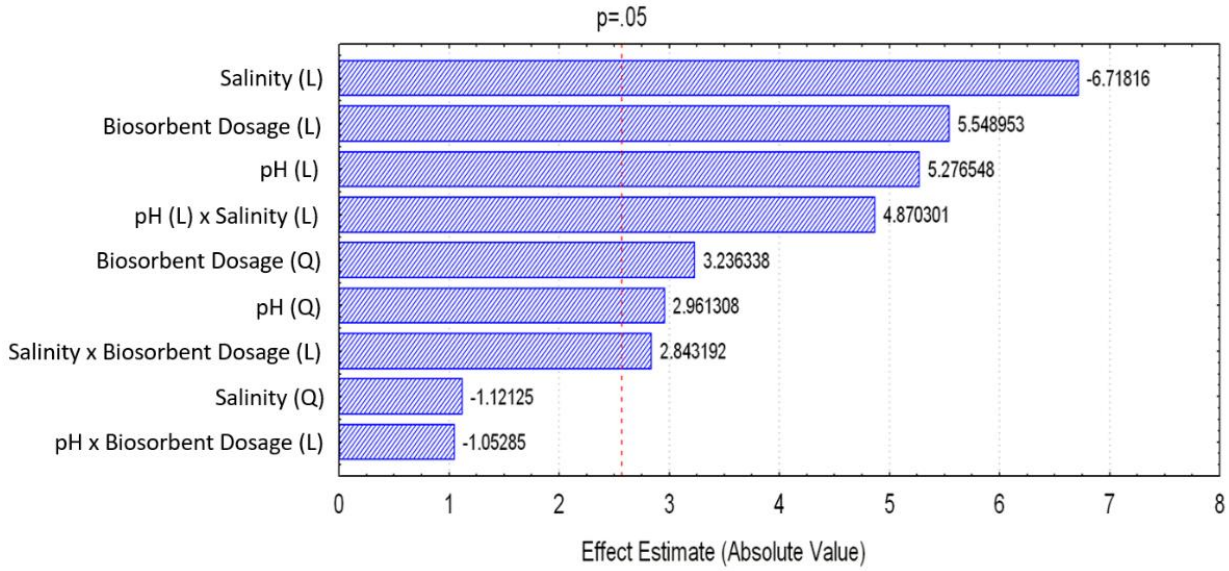

Figure III.3.4. Pareto chart with the impact of the factors studied

Table III.3.4. Regressed coefficients of the Eq. (III.3.4) obtained for the reduced model and individual significance.

Coefficients of the Eq. (III.3.4)	**Reduced model**	**p-value**
β_0	67.9	2.63E-08
β_1	9.6	1.33 E-03
β_2	-12.2	3.20 E-04
β_3	10.1	1.00 E-03
β_{11}	-8.2	2.05 E-02
β_{33}	-8.9	1.41 E-02
β_{12}	12.5	2.09 E-03
β_{23}	7.3	2.76 E-02

Figure III.3.5 exhibits the 3-D response surfaces obtained through the uncoded reduced model in Table III.3.5 by plotting two variables and remaining the other constant at its value of central point. Figure III.3.5a presents the plot of the influence of biosorbent

dosage and salinity, Figure III.3.5b shows the impact of salinity and pH and Figure III.3.5c shows the effect of biosorbent dosage and pH on the Hg(II) removal percentage.

Table III.3.5. Reduced model, coefficient of determination and adjusted coefficient of determination.

Reduced model of response	R^2	$R^2_{Adj.}$	Eq.
$\text{Removal}\ (\%) = 3.1 + 15.8\text{pH} - 3.8\text{Salinity} + 108.0\text{Biosorbent dosage} - 1.3\text{pH}^2 - 99.0\text{Biosorbent dosage}^2 + 0.3(\text{pH} \times \text{Salinity}) + 1.6(\text{Salinity} \times \text{Biosorbent dosage})$	0.954	0.793	(III.3.14)

It is possible to observe by the sloping profile of the surfaces the great importance of the concentration of salts in solution. In addition, more pronounced differences of this variable in the response were observed in lower pHs and biosorbent dosages. The effect of biosorbent dosage variation was more relevant in higher salinity and pHs, and the effect of pH was more impacting in higher salinity and biosorbent dosages.

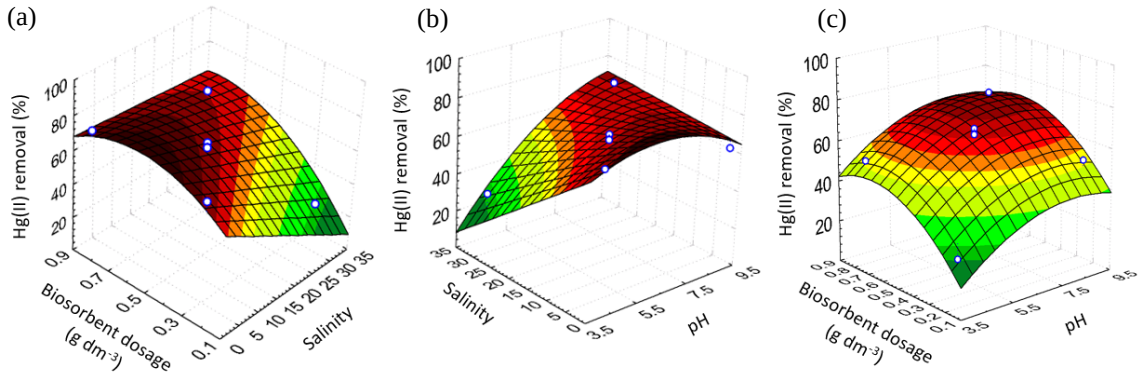

Figure III.3.5. Response surface plot of the interaction effect of variables: (a) biosorbent dosage and salinity, (b) salinity and pH, (c) biosorbent dosage and pH. Dots represent experimental values; the Hg(II) removal varies from 0 % (dark green) 100 % (dark red).

III.3.3.3. Kinetic modelling

The curves of the experiments 1-4 were modelled applying the most known kinetic models to adjust to the results obtained. The fittings are expressed in Figure III.3.6 in terms of the Hg(II) concentration on biosorbent *versus* time. Table III.3.6 summarizes the calculated values of the different kinetic parameters as well as the coefficients of determination (R^2) and the average absolute relative deviations ($AARD$).

Over all the models tested, the PSO equation describes better the experimental results for all the four curves, which suggests that Hg(II) sorption by *Eucalyptus globulus* bark occurs through a chemical reaction with kinetics of second order . That also can be observed in the higher values of R^2 found (between 0.973 and 0.996) and the low $AARDs$ (3.42 % to 9.69 %) in Table 5. The parameter values of q_{Ae} calculated from PSO equation agree well with the observed ones what is confirmed by the relative errors between them not greater than 3.77 %.

Although the slight difference observed at pH 4, the rate constants k_2 follow the biosorbent dosage tendency in the case of the PSO model, *i.e*. higher k_2 for higher masses and lower k_2 for lower masses of *E. globulus* bark. The increase in the biosorbent dosage enhance the number of the available active sorption sites and lead to faster removal of Hg(II) from solution. The same behavior does not take place in the case of the other models, probably because of the poorer fittings achieved.

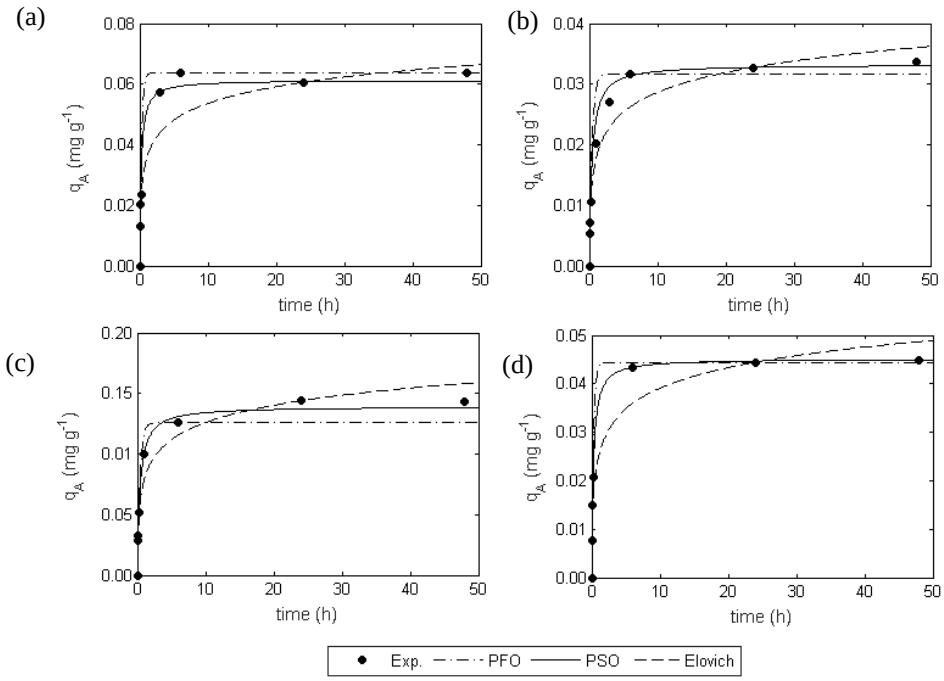

Figure III.3.6. Sorption kinetics modelling on the Eucalyptus globulus bark: (a) biosorbent dosage of 0.2 g dm^{-3} , salinity of 15 and pH 4.0, (b) biosorbent dosage of 0.8 g dm^{-3}, salinity of 15 and pH 4.0 (c) biosorbent dosage of 0.2 g dm^{-3}, salinity of 15 and pH 9.0, (d) biosorbent dosage of 0.8 g dm^{-3}, salinity of 15 and pH 9.0

Table III.3.6. Kinetic fitting parameters for the Hg(II) sorption.

	PPO				**PSO**				**Elovich**			
pH4.0	k_1 (h^{-1})	q_e (mg g^{-1})	R^2	$AARD$ (%)	k_2 (g $(mg \cdot h)^{-1}$)	q_e (mg g^{-1})	R^2	$AARD$ (%)	α (mg $(g \cdot h)^{-1}$)	β (g mg^{-1})	R^2	$AARD$ (%)
0.2 g dm^{-3}	3.81	0.0652	0.939	12.1	80.0	0.0613	0.973	7.73	0.667	126.0	0.918	8.10
0.8 g dm^{-3}	2.52	0.0317	0.908	15.8	81.3	0.0333	0.975	9.69	0.200	211	0.957	8.01
pH 9.0	k_1 (h^{-1})	q_e (mg g^{-1})	R^2	$AARD$ (%)	k_2 (g $(mg \cdot h)^{-1}$)	q_e (mg g^{-1})	R^2	$AARD$ (%)	α (mg $(g \cdot h)^{-1}$)	β (g mg^{-1})	R^2	$AARD$ (%)
0.2 g dm^{-3}	2.57	0.1260	0.945	13.7	18.5	0.1390	0.983	8.69	0.927	48.5	0.959	11.20
0.8 g dm^{-3}	3.78	0.0444	0.979	5.9	90.5	0.0452	0.996	3.42	0.355	163.0	0.955	10.70

III.3.4 Discussion

The DoE by the application of Box-Behnken method allowed obtaining relevant outcomes about the influence of different factors in the Hg^{2+} sorption efficiency. The most impactful factor, salinity, has been studied in a range from no salinity until salinity close of seawater. This wide interval provides information about the behaviour of the system from simple to complex matrices, where competitive elements may interfere in the removal process. Indeed, Carro et al. (2010) reported a drastic drop of mercury uptake (*ca.* 85 %) by bracken fern in the presence of 58.4 g dm^{-3} of NaCl. In another study using *Cystoseira baccat*, NaCl concentrations of 5.8 and 58.4 g dm^{-3} decreased mercury sorption by 8 % and 80 %, respectively, for solutions with initial Hg^{2+} concentration of 500 mg dm^{-3} and pH 6 (Herrero et al., 2005). In the case of our work, the impact of salinity is also negative, being the best removal accomplished for Exp. 7 (no salinity) in accordance with the above mentioned essays, *i.e.* ionic competition penalizes Hg(II) sorption.

Salinity not only affects sorption capacity but also has effects on mercury speciation. In line with previous investigations (Carro et al., 2010; Lopes et al., 2007), the Hg^{2+} ions exhibit high affinity to Cl^- ions and tend to form chloro-complexes with high stability constants (Stumm and Morgan, 1996). This fact may be explained because Hg^{2+} (as soft cation) coordinates preferentially with soft bases containing chloride as donor, establishing more stable bonds than those between Cl^- and hard cations mostly present in natural waters as, for instance, Na^+, Mg^{2+} or Ca^{2+} (Stumm and Morgan, 1996).

Figure III.3.7 presents the speciation of Hg in solutions containing 30 g dm^{-3} of NaCl as an example of this circumstance. In NaCl solutions with the pH range shown in this work, Hg was found as neutral and negatively charged complexes, considerably stable, which were more difficult to remove from the solution. Similar to the phenomenon observed in Figure III.3.5a for small biosorbent dosages, the efficiency of sorption reduced significantly with an increase of the salt in the solutions. The effect of the salinity was not impactful when larger amounts of biosorbent were used probably due to the higher presence of functional groups on the biosorbent surface interacting with the complexes in solution shifting the equilibrium of the species and contributing for

the removal of mercury through the formation of coordinate covalent bonds (Atkins and Jones, 2007; Stumm and Morgan, 1996).

The same behaviour is observed in the Figure III.3.5b, the salinity is impactful only at low pH. Acidic media may interfere in the stability of the chloro-complexes of mercury in solution and the excess of H^+ ions are possibly interacting with these complexes and consequently impairing their removal from solution. Moreover, the ionic state of functional groups on *E. globulus* bark surface is mainly affected by pH changes and play an important role in metal removal (Carro et al., 2010). It is important to mention that in these complexes matrices several equilibriums are involved on the sorption processes and each case needs to be evaluated separately.

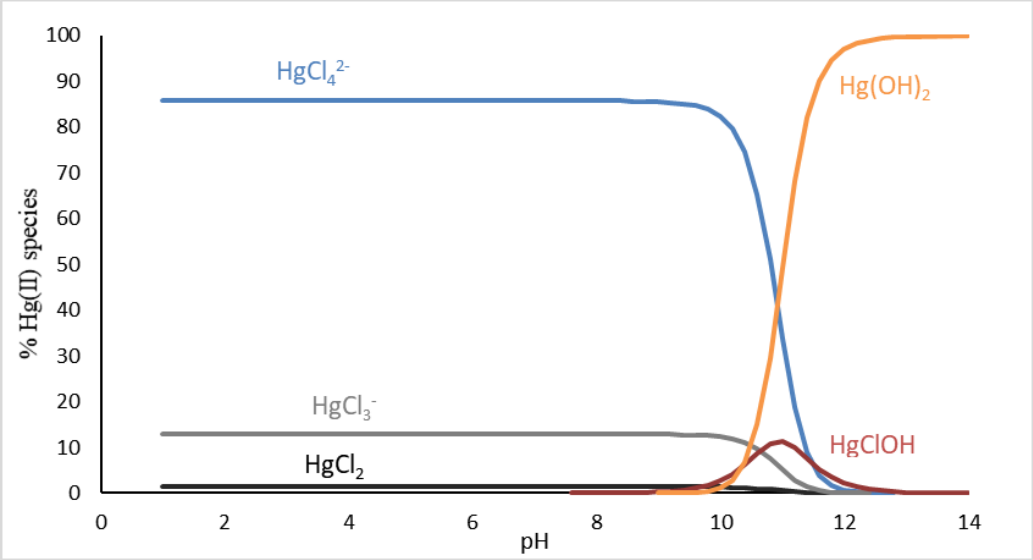

Figure III.3.7. Speciation diagram for Hg(II) in aqueous solution, with NaCl concentration of 30 g dm^{-3} at temperature of 22 °C.

Lastly, the plot of the interaction impact of biosorbent mass and pH is shown in the Figure III.3.5c. The increase in the biossorbent dosage is contributing positively for the removal efficiency until an optimal condition. This fact may be ascribed to the formation of agglomerates of biomass preventing the access to some sorption sites to the Hg(II) in solution. Besides that, the gradient of concentration becomes smaller as the sorption occurs and at some point, the driving force may be not strong enough to promote the removal.

In whole, calculations exhibited that the optimized operating conditions for the Hg(II) removal by *Eucalyptus globulus* bark under the range studied are 0.55 g dm^{-3} of biosorbent, no salinity and pH 6.0. The metal removal expected under these conditions is 81 %. Concerning the biomass features, the excellent performance of this biosorbent may be attributed to the high affinity between Hg(II) and functional groups on the solid surface like OH, CH_3, CH_2 and C-O.

It is possible to extract from the Figure III.3.5 and from the model obtained important information about the Hg(II) uptake by *E. globulus* bark for several operational conditions. In many cases, the optimized variables are not the more realistic or applicable conditions to treat real wastewaters. Nevertheless, through the large intervals between the variables conditions, most of the possible scenarios are covered. The salinity of 15 for instance, is more frequent in the aquatic or industrial environment and under this condition it is possible to achieve removals in the order of 74 % for pH 8.0 and 0.7 g dm^{-3} of biosorbent. The correction of pH is quite simple and despite the normal pH of the real wastewaters be around 6.5 this variable can easily be adjusted to the optimized values under low operational costs. The model provides information about the behaviour of the process (in the range of conditions studied) and avoids spending time with unnecessary experiments. Another advantage attained with the model is the overview of the interaction between the factors which is most of the times ignored and may bring unexpected results in the efficiency of the sorption.

The kinetic curves exhibited the large affinity of *E. globulus* bark to sorb mercury. In terms of industrial application, the sorption time, or residence time is an important variable to consider since it is directly related with profitability of the system. The more time, more energy consumption, more working hours and less volume treated. The high kinetic constants from the PSO model together with the fast equilibrium time, in which after 6 hours no relevant removal was observed, highlight this biosorbent for use in remediation technologies.

III.3.5. Conclusions

Impacts of diverse operational conditions on sorption of Hg(II) from aqueous solutions using *E. globulus* bark as biosorbent were evaluated. Optimal conditions for metal removal were pH of 6.0, no salinity and 0.55 g dm^{-3} of biosorbent to which correspond to 81 % of Hg(II) elimination. This remarkable performance noticed by *E. globulus* bark is highly influenced by its chemical characteristics as well as the sorption conditions. Salinity was the most significant factor for sorption of mercury, the increase of ionic strength resulted in metal removal reduction. The PSO model was the most appropriated equation to represent the experimental behaviour, and the kinetic constants increased with increasing the biosorbent dosage.

Taking into account the environmental concerns the use of small masses of sorbent promotes less generation of contaminated wastes and afford more sustainable and eco-friendly systems. The use of very small masses in this work evidenced the great affinity of *E. globulus* bark to Hg(II). The innovative application of RSM model to describe more realistic conditions gave an insight to an effective implementation of this biosorbent in wastewater clean-up technologies.

III.3.6. References

Aman, A., Ahmed, D., Asad, N., Masih, R., Muhammad Abd ur Rahman, H., 2018. Rose biomass as a potential biosorbent to remove chromium, mercury and zinc from contaminated waters Rose biomass as a potential biosorbent to remove chromium, mercury and zinc from contaminated waters. Int. J. Environ. Stud. 75, 774–787. https://doi.org/10.1080/00207233.2018.1429130

Atkins, P., Jones, L., 2007. Chemical Principles, 4th ed. New York.

Baeyens, W., Ebinghaus, R., Vasiliev, O., 1996. Global and Regional Mercury Cycles: Sources, Fluxes and Mass Balances. Springer Netherlands.

Balderas-Hernández, P., Roa-Morales, G., Ramírez-Silva, M.T., Romero-Romo, M., Rodríguez-Sevilla, E., Esparza-Schulz, J.M., Juárez-Gómez, J., 2017. Effective

mercury(II) bioremoval from aqueous solution, and its electrochemical determination. Chemosphere 167, 314–321. https://doi.org/10.1016/J.CHEMOSPHERE.2016.10.009

Boutsika, L.G., Karapanagioti, H.K., Manariotis, I.D., 2014. Aqueous mercury sorption by biochar from malt spent rootlets. Water. Air. Soil Pollut. 225, 2007–2013. https://doi.org/10.1007/s11270-013-1805-9

Carro, L., Anagnostopoulos, V., Lodeiro, P., Barriada, J.L., Herrero, R., Sastre de Vicente, M.E., 2010. A dynamic proof of mercury elimination from solution through a combined sorption–reduction process. Bioresour. Technol. 101, 8969–8974. https://doi.org/10.1016/J.BIORTECH.2010.06.118

Cecilia Soto-Ríos, P., Antonio León-Romero, M., Sukhbaatar, O., Nishimura, O., 2018. Biosorption of Mercury by Reed (Phragmites australis) as a Potential Clean Water Technology. Water, Air, Soil Pollut. 229, 328. https://doi.org/10.1007/s11270-018-3978-8

Choudhary, B., Paul, D., Singh, A., Gupta, T., 2017. Removal of hexavalent chromium upon interaction with biochar under acidic conditions: mechanistic insights and application. Environ. Sci. Pollut. Res. 24, 16786–16797. https://doi.org/10.1007/s11356-017-9322-9

Devani, M.A., Munshi, B., Oubagaranadin, J.U.K., 2015. Characterization and use of chemically activated Butea monosperma leaf dust for mercury(II) removal from solutions. J. Environ. Chem. Eng. 3, 2212–2218. https://doi.org/10.1016/J.JECE.2015.07.028

Directive 2008/105/EC of the European Parliament and of the Council of 16 December 2008 on environmental quality standards in the field of water policy, amending and subsequently repealing Council Directives 82/176/EEC, 83/513/EEC, 84/156/EEC, 84/491/EEC, 2008. . Off. J. Eur. Communities L 348, 84–97.

Directive 2013/39/EU of the European Parliament and of the Council of 12 August 2013 amending Directives 2000/60/EC and 2008/105/EC as regards priority substances in

the field of water policy, 2013. . Off. J. Eur. Union.

Dwivedi, A.D., Dubey, S.P., Gopal, K., Sillanpää, M., 2011. Strengthening adsorptive amelioration: Isotherm modeling in liquid phase surface complexation of Pb (II) and Cd (II) ions. Desalination 267, 25–33. https://doi.org/10.1016/j.desal.2010.09.002

Eom, Y., Won, J.H., Ryu, J.-Y., Lee, T.G., 2011. Biosorption of mercury(II) ions from aqueous solution by garlic (Allium sativum L.) powder. Korean J. Chem. Eng 28, 1439–1443. https://doi.org/10.1007/s11814-010-0514-y

Fiol, N., Villaescusa, I., 2009. Determination of sorbent point zero charge: usefulness in sorption studies. Environ. Chem. Lett. 7, 79–84. https://doi.org/10.1007/s10311-008-0139-0

Ho, Y.S., McKay, G., 1999. Pseudo-second order model for sorption processes. Process Biochem. 34, 451–465. https://doi.org/10.1016/S0032-9592(98)00112-5

Jiménez-Cedillo, M.J., Olguín, M.T., Fall, C., Colin-Cruz, A., 2013. As(III) and As(V) sorption on iron-modified non-pyrolyzed and pyrolyzed biomass from Petroselinum crispum (parsley). J. Environ. Manage. 117, 242–252. https://doi.org/10.1016/J.JENVMAN.2012.12.023

Krishnani, K.K., Meng, X., Christodoulatos, C., Boddu, V.M., 2008. Biosorption mechanism of nine different heavy metals onto biomatrix from rice husk. J. Hazard. Mater. 153, 1222–1234. https://doi.org/10.1016/J.JHAZMAT.2007.09.113

Lagergren, S., 1898. Zur theorie der sogenannten adsorption gel Zur theorie der sogenannten adsorption gelster stoffe, Kungliga Svenska Vetenskapsakademiens. Handlingar 24, 1–39.

Liang, S., McDonald, A.G., 2014. Chemical and thermal characterization of potato peel waste and its fermentation residue as potential resources for biofuel and bioproducts production. J. Agric. Food Chem. 62, 8421–8429. https://doi.org/10.1021/jf5019406

Lopes, C.B., Lito, P.F., Cardoso, S.P., Pereira, E., Duarte, A.C., Silva, C.M., 2012. Metal recovery, separation and/or pre-concentration, in: Inamuddin, Luqma, M. (Eds.), Ion

Exchange Technology II – Applications. Springer, pp. 237–322.

Lopes, C.B., Otero, M., Coimbra, J., Pereira, E., Rocha, J., Lin, Z., Duarte, A., 2007. Removal of low concentration Hg2+ from natural waters by microporous and layered titanosilicates. Microporous Mesoporous Mater. 103, 325–332. https://doi.org/10.1016/j.micromeso.2007.02.025

Marcilla, A., Beltrán, M.I., Navarro, R., 2007. Application of TG/FTIR to the study of the regeneration process of husy and HZSM5 zeolites. J. Therm. Anal. Calorim. 87, 325–330. https://doi.org/10.1007/s10973-005-7322-3

Montgomery, D.C., 2001. Design and Analysis of Experiments, 5th ed. John Wiley & Sons, Inc.

Neris, J.B., Luzardo, F.H.M., da Silva, E.G.P., Velasco, F.G., 2019. Evaluation of adsorption processes of metal ions in multi-element aqueous systems by lignocellulosic adsorbents applying different isotherms: A critical review. Chem. Eng. J. 357, 404–420. https://doi.org/10.1016/j.cej.2018.09.125

Nguyen, T.A.H., Ngo, H.H., Guo, W.S., Zhang, J., Liang, S., Yue, Q.Y., Li, Q., Nguyen, T.V., 2013. Applicability of agricultural waste and by-products for adsorptive removal of heavy metals from wastewater. Bioresour. Technol. 148, 574–585. https://doi.org/10.1016/J.BIORTECH.2013.08.124

Panayotova, M.I., 2001. Kinetics and thermodynamics of copper ions removal from wastewater by use of zeolite. Waste Manag. 21, 671–676.

Patnukao, P., Kongsuwan, A., Pavasant, P., 2008. Batch studies of adsorption of copper and lead on activated carbon from Eucalyptus camaldulensis Dehn. bark. J. Environ. Sci. 20, 1028–1034. https://doi.org/10.1016/S1001-0742(08)62145-2

Rafatullah, M., Sulaiman, O., Hashim, R., Ahmad, A., 2009. Adsorption of copper (II), chromium (III), nickel (II) and lead (II) ions from aqueous solutions by meranti sawdust. J. Hazard. Mater. 170, 969–977. https://doi.org/10.1016/J.JHAZMAT.2009.05.066

Rocha, L.S., Almeida, Â., Nunes, C., Henriques, B., Coimbra, M.A., Lopes, C.B., Silva, C.M.,

Duarte, A.C., Pereira, E., 2016. Simple and effective chitosan based films for the removal of Hg from waters: Equilibrium, kinetic and ionic competition. Chem. Eng. J. 300, 217–229. https://doi.org/10.1016/j.cej.2016.04.054

Roginsky, S., Zeldovich, Y.B., 1934. The catalytic oxidation of carbon monoxide on manganese dioxide. Acta Phys. Chem. USSR 1, 554.

Romera, E., González, F., Ballester, A., Blázquez, M.L., Muñoz, J.A., 2007. Comparative study of biosorption of heavy metals using different types of algae. Bioresour. Technol. 98, 3344–3353. https://doi.org/10.1016/J.BIORTECH.2006.09.026

Stumm, W., Morgan, J.J., 1996. Aquatic Chemistry: chemical equilibria and rates in natural waters. John Wiley & Sons, Inc.

Substance Priority List | ATSDR [WWW Document], 2017. URL https://www.atsdr.cdc.gov/spl/ (accessed 2.2.19).

Vinod, V.T.P., Sashidhar, R.B., Sivaprasad, N., Sarma, V.U.M., Satyanarayana, N., Kumaresan, R., Rao, T.N., Raviprasad, P., 2011. Bioremediation of mercury (II) from aqueous solution by gum karaya (Sterculia urens): A natural hydrocolloid. Desalination 272, 270–277. https://doi.org/10.1016/J.DESAL.2011.01.027

Witek-Krowiak, A., Chojnacka, K., Podstawczyk, D., Dawiec, A., Pokomeda, K., 2014. Application of response surface methodology and artificial neural network methods in modelling and optimization of biosorption process. Bioresour. Technol. 160, 150–160. https://doi.org/10.1016/j.biortech.2014.01.021

Zafar, M.N., Nadeem, R., Hanif, M.A., 2007. Biosorption of nickel from protonated rice bran. J. Hazard. Mater. 143, 478–485. https://doi.org/10.1016/J.JHAZMAT.2006.09.055

Chapter IV

Marine macroalgae towards water treatment

This chapter approaches two works in which six living macroalgae, namely *Ulva intestinalis*, *Ulva lactuca*, *Fucus spiralis*, *Fucus vesiculosus*, *Gracilaria* sp. and *Osmundea pinnatifida* were tested for mercury removal from synthetic seawater. The works are the integral form of the manuscripts submitted to scientific journals.

Initially a study of the ability of the six different macroalgae for mercury removal was carried out. Their performances were compared under three mercury initial concentrations (50, 200 and 500 μg dm^{-3}) in order to determine the best macroalgae as a promising alternative for remediation of Hg(II) contaminated waters.

Following the previous work, the competition effect by the presence of potential toxic elements (Cd, Cr, Cu, Ni and Pb) and rare earth elements (La, Ce, Pr, Nd, Eu, Gd, Tb and Y) were studied on the behavior of the six macroalgae for Hg(II) removal.

Index

Work submitted as scientific article

Fast and efficient removal of mercury from contaminated waters by green, brown and red living marine macroalgae: a promising alternative for water treatment

Abstract

Two green (*Ulva intestinalis* and *Ulva lactuca*), two brown (*Fucus spiralis* and *Fucus vesiculosus*) and two red (*Gracilaria* sp. and *Osmundea pinnatifida*) marine macroalgae were tested for the removal of mercury from spiked synthetic seawaters. Ability of each species was evaluated to the initial mercury concentrations of 50, 200 and 500 μg dm^{-3}. Kinetics were studied by measuring dissolved mercury concentrations along 72 hours. In general, all species exhibited good performances, removing 80.9-99.9% from solutions with 50 μg dm^{-3}, 79.3-98.6 % from solution with 200 μg dm^{-3} and 69.8-97.7 % from solutions containing 500 μg dm^{-3} of mercury after 72 hours, although the followed order was observed: green > brown > red macroalgae. *Ulva intestinalis* showed the highest affinity to mercury and it removed 1888 μg g^{-1} of Hg(II) from the 500 μg dm^{-3} spiked solution. Bioconcentration factors between 3803 and 3823 for the three contamination conditions

IV.1. Fast and efficient removal of mercury from contaminated waters by green, brown and red living marine macroalgae: a promising alternative for water treatment

IV.1.1. Introduction

Bioremediation technologies emerged as promising alternatives for the treatment of contaminated waters. Biosorption and bioaccumulation are the major processes related to the uptake of a sorbate by a sorbent of biological origin (Farooq et al., 2010). If the sorbent is a biomass metabolically inactive, the sorption and desorption occur on its surface until equilibrium is achieved. In the case of a living organism, sorption may be followed by the metabolically active transport systems into the cells (Chojnacka, 2010). The transport of the sorbate to the inside of cells makes available more active sites on sorbent surface and, hence, final concentrations in solution may be lower (Aryal and Liakopoulou-Kyriakides, 2015; Chojnacka, 2010). The metabolic active stage is normally slower than sorption (Kaduková and Virčíková, 2005). The limitations of these processes with living organisms are their resistance and adaptation to contaminants. Major environmental factors are those affecting biological processes, such as light exposure, temperature, pH and nutrient sources (Chojnacka, 2010; Kaduková and Virčíková, 2005). In the point of view of cost-effective application, the use of living organisms eliminates the step of biomass separation usually required in biosorption with non-living biomass. Moreover, it reduces expenses with other operations such as drying, milling and storage (Aksu and Dönmez, 2005; Chojnacka, 2010). Among the living organisms, macroalgae are pointed out as very resistant to extremely polluted medium and capable of retaining high concentrations of metals (Chojnacka, 2010; Kumar et al., 2006; Zhou et al., 2018). Along natural processes of nutrient uptake, contaminants may be removed from the medium. Examples of species tested as biosorbents are *Chlorella kessleri* for removal of Cu (Kaduková and Virčíková, 2005), *Zignema fanicum* (Shams Khoramabadi et al., 2008) and *Porphyridium cruentum* (Zaib et al., 2016) for Hg and *Fucus vesiculosus* for Cd (Holan et al., 1993), Ni and Pb (Holan and Volesky, 1994).

Macroalgae are commonly divided in three groups: Chlorophyta (green algae), Phaeophyta (brown algae) and Rhodophyta (red algae) (Romera et al., 2007). Although sharing common characteristic of containing chlorophyll, remarkable differences are noticed in pigmentation and composition of cell walls. The Chlorophyta pigments are chlorophylls, carotenes and xanthophylls, the Phaeophyta have in addition fucoxanthin, while the pigmentation of Rhodophyta is due to the chlorophylls, phycocyanins, phycoerythrins, carotenes and xanthophylls. The cell walls of all macroalgae are composed by cellulose. In addition, the green macroalgae cell walls have mannan and xylan, the brown macroalgae have alginic acid and fucoidan and the red macroalgae are formed by xylans and galactans. These compounds are formed by amine, carboxyl, sulphates and hydroxyl, with high tendency to bind with metals in solution (Bold and Wynne, 1978; Davis et al., 2003).

Mercury is the third most toxic element according to the list of priority pollutants created by the Agency for Toxic Substances and Disease Registry (ATSDR) ("ATSDR, Priority list of hazardous substances," 2017). Such position is attributed to its high frequency and persistence in the environment and its hazardous impacts on ecosystem and human health. Mercury forms are rapidly absorbed by organisms and slower eliminated, being transmitted and magnified along the food chain (Lopes et al., 2009). Trace Hg(II) concentrations in water are considered to represent dangerousness and therefore contaminated wastewaters must be remediated. In line with the present scientific knowledge, European Union promotes the improvement of surface water quality by reducing the discharges of priority hazardous substances like Hg(II), and by the development of new technologies more economic and effective to treat contaminated waters (Directive 2013/39/EU).

Accordingly, the present study aims to evaluate the ability of *Ulva intestinalis*, *Ulva lactuca*, *Fucus spiralis*, *Fucus vesiculosus*, *Gracilaria* sp. and *Osmundea pinnatifida* for the removal of Hg(II) from contaminated synthetic seawater. The macroalgae species were characterized and its relationship with removal efficiency was examined. Kinetic studies were performed and fitting of pseudo-first order, pseudo-second order and Elovich models to the experimental data were considered.

IV.1.2. Materials and methods

IV.1.2.1. Chemicals

The reagents used in this work were purchased by chemical suppliers: mercury stock solution (1000 ± 2 mg dm-3) from PanReac AppliChem and nitric acid (65 %) and sodium hydroxide (≥ 99 %) from Merck. The salt used to prepare the synthetic seawater was tropic Marin® SEA SALT acquired from Tropic Marine Center. The complete information about the salt composition is given by Atkinson and Bingman (Atkinson and Bingman (2010). The working solutions and the standards for calibration curves were prepared by diluting the stock solution to the desired concentration. All the glassware used in this work were prior washed with nitric acid (25 %, v/v) for at least 24 hours and ultrapure water (18 MΩ cm) afterwards.

IV.1.2.2. Macroalgae

Six macroalgae species were used in this study, two green (*U. lactuca*, *U. intestinalis*), two brown (*F. spiralis*, *F. vesiculosus*), and two red (*Gracilaria* sp., *O. pinnatifida*) macroalgae. Samples were collected from Ria de Aveiro, Portugal (40°38´39´´N, 8°44´43´´W) and washed with tap water and synthetic seawater for several times to eliminate some impurities or epibionts imbed on the macroalgae surface. Then biomasses were maintained in oxygenated aquaria with natural light exposure (about 12L:12D) for acclimation during one week before the experiments start. Nutrients were not added. Ten samples of each macroalgae were weighted and dried for determination of water content. Another portion of macroalgae was lyophilized for further quantification of Hg initial concentration and FTIR analysis

IV.1.2.3. Experiments

All the macroalgae were investigated for Hg(II) removal in 1 dm^3 transparent glass flasks and temperature of 22 ± 2 °C. Synthetic seawater of salinity 30 was prepared diluting tropic Marin® SEA SALT in distilled water. The macroalgae were cut in small

pieces and introduced into the flasks. The dosage of 3 g dm^{-3} (fresh weight) of each macroalgae were put in contact with Hg(II) solutions of 50 µg dm^{-3}, 200 µg dm^{-3} and 500 µg dm^{-3}. pH was adjusted to 8.5 with NaOH (1 M). Two assays of each condition (macroalgae species and initial concentration) were carried out together with control solutions (without macroalgae) with the aim to verify the experimental losses, and with blank solutions (without Hg(II)) to check the macroalgae health status. Results presented in this study correspond to one of the assays, because the variation in each pair of assays remained below 10 %. Liquid samples of 10 cm^{-3} were taken after 0, 1, 3,6, 9, 24, 48 and 72 hours, acidified with nitric acid (65 %, v/v) for pH ≤ 2 and stored at 4 °C for further Hg(II) quantification. The volume variation due to sampling was insufficient to significantly affect the results. In the end of each assay, the macroalgae was removed from the solution, weighted to quantify the growth rate, lyophilized and stored for FTIR characterization.

IV.1.2.4. Hg(II) quantification

Mercury quantification in the liquid samples was performed by cold vapour atomic fluorescence spectroscopy (CV-AFS), on a PSA cold vapour generator (model 10.003) connected to a Merlin PSA detector (model 10.023). Hg(II) in the samples was reduced by $SnCl_2$ and the response was obtained as signal converted to concentration through a calibration curve, constructed at least three times a day with the standards of 0.1, 0.2, 0.3 and 0.5 µg dm^{-3} of Hg(II). Three measures of each sample were performed with maximum acceptable variation between them of 10 % and the average value was used. The limit of quantification of this method was 0.02 µg dm^{-3}.

The concentration of Hg(II) in the macroalgae previous the bioaccumulation assays was quantified using LECO© AMA-254 by thermal decomposition atomic absorption spectrometry with gold amalgamation according to the method reported by Costley et al. (2000). The limit of quantification was of 0.03 ng of Hg. Samples were analyzed in duplicate with variation coefficients between concentrations lower than 10 %. The Certified Reference Material (CFR) ERM-CD200 (*Fucus vesiculosus*; 0.0186 ± 0.0016 mg kg^{-}

[1] of total Hg) was analyzed before and after the macroalgae samples to assure the quality of the results obtained. Average percentage of recovery was 100.8 %.

IV.1.2.5. Macroalgae characterization

The six macroalgae species studied were characterized by water content, external contact area and FTIR. External contact area was assessed by scanning the macroalgae with resolution of 200 ppi and the software Fiji scaled the image. Fourier Transform Infrared (FTIR) spectra of the macroalgae before and after contact with the contaminated solutions were recorded by Bruker optic tensor 27 spectrometer with an attenuated total reflectance (ATR), 256 scans with a resolution of 4 cm^{-1}. Spectra were obtained after baseline correction from the wavenumber 4000 to 500 cm^{-1}.

IV.1.2.6. Formula and data analysis

Removal of Hg(II) by the macroalgae (R, %) was calculated by the following equation:

$$R = 100 \times \frac{(C_0 - C_t)}{C_0} \quad \text{(IV.1.1)}$$

where C_0 (µg dm^{-3}) is the initial Hg(II) concentration in the spiked solutions and C_t (µg dm^{-3}) the concentration at time t.

The mass balance of each experiment allows to calculate the average Hg(II) concentration per mass of dry weight of macroalgae (q, µg g^{-1}) as follows:

$$q = \frac{V(C_0 - C_f)}{M} \quad \text{(IV.1.2)}$$

where V is the volume of solution in dm^3, C_f is the Hg(II) final concentration in solution (µg dm^{-3}) and M is the average mass between initial and final weights in dry weight (g).

Assuming an exponential growth of the macroalgae, the mean growth rate (GR % day^{-1}) of the experiment was mathematically expressed by (Gordillo et al., 2015):

$$GR = 100 \times \frac{\ln (W_f/W_i)}{t} \quad \text{(IV.1.3)}$$

where W_i is the initial fresh weight (g) of the macroalgae and W_f is the weight after 72 hours of exposure to Hg(II) contaminated solutions; t is the time of the experiment, 72 hours expressed in days.

The bioconcentration factor (BCF) was calculated by:

$$BCF = 1000 \times \frac{q}{C_i} \quad \text{(IV.1.4)}$$

where q (μg g^{-1}) is the macroalgae concentration obtained from the Eq. (IV.1.2) and C_i is the Hg(II) initial concentration in μg kg^{-1} (assuming that 1 dm^{-3} of solution is equal to 1 Kg).

The kinetic study was accomplished by fitting the most known kinetic models of pseudo-first order (Eq. (IV.1.5)) (Lagergren, 1898), pseudo-second order (Eq. (IV.1.6)) (Ho and McKay, 1999) and Elovich (Eq. (IV.1.7)) (Roginsky and Zeldovich, 1934) to the experimental results. These models give information about the viability of application of the process, taking into account the velocity and affinity of the macroalgae for Hg(II) bioaccumulation.

$$\frac{dq}{dt} = k_1(q_e - q) \quad \text{(IV.1.5)}$$

$$\frac{dq}{dt} = k_2(q_e - q)^2 \quad \text{(IV.1.6)}$$

$$\frac{dq}{dt} = \alpha e^{-\beta q} \quad \text{(IV.1.7)}$$

where q_e is the concentration on the macroalgae at equilibrium (μg g^{-1}), k_1 (h^{-1}) is the rate constant of pseudo-first order model, k_2 (g μg^{-1} h^{-1}) is the rate constant of the pseudo-second order model, α (μg g^{-1} h^{-1}) is the initial sorption rate and β (g μg^{-1}) is the desorption constant.

The parameters of the models were obtained by nonlinear optimization using the software Matlab R2014a in which the errors between experimental and calculated data ($AARD$, Eq. (IV.1.8)) were minimized by Nelder-Mead simplex algorithm. The goodness of the fits was evaluated by the average absolute relative deviation, $AARD$ (Eq. (IV.1.8)), and the coefficient of determination, R^2 (Eq. (IV.1.9)) represented by:

$$AARD(\%) = \frac{100}{N_{DP}} \sum_{i=1}^{N_{DP}} \frac{|\hat{y}_i - y_i|}{y_i} \quad \text{(IV.1.8)}$$

$$R^2 = 1 - \frac{\sum(\hat{y}_i - y_i)^2}{\sum(y_i - \bar{y})^2} \quad \text{(IV.1.9)}$$

N_{DP} denotes the number of experimental data, y_i, and $\hat{y}_i$ represent the observed and calculated values and $\bar{y}$ is the mean of experimental data.

Significance testes were done by one- way Analysis of Variance (ANOVA) test, with confidence interval of 95 %, using the data analysis extension of Microsoft® Excel™ 2016.

IV.1.3. Results and discussion

IV.1.3.1. Major characteristics of macroalgae

Water content (%), contact external area and initial concentration of Hg(II) of the macroalgae used in the experiments are presented in Table IV.1.1. Regarding water content, the six macroalgae can be separated in two groups, presenting statistic dissimilarities ($p < 0.05$): group I includes *U. intestinalis, Gracilaria* sp. and *O. pinnatifida*; and group II contains *U. lactuca*, *F. spiralis* and *F. vesiculosus*. *U. intestinalis* showed the

highest water content (91 %) and *F. vesiculosus* the lowest one (80 %). Contact external areas of the green macroalgae stand out due to their morphologies like thin leaves with round or tubular shapes. Brown macroalgae have a branched shape with alginate pouches which makes them denser. The red macroalgae *Gracilaria* sp. has filamentous shapes and thin branches, and *O. pinnatifida* has branched stems and flattened fronds. Although Hg(II) concentration differed significantly ($p < 0.05$) among the macroalgae species used in the experiments, values were characteristic of low contaminated regions (Coelho et al., 2005; Henriques et al., 2015).

Figure IV.1.1 depicts the FTIR spectra of the six macroalgae before and after the exposure assays. Major functional groups involved on the Hg(II) uptake were identified by the appearance, disappearance or shift of the peaks comparing the spectra of macroalgae before and after exposure to Hg(II) spiked solutions. All the macroalgae presented the O-H and N-H vibration at 3200-3400 cm^{-1}, the stretch at 2900 cm^{-1} related with the asymmetric C-H bonds, the peak of asymmetric C=O nearby 1600 cm^{-1} and symmetric C=O around 1400 cm^{-1}. The strong vibration at 1000-1100 is ascribed to the hydroxyl group of the characteristic main sugars present in the macroalgae. In the spectrum of *U. intestinalis/*Hg(II) there is the appearance of the peak at 1536 cm^{-1} correspondent to N-H of amide II groups of proteins (Murphy et al., 2009; Rodrigues et al., 2015), the formation of a double peak at 2910 and 2980 cm^{-1} of the C-H (Rodrigues et al., 2015) and the vanishing of the elbow at 1318 cm^{-1} of sulphonate groups ($-OSO_3$) (Murphy et al., 2009). In the case of *U. lactuca*, after contact with the Hg(II) solution there is the formation of a double peak at 2910 and 2990 cm^{-1} (C-H) (Rodrigues et al., 2015), elimination of the band at 1120 cm^{-1} (symmetric-OSO_3) (Murphy et al., 2009), shift of the peaks at 1090 and 1010 cm^{-1} due to involvement of the hydroxyl functionalities (Murphy et al., 2008), and shift at 1197 cm^{-1} assigned to the C-N stretching of the aromatic amine (Suganya and Renganathan, 2012). *F. spiralis*/Hg(II) and *F. vesiculosus*/Hg(II) spectra were very similar. Elimination of the double at 2850-2920 cm^{-1} (C-H) (Rodrigues et al., 2015), and disappearance of the vibrations at 1540 cm^{-1} (N-H) (Murphy et al., 2009) and 550 cm^{-1} (C–N–S) (Bulgariu and Bulgariu, 2014) were noticed. Regarding the red macroalgae spectra, both presented the vanishing of the band at 800 cm^{-1} ($-OSO_3$) attributed to the galactose

contained in carrageenan (Knutsen et al., 1994; Rodrigues et al., 2015). *Gracilaria* sp. Exposed to Hg(II) showed the shift of the peak at 1110 cm^{-1} (O-H) assigned to the presence of agar.

Table IV.1.1. Water content (%), external area of contact ($cm^2\ g^{-1}$) and Hg concentration ($\mu g\ g^{-1}$**)** of the living macroalgae used in the experiments.

Macroalgae	***Ulva Intestinalis***	***Ulva lactuca***	***Fucus spiralis***	***Fucus vesiculosus***	***Gracilaria* sp.**	***Osmundea pinnatifida***
Water content (%)	91.4 ± 0.6	82.8 ± 0.5	81.6 ± 3.1	80.2 ± 5.4	88.1 ± 5.5	88.8 ± 1.2
External contact area ($cm^2\ g^{-1}$)	148 ± 45	264 ± 31	29 ± 11	30 ± 9	79 ± 9	33 ± 2
Hg concentration ($\mu g\ g^{-1}$)	0.042 ± 0.002	0.034 ± 0.002	0.049 ± 0.002	0.032 ± 0.001	0.031 ± 0.002	0.082 ± 0.002

Growth rates (GR) of the macroalgae during the 72 hours of the experiments were calculated by the Eq. (IV.1.3) and values are given in Table IV.1.2. GR varied with narrow intervals in species exposed to 50 $\mu g\ dm^{-3}$ (-1.2 to 3.2 % day^{-1}) and 200 $\mu g\ dm^{-3}$ (-2.2 to 0.5 % day^{-1}). Exposure to 500 $\mu g\ dm^{-3}$ resulted in broader variation of weight, GR varying from -11.7 % day^{-1} for *O. pinnatifida* to 3.2 % day^{-1} for *U. lactuca*. The negative values of growth rates were probably associated with some losses in the recovery of the macroalgae and the highest loss of weight of *O. pinnatifida*, exposed to the Hg(II) concentration of 500 $\mu g\ dm^{-3}$, was associated with marked loss of color and deterioration in the end of the trial.

Table IV.1.2. Growth rates (GR, % day^{-1}) of the macroalgae during the 72 hours calculated by Eq. (IV.1.3).

GR (% day^{-1})	***Ulva Intestinalis***	***Ulva lactuca***	***Fucus spiralis***	***Fucus vesiculosus***	***Gracilaria* sp.**	***Osmundea pinnatifida***

50 µg dm^{-3}	0.6	3.2	-0.3	-0.6	1.1	-1.2
200 µg dm^{-3}	0.5	0.5	-1.7	-0.5	-0.7	-2.2
500 µg dm^{-3}	3.1	3.2	-1.6	-0.04	-4.5	-11.7

IV.1.3.2. Influence of Hg(II) initial concentrations on removal

Figure IV.1.2 shows the Hg(II) concentrations in solution at each time (C_t), normalized to the initial concentration (C_0), along 72 hours for the six macroalgae. Profiles for the initial concentrations of 50, 200 and 500 µg dm^{-3} are presented. For all the conditions, ratios $C_t: C_0$ decreased with time. Although slopes varied with the macroalgae species, only small differences were observed among the three spiking conditions. All the curves of *U. intestinalis* and the curves of *U. lactuca* and *Gracilaria* sp for 50 and 500 µg dm^{-3} were characterized by slopes with two stages: the first one shows a pronounced slope, the fast removal being most likely driven by the strong gradient of Hg between the solution and the clean macroalgae; in the second stage the removal slowed down towards an equilibrium. Change of removal rates suggest two dynamics of Hg(II) uptake: initially, Hg was extracellularly bound to the macroalgae by chemical or physical interactions, and then by intracellular accumulation driven by metabolic activities (Andrade et al., 2006; Henriques et al., 2015). In the profiles observed for the other studied species, the two stages were less pronounced. Decrease of $C_t: C_0$ in *F. spiralis*, *F. vesiculosus* and *O. pinnatifida* was almost linear, which may reflect lower affinity of the freshly arrived Hg cations to functional groups of the macroalgae surface, or difficult accessibility of Hg(II) to the active sorption sites. Diffusion towards the macroalgae surface should have increased as availability of Hg(II) was higher.

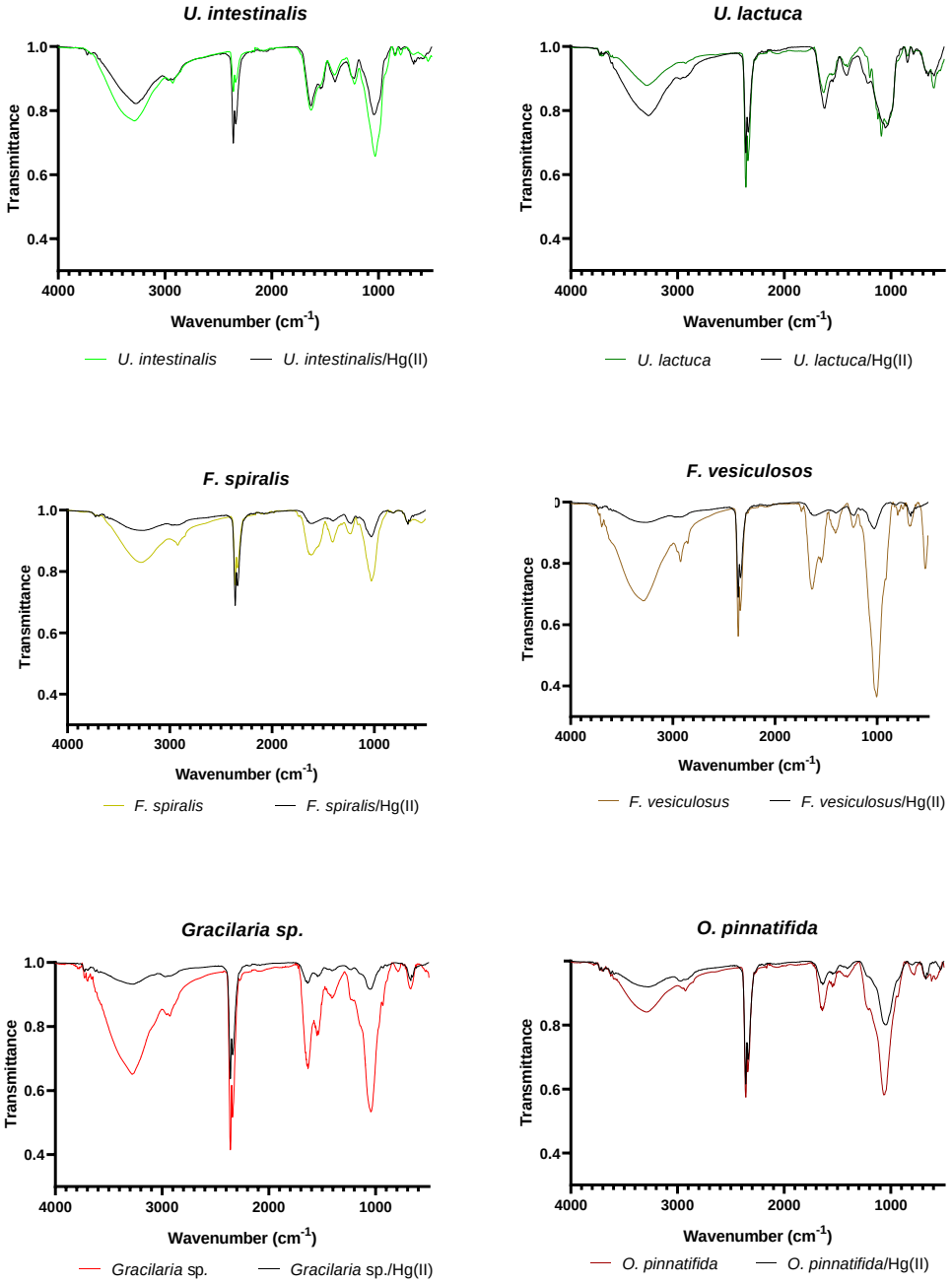

Figure IV.1.1. FTIR spectra of the six macroalgae before and after Hg(II) exposure.

For each time t, the differences among the C_t: C_0 ratios obtained for 50, 200 and 500 µg dm^{-3} experiments were minor for the macroalgae *U. intestinalis*, *F. spiralis*, *F. vesiculosus* and *O. pinnatifida*. The low variability suggests that increasing concentration of Hg(II) in solution, and consequently higher fluxes towards the macroalgae surface, led a

proportional uptake. Presumably, saturation of the sorption sites was not achieved for the tested concentrations. Although all the six macroalgae have achieved low final concentrations of Hg in solution, *U. intestinalis* appears as the most promising macroalgae.

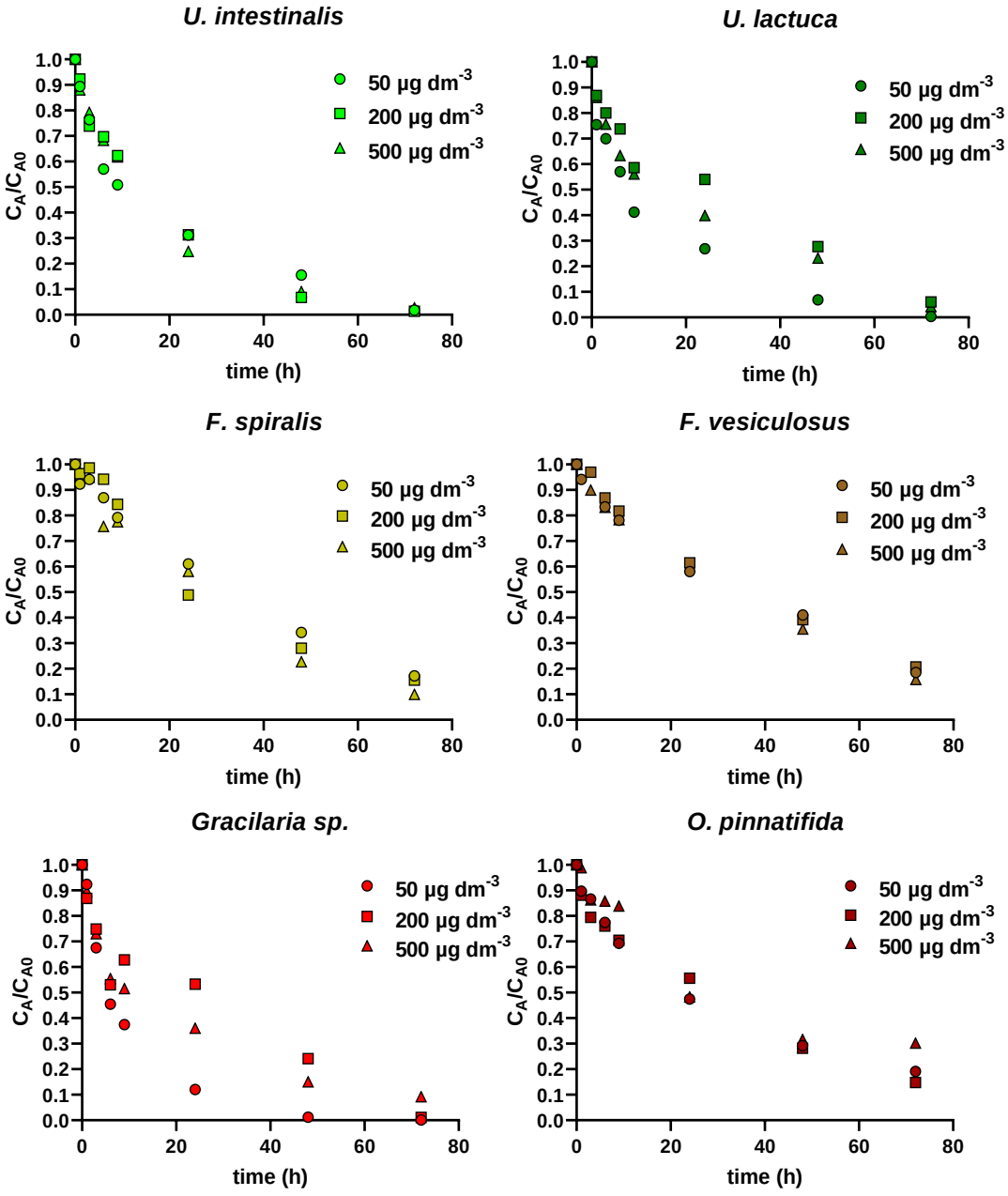

Figure IV.1.2. Normalized Hg(II) concentration of the solution along time for three different initial concentrations and six macroalgae.

Figure IV.1.3 shows the removal percentages by the six macroalgae (3 g dm^{-3}) for the three initial Hg(II) concentrations. After 72 hours of contact with the spiked solution of 50 µg dm^{-3}, *Gracilaria* sp., *U. lactuca* and *U. intestinalis* removed 99.9 %, 99.6 % and 98.2 % of Hg(II), respectively. And their final solutions have achieved concentrations of drinking water quality regulation (< 1 µg dm^{-3}) (Directive 2008/105/EC). *U. intestinalis* have got the best performance in the conditions of exposure to concentration of 200 and *ulva lactuca* to concentration of 500 µg dm^{-3}, with Hg(II) removal of 98.6 % and 97.7 %, respectively. The worst accomplishments were of *O. pinnatifida* (80.9 %) under the initial concentration of 50 µg dm^{-3}, *F. vesiculosus* (79.3 %) under 200 µg dm^{-3} and *O. pinnatifida* (69.8 %) under 500 µg dm^{-3}. Because biomass of *O. pinnatifida* decreased after being 72 hours in contact with the most contaminated solution, it should not be excluded the possibility of low removal being a consequence of toxicity effect.

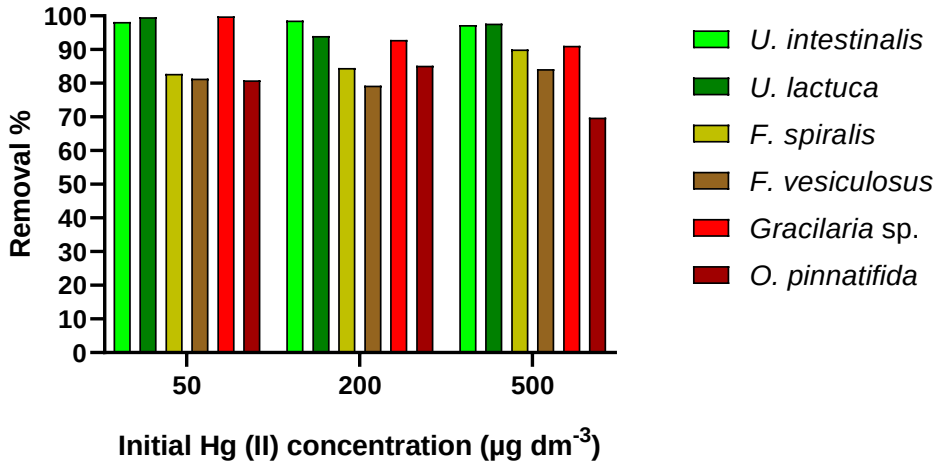

Figure IV.1.3. Removal percentages of Hg(II) after 72 hours of contact time from contaminated solutions with 50, 200 and 500 µg dm^{-3} for all the macroalgae studied

IV.1.3.3. Uptake of Hg(II) by macroalgae

Figure IV.1.4 presents the calculated mass of Hg uptake (q) by the green, brown and red macroalgae dry weight (Eq. (IV.1.2)) along time for the three initial concentrations. In line with the profiles of C_t: C_0 ratios, *U. intestinalis* showed the highest uptake for all the studied conditions. High external area of contact looks to be a plausible

explanation when comparing uptake with the other macroalgae, except *U. lactuca*. This species exhibited higher external contact area than *U. intestinalis* and the uptake was lower. Thin tubular structure of *U. intestinalis* may have facilitated the removal of cations from solution. For the two lower dissolved Hg concentrations, brown and red macroalgae showed similar behaviours, probably as result of their similar morphology and composition. The plateau observed in the case of *Gracilaria* sp. exposed to 50 µg dm^{-3} suggests an almost total removal of Hg(II) after 48 hours. It should not be excluded the possibility of living macroalgae incorporating Hg(II) by carrier proteins through nutrients transport processes, which would make available sorption sites (Stumm and Morgan, 1996). Under these conditions, equilibrium of the Hg sorption would be repeatedly adjusted (Stumm and Morgan, 1996). Higher values of *q* were obtained for higher initial Hg concentrations. For example, in the experiments of 50 µg dm^{-3} the quantities of Hg(II) retained in the macroalgae varied from 74 µg g^{-1} for *F. vesiculosus* to 209 µg g^{-1} for *U. intestinalis*, while for the initial concentration of 500 µg dm^{-3} *q* was between 727 µg g^{-1} for *F. vesiculosus* and 1888 µg g^{-1} for *U. intestinalis.*

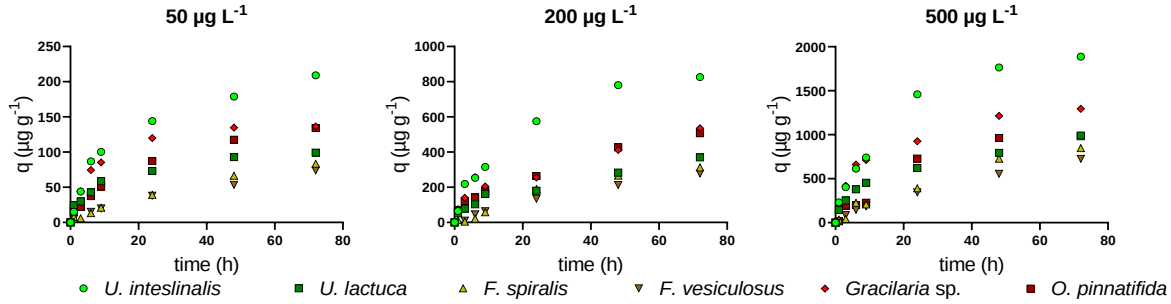

Figure IV.1.4. Hg(II) concentration on the macroalgae along time for the three different scenarios of contamination.

IV.1.3.4. Kinetics modelling

The kinetic models of PFO, PSO and Elovich were fitted to the experimental data of *U. intestinalis,* the macroalgae chosen due to its best performance on removal of Hg(II). The adjusted curves are plotted in Figure IV.1.5 and the parameters obtained are presented in Table IV.1.4. Good agreements were obtained between the fittings of the

models and the experimental data, with coefficients of determination in the range of 0.971 - 0.991 for PFO, 0.987 - 0.990 for PSO, and 0.986 - 0.989 for Elovich models. Globally, PSO and Elovich equations presented best combinations of higher values of R^2 and lower $AARD$ and, consequently, are better for description of Hg(II) kinetics by *U. intestinalis*. The constant of the PSO model k_2 decreased with the higher concentrations. This parameter is related with the time to reach the equilibrium and higher values represent shorter equilibrium time (Plazinski et al., 2009). Therefore, less contaminated solutions tend to get the steady state earlier. However, the initial sorption parameter of Elovich model α followed the initial concentration pattern, which corroborates with the enhance in the Hg(II) concentration gradient between solution and macroalgae surface that promoted higher uptake of Hg(II).

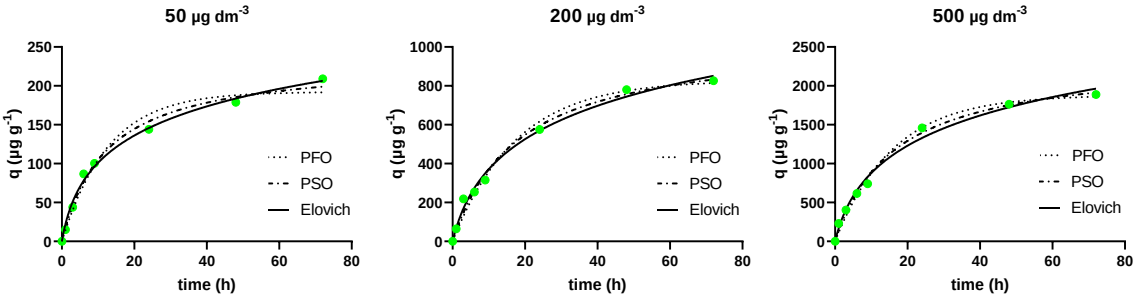

Figure IV.1.5. Kinetic fitting to the experimental data of U. intestinalis.

Table IV.1.3. Kinetic parameters of the models of PFO, PSO and Elovich models for U. intestinalis.

	PFO model				**PSO model**				**Elovich model**			
[Hg(II)] (µg dm^{-3})	k_1 (h^{-1})	q_e (µg g^{-1})	R^2	$AARD$ (%)	k_2 (g mg^{-1} h^{-1})	q_e (µg g^{-1})	R^2	$AARD$ (%)	α (µg g^{-1} h^{-1})	β (g µg^{-1})	R^2	$AARD$ (%)
50	0.090	181.2	0.971	5.33	3.602E-04	224.8	0.987	5.36	20.79	0.0151	0.989	6.74
200	0.061	824.4	0.983	10.46	5.330E-05	1040.2	0.989	8.18	73.22	0.0036	0.989	6.03
500	0.068	1833.8	0.991	10.26	3.252E-05	2246.8	0.990	8.55	193.48	0.0017	0.986	7.38

IV.1.3.5. Bioconcentration factor

Table IV.1.4 shows the bioconcentration factor (BCF) calculated by the Eq. (4) for the six macroalgae exposed for 72 hours to solutions with 50, 200 and 500 μg dm^{-3} of Hg(II). BCFs varied within the broad interval of 1357-3823. . The species of macroalgae contributed more to the variation of the BCF than the different contamination in solution. Narrow variation of BCFs for the three contamination conditions might be ascribed to the chemical equilibrium of Hg(II) between solution and macroalgae surface. This is a remarkable result because emphasizes the high capacity of the studied macroalgae to store the Hg, at least until the presence of 500 μg dm^{-3} in solution. *U. intestinalis* was much more efficient to concentrate Hg(II) than the other macroalgae, and brown and red macroalgae presented similar BCFs. In terms of practical aspects these outcomes are very promising, since even the species that performed worst were able to accumulate mercury three orders of magnitude above than the contaminated medium.

Table IV.1.4. Bioconcentration factor (BCF) of the macroalgae for the contaminated solutions with 50, 200, and 500 μg dm^{-3} of Hg(II).

	Bioconcentration factor (BCF)		
Macroalgae	**50 μg dm^{-3}**	**200 μg dm^{-3}**	**500 μg dm^{-3}**
U. intestinalis	3803	3823	3773
U. lactuca	1953	1738	1877
F. spiralis	1500	1531	1630
F. vesiculosus	1357	1321	1404
Gracilaria sp.	2775	2462	2574
O. pinnatifida	2450	2581	2115

IV.1.3.6. Comparison with different sorbents from literature

The removal efficiencies of the six macroalgae tested in this work have been compared with different sorbents used to remove Hg(II) in similar initial concentrations (50 and 500 μg dm^{-3}) and the results are displayed in Table IV.1.5. It is possible to observe that small doses of macroalgae as low as the ones used in this study were able to perform equally or even better than the sorbents reported in literature. *Gracilaria* sp. presented the same performance of the magnetic nanoparticles Fe_3O_4@SiO_2/SiDTC in similar matrices and spiked Hg(II) concentration of 50 μg dm^{-3} and its use allows to obtain a decontaminated solution. All the other biosorbents and synthetic materials showed worse performances than *Gracilaria* sp under this Hg(II) concentration, even the materials tested under simpler water matrices. Comparing the performances of the macroalgae under the highest Hg(II) initial concentration studied, *U. lactuca* presented best removal percentage than the biosorbents rice husks, cork stoppers, crab carapace and clam shell wastes. These results highlight the potential of using macroalgae as an alternative for water treatments in contrast with the other materials, which were less efficient or have cost and environment impact associated with their synthesis.

Table IV.1.5. Comparison of the Hg(II) removal efficiencies for different materials

Sorbent	Type of water matrix	Hg(II) initial concentration (μg dm^{-3})	Sorbent dosage (g dm^{-3})	Time of exposure (h)	Removal (%)	Ref.
U. intestinalis	Synthetic seawater	50	0.26	72	98.2	This study
U. lactuca	Synthetic seawater	50	0.52	72	99.6	This study
F. spiralis	Synthetic seawater	50	0.55	72	82.8	This study
F. vesiculosus	Synthetic seawater	50	0.59	72	81.4	This study
Gracilaria sp.	Synthetic	50	0.36	72	99.9	This study

	seawater					
O. pinnatifida	Synthetic seawater	50	0.34	72	80.9	This study
Rice husks	Ultrapure	50	0.25	168	82.0	(Rocha et al., 2013)
Rice husks	Ultrapure	50	0.50	168	84.0	(Rocha et al., 2013)
Cork stoppers	Seawater	50	0.25	96	48.0	(Lopes et al., 2014)
Crab carapace	Ultrapure	50	0.25	72	62.0	(Monteiro et al., 2016)
Clam shell wastes	Ultrapure	50	0.25	72	80.0	(Monteiro et al., 2016)
Graphene oxide	Seawater	50	0.01	48	42.0	(Henriques et al., 2016)
Fe_3O_4@SiO_2/ SiDTC	Seawater	50	0.01	48	99.9	(Tavares et al., 2016)
ETS-4	Ultrapure	50	0.016	24	99.5	(Lopes et al., 2009)
U. intestinalis	Synthetic seawater	500	0.26	72	97.3	This study
U. lactuca	Synthetic seawater	500	0.52	72	97.7	This study
F. spiralis	Synthetic seawater	500	0.55	72	90.0	This study
F. vesiculosus	Synthetic	500	0.59	72	84.2	This study

	seawater					
Gracilaria sp.	Synthetic seawater	500	0.36	72	91.1	This study
O. pinnatifida	Synthetic seawater	500	0.34	72	69.8	This study
Rice husks	Ultrapure	500	0.25	168	91.0	(Rocha et al., 2013)
Rice husks	Ultrapure	500	0.50	168	92.0	(Rocha et al., 2013)
Cork stoppers	Ultrapure	500	0.25	168	94.4	(Lopes et al., 2014)
Crab carapace	Ultrapure	500	0.25	72	62.0	(Monteiro et al., 2016)
Clam shell wastes	Ultrapure	500	0.25	72	83.0	(Monteiro et al., 2016)

IV.1.4. Conclusions

The performances of the six macroalgae to uptake Hg from solutions followed the sequence: green > red > brown. Green macroalgae is characterized by thinner structures with higher apparent contact external areas which may facilitate the Hg uptake. Uptake increased with time and with initial mercury concentration, although without reach a plateau. This pattern is indicative of lack of saturation for the active binding sites on the macroalgae surface. It may be hypothesised that Hg crossed the macroalgae surface and were stored in the inner parts of the cells, and new binding sites became available. Further studies should be performed to test this hypothesis. High bioconcentration factors of the macroalgae for the three spiking conditions, in particular *U. intestinalis,* point to the excellent performance of these species on mercury removal. In addition, the

comparison with different materials reported in literature highlighted the potential of using this simple sustainable and efficient alternative for the treatment of contaminated waters by using adequate living organisms.

IV.1.5. References

Aksu, Z., Dönmez, G., 2005. Combined effects of molasses sucrose and reactive dye on the growth and dye bioaccumulation properties of Candida tropicalis. Process Biochem. 40, 2443–2454. https://doi.org/10.1016/j.procbio.2004.09.013

Andrade, S., Contreras, L., Moffett, J.W., Correa, J.A., 2006. Kinetics of copper accumulation in Lessonia nigrescens (Phaeophyceae) under conditions of environmental oxidative stress 78, 398–401. https://doi.org/10.1016/j.aquatox.2006.04.006

Aryal, M., Liakopoulou-Kyriakides, M., 2015. Bioremoval of heavy metals by bacterial biomass. Environ. Monit. Assess. 187, 4173. https://doi.org/10.1007/s10661-014-4173-z

Atkinson, M.J., Bingman, C., 2010. Elemental composition of commercial seasalts. J. Aquaric. Aquat. Sci. 8, 39–43.

ATSDR, Priority list of hazardous substances [WWW Document], 2017. URL https://www.atsdr.cdc.gov/spl/ (accessed 2.22.17).

Bold, H.C., Wynne, M.J., 1978. Introduction to the algae : structure and reproduction. Prentice-Hall, Englewood Cliffs N.J.

Bulgariu, L., Bulgariu, D., 2014. Enhancing Biosorption Characteristics of Marine Green Algae (Ulva lactuca)for Heavy Metals Removal by Alkaline Treatment. J. Bioprocess. Biotech. 4, 1–8. https://doi.org/10.4172/2155-9821.1000146

Chojnacka, K., 2010. Biosorption and bioaccumulation – the prospects for practical applications. Environ. Int. 36, 299–307. https://doi.org/10.1016/J.ENVINT.2009.12.001

Coelho, J.P., Pereira, M.E., Duarte, A., Pardal, M.A., 2005. Macroalgae response to a mercury contamination gradient in a temperate coastal lagoon (Ria de Aveiro,

Portugal). Estuar. Coast. Shelf Sci. 65, 492–500. https://doi.org/10.1016/J.ECSS.2005.06.020

Costley, C.T., Mossop, K.F., Dean, J.R., Garden, L.M., Marshall, J., Carroll, J., 2000. Determination of mercury in environmental and biological samples using pyrolysis atomic absorption spectrometry with gold amalgamation. Anal. Chim. Acta 405, 179–183. https://doi.org/10.1016/S0003-2670(99)00742-4

Davis, T.A., Volesky, B., Mucci, A., 2003. A review of the biochemistry of heavy metal biosorption by brown algae. Water Res. 37, 4311–4330. https://doi.org/10.1016/S0043-1354(03)00293-8

Directive 2008/105/EC of the European Parliament and of the Council of 16 December 2008 on environmental quality standards in the field of water policy, amending and subsequently repealing Council Directives 82/176/EEC, 83/513/EEC, 84/156/EEC, 84/491/EEC, 2008. . Off. J. Eur. Communities L 348, 84–97.

Directive 2013/39/EU of the European Parliament and of the Council of 12 August 2013 amending Directives 2000/60/EC and 2008/105/EC as regards priority substances in the field of water policy, 2013. . Off. J. Eur. Union.

Farooq, U., Kozinski, J.A., Khan, M.A., Athar, M., 2010. Biosorption of heavy metal ions using wheat based biosorbents – A review of the recent literature. Bioresour. Technol. 101, 5043–5053. https://doi.org/10.1016/J.BIORTECH.2010.02.030

Gordillo, F.J.L., Aguilera, J., Wiencke, C., Jiménez, C., 2015. Ocean acidification modulates the response of two Arctic kelps to ultraviolet radiation. J. Plant Physiol. 173, 41–50. https://doi.org/10.1016/J.JPLPH.2014.09.008

Henriques, B., Gonçalves, G., Emami, N., Pereira, E., Vila, M., Marques, P.A.A.P., 2016. Optimized graphene oxide foam with enhanced performance and high selectivity for mercury removal from water. J. Hazard. Mater. 301, 453–461. https://doi.org/10.1016/j.jhazmat.2015.09.028

Henriques, B., Rocha, L.S., Lopes, C.B., Figueira, P., Monteiro, R.J.R., Duarte, A.C., Pardal, M.A., Pereira, E., 2015. Study on bioaccumulation and biosorption of mercury by living marine macroalgae: Prospecting for a new remediation biotechnology applied to saline waters. Chem. Eng. J. 281, 759–770.

https://doi.org/10.1016/J.CEJ.2015.07.013

Ho, Y.S., McKay, G., 1999. Pseudo-second order model for sorption processes. Process Biochem. 34, 451–465. https://doi.org/10.1016/S0032-9592(98)00112-5

Holan, Z.R., Volesky, B., 1994. Biosorption of lead and nickel by biomass of marine algae. Biotechnol. Bioeng. 43, 1001–1009. https://doi.org/10.1002/bit.260431102

Holan, Z.R., Volesky, B., Prasetyo, I., 1993. Biosorption of cadmium by biomass of marine algae. Biotechnol. Bioeng. 41, 819–825. https://doi.org/10.1002/bit.260410808

Kaduková, J., Virčíková, E., 2005. Comparison of differences between copper bioaccumulation and biosorption. Environ. Int. 31, 227–232. https://doi.org/10.1016/j.envint.2004.09.020

Knutsen, S.H., Myslabodski, D.E., Larsen, B., Usov, A.I., 1994. A Modified System of Nomenclature for Red Algal Galactans. Bot. Mar. 37, 163–169. https://doi.org/10.1515/botm.1994.37.2.163

Kumar, Y.P., King, P., Prasad, V.S.R.K., 2006. Removal of copper from aqueous solution using Ulva fasciata sp.—A marine green algae. J. Hazard. Mater. 137, 367–373. https://doi.org/10.1016/J.JHAZMAT.2006.02.010

Lagergren, S., 1898. Zur theorie der sogenannten adsorption gel Zur theorie der sogenannten adsorption gelster stoffe, Kungliga Svenska Vetenskapsakademiens. Handlingar 24, 1–39.

Lopes, C.B., Oliveira, J.R., Rocha, L.S., Tavares, D.S., Silva, C.M., Silva, S.P., Hartog, N., Duarte, A.C., Pereira, E., 2014. Cork stoppers as an effective sorbent for water treatment: the removal of mercury at environmentally relevant concentrations and conditions. Environ. Sci. Pollut. Res. 21, 2108–2121.

Lopes, C.B., Otero, M., Lin, Z., Silva, C.M., Rocha, J., Pereira, E., Duarte, A.C., 2009. Removal of Hg2+ ions from aqueous solution by ETS-4 microporous titanosilicate-Kinetic and equilibrium studies. Chem. Eng. J. 151, 247–254. https://doi.org/10.1016/j.cej.2009.02.035

Monteiro, R.J.R., Lopes, C.B., Rocha, L.S., Coelho, J.P., Duarte, A.C., Pereira, E., 2016. Sustainable approach for recycling seafood wastes for the removal of priority hazardous substances (Hg and Cd) from water. J. Environ. Chem. Eng. 4, 1199–1208.

https://doi.org/10.1016/J.JECE.2016.01.021

Murphy, V., Hughes, H., McLoughlin, P., 2009. Enhancement strategies for Cu(II), Cr(III) and Cr(VI) remediation by a variety of seaweed species. J. Hazard. Mater. 166, 318–326. https://doi.org/10.1016/j.jhazmat.2008.11.041

Murphy, V., Hughes, H., McLoughlin, P., 2008. Comparative study of chromium biosorption by red, green and brown seaweed biomass. Chemosphere 70, 1128–1134. https://doi.org/10.1016/j.chemosphere.2007.08.015

Plazinski, W., Rudzinski, W., Plazinska, A., 2009. Theoretical models of sorption kinetics including a surface reaction mechanism: A review. Adv. Colloid Interface Sci. 152, 2–13. https://doi.org/10.1016/J.CIS.2009.07.009

Rocha, L.S., Lopes, C.B., Borges, J.A., Duarte, A.C., Pereira, E., 2013. Valuation of Unmodified Rice Husk Waste as an Eco-Friendly Sorbent to Remove Mercury: a Study Using Environmental Realistic Concentrations. Water, Air, Soil Pollut. 224, 1599. https://doi.org/10.1007/s11270-013-1599-9

Rodrigues, D., Freitas, A.C., Pereira, L., Rocha-Santos, T.A.P., Vasconcelos, M.W., Roriz, M., Rodríguez-Alcalá, L.M., Gomes, A.M.P., Duarte, A.C., 2015. Chemical composition of red, brown and green macroalgae from Buarcos bay in Central West Coast of Portugal. Food Chem. 183, 197–207. https://doi.org/10.1016/j.foodchem.2015.03.057

Roginsky, S., Zeldovich, Y.B., 1934. The catalytic oxidation of carbon monoxide on manganese dioxide. Acta Phys. Chem. USSR 1, 554.

Romera, E., González, F., Ballester, A., Blázquez, M.L., Muñoz, J.A., 2007. Comparative study of biosorption of heavy metals using different types of algae. Bioresour. Technol. 98, 3344–3353. https://doi.org/10.1016/J.BIORTECH.2006.09.026

Shams Khoramabadi, G., Jafari, A., Hasanvand Jamshidi, J., 2008. Biosorption of Mercury (II) from Aqueous Solutions by Zygnema fanicum Algae. J. Appl. Sci. 8, 2168–2172.

Stumm, W., Morgan, J.J., 1996. Aquatic Chemistry: chemical equilibria and rates in natural waters. John Wiley & Sons, Inc.

Suganya, T., Renganathan, S., 2012. Optimization and kinetic studies on algal oil extraction from marine macroalgae Ulva lactuca. Bioresour. Technol. 107, 319–326.

https://doi.org/10.1016/j.biortech.2011.12.045

Tavares, D.S., Lopes, C.B., Daniel-da-silva, A.L., Vale, C., Trindade, T., Pereira, M.E., 2016. Mercury in river , estuarine and seawaters e Is it possible to decrease realist environmental concentrations in order to achieve environmental quality standards ? Water Res. 106, 439–449. https://doi.org/10.1016/j.watres.2016.10.031

Zaib, M., Makshoof Athar, M., Saeed, A., Farooq, U., Salman, M., Nouman Makshoof, M., 2016. Green Chemistry Letters and Reviews Equilibrium, kinetic and thermodynamic biosorption studies of Hg(II) on red algal biomass of Porphyridium cruentum. Green Chem. Lett. Rev. 94, 179–189. https://doi.org/10.1080/17518253.2016.1185166

Zhou, Y., Wei, F., Zhang, W., Guo, Z., Zhang, L., 2018. Copper bioaccumulation and biokinetic modeling in marine herbivorous fish Siganus oramin. Aquat. Toxicol. 196, 61–69. https://doi.org/10.1016/J.AQUATOX.2018.01.009

Work submitted as scientific article

Negligible effect of potential toxic elements and rare earth elements on mercury removal from contaminated waters by green, brown and red living marine macroalgae

Abstract

Mercury (Hg) removal by six different living marine macroalgae, namely, *Ulva intestinalis*, *Ulva lactuca*, *Fucus spiralis*, *Fucus vesiculosus*, *Gracilaria* sp. and *Osmundea pinnatifida* was investigated in mono and multi-contamination scenarios. All macroalgae were tested under the same experimental conditions and the competition effects were evaluated with all elements at the same initial molar concentration of 1 μmol dm^{-3}. The presence of the main potential toxic elements (Cd, Cr, Cu, Ni and Pb) and rare earth elements (La, Ce, Pr, Nd, Eu, Gd, Tb and Y) have not affected the removal of Hg. Characterizations of the macroalgae by FTIR before and after the sorption/bioaccumulation assays suggest that Hg was mainly linked to sulfur-functional groups, while the removal of other elements was related with other functional groups. The mechanisms involved point to sorption of Hg on the macroalgae surface followed by possible incorporation of this metal into the macroalgae by metabolic active processes. Globally, the green macroalgae (*Ulva intestinalis*, *Ulva lactuca*) showed the best performances for Hg, PTEs and REEs removal from synthetic seawater spiked with 1 μmol dm^{-3} of each element, at room temperature and pH 8.5.

IV.2. Negligible effect of potential toxic elements and rare earth elements on mercury removal from contaminated waters by green, brown and red living marine macroalgae

IV.2.1. Introduction

Among the major contaminants, mercury (Hg) has aroused worldwide concerns due to its accumulation in organisms and amplification along the food chain. Mercury and its compounds are classified as priority hazardous substances according to the European Union (EU) legislation, which promotes their cessation or phase-out, particularly by discharges or losses as a result of anthropogenic activities (Directive 2013/39/EU). Release of Hg to the environment is mostly by battery and lamps production, mining and metallurgical processes, and chlor-alkali, petrochemical and paint industries (Priyadarshini et al., 2019). Moreover, its dangerousness and impacts on environment and human health led the ratification of the Minamata convention emphasizing the importance of eliminating this contaminant.

The use of biological materials for the removal of metals from contaminated waters has emerged as potential alternative to conventional methods (Shams Khoramabadi et al., 2008). Biosorbents such as plants, fungi, bacteria and algae are feasible low-cost options for the treatment of contaminated waters (Park et al., 2010). Biosorption is the mass transfer process where the target metal remains on the surface of the biomass, while bioaccumulation is the passive incorporation of metals on the solid surface followed by active uptake triggered by metabolic means (Henriques et al., 2015; Shams Khoramabadi et al., 2008; Velásquez and Dussan, 2009). Several works have proposed the use of biosorbents to remove Hg by biosorption (Anagnostopoulos et al., 2012; Boutsika et al., 2014; Carro et al., 2011; El-Shafey, 2010; Esmaeili et al., 2015; Lohani et al., 2008; Shams Khoramabadi et al., 2008). Despite the advantages of this process, the separation of biomass from the solution may be a challenging task in the process and normally requires an additional step of filtration (Henriques et al., 2015).

Beyond that, bioaccumulation has been reported to be more efficient when compared with biosorption (Chojnacka, 2010; Henriques et al., 2017, 2015). Living marine macroalgae are excellent options for bioaccumulation, since they are known as organisms very resistant, being able to live under contaminated environments, including by toxic metals (Priyadarshini et al., 2019). Macroalgae can interact with metals in two ways: (i) externally, by active release of ligands or by complexation on surface and, (ii) carrying the metals through the membrane to the inside of the cells (Stumm and Morgan, 1996). The cell walls are formed by hydroxyl, amine, carbonyl, sulphur and phosphoryl groups with high affinity to metals, which make the macroalgae promising Hg scavengers (Priyadarshini et al., 2019). Furthermore, the application of living macroalgae to waste water treatments does not demand any solid separation systems, which could represent additional costs in industrial processes (Henriques et al., 2017; Mata et al., 2009).

The marine macroalgae can be divided in three groups: Phaeophyta (brown macroalgae), Rhodophyta (red macroalgae) and Chlorophyta (green macroalgae) (Romera et al., 2007). Besides the pigmentation, they present different chemical and structural compositions. Carbohydrates, proteins (Rodrigues et al., 2015) and polysaccharides are commonly used to identify the type of macroalgae (Rodrigues et al., 2015; Shanmugam and Mody, 2000). Vijayaraghavan and Joshi have studied the Hg(II) removal from synthetic solutions by two brown macroalgae namely *Sargassum* sp*.,* and *Turbinaria conoide* and a green macroalgae *Ulva* sp (Vijayaraghavan and Joshi, 2012). Esmaelli *et al*. have used *Gracilaria corticata* (red algae) and *Sargassum glaucescens* (brown algae) to remove Hg from mono-elemental solutions (Esmaeili et al., 2015). Henriques *et al*. have studied the Hg(II) bioaccumulation on *Ulva lactuca*, *Gracilaria gracilis* and *Fucus vesiculosus* (Henriques et al., 2015). Although the literature contemplates works applying macroalgae for Hg(II) removal, most of these studies only considered its removal from monometallic synthetic solutions. Consequently, there is still a lack of information about Hg removal by macroalgae from complex aqueous streams (like seawater) and how the presence of other elements in solution affect that process.

The main aim of this study was to identify potential interactions (antagonism or synergetic) of potential toxic elements (Cd, Cr, Cu, Ni and Pb) and rare earth elements (La,

Ce, Pr, Nd, Eu, Gd, Tb and Y) on the removal of Hg(II) by six macroalgae species (*Ulva intestinalis, Ulva lactuca*, *Fucus spiralis*, *Fucus vesiculosus*, *Gracilaria sp*. and *Osmundea pinnatifida*).

III.1.2. Materials and methods

IV.2.2.4. Chemicals and materials

The chemicals used in this study were purchased by commercial suppliers and used without any other purification. The standard solutions (1000 ± 2 mg dm^{-3}) of Hg and Cd were obtained from PanReac AppliChem, Pb, Cu, Cr and Gd from Merck, Ni from Spectrosol, Tb, Y and Pr from Alfa Aesar Specpure®, Eu and La from Plasma Cal, Dy from CPAchem and Nd, Ce and certified reference materials for ICP from Inorganic Ventures™. The nitric acid solution (65 %) and sodium hydroxide (≥ 99 %) were acquired from Merck. The artificial salt tropic Marin® SEA SALT was purchased from Tropic Marine Center and was used to prepare the synthetic seawater. Salt composition is described by Atkinson and Bingman (Atkinson and Bingman, 2010). Working solutions, including the calibration standards were prepared directly by dilution of the stock solutions or by intermediate solutions, in HNO_3 2% solution. All the glassware was prewashed with nitric acid (25 % v/v) for 24 hours and subsequently washed with ultrapure water (18 MΩ cm).

IV.2.2.2. Sampling of macroalgae biomasses

The macroalgae used in this work were *Ulva intestinalis, Ulva lactuca*, *Fucus spiralis*, *Fucus vesiculosus*, *Gracilaria sp*. and *Osmundea pinnatifida.* Specimens were collected in Ria de Aveiro (Portugal, 40°38´39´´N, 8°44´43´´W). In the laboratory, the macroalgae were washed with tap water and synthetic seawater to eliminate dirt and microorganisms that might be attached to their surface. Then, the macroalgae were maintained in aquariums with aerated seawater for one week under natural light (approximately 12L:12D) and room temperature (22 ± 2 °C), for acclimatization to the laboratory conditions. Previously, a sample of each macroalgae was taken and freeze-dried to quantify Hg(II) background levels and for FTIR analysis before contaminants

exposure. Other portions of each macroalgae were also collected for determination of the external contact area and to calculate the water content by weight loss.

IV.2.2.3. Experimental design

Laboratory experiments were designed to test the ability of the six collected macroalgae species to remove Hg(II) from mono- and multi-contaminated solutions. Synthetic seawater (salinity of 30) was prepared in transparent bottles of 1 dm^3, maintained at room temperature of 22 ± 2 °C, and pH adjusted to 8.5 with NaOH (1 M). Different volumes of standard solutions were added into the bottles to achieve the final concentration of 1 µmol dm^{-3} of each element. Three spiked solutions were prepared for the exposure of each macroalgae: solution 1 (S1) was prepared with 1 µmol dm^{-3} of Hg and the macroalgae; solution 2 (S2) with 1 µmol dm^{-3} of Hg, Cd, Cu, Cr, Ni and Pb and the macroalgae; solution 3 (S3) with 1 µmol dm^{-3} of Hg, Cd, Cu, Cr, Ni, Pb (as S2) plus 1 µmol dm^{-3} of La, Ce, Pr, Nd, Eu, Gd, Tb and Y (REEs). The elements: Hg, Cd, Cr, Cu, Ni and Pb are designated potential toxic elements (PTEs) because are common contaminants found in the water bodies (Henriques et al., 2017). REEs are known as critical technology elements used in various industrial fields, such as production of batteries, computer and monitors, fluorescent lamps, and electronical and medical devices (Costley et al., 2000; Liu et al., 2018). Wastewaters contain often a variable mixture of those elements.

Experiments with blank solutions (macroalgae exposed to uncontaminated synthetic seawater) and control solutions (spiked solution without macroalgae) run in parallel with the spiked solutions to check the adaptation of the macroalgae species to the experimental conditions and to assess possible losses or external contaminations. All the solutions were left to pre-equilibrate 24 hours before the beginning of the assays and then were exposed to natural light (approximately 12L:12D) during the trials. To 1 dm^3 of each type of spiked solution, 3 g (fresh weight) of small pieces of each macroalgae were added. In general, the size varied from 1x5 cm^2 for *F. spiralis, F. vesiculosus*, *Gracilaria sp.* and *O. pinnatifida*, 5x5 cm^2 for *U. lactuca,* and 1x10 cm^2 *U. intestinalis*. Different sizes resulted from specificity of each species structure combined with logistic constraints. The initial time of each experiment started with the addition of the macroalgae to the spiked

solution. Samples of 10 cm^3 were collected at increasing times from the mono-contaminated solutions (S1): 0, 1, 3, 6, 9, 24, 48 and 72 hours. Then samples were acidified to pH < 2 with HNO_3 65% and stored at 4 °C for total Hg(II) analysis. In addition, aliquots of 15 cm^3 were taken at 0, 24, 48 and 72 hours from solutions 2 (S2) and 3 (S3) for the determination of Hg(II), PTEs and REEs.

All experiments were run in duplicate. Values of the two assays did not varied more that 10 % for Hg and 20 % for PTEs and REEs. Low variability led us to consider a single value of each pair of values. At the end of each experiment, macroalgae were removed from solutions and weighted for the calculation of growth rates. Another portion was lyophilized and stored for further FTIR analysis.

IV.2.2.4. Analytical methods and quality control

Fourier Transform Infrared (FTIR) of the macroalgae was performed before and after exposure to spiked solutions in order to identify major functional groups involved on the removal processes. A Bruker optics tensor 27 spectrometer coupled to a horizontal attenuated total reflectance (ATR) cell using 256 scans at a resolution of 4 cm^{-1} was used and the spectra were recorded as transmittance from 4000 to 500 cm^{-1}. The external contact area was assessed with the Fiji software. Previously, different masses of fresh macroalgae were weighted (0.02-2.20 g) and then scanned with a resolution of 200 ppi. This resolution served to set the scale and the file was saved as TIFF format because this format stores the information of scale with the image.

The quantification of Hg(II) present in solution was performed by cold vapor atomic fluorescence spectroscopy (CV-AFS), on a PSA cold vapour generator (model 10.003) coupled to a Merlin PSA detector (model 10.023). Tin chloride ($SnCl_2$) solution was used as the reducing agent. Standards with concentrations of 0.1, 0.2, 0.3 and 0.5 µg dm^{-3} were used for the calibration curve. The samples were measured in triplicate and the average value was used, with maximum relative standard deviation between them of 10 %. The quantification limit of this method was 0.02 µg dm^{-3}. Concentrations of the other elements in the liquid phase were measured with inductively coupled plasma atomic emission spectrometry (ICP-OES) on a Horiba Jobin Yvon, Activa M. The limit of

quantification of this method was 10 µg dm^{-3} with acceptable relative standard deviation between replicates lower than 5 %.

Determination of the total Hg in macroalgae, before the exposure, was performed by thermal decomposition atomic absorption spectrometry with gold amalgamation using a LECO© AMA-254. The method followed is described by Costley *et al*. (Costley et al., 2000) and had the limit of quantification of 0.03 ng of Hg. Approximately 20 mg of samples were directly analyzed in duplicate (with relative standard deviations between replicates lower than 10 %). To ensure the quality of the results, the Certified Reference Material (CFR) ERM-CD200 (*Fucus vesiculosus*; 0.0186 ± 0.0016 mg kg^{-1} of total Hg) was analyzed prior and after the samples, and its recovery percentage was 100.8 %.

IV.2.2.5. Formulas and data analysis

The growth rate of the macroalgae (G, % day^{-1}) was calculated trough the logarithmic equation as follows (Gordillo et al., 2015):

$$G = 100 \times \frac{\ln (W_f / W_i)}{t} \quad \text{(IV.2.1)}$$

where $W_i$and W_f (g) are the initial and final masses of macroalgae in fresh weight and t (day) is the time of the experiments.

The removal percentage of the element (R, %) by the macroalgae were calculated through the differences of concentrations in the liquid phase, as represented bellow:

$$R\ (\%) = 100 \times \frac{(C_0 - C_t)}{C_0} \quad \text{(IV.2.2)}$$

where C_0 (µg dm^{-3}) is the concentration at the initial time and C_t (µg dm^{-3}) is the concentration at the time t of the experiment.

The average concentration of the element for unit mass of macroalgae (q, µg g^{-1}) was obtained by the global mass balance, mathematically expressed by:

$$q = \frac{V(C_0 - C_f)}{M} \quad \text{(IV.2.3)}$$

where C_f (µg dm^{-3}) is the element final concentration in the liquid phase, V (dm^3) is volume of solution and M (g) is the initial mass in dry weight, assuming no significant differences between initial and final mass of the macroalgae.

Tests of significance of the statistical analysis were performed by one- way Analysis of Variance (ANOVA) test, with confidence interval of 95 %, using the data analysis extension of Microsoft® Excel™ 2016.

IV.2.3. Results and discussion

IV.2.3.1. Water content, external area and growth rate of macroalgae

Table IV.2.1 presents the water content and external contact area of each macroalgae and the growth rate during the 72 hours of the experiment. Water content of *U. intestinalis, Gracilaria sp*. and *O. pinnatifida* was statistically ($p < 0.05$) higher than of *U. lactuca*, *F. spiralis* and *F. vesiculosus*. External contact area varied considerably among the macroalgae, with significant ($p < 0.05$) differences being obtained: *U. lactuca* > *U. intestinalis* > *Gracilaria sp*. > *O. pinnatifida*, *F. spiralis* and *F. vesiculosus*. The noteworthy external contact areas of *U. lactuca* and *U. intestinalis* provide larger surfaces of contact with the solution, which may facilitate the removal of elements from the spiked waters. The growth rates for 72 hours were negligible. For this reason, the further calculations of q (Equation (IV.2.3)) have considered the initial mass of the macroalgae.

IV.2.3.2. Mercury content in macroalgae used in experiments

Mercury concentrations in macroalgae biomasses sampled in Ria de Aveiro before exposure to the spiked solutions were: 0.042 ± 0.002 µg g^{-1} in *Ulva inteslinalis*, 0.034 ± 0.002 µg g^{-1} in *Ulva lactuca,* 0.049 ± 0.002 µg g^{-1} in *Fucus spiralis*, 0.032 ± 0.001 µg g^{-1} in *Fucus vesiculosus,* 0.031 ± 0.002 µg g^{-1} in *Gracilaria* sp. and 0.082 ± 0.002 µg g^{-1} in *Osmundea pinnatifida*. Despite these low concentrations, which are characteristic of non-

contaminated biosorbents (Bułkowska, K., Pawłowski, 2016; Henriques et al., 2015), values are significantly different ($p < 0.05$).

Table IV.2.1. Water content (%), external contact area ($cm^2\ g^{-1}$) and growth rate (% day^{-1}) of the six macroalgae.

Macroalgae	*U. Intestinalis*	*U. lactuca*	*F. spiralis*	*F. vesiculosus*	*Gracilaria* sp.	*O. pinnatifida*
Water content (%)	91.4 ±0.6	82.8 ±0.5	81.6 ±3.1	80.2 ±5.4	88.1 ±5.5	88.8 ±1.2
External contact area ($cm^2\ g^{-1}$)	148 ± 45	264 ± 31	29 ± 11	30 ± 9	79 ± 9.3	33 ± 2
Growth rate (% day^{-1})	-0.54	0.53	-1.70	-0.47	-0.74	-0.54

IV.2.3.3. Fourier Transform Infrared in macroalgae

FTIR was performed in macroalgae before and after exposure to the different conditions of contamination: macroalgae exposed to Hg solution (S1), macroalgae exposed to Hg and PTEs (S2), and macroalgae exposed to Hg, PTEs and REEs (S3). Comparison of the spectra provides information on major functional groups involved on Hg removal and the possible interaction with the additional elements (PTEs and REEs). Figure IV.2.1 presents the normalized infrared spectra for the six macroalgae under the three contaminated conditions. Most of the spectra exhibited five vibration regions in common: overlapping peaks of O-H and N-H stretching vibrations at 3280-3290 cm^{-1} (Kalavathy et al., 2005; Rodrigues et al., 2015), band at 2900 cm^{-1} attributed to the asymmetric C-H bonds (Figueira et al., 2011), asymmetric and symmetric bands of C=O presented at 1630 and 1410 cm^{-1}, respectively (Omar et al., 2018), and the strong stretch at 1000-1100 cm^{-1} related with the alcohol groups (Murphy et al., 2009). However, it was registered differences among the macroalgae species.

U. intestinalis spectra (Figure IV.2.1a) showed remarkable differences after being exposed to Hg, which give insights about the possible functional groups involved on the Hg uptake process. After exposure to S1 the macroalgae showed vibrations at 1536 cm^{-1} ascribed to N-H of amide II, and at 1318 cm^{-1} associated with sulfonate groups (asymmetric -OSO_3) (Murphy et al., 2009). This is in line with the strong affinity of Hg to sulfur groups and progressively lower affinity to amide, amine and carboxyl groups (Ferreira et al., 2009; Wang and Sun, 2013). Macroalgae in S2 showed the additional presence of the stretch at 2800 cm^{-1} (symmetric C-H) (Liu et al., 2018), and the loss of the band at 535 cm^{-1} of C–N–S (Bulgariu and Bulgariu, 2014; Henriques et al., 2015). For S3 it was vanishing the bands of of the glycosidic linkages of cellulose located at 840 and 790 cm^{-1} (Fan et al., 2012).

U. lactuca spectrum (Figure IV.2.1b) of S1 with respect to the unexposed species showed the disappearance of the peak at 644 cm^{-1} due to alkynes bonds (C-H) (Suganya and Renganathan, 2012). Most likely sulfur (symmetric-OSO_3) and carboxyl (C-O) groups contribute to Hg(II) removal, as it is suggested by the disappearance of the peaks at 1120 cm^{-1} and 1197 cm^{-1} (Murphy et al., 2009, 2008). Hydroxyl groups from rhamnose and glucuronic acid, the main sugars present in this macroalgae, played an important role in the uptake of the elements from S2 and S3 as pointed by the decrease of the wavenumber from 1100 to 1000 cm^{-1} (Murphy et al., 2008). The vibrations of two bands at 1242 cm^{-1} and 1220 cm^{-1} in solutions S2 and S3 instead of the band at 1197 cm^{-1} (on the free algae, blank) indicate involvement of aromatic amine (C-N stretching) (Suganya and Renganathan, 2012) and the new peak at 1323 cm^{-1} indicate asymmetric -OSO_3 (Murphy et al., 2008) bending. There is also a shift of the vibrations from 600 to 533 cm^{-1} related to C–N–S of the polypeptides (Bulgariu and Bulgariu, 2014; Henriques et al., 2015).

The brown macroalgae *F. spiralis* (Figure IV.2.1c) and *F. vesiculosus* (Figure IV.2.1d) presented characteristic peaks of alginate, a polysaccharide composed by guluronic and mannuronic acids evidenced by the peaks at 1025 cm^{-1} and at 800 cm^{-1}, respectively (Gómez-Ordóñez and Rupérez, 2011; Rodrigues et al., 2015). Hg(II) removal by *F. spiralis* might be ascribed to the appearance of the band at 1240 cm^{-1}, related with S=O sulphate

esters of the polysaccharide fucoidan (Pereira et al., 2013; Rodrigues et al., 2015) and the two bands at 616 and 582 cm^{-1}. S2 spectrum has an additional vibration at 1540 cm^{-1} (N-H) (Murphy et al., 2009) and in S3 the C-H stretching gave rise to a new frequency at 890 cm^{-1} (Gómez-Ordóñez and Rupérez, 2011; Rodrigues et al., 2015). For *F. vesiculosus* the peak at 1540 cm^{-1} is not observed after the contact with Hg(II) and there is also the rise of the peak at 1240 cm^{-1} related with fucoidan (Pereira et al., 2013; Rodrigues et al., 2015), as observed in *F. spiralis*. Both in S1 and S3 there was the absence of the peak at 535 cm^{-1} (C–N–S) (Bulgariu and Bulgariu, 2014).

Gracilaria sp. and *O. pinnatifida* are red macroalgae producers of agars rich in sulphate (Rodrigues et al., 2015). Agars representative bands are located at the wavenumber of 1040-1060 cm^{-1} (Figure IV.2.1d and e) (Knutsen et al., 1994; Rodrigues et al., 2015). In S1 spectrum of *Gracilaria* sp, the vanishing of the peaks at 2930 cm^{-1} (asymm. C-H) and 790 cm^{-1} assigned to galactose, present in carrageenan and agar polysaccharides points to coordination with Hg(II) (Rodrigues et al., 2015). For *O. pinnatifida* there is an evidence that Hg(II) accumulation is related with the absence of the peak at 580 cm^{-1} and the appearance of a new peak at 2820 cm^{-1} (symm. C-H) (Liu et al., 2018). The accumulation of the other elements from S2 and S3 might be associated with the loss of the galactose band at 800 cm^{-1} (Knutsen et al., 1994; Rodrigues et al., 2015).

IV.2.3.4. Removal of mercury by the six macroalgae

Figure IV.2.2 shows the concentration of Hg(II) in the liquid phase normalized to the initial concentration (1 µmol dm^{-3}) for several contact times, in the presence of the six macroalgae in mono-contaminated solutions (S1). Control values of each macroalgae experiment (not shown) varied less than 10 % with time. In general, the concentration profiles are characterized by two stages of Hg(II) concentration decrease. The first stage showed a faster removal, most likely due to the pronounced gradient of concentrations between the spiked solution and the macroalgae surface that was initially free of Hg(II). The number of available active sites in the macroalgae and the possible links to Hg favour its retention. In general, retention is the result of a passive surface uptake involving

physical forces and chemical links (Ishii et al., 2006). On the second stage, the decline of Hg(II) in solution was slower, probably because the sorption sites have been progressively occupied, the gradient was less accentuated, and consequently the driving force was weaker. However, it should be hypothesised that simultaneously with passive uptake, Hg is transported from the surface into the cell by helper proteins making available new sorption sites (Ishii et al., 2006). This would explain why the plateau was not reached in these experiments (Henriques et al., 2017).

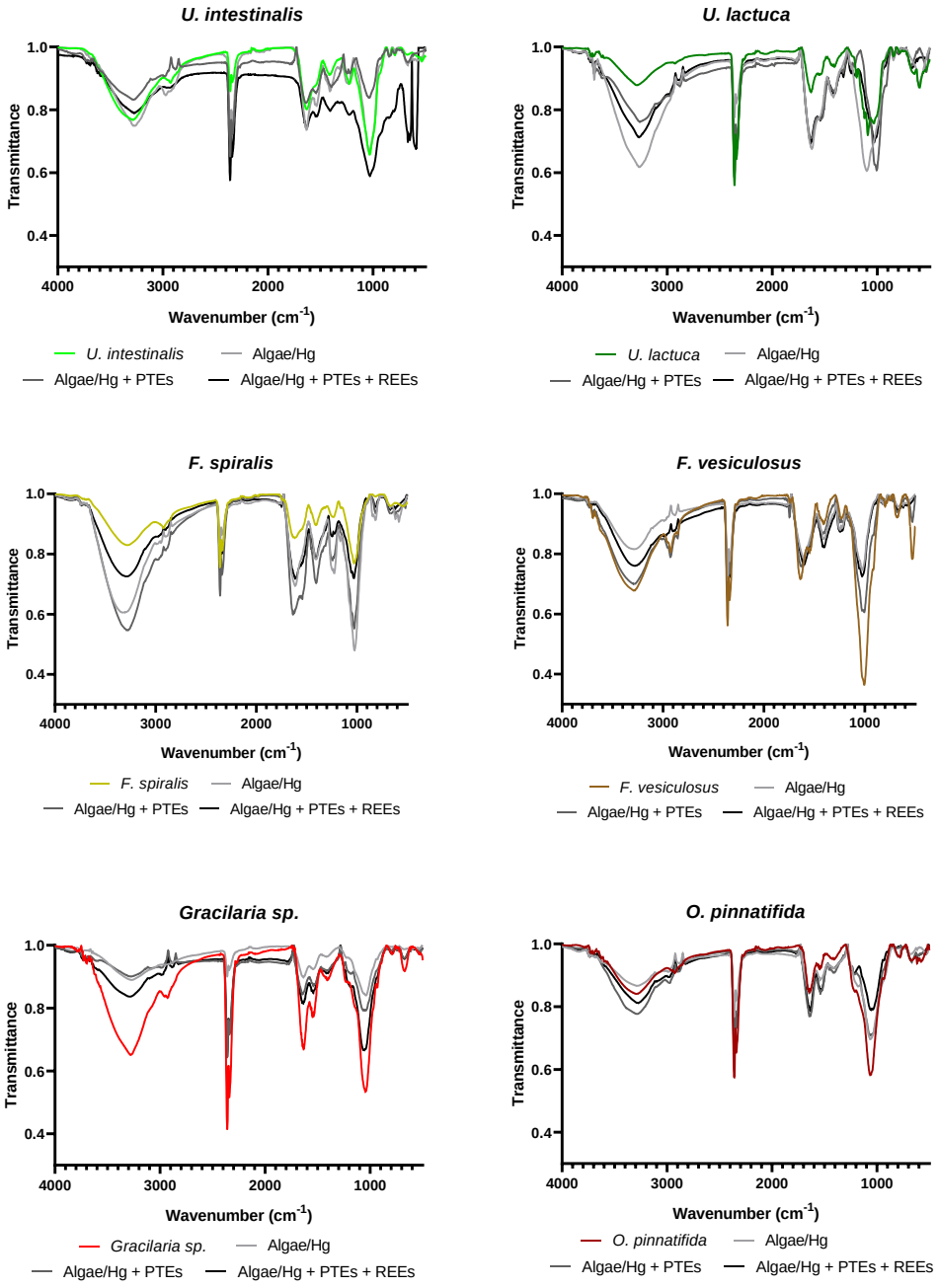

Figure IV.2.1. FTIR spectra of the six macroalgae before and after exposure in mono- and multi-contaminated solutions S1 (macroalgae + Hg), S2 (macroalgae + Hg + PTEs) and S3 (macroalgae + Hg + PTEs + REEs).

Regarding the three groups of macroalgae plotted in (brown, red and green), the two brown macroalgae (Figure IV.2.2) showed similar profiles (relative standard deviation of 9.3 % considering the pair *F. spiralis* and *F. vesiculosus*). Decline with time fits better to a straight line than macroalgae kinetic profiles of other two groups (red and green, Figure

IV.2.2), which may be due to the presence of less active sites, reduced accessibility to them or lower affinity to Hg(II). Red macroalgae have also presented similar kinetic curves, with relative standard deviation between *Gracilaria sp.* and *O. pinnatifida* concentrations of 7.0 %. These results are in line with their similar chemical and structural composition as mentioned above. On the other hand, *U. intestinalis* and *U. lactuca* showed different patterns probably reflecting interaction of Hg(II) with different functional groups. Despite these two macroalgae have presented the best Hg(II) removals, *U. intestinalis* has much higher affinity to Hg. This species stands out for having high content of sulfonate and amide groups and large available contact area, allowing the achievement of the very low Hg(II) concentration in solution after 72 hours, 2.8 µg dm^{-3}. This value is much lower than with other species: 22.8 µg dm^{-3} by *U. lactuca*, 31.1 µg dm^{-3} by *F. spiralis*, 41.6 µg dm^{-3} by *F. vesiculosus*, 22.8 µg dm^{-3} by *Gracilaria* sp. and 29.7 µg dm^{-3} by *O. pinnatifida*.

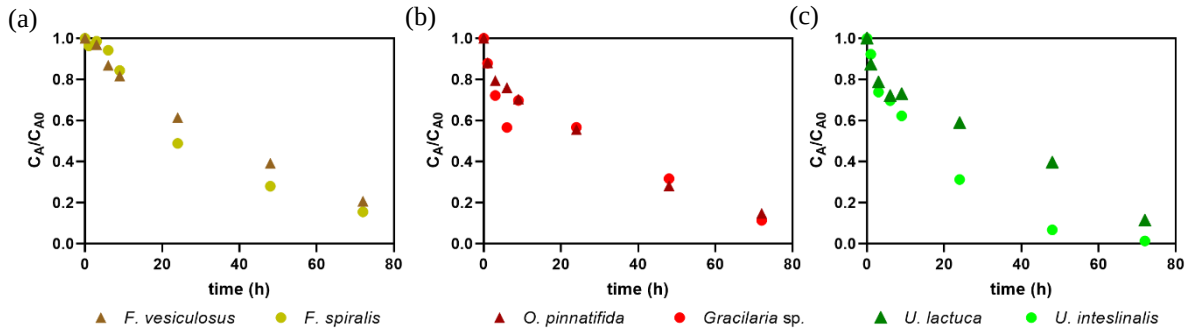

Figure IV.2.2. Normalized Hg(II) concentrations to the initial value (C_0) in solution *versus* time for: (a) brown, (b) red and (c) green macroalgae.

IV.2.3.5. Bioconcentration factors

The bioconcentration factor (BCF, dm^3 kg^{-1}, dry weight), calculated as the ratio between Hg concentration in macroalgae and in solution at 72 hours, corroborates the affinity of Hg to the macroalgae. The calculated BCF were: 3536 (*U. intestinalis*), 1733 (*U. lactuca),* 1497 (*F. spiralis),* 1257 (*F. vesiculosus),* 2463 (*Gracilaria* sp.*)* and 2629 (*O. pinnatifida).* These results highlight the excellent ability of living marine macroalgae to

capture Hg(II) from contaminated streams and their potential use in industrial application.

IV.2.3.6. Interaction of potential toxic elements and rare earth elements in Hg(II) removal

The influence of other solubilized elements on Hg(II) removal from solution was tested by exposing the six macroalgae to Hg(II) solution in the presence of other cations: PTEs and PTEs plus REEs (Figure IV.2.3). The use of the same initial concentration (1 μmol dm^{-3}) of all elements allows the comparison of the possible interaction or competitiveness for the binding sites in the macroalgae surface (Jacinto et al., 2018; Zhao et al., 2016). Removal percentages by the six macroalgae after 72 hours ranged within similar intervals in mono-contamination experiments (S1, 85-99 %), experiments with Hg+PTEs (S2, 86-94 %) and Hg+PTEs+REEs (S3, 85-93 %). These results suggest that the effect of the coexistent ions on the removal of Hg(II) was negligible. Most likely, Hg ions were linked preferentially to sulfur groups and the other elements (PTEs and REEs) were related with various functional groups. Comparison of the removal of Hg, Cd, Cr, Cu, Ni and Pb by the six macroalgae is shown in Figure IV.2.4. Mercury was removed above between 86 and 94 %, exceedingly largely the values observed for Cd (4-22 %), Ni (7-44 %), Cr (12-50 %), Cu (27-49 %) and Pb (17-52 %). These results are in line with the high affinity between Hg(II) and sulphated polysaccharides presented in the macroalgae (Castro et al., 2003)(Wang and Sun, 2013). Carro *et al*. have investigated the removal of divalent cations of Hg, Ca, Cd, Cu and Pb by the brown algal *Sargassum muticum* and found the affinity sequential order Hg > Pb > Cd > Cu > Ca (Carro et al., 2010). In the current study with the six macroalgae, Cu(II) and Cr(VI) were the elements more efficiently removed after Hg although the sequence varied with the species. These results corroborate the conclusion of a previous work with *F. vesiculosus* showing the removal sequence of Hg > Pb > Cd (Henriques et al., 2017). Plaza *et al*. indicated that the presence of divalent cations has declined the Hg(II) removal onto *M. pyrifera* and *U. pinnatifida* in the following order: Cd(II) ≥ Ni(II) > Zn(II) (Plaza et al., 2011).

Elements, like Cd, Cu, Cr, Ni and Pb are expected to be mainly in the cationic forms or present as carbonate and chloro-complexes (Stumm and Morgan, 1996). Macroalgae may have exudate organic compounds to solution that act as addition sequesters to dissolved elements (Stumm and Morgan, 1996). Removal of the elements by electrostatic interactions with active sites in the macroalgae surface, or remaining in solution depends on the stability constants. For example, high affinity of Hg to the sulfur groups may detached chloro-complexes forms (Stumm and Morgan, 1996). Lower affinity of Cd, Cu, Cr, Ni and Pb to the macroalgae surface than Hg implied that more than 50 % of the added quantities in the spiked solutions remained in dissolved forms. Cadmium was clearly the element in higher quantity in solution after the 72 hours of experiment, 78 to 96 % of the added quantity.

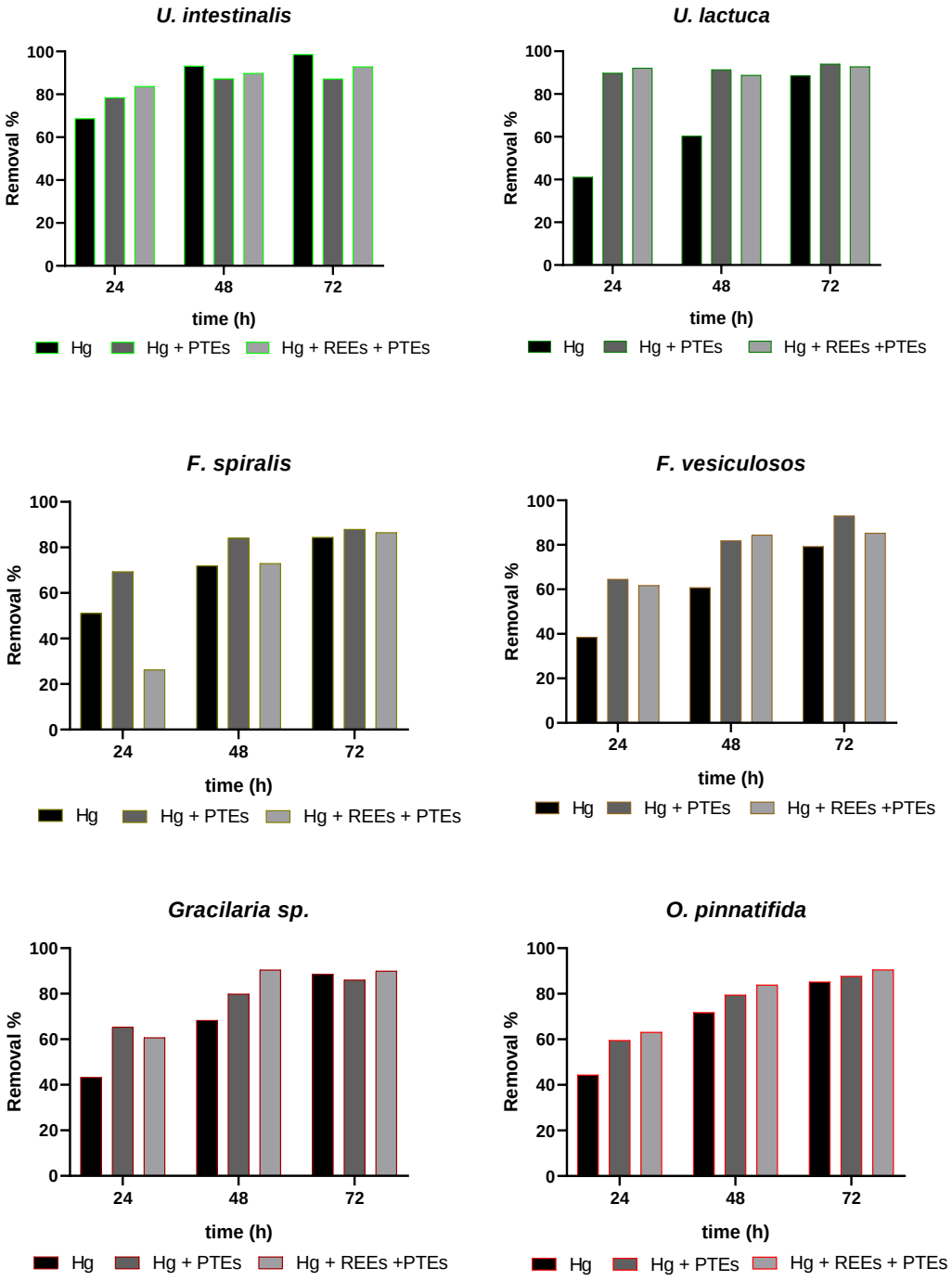

Figure IV.2.3. Hg(II) removal in mono- and multi-contamination solutions S1 (macroalgae + Hg), S2 (macroalgae + Hg + PTEs) and S3 (macroalgae + Hg + PTEs + REEs) by the six living macroalgae species

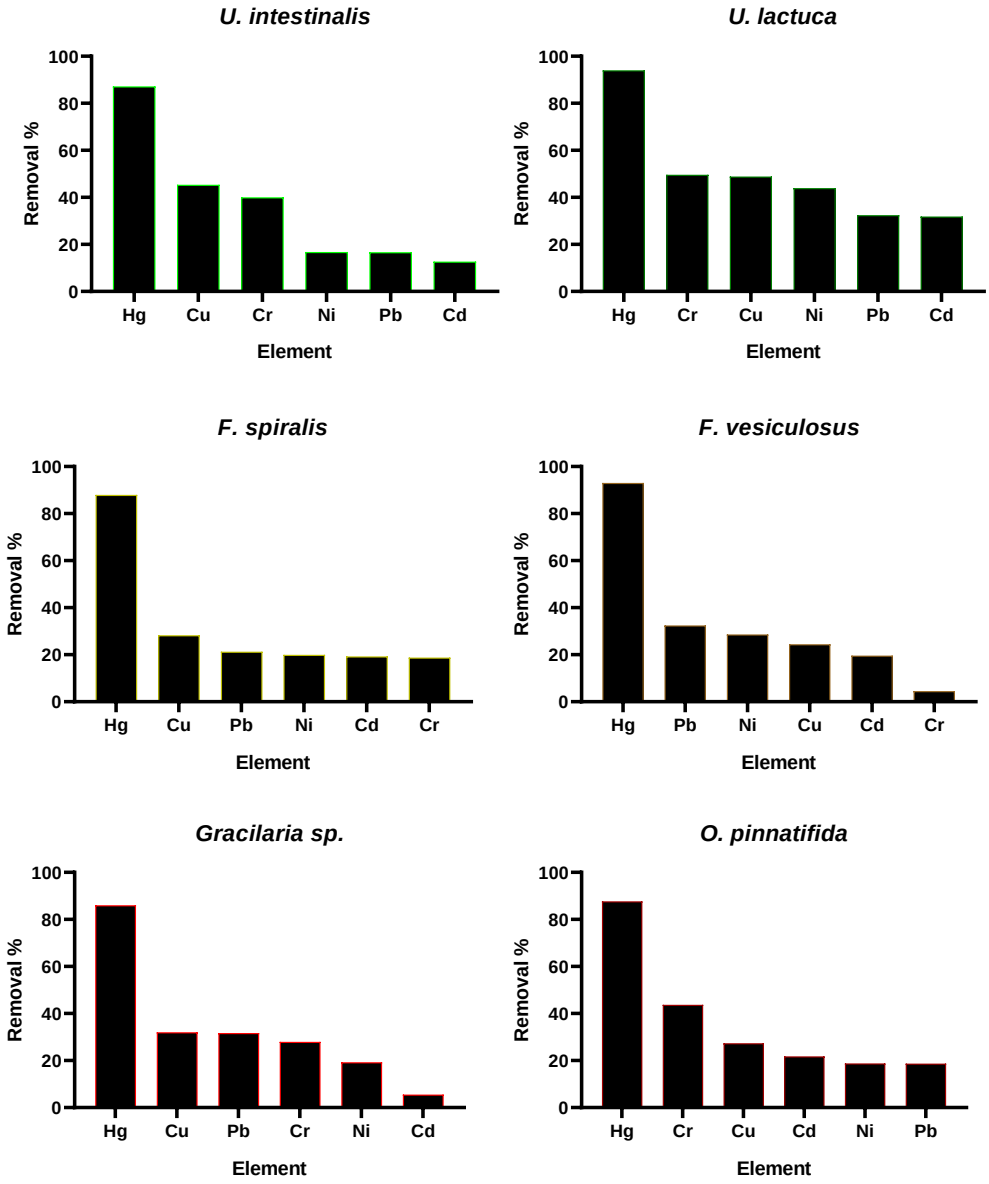

Figure IV.2.4. Removal percentages of Hg(II) and the PTEs in the solution 2 (S2) (Hg, Cd, Cr, Cu, Ni and Pb).

Figure IV.2.5 represents the removal percentages of all the elements present in solution S3 (Hg, Cd, Cr, Cu, Pb, Ni, La, Ce, Pr, Nd, Eu, Gd, Tb and Y) onto the six macroalgae. As in S2, Hg showed the highest removal by macroalgae among all the elements. Low affinity of REEs to S-H groups exclude these elements from competing with Hg(II) for binding with these functional groups on the surface of the macroalgae (Bulman,

2003). Despite the variation among macroalgae, removal of REEs (with few exceptions) exceeded the values of PTEs by all species. Higher removal of REEs than PTEs points to their lower affinity to dissolved anions, complexes formed with Cl^-, or organic compounds produced by the macroalgae. No pattern was observed regarding the groups of light REEs (La, Ce, Pr, Nd, Eu) and heavy REEs (Gd, Tb, Dy, Y). Similar results were observed with the removal of La, Ce, Nd, Eu and Y by *Gracilaria gracilis* from a multi-element spiked solution (Jacinto et al., 2018). The progressive filling of the 4f orbital of the lanthanides series elements from Ce to Lu and nearby ionic sizes makes the lanthanides very similar in chemical properties (Bulman, 2003; Yoshimura and Watanabe, 2003). However, Ishii *et al*. have obtained different outcomes by testing algal *Euglena gracilis* to remove sixteen types of REEs from aqueous solutions. They have found decrescent removals of REEs with decreasing atomic radius (Ishii et al., 2006). Results of the present study are in the same line in the way that differences were also noticed among REE behaviour with respect to sorption on macroalgae surfaces. Liu *et al*. suggest that ion exchange and surface complexation, mainly with the functional groups of cellulose are the mechanisms involved in the REEs elimination (Liu et al., 2018).

Dissimilarities were also notice among the macroalgae species tested in this study. Green macroalgae (*U. lactuca* and *U. intestinalis)* exhibited the best sequestration of REEs and of most of PTEs from solutions (Table IV.2.2), probably due to their larger external contact areas. The present study does not allow to distinguish whether elements were retained on the cell walls by physical-chemical sorption or crossed the membrane and were incorporated in other parts of the cells.

Highest and lowest removals of REEs were found for *U. lactuca* and *F. spiralis*: La (28-68 %), Ce (26-66 %), Nd (22-67 %), Eu (29-71 %), Gd (32-72 %), Tb (25-67 %), Dy (29-59 %) and Y (21-65 %), while Pr varied from 30 % for *O. pinnatifida* to 65 % for *U. lactuca*.

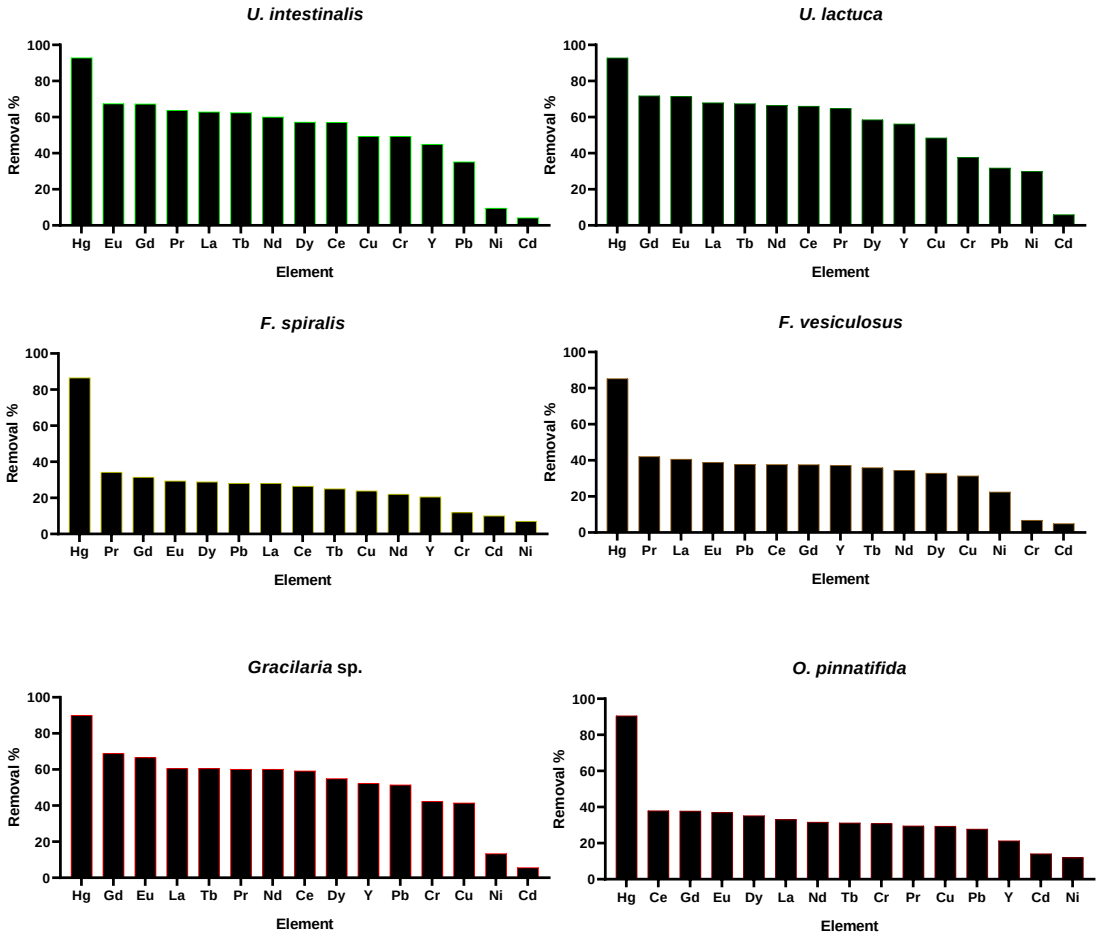

Figure IV.2.5. Removal percentages of Hg(II), PTEs and REEs in the solution 3 (S3).

Table IV.2.2. Removals of all the elements in the different multi-contaminated solutions, S2 (Hg + PTEs) and S3 (Hg + PTEs + REEs).

	Type of solution	***U. intestinalis***	***U. lactuca***	***F. spiralis***	***F. vesiculosus***	***Gracilaria* sp.**	***O. pinnatifida***	**Best**
Hg	S2	87.2 %	94.0 %	88.0 %	93.0 %	86.0 %	87.7 %	*U. lactuca*
	S3	92.9 %	92.8 %	86.5 %	85.3 %	90.0 %	90.5 %	*U. intestinalis*
Cd	S2	12.7 %	31.9 %	19.3 %	19.6 %	5.5 %	21.8 %	*U. lactuca*

	S3	4.2 %	6.0 %	10.0 %	5.0 %	5.7 %	14.1 %	*O. pinnatifida*
Cu	S2	45.4 %	48.8 %	28.3 %	24.5 %	32.0 %	27.3 %	*U. lactuca*
	S3	49.4 %	48.5 %	23.9 %	31.4 %	41.4 %	29.4 %	*U. intestinalis*
Cr	S2	40.0 %	49.5 %	18.8 %	4.6 %	27.9 %	43.7 %	*U. lactuca*
	S3	49.4 %	37.7 %	11.9 %	6.8 %	42.3 %	30.9 %	*U. intestinalis*
Ni	S2	16.8 %	43.9 %	20.0 %	28.6 %	19.3 %	18.8 %	*U. lactuca*
	S3	9.6 %	29.9 %	7.0 %	22.4 %	13.4 %	12.0 %	*U. lactuca*
Pb	S2	16.7 %	32.4 %	21.3 %	32.4 %	31.7 %	18.7 %	*U. lactuca*
	S3	35.2 %	31.8 %	28.1 %	37.8 %	51.5 %	27.8 %	*Gracilaria* sp.
Eu	S3	67.4 %	71.4 %	29.4 %	38.9 %	66.6 %	37.0 %	*U. lactuca*
Nd	S3	60.0 %	66.5 %	22.0 %	34.4 %	60.1 %	31.6 %	*U. lactuca*
Dy	S3	57.2 %	58.5 %	28.9 %	32.9 %	54.9 %	35.2 %	*U. lactuca*
Gd	S3	67.3 %	71.8 %	31.5 %	37.6 %	68.8 %	37.8 %	*U. lactuca*
La	S3	62.8 %	68.0 %	28.1 %	40.6 %	60.5 %	33.0 %	*U. lactuca*
Tb	S3	62.4 %	67.5 %	25.0 %	35.9 %	60.5 %	31.2 %	*U. lactuca*
Y	S3	45.0 %	56.2 %	20.6 %	37.2 %	52.3 %	21.3 %	*U. lactuca*
Pr	S3	63.7 %	64.9 %	34.5 %	42.1 %	60.2 %	29.6 %	*U. lactuca*
Ce	S3	57.2 %	66.1 %	26.4 %	37.7 %	59.2 %	37.9 %	*U. lactuca*

IV.2.3.7. Estimation of mercury loading

Calculated quantities of Hg uptake (*q*, Equation (IV.2.3)) by the six macroalgae under the three contamination conditions are presented in Figure IV.2.6. Values of *q* indicate that ability of the six macroalgae to uptake Hg from contaminated waters is virtually independent of the presence of other contaminants, either classic contaminants such as Cd, Cr, Cu, Pb and Ni that are commonly found in waste waters, or REEs that started to be found as result of their spread use, namely in electronic equipment. *U. intestinalis* has stood up, being able to achieve concentrations of 765 μg g^{-1} of Hg(II) in the mono-contamination scenario and 646 and 688 μg g^{-1} in the complex solutions S2 and S3. The lowest Hg(II) accumulation was performed by *F. vesiculosus* and differences of Hg uptake under competition was small, 264-310 μg g^{-1}.

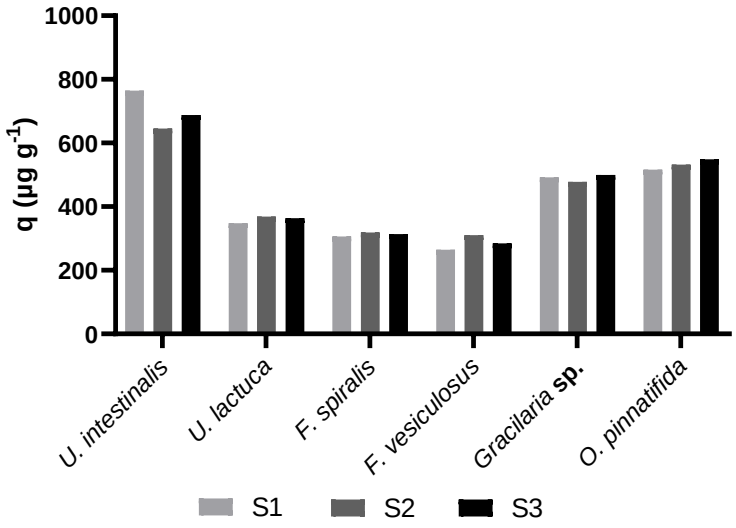

Figure IV.2.6. Concentration of Hg(II) in the six macroalgae under the contaminated solutions S1 (macroalgae, Hg), S2 (macroalgae, Hg+PTEs) and S3 (macroalgae, Hg+PTEs+REEs).

IV.2.4. Conclusions

Potential competition of various cations on the removal of mercury from contaminated waters by living marine macroalgae in mono and multi-element contaminated solutions indicated that: (i) Hg is the easiest element to remove among

potential toxic elements (Cd, Cr, Cu, Pb, Ni) and REEs (La, Ce, Pr, Nd, Eu, Gd, Tb, Dy and Y); (ii) removal percentage exceeded 86 % of the initial concentration by all tested macroalgae; (iii) removal of REEs were lower (21 to 71 %) and potential toxic elements were much lower (4 to 52%) and; (iv) the presence of other cations did not affect considerably the Hg uptake capacity of all studied species.

IV.2.5. References

Anagnostopoulos, V.A., Manariotis, I.D., Karapanagioti, H.K., Chrysikopoulos, C. V., 2012. Removal of mercury from aqueous solutions by malt spent rootlets. Chem. Eng. J. 213, 135–141. https://doi.org/10.1016/J.CEJ.2012.09.074

Atkinson, M.J., Bingman, C., 2010. Elemental composition of commercial seasalts, Journal of Aquariculture and Aquatic Sciences.

Boutsika, L.G., Karapanagioti, H.K., Manariotis, I.D., 2014. Aqueous mercury sorption by biochar from malt spent rootlets. Water. Air. Soil Pollut. 225, 2007–2013. https://doi.org/10.1007/s11270-013-1805-9

Bulgariu, L., Bulgariu, D., 2014. Enhancing Biosorption Characteristics of Marine Green Algae (Ulva lactuca)for Heavy Metals Removal by Alkaline Treatment. J. Bioprocess. Biotech. 04, 1–8. https://doi.org/10.4172/2155-9821.1000146

Bułkowska, K., Pawłowski, A., 2016. Biomass feedstock for biofuels production, in: Bułkowska, K., Gusiatin, Z.M., Klimiuk, E., Pawłowski, A., Pokoj, T. (Eds.), Biomass for Biofuels. CRC Press, pp. 37–61.

Bulman, R.A., 2003. Mobilization of Lanthanides through the Terrestrial Biosphere, in: Sigel, A., Sigel, H. (Eds.), Metal Ions in Biological Systems. Marcel Dekker, Inc., New York, pp. 39–67.

Carro, L., Anagnostopoulos, V., Lodeiro, P., Barriada, J.L., Herrero, R., Sastre de Vicente, M.E., 2010. A dynamic proof of mercury elimination from solution through a combined sorption–reduction process. Bioresour. Technol. 101, 8969–8974.

https://doi.org/10.1016/J.BIORTECH.2010.06.118

Carro, L., Barriada, J.L., Herrero, R., Sastre de Vicente, M.E., 2011. Adsorptive behaviour of mercury on algal biomass: Competition with divalent cations and organic compounds. J. Hazard. Mater. 192, 284–291. https://doi.org/10.1016/J.JHAZMAT.2011.05.017

Castro, M., Cruz, J., Otazo-Sánchez, E., Perez-Marín, L., 2003. Theoretical Study of the Hg 2+ Recognition by 1,3-Diphenyl-Thiourea. J. Phys. Chem. A 107, 9000–9007. https://doi.org/10.1021/jp030768g

Chojnacka, K., 2010. Biosorption and bioaccumulation – the prospects for practical applications. Environ. Int. 36, 299–307. https://doi.org/10.1016/J.ENVINT.2009.12.001

Costley, C.T., Mossop, K.F., Dean, J.R., Garden, L.M., Marshall, J., Carroll, J., 2000. Determination of mercury in environmental and biological samples using pyrolysis atomic absorption spectrometry with gold amalgamation. Anal. Chim. Acta 405, 179–183. https://doi.org/10.1016/S0003-2670(99)00742-4

Directive 2013/39/EU of the European Parliament and of the Council of 12 August 2013 amending Directives 2000/60/EC and 2008/105/EC as regards priority substances in the field of water policy, 2013. . Off. J. Eur. Union.

El-Shafey, E.I., 2010. Removal of Zn(II) and Hg(II) from aqueous solution on a carbonaceous sorbent chemically prepared from rice husk. J. Hazard. Mater. 175, 319–327. https://doi.org/10.1016/J.JHAZMAT.2009.10.006

Esmaeili, A., Saremnia, B., Kalantari, M., 2015. Removal of mercury(II) from aqueous solutions by biosorption on the biomass of Sargassum glaucescens and Gracilaria corticata. Arab. J. Chem. 8, 506–511. https://doi.org/10.1016/J.ARABJC.2012.01.008

Fan, M., Dai, D., Huang, B., 2012. Fourier Transform Infrared Spectroscopy for Natural Fibres, in: Salih, S. (Ed.), Fourier Transform - Materials Analysis. InTech China. https://doi.org/10.5772/35482

Ferreira, T.R., Lopes, C.B., Lito, P.F., Otero, M., Lin, Z., Rocha, J., Pereira, E., Silva, C.M., Duarte, A., 2009. Cadmium(II) removal from aqueous solution using microporous titanosilicate ETS-4. Chem. Eng. J. 147, 173–179. https://doi.org/10.1016/j.cej.2008.06.032

Figueira, P., Lopes, C.B., Daniel-da-Silva, A.L., Pereira, E., Duarte, A.C., Trindade, T., 2011. Removal of mercury (II) by dithiocarbamate surface functionalized magnetite particles: application to synthetic and natural spiked waters. Water Res. 45, 5773–5784. https://doi.org/10.1016/j.watres.2011.08.057

Gómez-Ordóñez, E., Rupérez, P., 2011. FTIR-ATR spectroscopy as a tool for polysaccharide identification in edible brown and red seaweeds. Food Hydrocoll. 25, 1514–1520. https://doi.org/10.1016/J.FOODHYD.2011.02.009

Gordillo, F.J.L., Aguilera, J., Wiencke, C., Jiménez, C., 2015. Ocean acidification modulates the response of two Arctic kelps to ultraviolet radiation. J. Plant Physiol. 173, 41–50. https://doi.org/10.1016/J.JPLPH.2014.09.008

Henriques, B., Lopes, C.B., Figueira, P., Rocha, L.S., Duarte, A.C., Vale, C., Pardal, M.A., Pereira, E., 2017. Bioaccumulation of Hg, Cd and Pb by Fucus vesiculosus in single and multi-metal contamination scenarios and its effect on growth rate. Chemosphere 171, 208–222. https://doi.org/10.1016/J.CHEMOSPHERE.2016.12.086

Henriques, B., Rocha, L.S., Lopes, C.B., Figueira, P., Monteiro, R.J.R., Duarte, A.C., Pardal, M.A., Pereira, E., 2015. Study on bioaccumulation and biosorption of mercury by living marine macroalgae: Prospecting for a new remediation biotechnology applied to saline waters. Chem. Eng. J. 281, 759–770. https://doi.org/10.1016/J.CEJ.2015.07.013

Ishii, N., Tagami, K., Uchida, S., 2006. Removal of rare earth elements by algal flagellate Euglena gracilis. J. Alloys Compd. 408–412, 417–420. https://doi.org/10.1016/J.JALLCOM.2004.12.105

Jacinto, J., Henriques, B., Duarte, A.C., Vale, C., Pereira, E., 2018. Removal and recovery of Critical Rare Elements from contaminated waters by living Gracilaria gracilis. J.

Hazard. Mater. 344, 531–538. https://doi.org/10.1016/J.JHAZMAT.2017.10.054

Kalavathy, M.H., Karthikeyan, T., Rajgopal, S., Miranda, L.R., 2005. Kinetic and isotherm studies of Cu(II) adsorption onto H3PO4-activated rubber wood sawdust. J. Colloid Interface Sci. 292, 354–362. https://doi.org/10.1016/j.jcis.2005.05.087

Knutsen, S.H., Myslabodski, D.E., Larsen, B., Usov, A.I., 1994. A Modified System of Nomenclature for Red Algal Galactans. Bot. Mar. 37, 163–169. https://doi.org/10.1515/botm.1994.37.2.163

Liu, C., Lin, H., Mi, N., Liu, F., Song, Y., Liu, Z., Sui, J., 2018. Adsorption mechanism of rare earth elements in *Laminaria ochroleuca* and *Porphyra haitanensis*. J. Food Biochem. 42, e12533. https://doi.org/10.1111/jfbc.12533

Lohani, M.B., Singh, A., Rupainwar, D.C., Dhar, D.N., 2008. Studies on efficiency of guava (Psidium guajava) bark as bioadsorbent for removal of Hg (II) from aqueous solutions. J. Hazard. Mater. 159, 626–629. https://doi.org/10.1016/J.JHAZMAT.2008.02.072

Mata, Y.N., Blázquez, M.L., Ballester, A., González, F., Muñoz, J.A., 2009. Biosorption of cadmium, lead and copper with calcium alginate xerogels and immobilized Fucus vesiculosus. J. Hazard. Mater. 163, 555–562. https://doi.org/10.1016/J.JHAZMAT.2008.07.015

Murphy, V., Hughes, H., McLoughlin, P., 2009. Enhancement strategies for Cu(II), Cr(III) and Cr(VI) remediation by a variety of seaweed species. J. Hazard. Mater. 166, 318–326. https://doi.org/10.1016/j.jhazmat.2008.11.041

Murphy, V., Hughes, H., McLoughlin, P., 2008. Comparative study of chromium biosorption by red, green and brown seaweed biomass. Chemosphere 70, 1128–1134. https://doi.org/10.1016/j.chemosphere.2007.08.015

Omar, H., El-Gendy, A., Al-Ahmary, K., 2018. Bioremoval of toxic dye by using different marine macroalgae. Turk. J. Botany 42, 15–27. https://doi.org/10.3906/bot-1703-4

Park, D., Yun, Y.-S., Park, J.M., 2010. The Past, Present, and Future Trends of Biosorption.

Biotechnol. Bioprocess Eng. 15, 86–102. https://doi.org/10.1007/s12257-009-0199-4

Pereira, L., Gheda, S.F., Ribeiro-Claro, P.J.A., 2013. Analysis by Vibrational Spectroscopy of Seaweed Polysaccharides with Potential Use in Food, Pharmaceutical, and Cosmetic Industries. Int. J. Carbohydr. Chem. 2013, 1–7. https://doi.org/10.1155/2013/537202

Plaza, J., Viera, M., Donati, E., Guibal, E., 2011. Biosorption of mercury by Macrocystis pyrifera and Undaria pinnatifida: Influence of zinc, cadmium and nickel. J. Environ. Sci. 23, 1778–1786. https://doi.org/10.1016/S1001-0742(10)60650-X

Priyadarshini, E., Priyadarshini, S.S., Pradhan, N., 2019. Heavy metal resistance in algae and its application for metal nanoparticle synthesis. Appl. Microbiol. Biotechnol. 103, 3297–3316. https://doi.org/10.1007/s00253-019-09685-3

Rodrigues, D., Freitas, A.C., Pereira, L., Rocha-Santos, T.A.P., Vasconcelos, M.W., Roriz, M., Rodríguez-Alcalá, L.M., Gomes, A.M.P., Duarte, A.C., 2015. Chemical composition of red, brown and green macroalgae from Buarcos bay in Central West Coast of Portugal. Food Chem. 183, 197–207. https://doi.org/10.1016/j.foodchem.2015.03.057

Romera, E., González, F., Ballester, A., Blázquez, M.L., Muñoz, J.A., 2007. Comparative study of biosorption of heavy metals using different types of algae. Bioresour. Technol. 98, 3344–3353. https://doi.org/10.1016/J.BIORTECH.2006.09.026

Shams Khoramabadi, G., Jafari, A., Hasanvand Jamshidi, J., 2008. Biosorption of Mercury (II) from Aqueous Solutions by Zygnema fanicum Algae. J. Appl. Sci. 8, 2168–2172.

Shanmugam, M., Mody, K.H., 2000. Heparinoid-active sulphated polysaccharides from marine algae as potential blood anticoagulant agents. Curr. Sci. https://doi.org/10.2307/24104127

Stumm, W., Morgan, J.J., 1996. Aquatic Chemistry: chemical equilibria and rates in natural waters. John Wiley & Sons, Inc.

Suganya, T., Renganathan, S., 2012. Optimization and kinetic studies on algal oil extraction from marine macroalgae Ulva lactuca. Bioresour. Technol. 107, 319–326.

https://doi.org/10.1016/j.biortech.2011.12.045

Velásquez, L., Dussan, J., 2009. Biosorption and bioaccumulation of heavy metals on dead and living biomass of Bacillus sphaericus. J. Hazard. Mater. 167, 713–716. https://doi.org/10.1016/J.JHAZMAT.2009.01.044

Vijayaraghavan, K., Joshi, U.M., 2012. Interaction of Mercuric Ions with Different Marine Algal Species. Bioremediat. J. 16, 225–234. https://doi.org/10.1080/10889868.2012.731443

Wang, T., Sun, H., 2013. Biosorption of heavy metals from aqueous solution by UV-mutant Bacillus subtilis. Env. Sci Pollut Res 20, 7450–7463. https://doi.org/10.1007/s11356-013-1767-x

Yoshimura, E., Watanabe, T., 2003. Lanthanide ions as probes in studies of metal ion-dependency enzymes, in: Sigel, A., Sigel, H. (Eds.), Metal Ions in Biological Systems. Marcel Dekker, Inc., New York, p. 161.189.

Zhao, F., Repo, E., Meng, Y., Wang, X., Yin, D., Sillanpää, M., 2016. An EDTA-β-cyclodextrin material for the adsorption of rare earth elements and its application in preconcentration of rare earth elements in seawater. J. Colloid Interface Sci. 465, 215–224. https://doi.org/10.1016/J.JCIS.2015.11.069

Chapter V

Final remarks and future work

Water scarcity is becoming a reality in many parts of the world and the projection for 2050 is not optimistic. In addition, water contamination as a result of toxic metals discharges is also a major problem that humanity is facing today. Population growth and the development of industrial activities will bring consuming water availability to the lowest levels in the coming years, and therefore, the treatment and reuse of aquatic sources has attracted more interest in order to contain or minimize this current problem. To accomplish that, the governmental entities have imposed more restrict regulations and incentive the development of efficient alternatives to remove pollutants from waters. One of the goals of 2030 Agenda for Sustainable Development of United Nations promotes improving water quality by minimizing the presence of hazardous chemicals and encourages substantial increase of water recycling and reuse.

Among the toxic metals that must be eliminated or phased out of discharges mercury is of great importance. It is classified as the third most hazardous substance in the rank of the Agency for Toxic Substances & Disease Registry (ATSDR), which was elaborated based on a combination of its environmental frequency, toxicity, and potential for human exposure. Moreover, the Directive 2013/39/EU of the European Union classifies mercury as a priority substance that must be progressive eliminated of the emissions by 2021. Although the attempts of banning or reducing its utilization, many industrial activities and illegal mining keep releasing this toxic metal to the environment. The aggravate of mercury emissions is the fact that it can persist in the atmosphere and be transported many kilometers before it be deposited in the aquatic systems. In water bodies, mercury rapidly accumulates in the living organisms and is transmitted and amplified along the food chain attaining the man in concentrations up to thousand folds than the ones found in waters. For that reason, even low concentrations in waters should be treated with the aim to reduce the mercury concentration and prevent its toxicity.

Various works are reported in literature for the removal of mercury from contaminated waters. However, most of them are focused on the removal of Hg(II) under conditions extremely different from the real systems, applying initial concentrations of Hg(II) very high, up to 2000 mg dm^{-3} and using simple matrices like deionized or distilled waters. Such conditions are more favorable for Hg removal, since the effects of ionic

strength and competitive ions are neglected, and higher gradients of concentration normally improve Hg(II) uptake. Hence, the solids tested are expected to perform well but frequently it is irreproducible in realistic conditions.

The present work intended to fulfill these gaps and offer reliable and effective alternatives for mercury removal from water bodies. Different conditions were applied to evaluate Hg(II) removal in diverse systems simulating the ones found in real applications. Natural waters, seawater and industrial effluents contain several other elements which may prevent Hg(II) removal by complexation or competition for the sorption sites. With the aim to find alternatives to replace the commonly used activated carbons and ion exchange resins the sorbents must be considered under these conditions, *ie.* low Hg(II) concentrations and real waters.

The use of synthetic zeolite-type materials presented the advantage of high efficiency due to their microporous structure, large surface areas, porosity and great ion exchange capacity. Despite the cost associated with their synthesis these sorbents may be easily regenerated in industrial applications which reduce substantially the operational costs. The sorbents had excellent performances and very low doses of the zeolite-type materials studied in this work were able to achieve final residual mercury concentrations. The limitation for the use of such materials is normally their large-scale synthesis to provide sufficient masses of these solids for the treatment of large volumes of contaminated solutions. In this sense, researching new and efficient materials is important to find the best ones that are worth producing and applying industrially.

On the other hand, the utilization of biosorbents represents an interesting and sustainable option for water treatment, because it allows to use residues from agriculture and industry or even organisms largely available in the environment. From the economic point of view, the less the pre-treatment of the biosorbents, the more attractive is the process. So, in this work, the biosorbents were tested in their natural forms or after simple physical transformations like drying, freeze-drying or milling. The performances varied according to the biosorbents used and the operation conditions. Considering more realistic Hg(II) concentrations as low as 50 μg dm^{-3}, banana peels and water hyacinth were found to be the best choices for spiked tap waters. However, under more complex

solutions like spiked seawater, the living macroalgae such as *Ulva intestinalis, Ulva lactuca* and *Gracilaria* sp. together with banana peels are great alternatives. Suitability to the water treatment installation will determine whether the living or dead biosorbents are the most promising technology. The current study showed that mercury concentrations of 50 μg dm^{-3} may decrease to values lower than 1 μg dm^{-3} using very low dosages (0.27 - 0.50 g dm^{-3}) of the biosorbents banana peels, *Ulva intestinalis, Ulva lactuca* and *Gracilaria* sp. The restrict guideline for drinking waters imposed by organisations such as W.H.O, European Commission and U.S.A Agencies was successfully achieved. In the case of the maximum allowed for Hg(II) concentration in drinking waters imposed by regulation in Brazil of 0.2 μg dm^{-3}, it was accomplished by using *Gracilaria* sp. and *Ulva lactuca.*

Comparing the use of synthetic materials with biosorbents (living or dead), different aspects can be considered. In terms of capacity, the isotherms of AM-11 (niobium silicate) and AM-14 (vanadium silicate) showed Langmuir capacities very high, of 161 and 304 mg g^{-1}, respectively. In contrast, banana peels (biosorbent that had excellent performance) presented Langmuir capacity of 0.75 mg g^{-1}. The differences between the results obtained are mainly due to the microporous structures of the zeolite-type materials, which provides larger surfaces areas and higher number of sorption sites for mercury removal. Despite the lower capacity, the use of biosorbents may be preferred in order to use materials with negligible costs associated, and need of few or no biomass pre-treatments. For water treatment units, the use of synthetic materials is viable when a regeneration system is added to the sorption process. In terms of installation, synthetic materials are used in substitution to the ion exchange resins in fixed-bed columns, while the biosorbents could be used in batch reactors. The time required to achieve the equilibrium is also an important factor to be evaluated, and generally AM-11 and AM-14 took *ca.* 96 hours to reach equilibrium while for banana peels the time required was *ca.* 72 hours and for *Gracilaria* sp. was 48 hours. Comparison between living macroalgae and banana peels in similar contaminated waters showed that macroalgae are more efficient, being able to remove 99.9 % of Hg(II) by *Gracilaria* sp. and 99.6 % by *Ulva intestinalis* with doses of 0.36 g and 0.26 g, respectively and 0.5 g of banana peels removed 93 % of Hg(II)

from seawater. Additionaly, the amount of biosorbent necessary to treat contaminated waters is also a relevant factor, the lower the biosorbent required the lower it will be the residues generation which may represent expensive disposal costs.Despite this work has focused on the investigation of different materials, understanding about the mechanisms involved on the mercury removal by them through equilibrium and kinetic study and the impact of different conditions were also extensively examined. Additionally, a two-stage batch contactor was proposed and depicted a simple system for real application in water treatments units.

Future work could comprises the evaluation of the ability of AM-11 and AM-14 for Hg(II) ion exchange under fixed-bed configuration and the obtention of the breakthrough curves. Methods of packing these solids to fill the column should be evaluated. For instance, they could be prepared as pellets, or impregnated in different supports. Moreover, regeneration studies in batch and fixed-bed systems using different acid and salt solutions would give more information for subsequently scale-up application.

In relation to the biosorbents, some work could be developed with the aim to evaluate more deeply the mechanisms involved using different desorption solutions and also by analysing the content of other cations in the remained water solution. Furthermore, some recover of Hg could be investigated. Using the response surface methodology, the impact of other operational conditions, such as temperature and stirring or other ranges of pH could be accessed. Combination of different biosorbents in series configuration or as mixtures could allow to use lower biosorbents dosages.

Regarding the promising potential of the living macroalgae, studies using living and dead macroalgae would give insights about the process involved in the mercury uptake, if it is mainly occurring by biosorption or bioaccumulation and which one is more efficient. Despite the equilibrium state does not exist in bioaccumulation, experiments similar to the ones for the determination of equilibrium isotherms could be performed as an attempt to get information about the capacity of the macroalgae. Combined with that, growth rates should be considered. Toxicity resistance could determine which macroalgae is more appropriated for each target treatment. The impact of parameters like light

exposure, temperature and nutrients sources could be evaluate on the uptake performances of these organisms.